

**A Descriptive Analysis of the Joint Reaction Forces  
and the Ground Reaction Forces in the Lower Limb  
During the Landing of a Triple Toe Loop.**

By

Daryl E. Boldt

A Thesis  
Submitted to the Faculty of Graduate Studies  
in Partial Fulfillment of the Requirements  
for the Degree of

MASTER OF SCIENCE

Faculty of Physical Education and Recreation Studies  
University of Manitoba  
November, 1993



National Library  
of Canada

Acquisitions and  
Bibliographic Services Branch

395 Wellington Street  
Ottawa, Ontario  
K1A 0N4

Bibliothèque nationale  
du Canada

Direction des acquisitions et  
des services bibliographiques

395, rue Wellington  
Ottawa (Ontario)  
K1A 0N4

*Your file* *Votre référence*

*Our file* *Notre référence*

The author has granted an irrevocable non-exclusive licence allowing the National Library of Canada to reproduce, loan, distribute or sell copies of his/her thesis by any means and in any form or format, making this thesis available to interested persons.

L'auteur a accordé une licence irrévocable et non exclusive permettant à la Bibliothèque nationale du Canada de reproduire, prêter, distribuer ou vendre des copies de sa thèse de quelque manière et sous quelque forme que ce soit pour mettre des exemplaires de cette thèse à la disposition des personnes intéressées.

The author retains ownership of the copyright in his/her thesis. Neither the thesis nor substantial extracts from it may be printed or otherwise reproduced without his/her permission.

L'auteur conserve la propriété du droit d'auteur qui protège sa thèse. Ni la thèse ni des extraits substantiels de celle-ci ne doivent être imprimés ou autrement reproduits sans son autorisation.

ISBN 0-315-92152-8

Canada

Name DARYL E. BOLDT

Dissertation Abstracts International is arranged by broad, general subject categories. Please select the one subject which most nearly describes the content of your dissertation. Enter the corresponding four-digit code in the spaces provided.

PHYSICAL EDUCATION

SUBJECT TERM

0523

SUBJECT CODE

U·M·I

**Subject Categories**

**THE HUMANITIES AND SOCIAL SCIENCES**

**COMMUNICATIONS AND THE ARTS**

Architecture	0729
Art History	0377
Cinema	0900
Dance	0378
Fine Arts	0357
Information Science	0723
Journalism	0391
Library Science	0399
Mass Communications	0708
Music	0413
Speech Communication	0459
Theater	0465

**EDUCATION**

General	0515
Administration	0514
Adult and Continuing	0516
Agricultural	0517
Art	0273
Bilingual and Multicultural	0282
Business	0688
Community College	0275
Curriculum and Instruction	0727
Early Childhood	0518
Elementary	0524
Finance	0277
Guidance and Counseling	0519
Health	0680
Higher	0745
History of	0520
Home Economics	0278
Industrial	0521
Language and Literature	0279
Mathematics	0280
Music	0522
Philosophy of	0998
Physical	0523

Psychology	0525
Reading	0535
Religious	0527
Sciences	0714
Secondary	0533
Social Sciences	0534
Sociology of	0340
Special	0529
Teacher Training	0530
Technology	0710
Tests and Measurements	0288
Vocational	0747

**LANGUAGE, LITERATURE AND LINGUISTICS**

Language	
General	0679
Ancient	0289
Linguistics	0290
Modern	0291
Literature	
General	0401
Classical	0294
Comparative	0295
Medieval	0297
Modern	0298
African	0316
American	0591
Asian	0305
Canadian (English)	0352
Canadian (French)	0355
English	0593
Germanic	0311
Latin American	0312
Middle Eastern	0315
Romance	0313
Slavic and East European	0314

**PHILOSOPHY, RELIGION AND THEOLOGY**

Philosophy	0422
Religion	
General	0318
Biblical Studies	0321
Clergy	0319
History of	0320
Philosophy of	0322
Theology	0469

**SOCIAL SCIENCES**

American Studies	0323
Anthropology	
Archaeology	0324
Cultural	0326
Physical	0327
Business Administration	
General	0310
Accounting	0272
Banking	0770
Management	0454
Marketing	0338
Canadian Studies	0385
Economics	
General	0501
Agricultural	0503
Commerce-Business	0505
Finance	0508
History	0509
Labor	0510
Theory	0511
Folklore	0358
Geography	0366
Gerontology	0351
History	
General	0578

Ancient	0579
Medieval	0581
Modern	0582
Black	0328
African	0331
Asia, Australia and Oceania	0332
Canadian	0334
European	0335
Latin American	0336
Middle Eastern	0333
United States	0337
History of Science	0585
Law	0398
Political Science	
General	0615
International Law and Relations	0616
Public Administration	0617
Recreation	0814
Social Work	0452
Sociology	
General	0626
Criminology and Penology	0627
Demography	0938
Ethnic and Racial Studies	0631
Individual and Family Studies	0628
Industrial and Labor Relations	0629
Public and Social Welfare	0630
Social Structure and Development	0700
Theory and Methods	0344
Transportation	0709
Urban and Regional Planning	0999
Women's Studies	0453

**THE SCIENCES AND ENGINEERING**

**BIOLOGICAL SCIENCES**

Agriculture	
General	0473
Agronomy	0285
Animal Culture and Nutrition	0475
Animal Pathology	0476
Food Science and Technology	0359
Forestry and Wildlife	0478
Plant Culture	0479
Plant Pathology	0480
Plant Physiology	0817
Range Management	0777
Wood Technology	0746
Biology	
General	0306
Anatomy	0287
Biostatistics	0308
Botany	0309
Cell	0379
Ecology	0329
Entomology	0353
Genetics	0369
Limnology	0793
Microbiology	0410
Molecular	0307
Neuroscience	0317
Oceanography	0416
Physiology	0433
Radiation	0821
Veterinary Science	0778
Zoology	0472
Biophysics	
General	0786
Medical	0760

Geodesy	0370
Geology	0372
Geophysics	0373
Hydrology	0388
Mineralogy	0411
Paleobotany	0345
Paleoecology	0426
Paleontology	0418
Paleozoology	0985
Palynology	0427
Physical Geography	0368
Physical Oceanography	0415

**HEALTH AND ENVIRONMENTAL SCIENCES**

Environmental Sciences	0768
Health Sciences	
General	0566
Audiology	0300
Chemotherapy	0992
Dentistry	0567
Education	0350
Hospital Management	0769
Human Development	0758
Immunology	0982
Medicine and Surgery	0564
Mental Health	0347
Nursing	0569
Nutrition	0570
Obstetrics and Gynecology	0380
Occupational Health and Therapy	0354
Ophthalmology	0381
Pathology	0571
Pharmacology	0419
Pharmacy	0572
Physical Therapy	0382
Public Health	0573
Radiology	0574
Recreation	0575

Speech Pathology	0460
Toxicology	0383
Home Economics	0386

**PHYSICAL SCIENCES**

Pure Sciences	
Chemistry	
General	0485
Agricultural	0749
Analytical	0486
Biochemistry	0487
Inorganic	0488
Nuclear	0738
Organic	0490
Pharmaceutical	0491
Physical	0494
Polymer	0495
Radiation	0754
Mathematics	0405
Physics	
General	0605
Acoustics	0986
Astronomy and Astrophysics	0606
Atmospheric Science	0608
Atomic	0748
Electronics and Electricity	0607
Elementary Particles and High Energy	0798
Fluid and Plasma	0759
Molecular	0609
Nuclear	0610
Optics	0752
Radiation	0756
Solid State	0611
Statistics	0463
Applied Sciences	
Applied Mechanics	0346
Computer Science	0984

Engineering	
General	0537
Aerospace	0538
Agricultural	0539
Automotive	0540
Biomedical	0541
Chemical	0542
Civil	0543
Electronics and Electrical	0544
Heat and Thermodynamics	0348
Hydraulic	0545
Industrial	0546
Marine	0547
Materials Science	0794
Mechanical	0548
Metallurgy	0743
Mining	0551
Nuclear	0552
Packaging	0549
Petroleum	0765
Sanitary and Municipal	0554
System Science	0790
Geotechnology	0428
Operations Research	0796
Plastics Technology	0795
Textile Technology	0994

**PSYCHOLOGY**

General	0621
Behavioral	0384
Clinical	0622
Developmental	0620
Experimental	0623
Industrial	0624
Personality	0625
Physiological	0989
Psychobiology	0349
Psychometrics	0632
Social	0451



A DESCRIPTIVE ANALYSIS OF THE JOINT REACTION  
FORCES AND THE GROUND REACTION FORCES IN THE  
LOWER LIMB DURING THE LANDING OF A TRIPLE TOELOOP

BY

DARYL E. BOLDT

A Thesis submitted to the Faculty of Graduate Studies of the University of Manitoba  
in partial fulfillment of the requirements of the degree of

MASTER OF SCIENCE

© 1993

Permission has been granted to the LIBRARY OF THE UNIVERSITY OF MANITOBA  
to lend or sell copies of this thesis, to the NATIONAL LIBRARY OF CANADA to  
microfilm this thesis and to lend or sell copies of the film, and LIBRARY  
MICROFILMS to publish an abstract of this thesis.

The author reserves other publication rights, and neither the thesis nor extensive  
extracts from it may be printed or other-wise reproduced without the author's written  
permission.

## TABLE OF CONTENTS

ABSTRACT.....	vi
ACKNOWLEDGMENTS.....	viii
List of Tables.....	ix
List of Figures.....	x
CHAPTER 1.....	1
Introduction.....	1
Injuries in Figure Skating.....	2
Landing Forces in Figure Skating.....	3
Jumping Skill Analysis.....	4
Statement of the Problem.....	6
Hypotheses.....	6
Rationale.....	7
Limitations and Delimitations.....	7
Assumptions.....	8
Definition of Terms.....	8
CHAPTER 2.....	12
Review of Literature.....	12
Anatomy of the Lower Limb.....	12
Bones of the Foot.....	12
The Calcaneus.....	13
The Talus.....	15
The Navicular.....	16
The Remaining Tarsal and Metatarsals Bones.....	16
Bones of the Shank.....	17
Tibia.....	17
Fibula.....	20
Patella.....	21
The Thigh.....	21
Femur.....	22
Pelvic Girdle.....	24
The Innominate Bone.....	24
Ligaments.....	25
Ligaments of the Ankle.....	25
Ligaments of the Knee.....	27
Ligaments of the Hip.....	30
The Articular Capsule of the Knee.....	31
Menisci.....	32
Muscles.....	33
Ankle Joint Muscles (Table 2-1).....	34
Intertarsal Joint Muscles (Table 2-2).....	34

Knee Joint Muscles (Table 2-3).....	35
Hip Joint Muscles (Table 2-4).....	36
Ankle Biomechanics.....	37
Ankle Joint.....	37
The Subtalar Joint.....	39
Ankle and Subtalar Joints.....	40
Knee Biomechanics.....	41
Range of Motion.....	42
Surface Motion.....	43
Function of the Menisci.....	45
Hip Biomechanics.....	46
Range of Motion.....	46
Surface Motion.....	47
Force Distribution.....	47
Cinematography.....	49
Purpose of Filming.....	49
Advantages and Disadvantages of Video/Film.....	50
Direct Linear Transformations.....	52
Data Smoothing.....	53
Centre of Gravity Calculations.....	57
Force Calculations.....	58
Ground Reaction Forces.....	65
Time to Impact Peak.....	67
Medial-Lateral and Braking-Propulsion GRF.....	68
Joint Reaction Forces (JRF).....	69
Moments.....	72
Impact Loading and its Relation to Injury.....	74
Bones.....	75
Cartilage.....	84
Ligament and Tendon Injuries.....	86
Training Effect.....	88
Landing Strategies and Injury Reduction.....	89
Mechanical Aspects of Figure Skating.....	93
Force.....	93
Torques.....	95
Frictional Forces.....	97
Inertia and Moment of Inertia.....	98
Impulse - Momentum.....	99
Projectile Motion.....	102
Skating.....	104
Equipment.....	104
The Boot.....	104
The Blade.....	105
Attachment of the Blade to the Boot.....	107
Figure Skating Injuries.....	108
Overuse Injuries.....	109

Acute Injuries.....	111
Toe Loop.....	111
Jumping.....	111
Preparation.....	112
Take-Off.....	114
The Flight.....	117
The Landing.....	118
CHAPTER 3.....	121
METHODS AND PROCEDURES.....	121
Subjects.....	121
Data Collection.....	122
Camera Setup.....	122
Pilot Study.....	124
Test Procedure.....	125
Data Reduction.....	126
Setup Before Digitizing.....	126
Digitizing Process.....	128
Legend.....	131
Force Calculations.....	132
Calculation of Moments.....	142
CHAPTER 4.....	147
RESULTS.....	147
Subjects.....	147
Time Intervals of the Triple Toe Loop.....	148
Ground Reaction Forces (GRF).....	150
Subject GRF Differences.....	151
Segmental vs. CG Methods of Force Calculations.....	153
Joint Reaction Forces.....	154
Moments.....	157
Accelerations and Angles of Support Limb.....	158
CHAPTER 5.....	163
DISCUSSION.....	163
Time - Airborne Phase.....	163
Landing Pattern.....	165
Force Interpretation.....	168
Vertical Ground Reaction Forces.....	169
Horizontal Ground Reaction Forces.....	172
Joint Reaction Forces (JRF).....	175
Moments.....	180
Acceleration and Angles of the Lower Extremity.....	182
Implications - Bone.....	185
Joint Related Injuries.....	188
Ligament Injuries.....	190

Strain Injuries.....	191
Limitations and Future Considerations.....	193
CHAPTER 6.....	195
SUMMARY.....	195
CONCLUSION.....	197
RECOMMENDATIONS.....	198
REFERENCES.....	200
APPENDIX A.....	221
PERSONAL CONSENT FORM.....	222
LOCATION RECORD.....	223
SUBJECT RECORD.....	224
APPENDIX B.....	230
Digitizing Reference Frame.....	231
APPENDIX C.....	232
Linear Accelerations.....	233
Angular Accelerations.....	252
Segment Angles.....	258
APPENDIX D.....	264
Sample GRF, JRF, and Moments.....	265
Statistics for Ground Reaction Forces.....	266
Statistics for Joint Reaction Forces.....	269
Statistics for Moments.....	272
APPENDIX E.....	275
Computer Program Used to Calculate Forces and Moments.....	276

## ABSTRACT

The examination of ground and joint forces produced during jump landings is important in assessing injury risk and etiology. Testing ground reaction forces (GRF) using force platforms in normal sport settings is very difficult, due to the sophisticated instrumentation required. It is for this reason that alternate methods of calculating GRF have been developed. The inverse dynamics approach involves calculating accelerations of body segments from digitized positional film data. The subsequent placement of the acceleration values into the inverse dynamic equations allows forces and moments to be calculated at each of the joints of interest. The purpose of this study was to calculate the impact GRF, as well as the joint reaction forces (JRF), for the ankle, knee, and hip upon landing of a triple toe loop in figure skating. The magnitude of GRF and JRF in sports skills are likely related to the occurrence of acute and chronic injuries to athletes. An examination of these forces may lead to insights into the high incidence of injuries in elite figure skating. Nine subjects were filmed performing the Triple Toe Loop. Using the Peak Performance Software, the skater's positional data was analyzed in order to calculate linear and angular accelerations of each segment. The acceleration values were then placed into a series of inverse dynamic equations in order to calculate GRF (segmentally and using the entire body's CG), the JRF, and the moments of force at each joint throughout the landing of the jump. Statistically there was no difference found between the segmental method of force calculation and the force calculation using the entire body's Centre of Gravity. The peak horizontal GRF was found to be 7.013 BW, and took an average of 0.044 seconds to occur. In the vertical direction the same values were 6.482 BW and 0.045 seconds. The horizontal

JRF at the ankle, knee, and hip reached peak values of 7.040, 6.970, and 6.465 BW, while the vertical JRF values were 6.501, 6.337, and 5.703 BW respectively. The peak moment values at the ankle, knee, and hip were 76.513, 388.077, and 501.731 N·m respectively. Again, there were no statistically significant differences found between the JRF and moments at the joints of the support limb during the landing of the Triple Toe Loop. Finally, using the values obtained from the JRF calculation it is unlikely that the tissues of the lower extremity will suffer acute injury during landings. However, the combination of repeated jumping and the long hours of practice may predispose the figure skater to chronic overuse injuries.

## ACKNOWLEDGMENTS

I would like to thank my thesis committee, Dr. Cooper, Dr. Giesbrecht, and especially my advisor, Dr. Marion Alexander, for all the guidance and knowledge they have provided during the writing of this paper.

I would also like to thank the Statistical Advisory Services at the University of Manitoba for their consultations and assistance with the processing of my data. Specifically, I would like to thank Rob Platt for all his effort.

I would also like to thank Syl Lemelin, Chuck Holmes, and John Woodard for their help during the collection of my data, and specifically my parents for their continued support during the writing of this paper, and throughout my University years.

## List of Tables

Table 2-1: Ankle Joint Muscles	34
Table 2-2: Intertarsal Joint Muscles	35
Table 2-3: Knee Joint Muscles	35
Table 2-4: Hip Joint Muscles	36
Table 2-5: Joint Reaction Forces (JRF)	71
Table 2-6: Moments of Force	73
Table 2-7: Muscle Moment Arm Length	74
Table 2-8: Bone Ultimate Stress Levels	76
Table 2-9: Tendon and Ligament Ultimate Stress Levels	87
Table 4-1: Subject Height and Weight	147
Table 4-2: Subject, Jumps, Date, and Location of Research	148
Table 4-3: Time Spent in the Air	149
Table 4-4: Time Spent During Landing	150
Table 4-5: Horizontal and Vertical JRF	155
Table 4-6: Subject #6 and #8 Horizontal and Vertical JRF	157
Table 4-7: Peak Moment Values	157
Table 5-1: JRF From Previous Studies	175
Table 5-2: Moments From Previous Studies	180
Table 5-3: Calculated Pressure in Bone	186
Table 5-4: Joint Stresses	189
Table 5-5: Muscle/Tendon Stresses	192

## List of Figures

Figure 2-1: Bones of the Foot and Lower Shank	13
Figure 2-2: The Hip Joint and Surrounding Muscles	25
Figure 2-3: The Knee Joint	27
Figure 2-4: The Ankle Axis of Rotation	37
Figure 2-5: Instant Centre of Rotation (Knee)	44
Figure 2-6: Femoral Head Force Distribution	48
Figure 2-7: Digital Filtering Accuracy	56
Figure 2-8: Inverse Dynamic Force Calculation (Example 1)	60
Figure 2-9: Inverse Dynamic Force Calculation (Example 2)	61
Figure 2-10: Inverse Dynamic Force Calculation (Example 3)	63
Figure 2-11: Moments and Forces in the Lower Limb	64
Figure 2-12: Example GRF and Limb Positions	67
Figure 2-13: Medial - Lateral GRF	69
Figure 2-14: Load - Repetition Graph as Related to Injury	80
Figure 2-15: Theory of Muscle Fatigue and Stress Fractures	81
Figure 2-16: Mechanical Axes of the Tibia and Femur	83
Figure 2-17: Segmental Contributions to Force Absorption	93
Figure 2-18: Production of Torque in Figure Skating	96
Figure 2-19: The Figure Skate	108
Figure 2-20: Preparation of Triple Toe Loop	113
Figure 2-21: Take - Off of Triple Toe Loop	116
Figure 2-22: Airborne Phase of Triple Toe Loop	118
Figure 2-23: Landing of Triple Toe Loop	119
Figure 2-24: The Skate's Path During a Triple Toe Loop	120
Figure 3-1: Camera Set - Up	123
Figure 3-2: Digitizing Stick Figure	127
Figure 3-3: Force Calculation Stick Figure	133
Figure 3-4: Free Body Diagram (FBD) of Forearm - Hand Complex	135
Figure 3-5: FBD of the Head	136
Figure 3-6: FBD of the Left Lower Limb	137
Figure 3-7: FBD of the Trunk	139
Figure 3-8: FBD of the Support Limb	140

Figure 4-1: Comparison of Horizontal and Vertical Forces	151
Figure 4-2: Comparison of Horizontal and Vertical GRF Using the Segmental Method and the Centre of Gravity Method	153
Figure 4-3: Comparison of Horizontal and Vertical JRF	154
Figure 4-4: Comparison of Vertical GRF and JRF	156
Figure 4-5: Comparison of Joint Moments	158
Figure 4-6: Comparison of Shank Angles	159
Figure 4-7: Landing Positions for Three Subjects (Example 1)	161
Figure 4-8: Landing Positions for Three Subjects (Example 2)	162
Figure 5-1: Typical Horizontal GRF Curve	173
Figure 5-2: Comparison of Vertical GRF and JRF	177
Figure 5-3: Comparison of Vertical JRF	179
Figure 5-4: Single Subject Moment Curve	182
Figure 5-5: Vector Resolution of JRF	184

## CHAPTER 1

### INTRODUCTION

In order to be a successful skater at the national or international level, there are a number of requirements that must be met by the skater. The first is that the skater must be strong. The stronger the athlete, the higher the skater can jump, this will allow for more revolutions to be completed, and in turn this will increase both his/her technical merit and artistic impression scores (Podolsky, Kaufman, Cahalan, Aleshinsky, & Chao, 1990).

To reiterate, figure skating is a very demanding sport both physically and financially. In order to compete at a national level, the amount of time and work required is tremendous. Figure skating practices can last between four and six hours a day, six days a week, for many weeks. In addition, there is an off-ice training session that takes one hour and must be performed each day (Petkevich, 1984). However, according to Wright (1987), these levels of training are not necessary for the entire year. Wright's article on Brian Orser highlighted the fact that in the early part of the season the practice length is considerably shorter, and lasts approximately three hours a day. However, as competitions approach, the training time increases to 5<sup>1</sup>/<sub>2</sub> hours of on-ice training, as well as the usual one hour off-ice session that follows.

Until 1990 compulsory figures were an essential part of figure skating. These figures were a series of modified figure eights that the skater traced on the ice with his/her skate blades. However, on July 1, 1990 these figures were removed from all international competitions (Petkevich, 1989). According to Petkevich, the removal of these compulsory figures will place more emphasis on free skating, which is more athletic, more artistic, and more appealing to

the spectators.

### Injuries in Figure Skating

These rule changes may have made the sport more appealing to the spectator, and according to Smith (1990), triple and quadruple jumps are being performed at much younger ages, which may increase the chance of injury. In a previous study by Smith and Micheli (1982), it was found that young skaters do not seem to be any more prone to injury than older skaters. While the results of the two studies are contradictory, the original study by Smith and Micheli (1982) was performed before compulsory figures were removed from competition. Therefore, the findings may not be valid at the present levels of competitive skating in which all practice time is devoted to free skating.

Of all the injuries sustained in figure skating, most occur in the lower limb, particularly the feet, ankles, and other parts of the lower limb (Comper, 1990; Smith, 1990). The chance of sustaining an injury that prevents the athlete from practicing or competing ranges from 40% (Davis & Litman, 1979) up to 46.6% (Brock & Striowski, 1986) for a single year of competition.

In 1982, Smith and Micheli studied figure skating injuries and found that the average age of injured subjects was greater than the age of his/her uninjured counterparts. The average age of the injured group was 14.4 years, while the uninjured groups average age was 12.2 years. Their results also showed that average acute injury rate was 18-22% per year for competitive skaters, while the overuse injury rate was 61-78% per year. The additional finding was that the skaters had a high incidence of low back pain. Low back injuries were suspected to be related to the "repeated hyperextension of the low back and frequent jumping and landing, which are all common activities

in figure skating..." (Smith and Micheli, 1982, p. 44).

As mentioned above, the type of injury can be broken down into two groups, acute and overuse injuries. On the other hand, Brock and Striowski (1986) found that acute injuries occurred more often than overuse injuries, and surprisingly, the time of inactivity was less for acute injuries than overuse injuries. In 1990, Smith found that these two types of injuries occur in similar proportions. Furthermore, the findings of Smith (1990) may be related to the removal of the compulsory figures.

Hage (1982) studied the two types of injuries and tried to categorize the injuries by gender. His findings showed that women were more susceptible to overuse injuries, while men were more liable to sustain acute injuries. In another study, the most common overuse injury was stress fractures, and the occurrence of these injuries were similar to the occurrences found in runners (Pecina, Bojanic, and Dubravacic, 1990). The location of the most common stress fractures occur in the tibia and fibula with some occurring in the metatarsals, femur, and pelvic girdle (Sullivan, Warren, Pavlov, & Kelman, 1984; Hulkko & Orava, 1987; Markey, 1987;). Furthermore, Pecina et al (1990) believed that the occurrence of stress fractures was not rare, and should always be considered as a possibility when a skater complains of pain. In another paper, it was suggested that the torque placed on the body during figure skating jumps was great enough to tear the femur apart (Wright, 1987). With this type of information, it is surprising that there are not more acute injuries in figure skating.

#### Landing Forces in Figure Skating

Ground reaction forces (GRF) from force platform data range from 1.98 to 11.0 times body weight in related jumping skills (Valiant & Cavanagh,

1985; Ricard & Veatch, 1990; Dufek & Bates, 1991). These forces produce a force time curve with two distinct peaks, the first peak represents toe contact while the second represents heel contact. The wide range of differences in the GRF is due to the height of the jump. As the height of the jump increases, so does the peak force at toe and heel contact (Bobbert, Huijing, & van Ingen Schenau, 1987). Therefore, as the jumps in figure skating become more difficult, the height of the jump must increase, and the chance of injury increases because of the increased forces at landing.

One problem associated with figure skating that makes force platform data collection impossible, is the inability to use a force platform. The reason this is not feasible is the difficulty of trying to mount the platform in or on the ice and to provide a substance to cover the platform that resembles the characteristics of ice. Furthermore, the covering must be flexible enough to allow the forces to be transferred to the force platform, and strong enough to resist being cut by the skaters skate blade. It is for this reason that a video filming technique will be used to record positional data, and inverse dynamics will be used to estimate GRF.

### Jumping Skill Analysis

In a number of studies (Denoth, Gruber, Ruder, & Keppler, 1984; Abraham, 1987; & Kennedy, Wright, & Smith, 1989), it has been shown that video film studies are as accurate as high speed filming techniques. The two disadvantages of video taping events are the reduced clarity and accuracy (Denoth et al, 1984). However, Higgs (1984) showed that jumping skills can be accurately digitized and produce meaningful results at speeds of 64-100 frames per second. The filming speed of this study (60 frames/second) will be close to the lower end of these two values, but is expected to produce accurate results.

Finally, other studies (Bobbert, Schamhardt and Nigg, 1991; Lamb and Stothart, 1978; & Roberts, 1970) have shown that film data can provide accurate representations of the GRF that are present during contact with the ground.

Since force platforms are unusable, an alternative method must be used if a study of the impact forces of figure skating jump is to be undertaken. Therefore, using video analysis techniques is useful in order to calculate forces which, in turn, may help to reduce the chance of injury, inform the coaches of the risk of repeated jumps, and aid in the rehabilitation of injuries.

## Statement of the Problem

The purpose of this study is to provide a two dimensional description of the moments and forces that occur in the muscles and joints of the lower limb during the landing of the triple toe loop. Furthermore, the ground reaction forces will also be calculated from the film data.

## Hypotheses

The greatest force will be located in the ankle, with a gradual decrease as the forces are transmitted from the ankle upwards to the hip (Brown, Abani, Usman, 1986). Second, the forces that are present in the lower limb of the skater will be similar to those of other sports where landings from jumps occur. Third, the forces calculated will exceed the forces required to fracture bone and damage muscle tissue of a normal subject, however, due to the strength, young age, and training of the competitive skater, there will be less of a chance that damage will occur to these tissues (Tipton & Vailas, 1990).

## Rationale

Over the last few years, the number of jumps and difficulty of these jumps has increased considerably. As a result, there has been a corresponding increase in the number of injuries to figure skaters (Smith, 1990). There has been no scientific research describing the impact forces, there is a need for further research in this area of figure skating to determine what the forces are, and if the torques are, in fact, great enough to fracture the femur or tibia (Wright, 1987). This information may provide further insight into preventing injuries and provide a basis for new or improved training methods. Moreover, the information found in this study may have an effect on the time spent in training. Finally, since all the figure skating studies to date have calculated the forces at take-off in figure skating, a study of the landing forces is required in order to obtain an overall understanding of the stresses placed on the body during a triple toe jump.

## Limitations and Delimitations

- 1) The forces will not be measured directly, rather they will be calculated from the film data. Errors present during the analysis section may be enhanced due to the relatively slow filming speed, digitization errors, perspective errors, errors in identifying anatomical landmarks (Robertson & Sprigings, 1987), and the subsequent double differentiation of the positional data. Therefore, the force calculations will not be the actual forces present in the muscles and bones of the figure skater, but instead they will be estimates of the actual forces.

- 2) To date, most of the body mass, centre of gravity, and inertia experiments have been performed on cadavers, and as a result the values obtained may not be applicable to young athletes. One reason for this is the between subject variability, and second, most cadaver studies are performed on elderly subjects, and as a result, the values may be considerably different from the young athletes.
- 3) Muscle force calculations will be representative of the net muscle force. The resulting muscle moment does not take into consideration the muscular force produced by antagonistic muscles groups (Gagnon, Robertson & Norman, 1987).
- 4) The subject group will be regional skaters who are able to perform the triple toe loop and therefore, the results may not be generalizable to all skaters, but just those of this caliber.

### Assumptions

- 1) The muscles acting across a joint, performing one movement, will be considered as a single muscle for the calculation of forces. The problem with this type of assumption is that the forces calculated may be beyond the limits of an individual muscle, but because there is more than one muscle producing the movement, these muscles may act together to help produce and absorb some of the forces (Procter & Paul, 1982; Zajac & Gordon, 1989).

### Definition of Terms

Back Inside Edge - The subject is skating backward and has his/her weight on

the inside (medial) edge of the skate. (May, 1980).

Back Outside Edge - The subject is skating backward and has his/her weight on the outside (lateral) edge of the skate. (May, 1980).

Centre of Gravity - "The total effect of the force of gravity on a whole body, or system, is as if the force of gravity were concentrated at a single point..." (Kreighbaum & Barthels, 1985, p. 70). The centre of gravity is not a fixed spot, but is dependent on the arrangement of the segments and their relative masses.

Digitizing - this process is most frequently used " ... to convert the location of body markers on the projected image of a film into numbers that can be processed by a computer." (Rodgers & Cavanagh, 1984, p. 1898)

Direct Linear Transformation (DLT) - This is a three dimensional reconstruction of two planar camera views with the use of a sturdy three dimensional calibration structure (Wood & Marshall, 1986)

Edges - Petkevich (1984) defines an edge as follows:

The two razor-sharp sides of the hollow of the blade; when skaters lean, they "take an edge"; edges and radius make skating a circle possible; there are forward and backward inside and outside edges; a skater spends 99.9 percent of the time on edges. (p. 136).

Front Inside Edge - The subject is skating forward and has his/her weight on the inside (medial) edge of the skate. (May, 1980).

Front Outside Edge - The subject is skating forward and has his/her weight on the outside (lateral) edge of the skate. (May, 1980).

Moment arm - is the perpendicular distance from the line of action of the force to the axis of rotation of the segment (Nordin & Frankel, 1989).

Moment of Inertia - The resistance of a body to change in its angular motion. The moment of inertia takes into consideration the mass of the body and how this mass is distributed around an axis of rotation. The representation of this quantity is described in the equation  $I = m r^2$  where (r) is the distance the mass (m) is from the axis of rotation (Hay, 1985).

Noise - "Error present in data collected that is unrelated to the process being studied. Some noise is almost always present in data collected in biomechanics and most other fields. Some typical examples are noise caused by human error in digitizing film, electrical interference in EMG, or mechanical vibration in a force platform. Noise may be random or systematic, and different techniques must be used to eliminate different kinds of noise." (Rodgers & Cavanagh, 1984, p. 1893)

Scaling Factor - This is a value obtained from an object of known length that represents a ratio of the actual size and the size in screen pixal units. This ratio is then used to convert the digitized screen units to real life units (Peak Performance Technologies, 1992).

Smoothing - The elimination of data scatter that arises from experimental error. This provides the researcher with "the simplest representation of the data that adequately describes the underlying process." (Wood, 1982, p. 310).

Toe Loop - This jump is a figure skating jump that uses the free lower limb to assist in the jumping action. The jump consists of a right back outside edge at take-off, a left toe assist, the number of rotations required, and a landing on a right back outside edge. This is the easiest of the toe jumps (Petkevich, 1990).

## CHAPTER 2

### REVIEW OF LITERATURE

#### Anatomy of the Lower Limb

The anatomy section will contain a brief overview of the main connective tissues found in the lower extremity of humans. The main tissues will include the bones, ligaments, muscles, and cartilage. However, due to the large number of tissues involved, and the scope of this paper, the descriptions of most tissues will be short, and will provide only a brief overview of the tissues involved.

#### Bones of the Foot

The foot consists of 26 bones, of which there are seven tarsal bones; the medial, intermediate, and lateral cuneiforms, the cuboid, navicular, talus, and calcaneus, whose role is to support and distribute the body's weight (Williams, Warwick, Dyson, & Bannister, 1989). The most important of these bones, related to this paper, are the calcaneus, talus and navicular. In normal heel walking, the calcaneus comes into contact with the ground first. Above the calcaneus rests the talus, which in turn supports the tibia and fibula, and articulates with the malleoli. Anteriorly, the surface of the talus articulates with the navicular (Williams et al., 1989).

Figure 2-1, located below, is a drawing of the shafts and distal ends of the tibia and fibula, as well as all the bones of the foot.

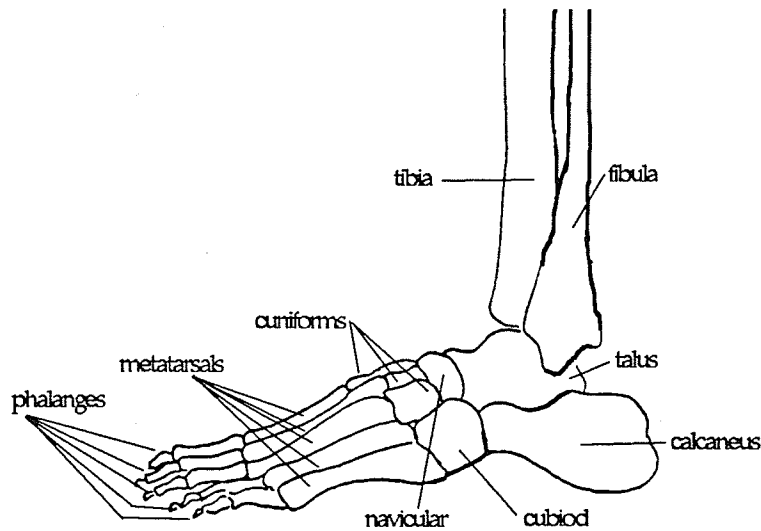


Figure 2-1 - The bones of the foot and distal half of the shank. The combination of these bones produce the ankle joint (modified drawing from Warfel, 1985, p. 100).

### The Calcaneus

The calcaneus is the largest of all the tarsal bones, and projects posteriorly to produce the heel (Moore, 1985) and thus produces a short lever for the posterior muscles of the calf (Williams et al., 1989). The calcaneus has the shape of an irregular cube (Williams et al., 1989).

The superior surface of the calcaneus can be divided into three distinct sections- posterior, middle, and anterior. The posterior third is convex mediolaterally and concave anteroposteriorly. This section is nonarticular, but instead is covered with fibroadipose tissue. This layer of tissue provides a barrier between the calcanean tendon and the ankle joint, keeping the two structures separated. The middle third is articular, is oval and convex in shape. The articular surface is called the posterior talar facet which provides support for the talus. The anterior third of the calcaneus consists of two articular surfaces for the talus, the anterior articular surface and the middle articular surface. Between the posterior talar facet and the two anterior facets

is a rough depression, the sulcus calcanei, which narrows medially (Williams et al., 1989).

Anteriorly the surface of the calcaneus is the smallest and is concavoconvex. This surface is orientated obliquely and articulates with the cuboid (Williams et al., 1989).

The posterior surface of the calcaneus, like the superior aspect, can be divided into three sections, superior, middle, and distal. Between each surface is a distinct line that acts as a border, separating the sections. The superior segment is separated from the middle by a groove, while the distal separator is a rough ridge. The superior surface is covered with adipose tissue, the middle section is the attachment site of the calcaneal tendon, and the distal surface supports the weight of the body (Williams et al., 1989).

The plantar surface is rough. The calcanean tuberosity is located posteriorly and consists of a long and broad medial process and a shorter, narrower lateral process. Between the two processes is a notch, which acts as a separator between the weight bearing surfaces. At the extreme anterior aspect of the plantar surface is a tubercle which is the attachment site of the short plantar ligament (Williams et al., 1989).

The lateral surface is almost completely flat with the exception of two small tubercles. The first tubercle is palpable two centimeters distal to the lateral malleolus, while the second tubercle is located one centimeter above and behind the first. The first tubercle is grooved, providing passage for the peroneus longus and peroneus brevis tendons, and the second is the attachment site of the calcaneofibular portion of the lateral ligament (Williams et al., 1989).

Medially, the calcaneal surface is concave, with the sustentaculum tali forming a superior process which further increases the concavity. On the

superior surface of the sustentaculum tali is the middle talar facet, and inferiorly there is a groove for the tendon of the flexor hallucis longus muscle. The sustentaculum tali is also an attachment site for ligaments and tendons (Williams et al., 1989).

### The Talus

The shape of the talus is the key to proper movement at the ankle (Williams et al., 1989). According to Williams et al. (1989), the "...rounded head, proximal trochlear surface for the tibia, facet for the lateral malleolus, and its neck and body are its main features." (p. 449).

The head of the talus is directed inferiorly and medially to articulate with the proximal surface of the navicular. The head of the talus is oval and convex, with the plantar surface having three articulating surfaces. The posterior surface rests on the sustentaculum tali, while the proximal anteromedial surface rests on the dorsal surface of the calcaneus and distally becomes continuous with the navicular surface. Medially, the head is covered by articular cartilage and is continuous with the calcaneonavicular area. The medial portion of the talar head is also in contact with the plantar calcaneonavicular ligament (Williams et al., 1989).

The neck of the talus is narrower than the head and body, has a rough surface inferiorly for ligament attachment and is inclined medially. When the talus and calcaneus are articulated, the inferior aspect of the neck forms the ceiling for the sinus tarsi, which contains the interosseous talocalcaneal and cervical ligaments (Williams et al., 1989).

The talar body is cuboidal; the superior surface is convex and articulates with the distal end of the tibia. The plantar surface has an oval concave surface which articulates with the calcaneus. The medial surface is rough

with many vascular foramina, while the proximal portion of this surface is covered by a comma-shaped facet that extends posterosuperiorly, articulating with the medial malleolus of the tibia. Finally, the lateral surface is vertically concave, smooth, triangular, and articulates with the lateral malleolus of the fibula (Williams et al., 1989).

The posterior surface of the talus is for the attachment of ligaments and consists of the medial and lateral tubercles. According to Williams et al (1989), the medial tubercle is the attachment site of the talocalcanean ligament and the superficial fibres of the deltoid ligament, while the lateral tubercle is void of ligament or tendon attachments. Between the medial and lateral tubercles is a groove that contains the tendon of the flexor hallucis longus and is the attachment site of the talofibular ligament.

#### The Navicular

This bone is sandwiched between the head of the talus and the cuneiform bones. The distal surface is transversely convex and is divided into three facets, each articulating with a different cuneiform bone. The proximal surface is concave, oval, and articulates with the head of the talus. The medial surface is rough and has a large tuberosity which is the main attachment of the tibialis posterior tendon. Laterally, the navicular is rough, irregular in shape, and often has an associated facet that articulates with the cuboid (Williams et al., 1989).

#### The Remaining Tarsal and Metatarsals Bones

The cuboid bone is located on the lateral aspect of the tarsus and forms a saddle-shaped joint with the calcaneus. This joint allows for moderate range of motion. The cuboid also articulates medially with the navicular and

the lateral cuneiform bone. The surfaces between the latter two bones and the cuboid are flat, providing limited movement. The remaining tarsal and tarso-metatarsal joints are all flat, and therefore, provide very little motion. The tarsal joints are formed between the lateral, intermediate, and medial cuneiforms, and the cuboid bone. The tarso-metatarsal joints are formed between the five metatarsal bones and the distal ends of the lateral, intermediate, and medial cuneiforms, and the cuboid bone. Beyond the metatarsals are fourteen phalanges (Romanes, 1986).

### Bones of the Shank

The shank "...is the part of the lower limb that is located between the knee and ankle joints" (Moore, 1985, p. 464). Two bones form the shank - the tibia and fibula. The tibia, on the medial aspect of the shank, bears most of the weight, articulating proximally with the femoral condyles and distally with the talus. The fibula, on the lateral aspect of the shank, articulates proximally with the tibia, and distally with the talus. The main functions of these bones are to provide stability to the ankle joint and attachment of muscles. The tibia and fibula are held together by a strong set of fibers known as the interosseous membrane (Moore, 1985).

### Tibia

The tibia is the second longest bone in the body and can be subdivided into three sections, the proximal, shaft, and distal regions (Williams et al., 1989). The distal end is smaller than the proximal, with facets for the talus and fibula. The shaft is triangular in cross-section, and the proximal end is large, with an almost flat superior surface (Moore, 1985).

The distal end of the tibia has five sides, anterior, posterior, medial,

lateral, and distal and a process known as the malleolus. The anterior surface is continuous with the lateral surface of the shaft and bulges beyond the edge of the distal surface. The medial surface is smooth, and continuous above and below with the medial surfaces of the shaft and malleolus respectively. The entire medial surface is completely subcutaneous. The posterior surface is smooth and continuous with the posterior surface of the shaft. The lateral surface is triangular and known as the fibular notch. This portion of the tibia is bound to the fibula by a ligament, with the raised posterior and anterior edges of the fibular notch converging superiorly to form the interosseous border (Williams et al., 1989).

Because the tibial shaft is triangular in cross-section it has medial, interosseous (lateral), and posterior surfaces. Each surface is separated from the others by distinct borders known as the anterior, lateral, and medial borders (Williams et al., 1989). The anterior border is subcutaneous and extends from the medial malleolus distally to the tibial tuberosity proximally. The interosseous border starts immediately below and anterior to the superior tibiofibular joint and extends distally to the anterior border of the fibular notch. This border is the attachment site of the interosseous membrane, which ties the tibia to the fibula. Finally, the medial border extends from the anterior aspect of the medial condyle to the posterior margin of the medial malleolus (Williams et al., 1989). The surfaces are easy to distinguish because of the distinct shape and prominence of the borders. The medial surface lies between the anterior and medial borders, it is smooth, broad and almost entirely subcutaneous. The lateral surface is broad, smooth, transversely convex, and located between the interosseous and anterior borders. The lateral surface faces laterally in the proximal three-fourths, and rotates anteriorly in the distal fourth. Finally, the posterior surface is located

between the interosseous and medial borders. This surface is widest proximally and narrows distally (Williams et al., 1989).

The proximal end of the tibia is a large, flattened area with two large articular condyles. The superior surface of the tibia is tilted slightly backward and has two flat surfaces, known as tibial plateaus, separated by the intercondylar area (Moore, 1985). The plateaus are not completely flat but in fact have a slight concavity. While both tibial plateaus are concave, their shapes are different. The medial condyle is oval in the anteroposterior direction with the deepest portion being lateral to the centre of the plateau. The lateral plateau is more circular, with the deepest portion of the concavity being more central. The differences in the tibial plateaus correspond directly to the differences between the femur condyles (Williams et al., 1989).

Between the two plateaus lies a raised bony structure known as the intercondylar area and the edges of this area form the borders of the tibial condyles. This bony structure is narrow in the middle and widens anteriorly and posteriorly. The intercondylar area is non-articular and is therefore non-weight bearing (Williams et al., 1989). This area is rough, and narrowest centrally, projects proximally and produces lateral and medial tubercles. These tubercles are the attachment sites of the anterior and posterior cruciate ligaments (Williams et al., 1989)

Proximal to the shaft, but below the tibial plateaus, is a prominent tuberosity known as the tibial tuberosity. The distal section of the tibial tuberosity is rough, subcutaneous, and is the attachment site of the patellar ligament. The proximal section of the tibial tuberosity is smooth. The distal section is level with the neck of the fibula, while the proximal is level with the head of the fibula (Moore, 1985).

## Fibula

The fibula is a long, thin bone on the lateral side of the shank posterolateral to the tibia. This bone has a very slender shaft which provides for little or no function in weight bearing. The main function of the fibula is to support the tibia, enabling it to bend and twist without fracturing. The other two functions of the fibula are for attachment of muscles and maintenance of the talus in its socket (Moore, 1985).

The distal end of the fibula extends further distally and more posterior than the tibia forming "... a knob-like subcutaneous prominence on the lateral surface of the ankle" (Moore, 1985, p. 465). The lateral aspect is subcutaneous, the anterior aspect is rough, rounded, and continuous with the tibia's inferior border, while the medial border forms a triangular articular facet for the talus, and is vertically convex (Williams et al., 1989).

The shaft of the fibula, like the tibia, has three borders and three surfaces. The three borders are the anterior, posterior, and interosseous. The anterior border extends from the anterior aspect of the lateral malleolus to the anterior aspect of the fibular head. The posterior border is continuous with the medial margin of the lateral malleolus to the anterior aspect of the fibular head. The interosseous border is medial to the anterior border, and usually more posterior, however, the proximal third of the border approaches the anterior border, coming within one millimeter or less of each other (Williams et al., 1989).

The head of the fibula is slightly expanded, projecting forward, behind and lateral to the shaft. There is a round facet on the proximomedial aspect which articulates with the lateral aspect of the tibial condyle. On the posterolateral aspect there is an apex that extends proximally and is palpable two centimeters distal to the knee joint (Williams et al., 1989).

## Patella

The patella is a sesamoid bone embedded in the quadriceps femoris tendon, composed mainly of dense trabecular bone surrounded by a thin lamina of compact bone (Williams et al., 1989). The patella is subcutaneous and its posterior surface articulates with the femur (Moore, 1985), however, it does not articulate with the tibia (Nordin & Frankel, 1989). The function of the patella is to increase the strength of the quadriceps femoris by increasing the muscles' leverage (Moore, 1985).

The general shape of the patella is triangular with the base orientated proximally and the apex distally. The proximal border is thick, sloped forward, and slightly curved. The medial and lateral borders are thinner and converge to form the apex. The anterior surface of the patella is convex, covered by the continuation of the quadriceps femoris tendon, and is continuous with the ligamentum patellae. The posterior surface is flat, smooth, and oval crossed by a smooth vertical ridge. This surface articulates with the patellar surface of the femur and the patellar groove, and the vertical ridge separates the articular area into medial and lateral surfaces, each articulating with its corresponding groove on the femur (Williams et al., 1989).

## The Thigh

The thigh extends from the hip joint distally to the knee joint and represents approximately one fourth of a person's overall height (Moore, 1985). This section of the lower extremity contains only one bone, the femur.

## Femur

"The femur (thigh bone) is the longest, strongest, and heaviest bone in the body" (Moore, 1985, p. 403). It consists of three distinct sections: the first is the proximal end, consisting of the head, neck, greater and lesser trochanters; the second is the shaft; and the third is the distal end, which forms two condyles that articulate with the tibia (Williams et al., 1989).

The distal end is broader than the shaft and consists of two large eminences, called condyles. This section of the bone is important for articulation with the tibia and patella, as well as for transfer of body weight from the femur to the tibia and ground reaction force from the tibia to the femur (Williams et al., 1989).

The distal articular surface of the femur is U-shaped, with the open end of the U facing posteriorly. This open end is known as the intercondylar fossa, and is the attachment site of the anterior and posterior cruciate ligaments. This fossa also provides space for the intercondylar eminence. The closed anterior surface is slightly concave transversely and convex vertically providing an articular surface for the patella. The grooved surface is speculated to stop lateral patellar dislocations (Williams et al., 1989).

The long axes of the condyles are not parallel but converge posteriorly with the medial condyle jutting out further than the lateral condyle (Kapandji, 1987). The lateral condyle is large, laterally flat, in line with the femoral shaft, and therefore, transmits more weight to the tibia than the medial condyle. The most prominent structure of the lateral condyle is its epicondyle, which is the site of attachment of the fibular collateral ligament (Williams et al., 1989).

The medial condyle projects further distally than the lateral condyle, however, this is only noticeable when the femur is disarticulated and held

vertically (Wells & Luttgens, 1976). As noted by Williams et al. (1989), the profile of the distal end of the condyles is almost horizontal as a result of the difference in length between the medial and lateral condyle, and because of the natural tilt of the femur. Finally, the summit of the medial condyle forms the medial epicondyle which is the attachment site of the medial collateral ligament (Williams et al., 1989).

The shaft is the section of bone that extends from the head and neck distally to the condyles. The shaft is almost completely cylindrical, and is bowed forward. The shaft is completely surrounded by muscles, and as a result is completely impalpable. The only structural differences between the sides are that the lateral surface is augmented to withstand the compressive forces placed on this section by the anterior curvature of the shaft; and the posterior surface is triangular in shape (Williams et al., 1989).

The head of the femur is spherical in shape and is covered with articular cartilage. However, there is one place on the femoral head that does not have cartilage, this is a depressed area that is the attachment point of the ligament of the head of the femur. This ligament is entirely covered by a synovial membrane, supplies blood to the head of the femur, but provides no mechanical support to the hip (Romanes, 1986).

The neck of the femur is smaller in diameter than the head; it joins the head to the shaft of the femur. The neck forms two angles between the head and the shaft of the femur. The first angle, the neck to shaft angle, is that formed between the long axis of the neck and the long axis of the shaft of the femur. The normal neck-to-shaft angle is  $125^{\circ}$ . The second angle, the angle of anteversion, forms a  $12^{\circ}$  angle between the long axis of the head and transverse axis of the two femoral condyles (Nordin & Frankel, 1989). According to Nordin and Frankel (1989), these angles provide the hip with

the large range of motion present at the joint.

The greater and lesser trochanters mark the end of the neck of the femur and the start of the shaft. These two structures are prominent processes of bone that are the attachment site of many muscles. These trochanters provide the muscles with leverage to perform the tasks they are required to execute (Williams et al., 1989).

### Pelvic Girdle

The hip joint is formed by four bones, three from the pelvic girdle and the fourth bone is the femur. The three bones of the pelvic girdle are the ilium, ischium, and pubis which are fused to form the innominate bone (Williams et al., 1989).

### The Innominate Bone

As mentioned above, the innominate bone consists of three fused bones. In the area where all three of these bones are fused is a cavity known as the acetabulum. This concave structure is the site of articulation with the femoral head. The acetabulum itself does not face directly laterally, but instead faces "...obliquely forward, outward, and downward." (Nordin & Frankel, p. 135, 1989). The entire surface of the acetabulum is covered with articular cartilage which becomes thicker close to the perimeter of the cavity (Nordin & Frankel, 1989).

Attached to the rim of the acetabulum is a ring of fibrocartilage called the labrum. The function of this structure is to deepen and reduce the size of the acetabular opening. The labrum fits snugly on the head of the femur, tilts slightly inward and thereby seals the femoral head into the acetabulum (Romanes, 1986).

Figure 2-2 provides an example of the hip joint including the acetabulum, labrum, and femur.

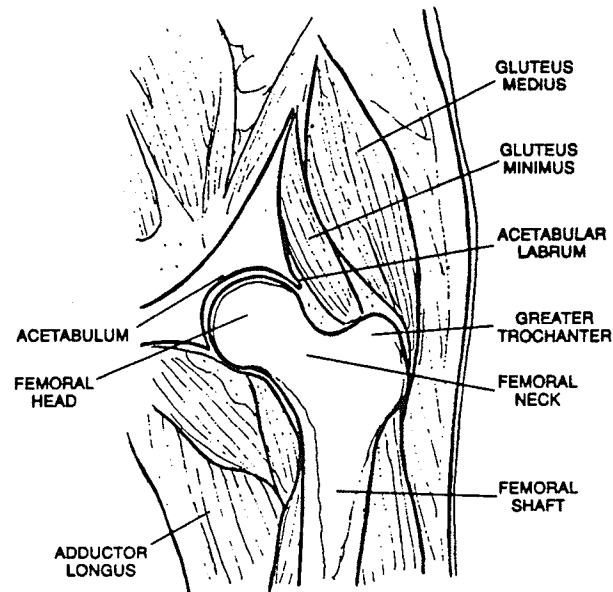


Figure 2-2 - a representation of the hip joint, including the innominate bone, femur, and some of the associated muscles (Nordin & Frankel, p. 136, 1986)

## Ligaments

There are too many ligaments in the lower limbs to describe each separately, and to do so is beyond the scope of this paper. Therefore, in order to keep the description simple, only the ligaments that resist excessive motion in each of the ankle, knee, and hip joints will be described as they pertain to this paper.

### Ligaments of the Ankle

According to Williams et al. (1989), the lateral aspect of the ankle

contains three main ligaments. The first of these is the anterior talofibular ligament. This ligament extends from the anterior margin of the lateral malleolus forward, and medially to the neck of the talus. The purpose of this ligament is to prevent forward displacement of the talus and to limit plantar flexion. The second lateral ligament is the calcaneofibular ligament. This ligament is described as being long, narrow, and rounded, passing from the tip of the lateral malleolus posteriorly and inferiorly to a tubercle on the lateral surface of the calcaneus. The purpose of this ligament is to prevent displacement in all directions and to limit dorsiflexion. The last lateral ligament is the posterior talofibular ligament and its fibers are orientated almost completely horizontally. This ligament originates on the upper and posterior surface of the lateral malleolus, and attaches to the lateral tubercle on the posterior surface of the talus. The ligament prevents posterior displacement of the foot and deepens the cavity for the talus (Williams et al., 1989).

On the medial side of the ankle is a strong triangular-shaped ligament called the deltoid ligament. The ligament is attached to the apex, anterior, and posterior borders of the medial malleolus, and has four distal connection sites. There are three parts to the superficial fibers, all attaching at different locations. The first distal attachment point for this ligament is the navicular tuberosity and the plantar calcaneonavicular ligament. The middle portion descends distally and attaches to the sustentaculum tali of the calcaneus. The posterior section passes back and laterally to connect to the medial tubercle of the talus. The deep fibers pass from the apex of the medial malleolus to the non-articular surface of the medial talar surface (Williams et al., 1989).

The plantar calcaneonavicular ligament is attached to the anterior margin of the sustentaculum tali and to the plantar surface of the navicular.

The ligament is a broad, thick band of tissue and performs some of the same functions as the deltoid ligament. The second function of the plantar calcaneonavicular ligament is to tie the calcaneus to the navicular, and sustains the foot's medial longitudinal arch (Williams et al., 1989).

### Ligaments of the Knee

The strength of the knee joint is a direct result of the soft tissue found around the knee (Romanes, 1986). There are five major ligaments in the knee joint, they are 1) the lateral collateral ligament (LCL), 2) the medial collateral ligament (MCL), 3) the anterior cruciate ligament (ACL), 4) the posterior cruciate ligament (PCL), and 5) the ligamentum patellae. Each of these ligaments will be discussed in more detail below.

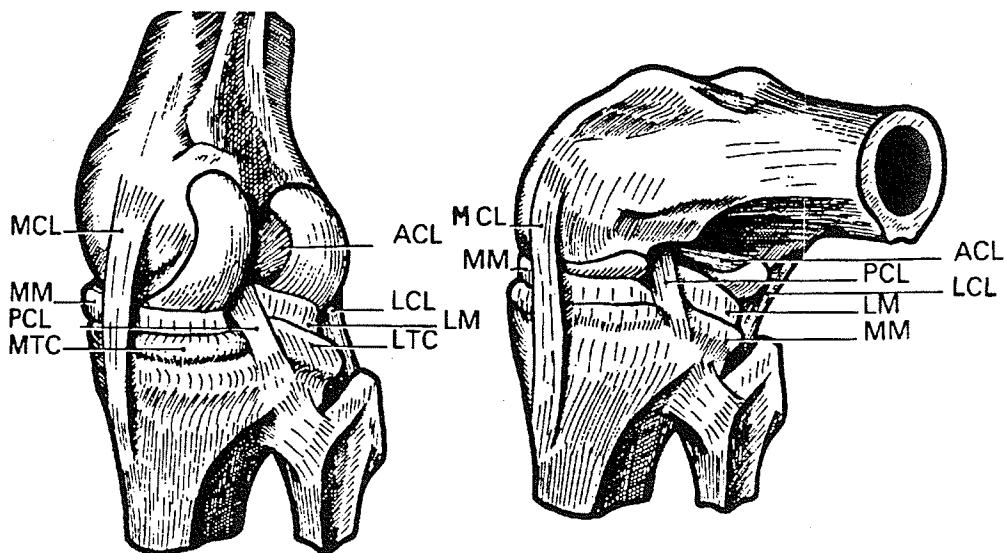


Figure 2-3 - A graphic representation of the ligaments and menisci in the knee joint as presented by Kapandji (1987, p. 95).. The medial and lateral menisci are MM and LM respectively and MTC and LTC represent the medial and lateral tibial condyles.

The MCL originates on the medial epicondyle of the femur and descends to the point where fibres from the adductor magnus integrate with the ligament. After joining with the fibers of the adductor magnus, the MCL splits into a superficial and a deep layer. The superficial layer continues inferiorly to insert on the medial surface of the tibia above the insertion of the sartorius, gracilis, and semitendinosus muscles. The deep layer continues inferiorly and attaches to the medial meniscus and inserts on the medial tuberosity of the tibia (Romanes, 1986).

The LCL "is a round, pencil-like cord" (Moore, 1985, p. 526) that extends from the lateral epicondyle of the femur and attaches to the lateral surface of the fibular head (Moore, 1985). The LCL is separated from the lateral meniscus by the tendon of the popliteus muscle, and splits the tendon of the biceps femoris muscle into two parts. Superiorly, the ligament is fused with the capsule of the knee joint, while inferiorly it is separated from the capsule by a fatty deposit of tissue (Moore, 1985).

The functions of the medial collateral ligaments are to prevent lateral displacement of the knee, to check extension (Wells & Luttgens, 1976), and prevent rotation throughout the range of motion (Morrison, 1970). The lateral collateral ligament also checks extension, but it also prevents medial displacement (Wells & Luttgens, 1976) and prevents lateral rotation of the knee when the knee joint is extending (Morrison, 1970).

The ACL is a narrow band of tissue that originates on the posteromedial aspect of the lateral condyle of the femur and extends inferiorly and anteriorly to attach on the anterior intercondylar area of the tibia. Distally the ACL fans out and forms an oval attachment site on the tibia. As a result of the fanning, and the large range of flexion and extension at the knee, the ligament twists upon itself during flexion. The fanning of the

ligament also places the ligament fibers at different angles to each other and, as a result, during flexion and extension the fibers of one part of the ligament will be under tension, while other sections will be under different amounts of tension. Furthermore, all the fibers of the ACL are under tension in full extension of the knee, making the ligament easily susceptible to failure in hyperextension (Dye and Cannon, 1988). Finally, according to Romanes (1986), the ACL acts to prevent anterior displacement of the tibia with reference to the femur.

The name of the PCL comes from its posterior attachment to the tibia. In order to further define the position of this attachment, Van Dommelen and Fowler (1989) describe the position as being located near the longitudinal axis of rotation of the femur and just medial to the centre of the knee. The orientation of the fibres at the distal attachment is such that the fibres run antero-posteriorly. The ligament extends vertically and anteriorly to attach to the medial femoral condyle's lateral surface (Romanes, 1986). The proximal attachment of the ligament is similar to that of the ACL in that it forms a semicircle, with the superior fibers running in a near horizontal direction and the inferior fibers in line with the articular surface of the femoral condyles (Van Dommelen & Fowler, 1989). The anterior fibres of the PCL are taut in flexion and lax in extension, while the posterior fibers are taut in extension and lax in flexion (Van Dommelen & Fowler, 1989). The purposes of this ligament are to aid in the "screw-home" mechanism of the knee, prevent excessive medial rotation of the tibia (Van Dommelen & Fowler, 1989), and to prevent posterior displacement of the tibia on the femur (Romanes, 1986).

According to Van Dommelen and Fowler (1989), there are three main reasons for injury and failure to the PCL, they are: "1) hyperextension of the

knee, 2) hyperflexion of the knee, and 3) posterior displacement of the tibia on the femur with the knee in flexion." (p. 26).

The final ligament of interest is the ligamentum patellae. This ligament is continuous with the extensor muscles of the knee and is a strong, flat ligament that extends from the apex of the patella to the tibial tuberosity (Moore, 1985). The ligamentum patellae is primarily responsible for the extension of the knee joint, in conjunction with the knee extensor muscles. A second function of this ligament is to maintain the position of the patella in front of the knee joint (Romanes, 1986). According to Romanes (1986), the ligament itself is not responsible for the extension of the knee or the positional maintenance of the patella. Instead the ligamentum patellae is controlled by the attachment of the extensor muscles to the patella, the attachment of the extensor muscles to the ligament itself, and by the bony structures of the knee. For example, the patella is held in position by the bony contact between the patella and femur, and by the attachment of the vastus medialis tendon fibers to the ligamentum patellae (Romanes, 1986).

### Ligaments of the Hip

While the ball and socket configuration of the hip forms a fairly secure joint, there are other structures that help maintain the femur in the acetabulum during motion. In the hip there are five major ligamentous structures holding the joint together.

The articular capsule is the first of these structures. The capsule surrounds the entire joint, with a majority of its fibers running obliquely from the acetabulum to the femur. These fibers are extremely strong anteriorly, and provide great strength in this region. The remainder of the fibers in the capsule encircle the capsule and run parallel to the border of the

acetabulum and are relatively weak (Romanes, 1986).

The iliofemoral ligament, located on the anterior aspect of the joint, is the strongest of all the hip ligaments. Its proximal attachment is to the anterior inferior iliac spine, and its distal attachment is to the intertrochanteric line of the femur. The ligament fans out distally, giving it the appearance of an inverted "Y". This ligament is so strong that it can prevent the body from falling back upon itself, without the help of active muscle control (Romanes, 1986).

The ligament of the head of the femur forms a secure bridge of fibers from the acetabulum to the head of the femur. The function of this structure is to transmit blood vessels and nerves from the pelvic girdle to the head of the femur and to prevent displacement of the femur (Romanes, 1986).

The other two ligaments are the pubofemoral, which is attached to the pubis and femur, and the ischiofemoral, which is attached to the ischium and femur. Romanes (1986) described both ligaments as being relatively weak, however, they function to support, and increase the strength of the fibrous capsule.

### The Articular Capsule of the Knee

This fibrous capsule is thin posteriorly, however, it becomes thicker and shorter on the sides. In front of the knee joint the capsule is replaced by the ligamentum patellae, patella, and the tendon of the quadriceps femoris (Romanes, 1986). The capsule is also fairly strong, increasingly so where it becomes continuous with local ligaments (Moore, 1985).

The posterior fibres of the capsule are orientated vertically, and attach to the proximal surface of the femoral condyles, the posterior margins of the

tibial condyles, and the intercondylar area. The medial fibres of the capsule blend with the medial collateral ligament and attach to the femoral and tibial condyles, and medial meniscus. The lateral fibres attach to the femoral condyles, above the popliteus tendon, down to the tibial condyle and head of the fibula. Anteriorly, the capsule does not extend above the patella or over the patella, instead it blends with the expansions of the vasti medialis or lateralis (Moore, 1985).

### Menisci

The femur and tibia are separated by two semilunar fibrocartilage structures known as the menisci. The menisci have thick, convex peripheral borders, thin concave free borders, and are crescentic. The menisci cover two-thirds of the tibial surface and deepen the articulating surfaces of the tibia that receive the femoral condyles (Williams et al., 1989). The shape of the lateral meniscus is nearly circular, while the medial meniscus is oval and elongated anteroposteriorly (Romanes, 1986).

The lateral meniscus forms four fifths of a circle, is uniform in breadth, and covers a larger area than the medial meniscus. The anterior portion of the meniscus is attached to the tibia's intercondylar eminence, while the posterior portion is attached to the intercondylar area anterior to the medial meniscus. Three other attachment sites for the lateral meniscus are the anterior and/or posterior menisiofemoral ligament and the popliteus muscle (Williams et al., 1989).

The medial meniscus is semi-circular, broader behind, with its anterior end attached to the tibial condyle in front of the attachment of the anterior

cruciate ligament. The posterior fibres are continuous with the transverse genual ligament, and the posterior end is attached to the posterior tibial intercondylar area. The peripheral border is also attached to the fibrous capsule and the deep fibres of the medial collateral ligament (Williams et al., 1989).

The medial meniscus is the most stable of the two menisci because of its shape and attachments. The elongated shape of the medial meniscus increases the distance between the anterior and posterior attachment sites, and thus increases its stability. In addition, the attachment of the medial meniscus to the medial collateral ligament further increases its stability (Romanes, 1986). As a result, the increased stability of the medial meniscus reduces the ability of the meniscus to escape being pinched between the femur and tibia during movements (Romanes, 1986).

### Muscles

According to the tables provided by Moore (1985), there are a total of 41 muscles providing active support for the hip, knee, and ankle. However, since figure skating injuries are seldom related to muscles, it is beyond the scope of this paper to describe each muscle in detail. Therefore, the muscles of the hip, knee and ankle joints will be outlined in a table format which will include the name and function performed. It should be noted that the muscles in bold print are considered, by Moore (1985), to be the primary movers while the normal print muscles provide support to the primary movers.

### Ankle Joint Muscles (Table 2-1)

The ankle joint is formed by the tibia, fibula, and talus. This is a hinge joint producing only two movements, dorsiflexion and plantarflexion. The muscles that are responsible for the movements of this joint are:

Table 2-1: Muscles producing movements at the ankle joint. Adapted from Moore (1985, p. 543).

Dorsiflexion	Plantarflexion
Tibialis Anterior	Triceps Surae
Extensor Digitorum Longus	Gastrocnemius
Extensor Hallucis Longus	Soleus
Peroneus Tertius	Plantaris
	Tibialis Posterior
	Flexor Hallucis Longus
	Flexor Digitorum Longus

### Intertarsal Joint Muscles (Table 2-2)

The intertarsal joints are those formed between the calcaneus, talus, cuboid, navicular, and the three cuneiform bones. The three that are of most importance are the subtalar, talocalcaneonavicular, and the calcaneocuboid joints. The movements produced at these joints by the surrounding muscles are inversion, eversion, and plantarflexion (Moore, 1985).

Table 2-2: The muscles performing movement at the intertarsal joints divided into groups according to their function. Adapted from Moore (1985, p. 546).

Inversion	Eversion	Plantarflexion
<b>Tibialis Anterior</b>	<b>Peroneus Longus</b>	<b>Peroneus Longus</b>
<b>Tibialis Posterior</b>	<b>Peroneus Brevis</b>	<b>Tibialis Posterior</b>
	<b>Peroneus Tertius</b>	<b>Abductor Hallucis</b>
		<b>Abductor Digiti Minimi</b>
		<b>Flexor Digitorum Brevis</b>
		<b>Peroneus Brevis</b>

### Knee Joint Muscles (Table 2-3)

The major motions that occur at the knee joint are flexion and extension however, medial and lateral rotation occur when the knee joint is flexed. The muscles that produce these four movements are listed in Table 2-3.

Table 2-3: Muscles producing movement at the knee. Adapted from Moore (1985, p. 529).

Flexion	Extension	Medial Rotation of Flexed Knee	Lateral Rotation of Flexed Knee
<b>Hamstrings</b>	<b>Quadriceps Femoris</b>	<b>Popliteus</b>	<b>Biceps Femoris</b>
<b>Semimembranosus</b>	<b>Rectus Femoris</b>	<b>Semimembranosus</b>	
<b>Semitendinosus</b>	<b>Vastus Lateralis</b>	<b>Semitendinosus</b>	
<b>Biceps Femoris</b>	<b>Vastus Intermedius</b>	<b>Sartorius</b>	
<b>Gracilis</b>	<b>Vastus Medialis</b>	<b>Gracilis</b>	
<b>Sartorius</b>	<b>Tensor Fasciae Latae</b>		
<b>Popliteus</b>			

### Hip Joint Muscles (Table 2-4)

The movements that can be performed at the hip joint are flexion, extension, abduction, adduction, internal and external rotation (Romanes, 1986) and circumduction (Kapandji, 1987). With such a wide range of motions available at the hip, there are a large number of muscles that produce and resist movements, the muscles involved in producing these movements are as follows:

Table 2-4: The muscles that perform movements at the hip. Adapted from Moore (1985, p. 518).

Flexion	Extension	Abduction
Iliopsoas Tensor Fasciae Latae Rectus Femoris	Gluteus Maximus	Gluteus Medius
	Semitendinosus	Gluteus Minimus
	Semimembranosus	Tensor Fascia Latae
Sartorius	Biceps Femoris (Long head)	Sartorius
Adductor Longus		Piriformis (in flexion)
Adductor Brevis	Adductor Magnus (Ischial fibers)	Obturator Externus (in flexion)
Pectineus		
Adduction	Medial Rotation	Lateral Rotation
Adductor Magnus	Tensor Fascia Latae	Obturator Internus
Adductor Longus	Gluteus Medius	Gemelli
Adductor Brevis	Gluteus Minimus (anterior fibres)	Obturator Externus
Pectineus		Quadratus Femoris
Gracilis		Piriformis
		Gluteus Maximus
		Sartorius

## Ankle Biomechanics

In the ankle complex, there are two main axes of rotation. The first axis is referred to as the ankle joint, and articulation occurs between the tibia, fibula and talus. The second axis is the subtalar joint, which occurs at the articular surfaces of the talus and calcaneus. In the following section these two joints are reviewed and the movements that occur at each joint are outlined.

### Ankle Joint

The ankle joint connects the shank to the foot and forms a hinge joint. Kapandji (1987) represented this joint as shown in Figure 2-4. His diagram showed the axis of rotation to be perfectly horizontal between the tibia and fibula. On the other hand, Inman (1976) described the axis as running

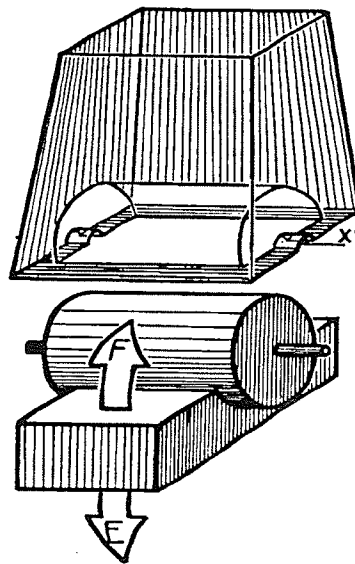


Figure 2-4 - The axis of rotation of the ankle according to Kapandji (1987, p.155).

obliquely between the tibia and fibula. This description had the axis deviating approximately  $6^{\circ}$  from the transverse plane, and  $12^{\circ}$  from the frontal plane. In other words, the axis runs obliquely from the lateral malleolus anteriorly, and superiorly toward the medial surface of the ankle. Therefore, the angle of the axis causes plantarflexion and dorsiflexion to occur about an oblique axis between the sagittal and frontal planes. As a result, toeing-out occurs in dorsiflexion and toeing-in occurs in plantarflexion.

Furthermore, Lundberg, Svensson, Nemeth, and Selvik (1989) described the axis of rotation for plantarflexion, dorsiflexion, pronation, supination, as well as medial and lateral rotation as running through a common central point in the talus. However, their findings also indicated that the orientation of the axis changes as the angle of the ankle joint changes. For example, in dorsiflexion, instead of the axis remaining as described above, the axis of rotation runs obliquely down and laterally, instead of down and medially. Therefore, the position of the foot, with regard to the shank, is vitally important in the determination of the axis of rotation for the ankle.

Sammarco, Burstein, and Frankel (1973) calculated the instant centre of rotation of the ankle. Their results showed that for plantarflexion and dorsiflexion in the sagittal plane, the centre of rotation remained in the talus. However, even though the instant centre was within the talus, no definable pattern of movement was found. Furthermore, the authors discovered that distraction occurred in the early phase of movement, sliding in the mid-portion, and compression near the end of the range of motion. They also found that the average range of motion was  $44^{\circ}$ .

The aforementioned limited range of motion is due to four main reasons. In dorsiflexion the range of motion is prevented by the contact of the

neck of the talus and the anterior margin of the tibia. This range is also limited by the tautness of the posterior capsule and ligaments, and by the active and passive contraction of the plantarflexor muscles (Kapandji, 1987). Plantarflexion is limited by a taut capsule, ligaments and by the bony contact between the posterior tubercle of the talus and the tibia. In both dorsiflexion and plantarflexion the capsule is prevented from being pinched between the bony surfaces by the attachment of muscle sheaths to the capsule. Therefore, during active contraction of the muscles the capsule is pulled by the muscle and thereby lifts the capsule out from between the talus and tibia (Kapandji, 1987).

#### The Subtalar Joint

Plantarflexion and dorsiflexion occur at the ankle joint while the remaining movements of the foot occur at the subtalar joint. This joint is described as a mitered hinge joint, with its axis at  $42^\circ$  to the "...horizontal in a sagittal plane and  $16^\circ$  from the longitudinal axis of the foot...in a transverse plane..." (McPoil & Knecht, 1985, p.69). This orientation of the axis is at an oblique angle to the cardinal planes and runs from the lateral, plantar, and posterior side of the ankle, anteriorly, medially, and dorsally.

The movements at the subtalar joint were described by McPoil and Knecht (1985) to be pronation and supination. Pronation consists of calcaneal eversion and adduction at the subtalar joint, and plantarflexion at the talus. Supination consists of inversion of the calcaneus, abduction, and talar dorsiflexion.

There are two functions performed by the subtalar joint. The first is to absorb rotational forces of the lower extremity during stance. During the stance phase the femur and tibia medially rotate, and the forces are absorbed

by the subtalar joint during pronation. Pronation, therefore, reduces the torsional forces transmitted to the lower limb. The second function of the subtalar joint is to provide shock absorption to the body at heel strike. At heel strike pronation at the subtalar joint shortens the lower limb, and the tibia rotates faster than the femur. This causes the knee to become unlocked, and as a result the knee flexes, and shock is absorbed by the muscles surrounding the knee (McPoil & Knecht, 1985).

### Ankle and Subtalar Joints

The combined effects of each joint are then combined in order to provide an accurate understanding of the overall working of the ankle complex. According to Inman (1976), "the ankle and subtalar joints constitute an integrated mechanism ... [and] one can not [sic] be studied to the exclusion of the other." (p. 67). Furthermore, the axis of rotation changes as motion occurs, and therefore, the amount of contribution of each joint to the range of motion also changes.

Inman (1976), described three phases that require the combined effort of both the ankle and subtalar joints during the stance phase of locomotion, these being heel contact, foot flat, and toe off. During the first phase or heel contact to foot flat, the foot plantarflexes and pronates. The second phase involves the stationary foot in full contact with the ground, while the shank moves over the foot. The ankle dorsiflexes and simultaneously supinates during this phase. Finally, during heel off to toe off the foot quickly plantarflexes and continues to supinate (Inman, 1976).

The ratio of the range of motion during normal gait is approximately 2:1 for the ankle and subtalar joints respectively. Furthermore, toeing-in and toeing-out causes large differences in the walking pattern and the range of

motion at each joint. Toeing-out increases rotation about the subtalar joint while subsequently decreases displacement of the ankle joint. On the other hand, toeing-in decreases the range of motion while the foot is flat, but at heel off supination is rapid and over exaggerated (Inman, 1976).

### Knee Biomechanics

The knee is particularly susceptible to injury for two reasons, first, because it forms the joint between the two longest bones in the body (Nordin & Frankel, 1989) and second, because the strength of the joint is directly related to the surrounding soft tissue rather than osseous configuration (Romanes, 1986). In other words, the strength of the joint is not the result of the tight, close proximity of the bony structures, but instead the joint is held together by muscles and ligaments.

According to Kapandji (1987), the knee has two distinct functions, the first is to supply stability in full extension, the second is to provide mobility at certain degrees of flexion. Stability is important in order to withstand the stresses of body weight and external loads, while mobility is required to maintain the proper orientation of the foot relative to the irregularities of the ground.

The knee is constructed to act primarily as a hinge, however, as will be shown, there are more movements occurring at the knee than just flexion and extension. In the knee there are three bones that are responsible for the actions that take place at the joint. The femur articulates with both the tibia and the patella, however, the patella and tibia do not articulate with each other (Nordin & Frankel, 1989). Furthermore, the cruciate ligaments and menisci are susceptible to injury under flexion, while the articular capsule

and collateral ligaments are susceptible in extension (Kapandji, 1987).

### Range of Motion

The first axis of the knee joint is one that runs horizontally through the femoral condyles. However, because the longitudinal axis of the femur does not coincide with the one of the tibia, the flexion-extension of the joint is not entirely in one plane. The difference in angle between the tibia and femur causes the shank to be positioned posteriorly, and slightly medial to the femur (Kapandji, 1987).

The second axis of rotation occurs about the longitudinal axis of the shank, allowing medial and lateral rotation of the shank. The key to this rotation is that it can only occur while the knee is being flexed or extended. This rotation is known as the screw-home mechanism. The rotation of the knee occurs automatically at the beginning of flexion and near the end of extension (Kapandji, 1987). The rotation occurs as the result of the uneven size of the femoral condyles. The medial femoral condyle is approximately 1.7 cm longer than the lateral condyle. As a result, as the tibia glides on the femur, it must descend or ascend around the medial condyle causing the tibia to rotate during flexion and extension. The result of the screw-home mechanism is a more stable joint, through the whole range of motion, than a normal hinge joint (Nordin & Frankel, 1989).

From a position of full extension, the knee can flex through an angle of approximately  $140^{\circ}$ . As the knee begins to flex, there is a gradual increase in the amount of rotation that can occur at the joint. At an angle of  $90^{\circ}$  of flexion, the knee reaches its maximum rotation capacity, with  $45^{\circ}$  of external rotation and  $30^{\circ}$  of internal rotation. Flexion, external and internal rotation are all limited by soft tissue interference (Nordin & Frankel, 1989).

## Surface Motion

The type of motion that occurs between the femur and tibia is a combination of sliding, rolling, and spinning (Rasch & Burke, 1978; Kapandji, 1987; Nordin & Frankel, 1989; Williams et al., 1989). Sliding and rolling occur as a result of the flexion and extension of the knee, while the spinning motion is a result of the femur medially rotating on a fixed tibia. This action is known as the screw-home mechanism (Rasch & Burke, 1978). Flexion and extension are the two movements that are most associated with the knee. Therefore, these two movements will be addressed first, with the action of the patella included, then the medial and lateral rotation of the knee will be addressed.

During flexion, the point of contact moves back on the tibia, indicating a rolling of the femur on the tibia. Sliding also occurs because the distance between the points of contact in extension and flexion are in a ratio of approximately 2:1 in favour of the femur (Kapandji, 1987).

The combination of both rolling and sliding must take place because of the difference in size and shape of the tibial and femoral condyles. If rolling and sliding did not take place, the femur would simply roll off the back of the tibial condyles. However, if sliding were the only motion occurring at the joint, then the tibia would prematurely stop flexion because of bony contact between the tibia and femur (Kapandji, 1987).

The range over which pure rolling occurs is different for each condyle. The medial condyle undergoes pure rolling for only the first 10°-15° of flexion. On the other hand, the lateral condyle undergoes pure rolling for up to 20°. After the rolling limits have been reached, the rolling continues but it is joined by sliding of the joint surfaces (Kapandji, 1987).

The instant centre of the knee joint is located in the femoral condyles,

but as the knee is flexed this position changes. The pathway of the instant centre remains within the femoral condyles, however, the path of the instant centre follows a semi-circle, as depicted below (Nordin & Frankel, 1989). The changing of the instant centre pathway is a key to the combination of the two types of motion that occur at the knee joint (Kapandji, 1987).

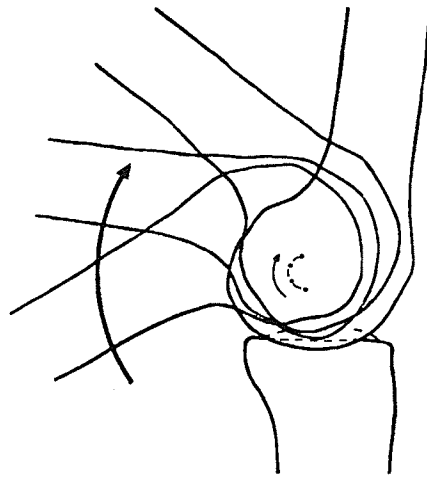


Figure 2-5 - the path of the instant centre of rotation of the knee as the knee joint goes from flexion to extension (Nordin & Frankel, 1989, p. 120).

According to Nordin and Frankel (1989), the patella glides on the femur for the first 90°, but beyond that point, the patella begins to rotate externally on the medial facet of the femur. The functions performed by the patella, as presented by Nordin and Frankel (1989), are to change the length of the quadriceps' lever arm, making the muscles' pull more effective, and to decrease the force per unit area placed on the femur by the quadriceps tendon. A third reason, presented by Pick and Howden (1974), is to protect the front of the knee.

The motions mentioned above, however, are not the only movements at the knee joint. Spinning occurs, in conjunction with flexion and extension, producing a spiral, or helical motion (Nordin & Frankel, 1989). The spinning motion is completely dependent on the medial femoral condyle, and the fact that it is approximately 1.7 cm longer than the lateral condyle (Nordin & Frankel, 1989). During knee extension, the lateral femoral condyle reaches its final resting place first, while the medial femoral condyle is still free to move. At this point the knee joint begins to rotate and continues until the medial femoral condyle reaches its final resting place. This rotation, known as the screw-home mechanism, locks the knee in extension and increases stability (Rasch & Burke, 1978).

The amount of spinning is highly dependent on the position of the knee joint in the sagittal plane. In complete extension, the amount of rotation is zero, however, as the knee is flexed the amount of spinning increases, reaching a maximum at 90 degrees of flexion. In this position, lateral rotation can range from 0-45 degrees, and medial rotation ranges from 0-30 degrees. In general, lateral rotation occurs during extension, while medial rotation occurs during knee flexion (Nordin & Frankel, 1989).

#### Function of the Menisci

The menisci are presumed to have several functions. The main function of these structures is to reduce the joint reaction forces present in the knee, by increasing the area of contact between the femur and tibia, (Wells & Luttgens, 1976; Gozna & Harrington, 1982; Peterson & Frankel, 1986; Romanes, 1986; Nordin and Frankel, 1989), however, Radin and Paul (1970), believe that the cartilage does not aid in the absorption of forces. A second function of the menisci is to deepen the articular facets of the tibia (Wells &

Luttgens, 1976), which in turn provides a better fit between the tibial plateaus and the femoral condyles (Rasch & Burke, 1978). Thirdly, the menisci function to reduce the frictional wear between the tibia and femur (Rasch & Burke, 1978), and finally they act as stabilizers (Gozna & Harrington, 1982). According to Renstrom and Johnson (1990), stability is increased by the menisci because they maintain proper positioning between the femur and tibia, they deepen the articular surfaces, and fill the empty space on the periphery of the condyles.

### Hip Biomechanics

The following section will describe how the hip joint functions, how force is distributed, and the range of motion that is available.

#### Range of Motion

The largest range of motion occurs in the transverse plane. The two joint motions in this plane are known as internal and external rotation. Ninety degrees of motion is contributed by external rotation, while 70° of motion is contributed by internal rotation (Nordin & Frankel, 1989). Therefore, the total range of motion in the transverse plane is 160°.

The sagittal plane also accounts for a considerable amount of the motion at the hip joint. The average range of flexion at the hip is 140° (Nordin & Frankel, 1989). Because the hip joint is so free to move, further flexion of the joint is prevented only by the contact made between the thigh and the anterior abdominal wall (Romanes, 1986). To further increase the motion available in the sagittal plane, the hip can be extended 15° (Nordin & Frankel, 1989), which increases the total range of motion in the sagittal plane

to 155°.

In the frontal plane, the range of motion is considerably less than the previous two planes. Abduction accounts for 30° of motion while adduction only contributes 25° (Nordin & Frankel, 1989) for a total range of motion of 55°.

Circumduction is the combination of flexion, extension, adduction and abduction. As a result, the pattern traced by the hip is a cone, with the apex of the cone located at the centre of the hip joint (Kapandji, 1987). Furthermore, it should be noted that the path of circumduction is not a symmetrical cone, due to the limited ranges of motion available in each of the planes and the interference of the support limb (Kapandji, 1987).

#### Surface Motion

There is only one type of motion occurring between the femur and acetabulum, that is gliding. Gliding is the only motion occurring between the surfaces because the femoral head is held securely in the acetabulum, and motion of the joint occurs around the centre of rotation of the femoral head. As a result, the femoral head does not experience rolling or spinning, and all motion at the hip is gliding (Nordin & Frankel, 1989).

#### Force Distribution

According to Brussatis, Dupuis, Hartung and Steeger (1976), the forces on the acetabulum are located on the upper lateral aspect. In an unpublished paper, presented at the University of Manitoba, Aiken (1988) described the forces of the femur to be on the superior aspect of the femoral head.

From the femoral head, the forces must be transmitted to the shaft of the femur. In order to transmit these forces, Benedik and Villars (1973)

concluded that the joint reaction forces must be directed down the neck of the femur. Again, Aiken (1988) took the study one step further, and showed that all the forces produced on the surface of the femur, converge to produce a cone of forces with the maximum force occurring at the vertex of this cone. This force is then transmitted to the shaft, via the neck.

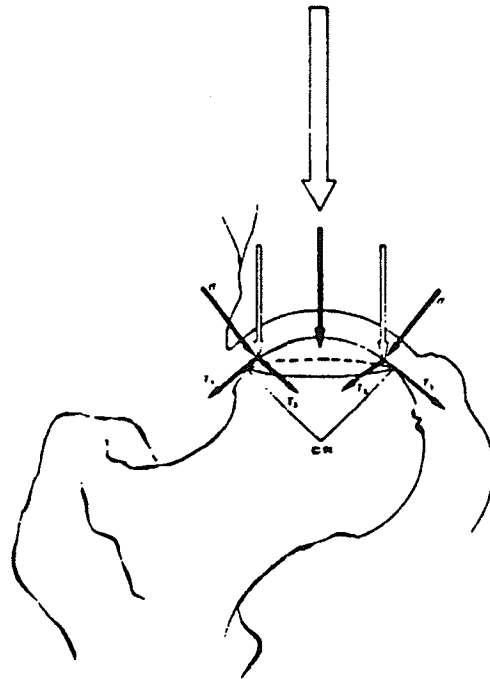


Figure 2-6 - A conical representation of the forces that occur in the head of the femur as a result of forces on the superior aspect of the head of the femur (Aiken, 1988, p. 25).

The unique shape of the femur places the bone at risk under extreme loading conditions. Because the load is placed on the head of the femur, and the shaft is tilted medially from the hip to the knee, this predisposes the neck of the femur to bending forces (Aiken, 1988). In other words, as the forces placed on the femur increase, the potential for injury increases because the

compressive and bending forces in the neck of the femur increase.

### Cinematography

There are two techniques that can be used when filming a sporting event - high speed cinematography (Lamb & Stothart, 1978; Muraki, Sakamoto, Asito & Shibukawa, 1982; Kennedy et al, 1989) and video taping methods (Abraham, 1987; & Kennedy et al, 1989).

#### Purpose of Filming

The purposes of filming sporting events are to calculate the following parameters: linear and angular displacement, linear and angular velocities (Bartee and Dowell, 1982), accelerations and centre of mass (Denoth et al, 1984), and the centre of rotation of a joint (Allard, Nagata, Duhaime, & Labelle, 1987).

As mentioned, force platforms are the main method of determining reaction forces in biomechanics (Nelson & Martin, 1985; Nigg, 1985; Valiant and Cavanagh, 1985; Zatsiorsky & Prilutsky, 1987; and Gross & Nelson, 1988), however, they can seldom be used in a natural sports setting. Film analysis can, therefore, be a substitute for force platforms in this type of setting. Roberts (1970) conducted an experiment that compared the forces produced on a force platform to those from film calculations. The results of the study showed that the forces calculated from film data were very close to force platform values. The problem with the study was that no specific numbers were given for the comparisons. Therefore, formal proof of the similarity between the two methods of force calculations was lacking. On the other hand, Lamb and Stothart (1978) provided substantial statistical proof that the

comparison between film and force platform calculations was accurate. The correlation found between the film and force platform calculations was 0.938. While the authors compared velocities, they believed that this relationship provided strong evidence for the impulse-momentum relationship because it applied "... to ground reaction force-time records, and is an accurate technique for measuring the vertical component of take-off velocity of the center [sic] of gravity." (p. 391). In other words, forces can be calculated from film data if the appropriate equations were used. In this case, GRF values from the force platform were converted into velocities, and the film data provided the appropriate velocities for comparison. As a result, the Lamb and Stothart (1978) comparison of velocities indirectly showed that force platform and film data were interchangeable in the calculation of forces.

Finally, Bobbert et al (1991) used the second derivative of positional data, accelerations, to calculate the vertical GRF of a runner. A direct measurement from the force platform was compared to the indirect method used by Newton's equations of motion, namely the direct relationship between the product of mass and acceleration and the force. The result showed that film data provided an accurate representation of the GRF peaks because the two methods of GRF calculations did not differ by more than 10 per cent, and time of GRF did not differ by more than 5 milliseconds.

#### Advantages and Disadvantages of Video/Film

The use of video taping "...for qualitative movement analysis has led to affordable systems..." (Abraham, 1987, p.1107) for researchers who could not afford the more expensive high speed cameras. Abraham also stated that this method provided reasonable clarity of the image, while allowing for freeze frame analysis and slow motion analysis. Kennedy et al (1989) supported

these findings and believed that video analysis was a more attractive form of analysis because of the "...low cost, ease of use, and short processing time,..." (p. 457) for the film.

The advantage of high speed film analysis was the number of frames that could be filmed per second. According to Kennedy et al (1989), film cameras can record at speeds of 500 Hz, whereas standard video cameras can only record movements to a maximum of 60 Hz. Therefore, the more frames recorded per second, the clearer the final image, which makes single frame analysis much easier.

Although the high speed filming may seem quick, this filming speed still has some problems. Denoth et al (1984) described the problems inherent in high speed film analysis. They found accelerations of  $600 \text{ ms}^{-1}$  and  $10^5$  degrees per second and this made kinematic recording with high speed film very difficult. Therefore, with sports skills that have velocity values as high as those mentioned by Denoth et al., it seems unlikely that video recording would prove as accurate or reliable as the high speed film analysis.

Another advantage found in favour of high speed cinematography was that the digitizing process was more accurate. Kennedy et al (1989) compared video and high speed film and found that the results for the x, y, and z coordinates were more accurate when high speed film techniques were used. However, the authors believed that little confidence should be placed on the statistical difference ( $p < 0.05$ ) found between the two mediums. With errors values of 4.8 mm and 5.8 mm for the high speed film and video techniques respectively, a difference of only one millimeter, the authors believed that the statistical difference should not be taken seriously, and that video analysis should be considered as accurate as high speed cinematography.

Finally, there was one problem that was inherent in both video and

high speed film analysis techniques, the time required to digitize the film (Higgs, 1984). According to Roberts (1970), digitizing can be very time consuming, even with semi-automatic forms of digitizing equipment. However, Roberts believed that the time required to analyze the data was worth the effort, because the value of the results outweighed the amount of time taken to analyze the data.

### Direct Linear Transformations

Direct Linear Transformation (DLT) is a process by which an investigator records an event with a minimum of two cameras, and a computer algorithm converts the two-dimensional data to three-dimensional data (Wood & Marshall, 1986). The general procedure involves the filming of a reference structure, the removal of the structure and the substitution of the subject in the same object space. Once the reference structure has been filmed, the cameras must remain stationary during the filming (Wood & Marshall, 1986). Shapiro (1978) also stated that several ground reference markers should be placed in the field of view for each camera to accommodate for any movement that might take place during the filming procedure.

Next the film must be processed. In this step, the reference structure and subject are digitized, and the computer calculates the parameters required to change two dimensional data to three dimensional data (Shapiro, 1978). Shapiro (1978) explained that the minimum number of reference points that can be digitized is six, which represents a cube. These six points are required in order to develop a set of equations to calculate the three dimensional representation of the data. The best estimates of DLT occur when between 12 and 20 reference points are used (Shapiro, 1978).

The advantage of this method of analysis is its flexibility. The cameras

can be set up at any particular angle to one another (Shapiro, 1978). However, Wood and Marshall (1986) stated that the best results are obtained by placing the cameras at 90<sup>0</sup> to each other.

When the cameras are placed in this configuration, the errors for both the calculated positional and acceleration data resulted in less than a 5% error of the actual values (Shapiro, 1978). However, according to Wood and Marshall (1986), the chance of error significantly increases as the points of interest move outside the space occupied by the scaled control points. Because these points lie outside the scaled control area, their positions must be interpolated by the computer since there are no surrounding values with which they can be compared. Therefore, this causes an increase in the likelihood of an error being introduced into the data collection.

#### Data Smoothing

When the measurement of segments of whole body energetics is required, a problem that arose was how to measure variables. They cannot be measured directly and, as a result, must be calculated by inverse mechanics. This approach, according to Wood (1982), involves the Newtonian equations:

$$\Sigma F = ma$$

$$\Sigma M = I\alpha$$

"That is, the resultant force (F) and moment (M) acting on a body of known mass (m) and moment of inertia (I) can be indirectly determined from its acceleration behaviour (linear a and angular  $\alpha$ )." (Wood, 1982, p. 310). The problem with using these equations arises when the velocities and accelerations are calculated from positional data. Velocity calculations require the positional data to be differentiated once and accelerations require double

differentiation of the positional data (Wood, 1982).

While differentiation of positional data provides adequate results, there was a problem associated with the results. Accelerations and velocities calculated by differentiation result in an increase in the measurement errors (Chao & Rim, 1973; Wood, 1982). The error associated with positional data is referred to as noise. This "noise is the term used to describe components of the final signal, which are not due to the process itself" (Winter, 1990). Sources of noise can be caused by vibration or improper alignment of the cameras, improper alignment of film, human error in digitizing, and machine error. As a result, the signal has an additional random component of error (Winter, 1990).

In order to reduce the signal to noise ratio, Wood (1982) suggests using 1) digital filtering, 2) Fourier or 3) spline smoothing routines. These routines will provide an adequate description of the displacement-time data, while at the same time minimizing measurement errors.

Digital filtering is designed to read data from equally spaced time intervals, reduce the noise, and produce data that closely resembles the original data (Wood, 1982). The initial positional data is passed through a series of formulae, which remove some of the noise, and produce uniform, flowing lines with few sharp peaks. One problem associated with this method is that the user is required to make the decision of which frequency must be used to smooth the data (Wood, 1982). Another problem associated with digital filtering is the slight distortion that occurs where the signal and noise overlap (Winter, 1990). The recommended frequency for digital filtering is around 6 Hz when the filming speed is 60 Hz (Winter, 1990).

Spline functions, on the other hand, pieces together a number of different polynomials of low degree with the junction point of the different

functions known as knots. The fact that the final smoothed data is represented by a series of equations allows the line to adapt quickly to rapid changes in direction (Wood, 1982). There are three decisions that need to be made when using this method of smoothing: which degree of spline, how accurate the spline is to be, and the number of knots to be used. The general rule of thumb when using splines is

1. there should be as few knots as possible, ensuring that there are at least four or five points per interval;
2. there should not be more than one extremum point ... or one inflection point per interval;
3. extremum points should be centered [sic] in the interval;
4. inflection points should be close to the knots (Wood, 1982, p. 327).

While Wood (1982) and Challis and Kerwin (1988) believed that splines are an acceptable method of data smoothing, there are a large number of variables that must be taken into consideration when using this method. However, Wood (1982) also stated that the use of this method requires that there be enough data points and that the accuracy of the data is well known.

The Fourier series uses sine and cosine curves of increasing frequency to fit the curve. The first sine curve is drawn within the data, and is known as the first harmonic. Subsequently, the amplitude and frequency of the signals are changed in multiples of the first harmonic until the proper weighting of the appropriate sine and cosine values results in an approximation of the displacement-time curve (Winter, 1990). Furthermore, it has been shown that little of the signal exists beyond the seventh harmonic for normal walking (Wood, 1982). This method has been proven to be very effective, and a better approximation than polynomial approximations (Wood, 1982).

An example of the results from a second-order Butterworth filtering procedure of a set of angular acceleration data is depicted in Figure 2-7. The smoothed graph was not identical to the original data, however the results were considered to be statistically similar and provided a reasonable estimate of the acceleration.

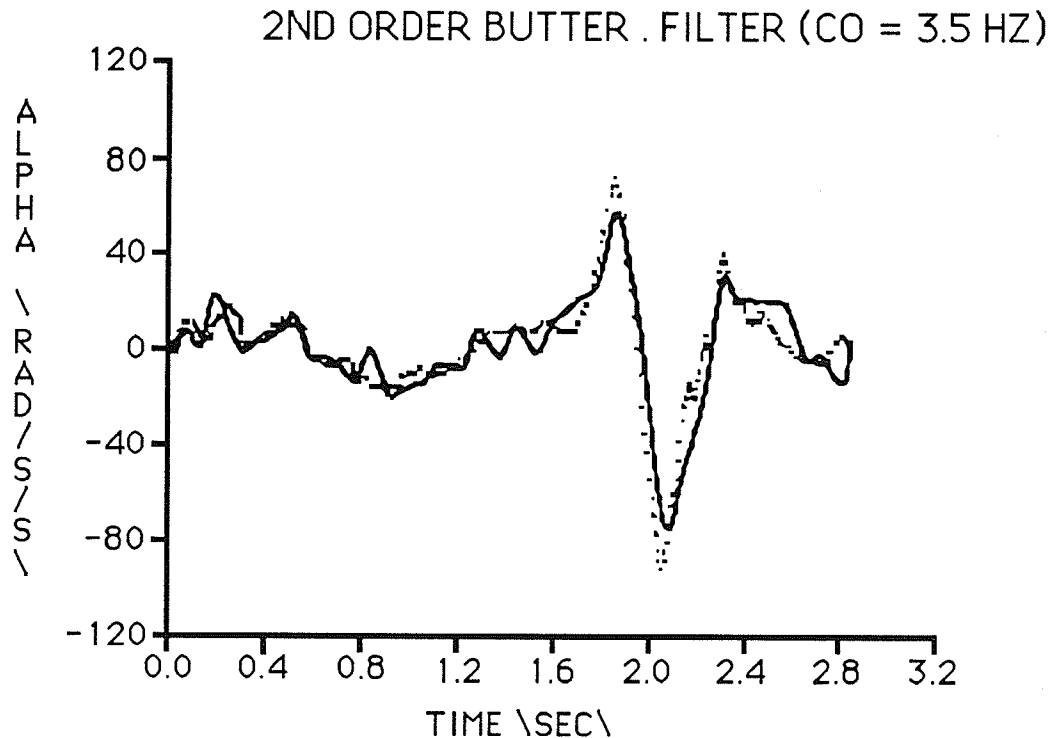


Figure 2-7 - A representation of the accuracy of the digital filtering as a smoothing function on angular acceleration data. The solid line is the filtered data (3.5 Hz), and the dotted line is the raw data (Wood, 1982, p. 353). As can be noted, the smoothed data is not very accurate using this method, therefore, alternative smoothing methods may provide a closer fit to the original data.

In conclusion, Wood (1982) found that digital filtering, Fourier smoothing, and spline smoothing produce valid results for motion analysis. Therefore, the method of filtering to be used depends on the data to be smoothed, the investigator's preference and the availability of the program routine.

## Centre of Gravity Calculations

Before any accurate force calculations can be made, the body should be divided into segments, weighed, and have the centre of gravity (CG) of each segment calculated. The position of the CG of each segment is important to the overall CG of the body and the moments created in the body (Le Veau, 1992). However, since this is not feasible on living beings, these values will be taken from tables of cadaver data, namely Humanscale and Hinrichs (1988).

The CG of each segment is an imaginary point that represents the mass of the entire segment. For each segment, this is the point through which the force of gravity acts (Le Veau, 1992). After the individual segmental CG's have been calculated, the entire body's centre of gravity can be calculated in a similar manner.

The CG of the entire body is an imaginary point which is represented by the sum of the moments of each individual segment (Le Veau, 1992). Since the position of CG of the human body is not constant, any movement of segments will cause the CG to shift within the body, and possibly even move outside of the body (Le Veau, 1992). An example of having the CG lying outside the body can be shown using a doughnut. The mass of a doughnut is around the hole in the middle of the doughnut, but the CG of the entire system is located in the centre of the doughnut where there is no mass whatsoever. This is the point that represents the total body's CG (Le Veau, 1992). Therefore, the CG of the entire body is not only related to the mass of each segment, but also the orientation of the segment in space. The position of the body's CG is important for two reasons, first, for the accurate measurement of forces and moments, and second, for the stability of the subject (Le Veau, 1992).

## Force Calculations

Since figure skating jumps are a dynamic activity, there are a number of forces that must be considered. Among these forces are the weight of the subject, the muscular force, other soft tissue forces (ligaments), and the externally applied force (Nordin & Frankel, 1989). According to Nordin and Frankel (1989), the forces must be calculated from the accelerations of the body segment under consideration and the moment of inertia of the segment.

Nordin and Frankel (1989) listed six steps that must be followed when calculating the joint reaction forces (JRF) and ground reaction forces (GRF) of the body:

1. The anatomic structures involved in the production of forces are identified. These are the segments of interest, or any of the segments that have an effect on the part of interest.
2. The angular acceleration of the moving body part is determined.
3. The mass moment of inertia of the moving body part is determined. (This is the resistance of the body to rotation of a body segment during a dynamic activity, (Chaffin & Andersson, 1991).
4. The torque (moment) acting about the joint is calculated. This is simply the product of the mass moment of inertia and the angular acceleration of the segment ( $M=I\alpha$ ).
5. The calculation of the magnitude of the main muscle force accelerating the body part.
6. The calculation of the magnitude of the joint reaction force at a particular instant in time.

Seireg and Arvikar (1975), separated the muscles of the lower limb and produced 42 force equations, and 104 unknown variables. Since these

equations produced an infinite number of solutions, Zajac and Gordon (1989) suggested calculating the total force, and then calculating the individual muscle force as a per cent of the total cross-sectional area occupied by the muscles.

In order to calculate the forces present in a given muscle, dividing the body into segments is a useful way to begin calculations. By doing this, Zajac and Gordon (1989) isolated each segment, and calculated the forces and moments of one segment at a time. The calculation of forces should also start at the free end of the segment and then work toward the fixed points (Zatziorsky & Aleshinsky, 1975). The advantage of this method is the ease with which the JRF can be calculated. The disadvantage is the large number of equations produced, and the time required to produce and use the equations.

One important consideration is the transfer of forces from one segment to the next. When using segments to calculate forces, the forces and moments of one segment will have a direct effect on the adjacent segment. Chaffin and Andersson (1991) diagrammed the effect that one segment had on an adjoining segment (Figure 2-8). At the ankle, the joint reaction forces in the talus were  $-R_{ax}$  and  $-R_{ay}$ , while in the attached segment the same forces were  $R_{ax}$  and  $R_{ay}$ . The moment at the ankle was  $-M_a$ , and it was  $M_a$  in the shank. In other words, the joint reaction forces and joint moments in the adjacent segment were of the same magnitude, but opposite in direction (Marshall, Jensen, & Wood, 1985, Chaffin and Andersson, 1991).



$$M_j = M_{j-1} + jCM_L(\cos \theta_j)m_Lg + jCM_L(\cos \theta_j)m_La_{Ly} + \\ jCM_L(\sin \theta_j)m_La_{Lx} + jj-1(\cos \theta_j)R_{(j-1)y} \\ + jj-1(\sin \theta_j)R_{(j-1)x} + I_L\theta_j$$

where  $M_j$  and  $M_{j-1}$  were the proximal and distal joint moments;  $\theta_j$  was the angle made by the segment and the horizontal;  $m_L$  was the mass of the link;  $jj-1$  was the segment link length;  $jCM_L$  was the distance from the joint  $j$  to the centre of mass;  $a_{Ly}$  and  $a_{Lx}$  were the linear accelerations of the segment;  $I_L$  was the moment of inertia of the segment about the centre of mass of the segment;  $\theta_j$  was the angular acceleration of the segment about joint  $j$  (Chaffin & Andersson, 1991).

A second example of the calculation of the joint reaction forces and moments at the ankle joint was presented by Bobbert, Huijing and van Ingen Schenau (1986). In this example, the researchers used the following diagram, and the associated equations.

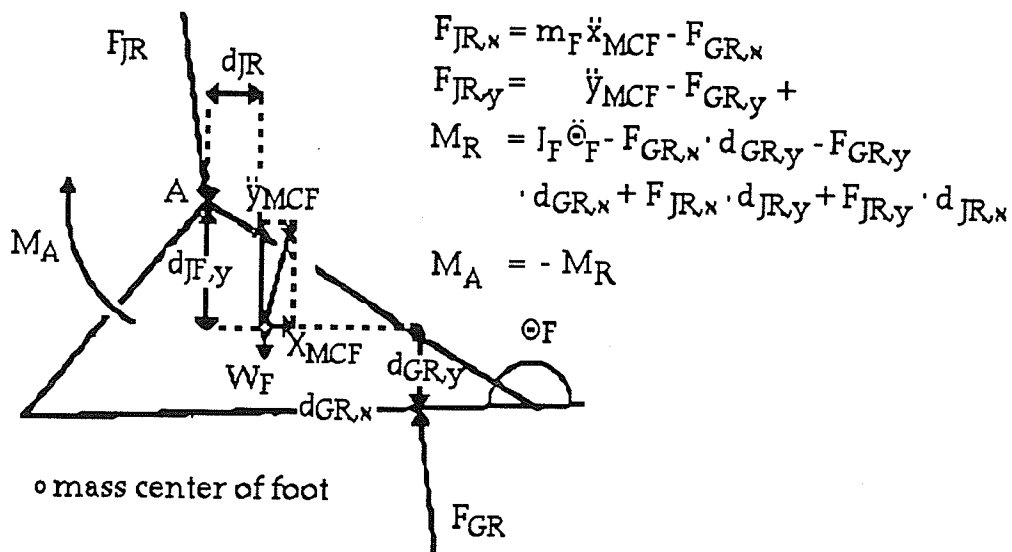


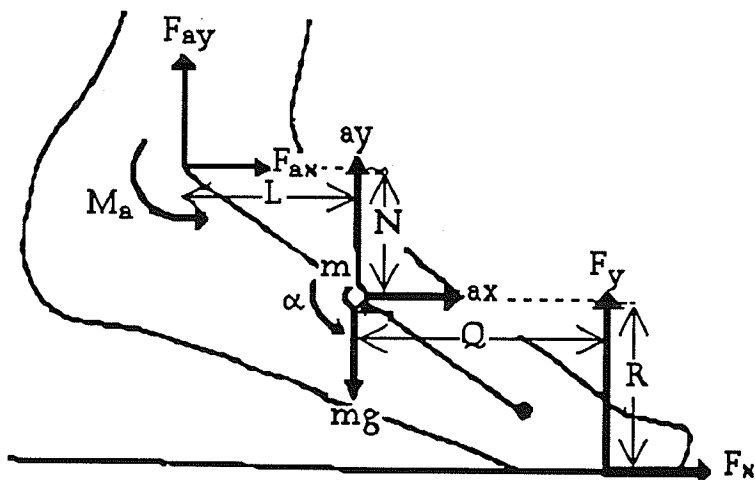
Figure 2-9 - Free body diagram of the foot, and equations used for calculating a plantar flexing moment (adapted from Bobbert et al, 1986, p. 889).

where:

- $F_{JR,x}$  and  $F_{JR,y}$  are the components of the resultant muscle and reaction forces at the ankle.
- $F_{GR,x}$  and  $F_{GR,y}$  are the components of the ground reaction force
- $\ddot{x}_{MCF}$  and  $\ddot{y}_{MCF}$  are the components of the acceleration of the mass center of the foot.
- $m_F$  is the mass of the foot.
- $W_F$  is the weight of the foot.
- $M_R$  is the resultant moment about the ankle.
- $M_A$  is the plantar flexing moment.
- $\theta_F$  is the angle between the foot and horizontal axis.
- $d_{.,y}$  and  $d_{.,x}$  are the components of moment arms of force.
- $J_F$  is the moment of inertia of the foot about its mass center (Bobbert et al, 1986, p. 889).

Once the free body diagram was constructed, the calculation of the forces acting on the body, in each of the cardinal planes was performed. Above, Bobbert et al (1986), provided the equations for the joint reaction forces in the x direction ( $F_{JR,x}$ ) and the y direction ( $F_{JR,y}$ ). The next step was to calculate the moment ( $M_R$ ) present at the ankle joint. The equations used in Figure 2-9 provided values of 5580 ( $\pm 634$ ) N. Because the study was coplanar, only one moment could be calculated. In a three dimensional study, there would be three moments acting at the joint. This procedure can be performed on many of the joints in the body if a force platform is present, and the forces are transferred from one limb to the next.

A second example of the calculation of forces and moments about the ankle was performed by Fukashiro and Komi (1987). Their equations and free body diagrams were as follows:



$$1. F_{ax} = m a_x - F_x$$

$$2. F_{ay} = m a_y - F_y + m g$$

$$3. \sum M = I \alpha$$

$$\therefore M_a = -(F_x R) - (F_y Q) + (F_{ay} L) + (F_{ax} N) + I \alpha$$

$F_{ax}, F_{ay}$  = joint reaction force

$M_a$  = moment of the joint

$F_x, F_y$  = ground reaction force

$a_x, a_y$  = acceleration of the center of gravity of segment

$m$  = segment mass

$g$  = acceleration due to gravity

$I$  = inertia moment of the segment

$\alpha$  = angular acceleration of the segment

$L, N, Q, R$  = distance

Figure 2-10 - A second example of the GRF from a force platform, and the forces that are occurring at the ankle joint (adapted from Fukashiro and Komi, 1987, p. 20 ERRATUM)

The values calculated by Fukashiro and Komi (1987) ranged from 2011 N to 3060 N depending on the activity the subjects were performing. The joint moments were calculated to be in the range from 120 Nm to 313 Nm. A representation of the forces and moments for the counter movement jump are presented below.

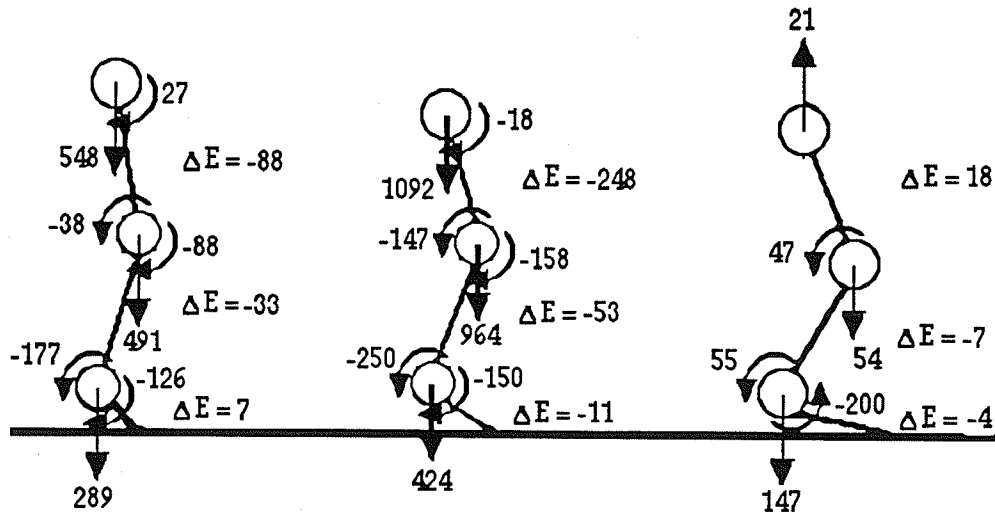


Figure 2-11 - The forces and moments on the lower limb as a subject lands from a jump (Fukashiro and Komi, 1987, p. 18).

Finally, Winter (1990) provided an example of the calculation of the forces and moments at the ankle and knee using this type of calculation. In the example, the subject had a segment mass of 1.16 kg, a segment length of 0.2 m, a moment of inertia of 0.0105 kgm<sup>2</sup>, and an angular velocity of 21.69 m/s<sup>2</sup>. The forces at the proximal joint for these variables was calculated as follows

$$1. \Sigma F_x = ma_x$$

$$R_{x1} = 1.16 \times 9.07 = 10.52 \text{ N}$$

$$2. \Sigma F_y = ma_y$$

$$R_{y1} = 1.16 \times 9.8 - 1.16 \times 6.62 = 3.69 \text{ N}$$

$$3. \Sigma M = I\alpha$$

$$\begin{aligned} M1 &= 0.0105 \times 21.69 + 10.52 \times 0.0985 + 3.69 \times 0.0195 \\ &= 0.23 + 1.04 + 0.07 = 1.34 \text{ N}\cdot\text{m} \end{aligned}$$

Winter (1990), continued the calculations for the next segment, by incorporating the above results into the next set of equations. This is done for every segment at this instant in time. Therefore, the more segments in the chain, the longer it will take to calculate the values, and the more equations that will be needed.

### Ground Reaction Forces

In order to accurately calculate GRF, the use of a force platform is the desired method. There have been a large number of articles written (Valiant and Cavanagh, 1985; Bobbert et al, 1987; Stacoff, Kaelin & Stuessi, 1988; Ricard and Veatch, 1990; Dufek & Bates, 1991; McNitt - Gray, 1991;) which investigate the forces applied to the body upon landing from heights.

In most of the studies, the vertical GRF time curves consist of two distinct peaks (Valiant & Cavanagh, 1985; Bobbert et al, 1987; Gross & Nelson, 1988; Stacoff, Kaelin, & Stuessi, 1988; Dufek & Bates, 1991). These authors believe that the first peak is associated with the initial contact of the toes with the ground, while the second peak corresponds to heel contact, which according to Gross and Nelson (1988), produced a toe - heel force ratio of 1: 2.2. Kaelin, Stacoff, Denoth and Stuessi (1988) explained toe impact as being lower than heel impact, due to the ankle's ability to dorsiflex and absorb the forces over a longer period of time, compared to the short, abrupt, change that occurs at heel contact. At heel contact, the impact forces are blocked and no movement occurs at the foot to absorb the forces, and as a result, forces were higher at heel contact (Kaelin et al., 1988).

In the non-sport related studies, the subjects simply stepped off a platform of predetermined height, and the resulting GRF ranged from 2.6 -11

times body weight (BW) (McNitt - Gray, 1991) or 4496 ( $\pm 693$ ) N (Bobbert et al, 1987). In sports related tests, Stacoff et al (1988) found impact values of between 1000 N and 6500 N for the volleyball block, while Valiant and Cavanagh (1985) found a value of 1.3 BW for rebounding a basketball.

The above information has one inherent problem, the lack of consistency between tests. Some investigators made their subjects jump onto a force platform with both feet (Gross & Nelson, 1988; Bobbert et al, 1987, Ricard & Veatch, 1990; McNitt - Gray, 1991; and Dufek & Bates, 1991) while others used single foot impacts (Valiant & Cavanagh, 1985; Stacoff et al, 1988). Other investigators studied athletes simulating the desired sporting events (Ricard & Veatch, 1985; Valiant & Cavanagh, 1985; Steele & Milburn, 1987; and Stacoff et al, 1988) while the remaining investigators either studied drop-jumping (Bobbert et al, 1987; McNitt - Gray, 1991), shoe absorption (Steele and Milburn, 1987; Dickinson, Cook, & Leinhardt, 1985), or landing surface differences (Fukuda, 1988; Gross & Nelson, 1988; Dufek & Bates, 1991).

Due to the lack of similarity between experiments, it is difficult to provide comparisons between these tests. Furthermore, the fact that some of the studies were performed in the laboratory, while others were performed in a natural setting further prevents comparisons between experiments. Finally, the wide range of values that have been found between subjects shows that there is no consistent pattern present that best describes the population as a whole (Steele & Milburn, 1987). Nevertheless, a force - time curve that best describes the general pattern of the vertical impact forces present during landing, is shown below.

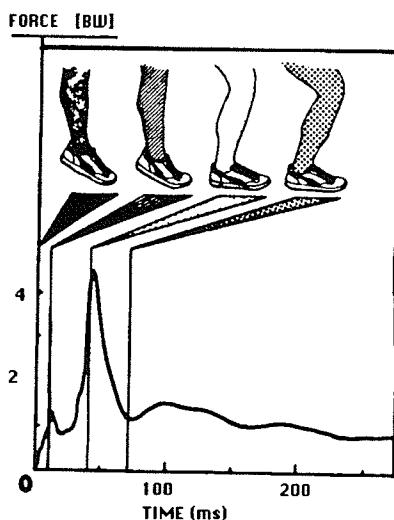


Figure 2-12 - The mean vertical GRF for a forefoot lander (Valiant & Cavanagh, 1985, p. 119).

#### Time to Impact Peak

While the heel impact produced the larger of the two vertical GRF values, McNitt - Gray (1991) found that the time from original contact to peak GRF decreased as the height of the jump increased. Furthermore, the author found that an increase in the GRF was directly related to the skill level of the athlete and to the impact velocity of the athlete. In addition, Dufek and Bates (1991) found that as the surface became harder, the time to peak impact decreased. Contrary to the results of Dufek and Bates (1991), Dickinson et al (1985) found that athletes continually alter their landing pattern in order to land jumps with the same time to peak impact.

The time required for peak impact to occur, ranges from 18 ms to 52 ms (Dickinson et al, 1985; Valiant & Cavanagh, 1985; Bobbert et al, 1987; Steele and Milburn, 1987; Panzer, Wood, Bates & Mason, 1988), depending on the height, velocity, surface, and skill of the athlete. According to a number of authors (Dickinson et al, 1985; Nigg, 1985; Nigg, 1988; and Panzer et al., 1988), the initial active muscle force does not occur until after the first 50 ms of

contact with the ground. Therefore, the forces that occur in the first 50 ms are all absorbed passively by the bones, muscles, tendons, ligaments, and cartilage (Nigg, Denoth, & Neukomm, 1981). It is this repetitive, passive impact force, and its relationship to injury that is of primary concern to the performer (Dufek & Bates, 1991).

Finally, Nigg and Morlock (1987) stated that footwear, namely running shoes, should be constructed to reduce stresses present in the first 30 to 50 ms. The reduced stress may then reduce the associated injuries such as fatigue fractures, tendinitis and cartilage damage.

#### Medial-Lateral and Braking-Propulsion GRF

Anterior-posterior GRF are the propulsive and braking forces. In heel toe running, the initial forces at impact act to stop the motion of the athlete and are the braking forces. Propulsive forces, on the other hand, tend to cause the runner to be accelerated forward (Miller, 1990). The author also states that the braking and propulsive values differ greatly from subject to subject. As a result, the force-time pattern may consist of single, double or multiple force peaks for each foot strike (Miller, 1990).

Medial-lateral forces generally contain no quantifiable characteristics that can be readily defined. The magnitude and direction are highly variable, from subject to subject, and often within individual subjects (Miller, 1990). Holden (1984) found that the greatest variability in the force curve occurred between the first 35 to 40 ms of contact with the ground. Therefore, Miller (1990) believed that it is essential to consider the direction of motion and which foot is in contact with the ground at any given instant.

While the braking and propulsive force values were not presented, graphical representation of these forces by Miller (1990), showed that the

forces were less than 1 BW. However, a study by Panzer, Wood, Bates, and Mason (1988) found the braking - propulsive forces as large as 8.8 BW. The medial - lateral forces, were also below BW for all but one study. Miller (1990) found values of 0.10 BW, Valiant and Cavanagh (1985) found values as high as 0.25 BW, but Panzer et al (1988) found medial - lateral forces as high as 2.1 BW. Therefore, for normal gait, these forces do not appear to be large enough to induce injury. The medial-lateral forces of four subjects are presented below (Figure 2-13). Note there is a large degree of variability between the peak forces and the general shape of the curves.

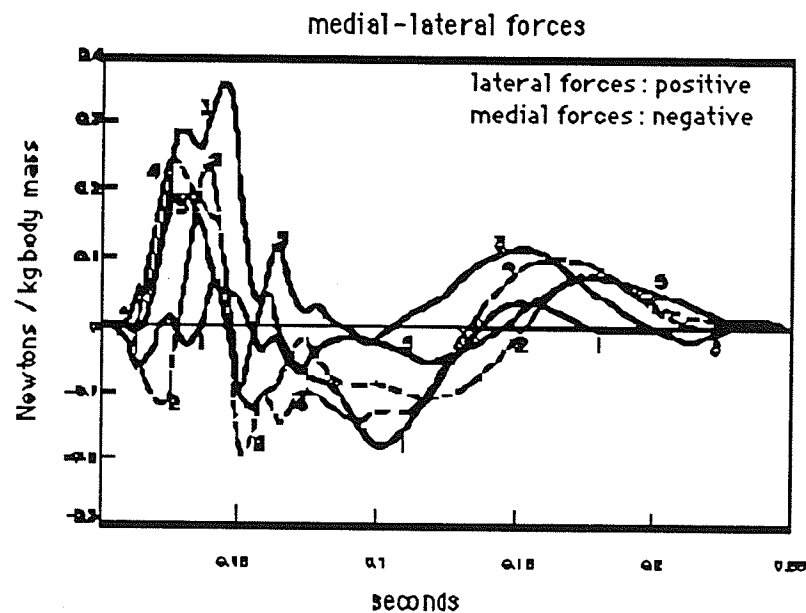


Figure 2-13 - The medial - lateral forces present for five different heel-toe footfalls while running at 3.6 m/s (Bates, Osternig, Sawhill & James, 1983, p. 184).

#### Joint Reaction Forces (JRF)

The result of landing from vertical jumps, as mentioned above, places large forces on the lower limb. As a result, these forces must be transferred from the ground, through the footwear to the athlete's body (Dufek & Bates,

1991; Steele & Milburn, 1987). The role of footwear is to reduce the GRF by absorbing the forces and reducing the stress passed to the body (Steele & Milburn, 1987; Nigg, 1988; Robbins & Gouw, 1990; Demak, 1987). In figure skating, the skate does not provide the shock absorption characteristics of normal footwear because of the attachment of blade to the underside of the boot, and a reinforced steel instep (Fassi, 1980) which prevents the shock from being absorbed by the boot. Furthermore, the heel of the boot is made of layers of leather, vinyl or thick rubber (Dainty, Cotton, & Morrison, 1978), which provide little, if any, shock absorbing characteristics. Therefore, the forces present at impact are transferred directly to the body thereby increasing the chance of injury.

The JRF values for a number of studies are located in Table 2-5. Similar to the findings of the GRF studies, the magnitude of these values vary significantly from activity to activity and from study to study.

Table 2-5 - The JRF values for the three joints of the lower limb from previous studies.

Author	Activity	Joint	Vertical JRF (BW)	Shear JRF (BW)
Smith (1975)	Jumping	Ankle Knee	7.4 24.0	2.9
Crowninshield, Johnston, Andrews, & Brand (1978)	Walking	Hip	7.0	
Burdett (1982)	Running	Ankle	13.0	5.5
Brüggemann (1985)	Gymnastics	Ankle	5.6	2.5
Ericson & Brand (1986)	Cycling	Knee		1.0
Harrison, Lees, McCullagh, & Rowe (1986)	Running	Knee Ankle	33.0 9.0	
Panzer et al (1988)	Gymnastics	Knee Hip	6.6 4.9	2.8 1.7
Skelly & DeVita (1990)	Jump Landing	Ankle	15.8	
Kaufman et al (1991)	Isokinetic Knee Exercises	Knee	4.0	1.7
Read & Herzog (1992)	Alpine Skiing	Knee		0.5

In general, the findings of Zarrugh (1981) and Brown et al. (1986) were that the JRF decrease as the joints become further from the point of force application, and these findings were supported by a number of other studies (Panzer et al., 1988; Skelly & DeVita, 1990). However, two studies that

contradicted these findings were reported by Smith (1975) and Harrison et al. (1986). In both of these cases the knee JRF was significantly greater than the ankle value. The problem associated with these studies was that since the muscles surrounding each joint absorb forces (Valiant, 1990), it seems unlikely that the JRF of the knee could be greater than the ankle.

In the vertical direction the largest force value at any of the joints (knee = 33BW, Harrison et al., 1986) was greater than the maximum GRF of 14 BW reported by Panzer et al (1988). In the horizontal direction, the maximum JRF value at any of the joints was 5.5 BW (Burdett, 1982), which was less than the maximum GRF of 8.8 BW reported by Panzer et al (1988). Therefore, from this data it is evident that the GRF are damped as the force is transferred from the ground, up the support leg.

### Moments

While the JRF and GRF values are widely publicized, the number of studies that have calculated the moments is considerably less. Table 2-6 provides a list of a majority of the moment values that are related to impact landings.

Unlike the JRF and GRF, the moment value is somewhat deceiving because the units of moments are Newton - meters. In order to obtain information from these values the moment must be divided by the moment arm length. The result is a value that is in Newtons, and this can be expressed as a percentage of body weight and is easily compared to other studies.

Table 2-6 - The maximum moments of force recorded for a number of studies.

Author	Activity	Joint	Moment (N· m)
Zernicke, Garhammer, & Jobe (1977)	Jumping	Knee	550 - 560
Pedotti, Krishnan, & Stark (1978)	Gait	Hip	74.4
		Knee	45.5
		Ankle	161.4
Bobbert et al (1986)	Counter Movement Jump	Hip	366
		Knee	279
		Ankle	266
Brüggemann (1985)	Gymnast	Ankle	345
Fukashiro & Komi (1987)	Counter Movement Jump	Hip	313
		Knee	153
		Ankle	125
	Squat Jump	Hip	183
		Knee	145
		Ankle	120
Read & Herzog (1992)	Alpine Skiing	Knee	400

Therefore, by dividing any moment by its moment arm, the force exerted on the muscles can be calculated and the force produced by the muscle is equal to this value. However, one important point is the fact that the calculated moment is only an average moment. In other words, the moment calculation assumes that during any motion, the antagonistic muscle groups are inactive and not producing any force of their own (Gagnon et al, 1987). Therefore, if the antagonistic muscle groups were active during the moment calculation the force produced in the muscles would be greater than the value produced from the moment equations. One further problem with the

calculation of moments is that the final calculated value can be over estimated or under estimated by as much as  $\pm 50\%$  (Smith, 1975).

Table 2-7 - Moment arm lengths of certain muscles and muscle groups.

Author	Muscle/ Tendon	Moment Arm (meter)
Alexander & Vernon (1975)	Achilles	0.047
Hawkins (1992)	Gluteus Maximus	0.090 (maximum)
	Biceps Femoris	0.090 (average)
	Quadriceps (knee)	0.06 (average)

#### Impact Loading and its Relation to Injury

A number of authors (Nigg, 1988; Frey & Shereff, 1988; Stacoff et al, 1988; and McNitt - Gray, 1991) believe that the high impact forces are one of the major causes of running and jumping injuries. The other variables believed to contribute to injury rate were, velocity of impact which increases the rate of loading (Frey & Shereff, 1988; McNitt - Gray, 1991), eccentric muscle contractions (Frey & Shereff, 1988; Ricard & Veatch, 1990; Bruns & Yngve, 1989), and fatigue (Dickinson et al, 1985; Nigg, 1988; and Bruns & Yngve, 1989).

Furthermore, McNitt - Gray (1991) found that landings from low heights may significantly load the passive structures of the ankle and foot. Together with the passive forces, ankle and knee forced flexion, and eccentric

muscle contractions all place increased stresses on the Achilles tendon, patellar tendon, and medial quadriceps muscles (Stacoff et al., 1988). Furthermore, Fukuda (1988) found that a hard landing surface increased the rate of energy absorption in the knee extensors, and thus increased the load on the knee musculature. All of these situations tend to increase the impact loads, which in turn increases the chance of injury.

Therefore, regardless of whether the impact forces are above or below the threshold limits of the individual tissues, the impact can have a serious effect on the performance of sports skills. High-performance athletes who continually perform repetitive loading skills may be subject to injury. Therefore, it is important to study all aspects of the skill, and to obtain an accurate diagnosis when an injury does occur (Hanks et al, 1989). Therefore, the following section includes the ultimate tissue limits and fatigue effect as they relate to the occurrence of acute and overuse injuries.

### Bones

According to Nordin and Frankel (1989), bones are irregular in shape and undergo tension, compression and torsion in everyday activities. As a result, the bone must withstand a number of different forces in small periods of time. Nordin & Frankel (1989) used normal gait and jogging to stress the changing forces during the support phase of one foot. "...during normal walking the stresses were compressive during heel strike, tensile during the stance phase, and again compressive during push-off" (Nordin & Frankel, 1989, p. 15). However, during jogging the forces change with the high compressive forces occurring at toe touchdown, and high tensile forces at push-off.

The forces required to cause acute fractures to the bones are located in

Table 2-8. While these are the maximum forces sustainable for the bones listed, stress fractures and/fatigue fractures occur at levels lower than those listed and depend on the size of the load, and the frequency with which it is repeated (Carter & Hayes, 1977b; Martin & McCulloch, 1987; Oakes & Parker, 1990; Chaffin & Andersson, 1991).

Table 2-8 - The bones (where applicable) and their ultimate stress levels.

Author	Bone	Ultimate Stress (MPa)	Direction of Load
Frost (1967)		27.6	shear
		82.8	tensile
		103.5	compressive
Evans (1973)	cortical (endurance limit)	27.6	tensile
	cortical (ultimate strength)	82.8	tensile
Carter & Hayes (1977b)	beef femur	127.8	tensile
	beef femur (after repetitive loading)	117.5	tensile
Le Veau (1992)	femur	172	tensile
	tibia	140 - 174	tensile
	fibula	146 - 165.5	tensile
	femur	170 - 209	compressive
	tibia	213	compressive
		50 - 100 132 - 181	shear bending

In order to compare the results of a number of studies, it is important to have an approximation of the cross - sectional area of the bone in question. According to Viano (1986), "if the force applied to a structure is divided by the original cross - sectional area, this is a measure of local stress on the material and is independent of the cross - sectional size of the sample" (p. 38). In other words, by dividing the force by the cross - sectional area, the force per unit area is normalized across all subjects and forces are comparable from subject to subject.

One problem with using the cross sectional area of bones is the lack of published data on bone dimensions. There have been a number of articles that refer to the cross - sectional area of bone, but do not provide the exact values for these calculations (Churches, Howlett, Waldron, & Ward, 1979; Moyle & Bowden, 1984; Chu et al., 1986; Viano, 1986; Ackland, Henson & Bailey, 1988; MacDougall et al, 1992). There are a few articles, however, that do provide enough information to allow the cross - sectional area to be calculated.

Ackland, Henson, and Bailey (1988), provide the cross - sectional area for six different positions of the leg. These start at the knee axis and end at the ankle. However, these cross sectional areas include tibia, fibula, and the surrounding soft tissue. While the article does not directly supply the bones' cross sectional area, the percentage of total cross sectional area taken up by the tibia and fibula was provided. At the knee axis, the overall cross - sectional area was 117.35 cm<sup>2</sup>, and 46 % of this area was bone. Therefore, the cross - sectional area of bone was 53.98 cm<sup>2</sup>. Midway down the shaft the overall cross - sectional area, percent bone, and bone cross - sectional area were 70.46 cm<sup>2</sup>, 10 %, and 7.05 cm<sup>2</sup> respectively. At the ankle these same values were 47.66 cm<sup>2</sup>, 45 %, and 21.45 cm<sup>2</sup> respectively.

In a similar study, Mungiole and Martin (1990), found that the percentage of the cross sectional area for the knee axis, mid shank, and ankle were 39 %, 11 %, and 36 % respectively. The proximal and distal cross - sectional areas were smaller than those of the previous study, while that of the mid shank cross - sectional area was larger. As a result, the cross - sectional areas for the knee axis, mid shank, and ankle were 45.77 cm<sup>2</sup>, 7.75 cm<sup>2</sup>, and 17.16 cm<sup>2</sup> respectively.

The cross sectional area for the femur was calculated by Overend, Cunningham, Paterson, and Lefcoe (1993). In this study, CT scans were performed on the femur and the area was found to be 8.5 cm<sup>2</sup> in the mid-shaft.

While the previous studies provide the cross sectional area of the leg and thigh bones, others such as Chu et al (1986) provide information that allows the cross sectional area of bones to be estimated. The cross sectional area can only be estimated because the assumption made was that the bones were cylindrical, when in fact they are not. However, using this assumption, with a diameter of the tibia being 3.5 cm (Chu et al., 1986), and the cross sectional area of a circle being ( $\pi r^2$ ) (Van Heuvelen, 1982), the resulting cross - sectional area of the tibia was 9.62 cm<sup>2</sup>.

While the forces mentioned above may not be sufficient to cause acute fractures in bones, the repetition of these forces may still cause stress fractures (Ting et al, 1988; Hanks, Kalenak, Bowman, Sebastianelli, 1989; Nordin & Frankel, 1989). The ability of the body to withstand these forces, without sustaining damage depends on the "... amplitude, temperature, density and microstructure of the tissue" (Hughes, 1985, p. 96).

On the other hand, stress fractures are an overuse injury that occur in the long bones of the athlete. The mechanism that causes bone tissue to

become susceptible to overuse injuries is very complicated. To simplify, Wolff's Law states that bone is deposited where needed and removed from where it is not needed (Chaffin & Andersson, 1991). However, when bones sustain repeated forces, the amount of osteoclast and osteoblast activity increases (Hughes, 1985). While this process takes place, the osteoblast activity lags behind that of the osteoclast activity and the bone becomes weakened and more susceptible to injury (Taunton, Clement, & Webber, 1981; Hughes, 1985). As a result, the initial remodeling of bone leads to a decrease in the ultimate strength of the bone and increases the susceptibility of the bone to injury (Carter & Hayes, 1977a). However, if the activity is kept within the tolerance level of the bone's reconstruction rate, the bone will remodel itself and become stronger than it was before exercising (Nordin & Frankel, 1989).

Overuse injuries are produced by the repeated application of a force lower than that required to create fracture from a single loading situation (Martin & McCulloch, 1987). There are three general causes of stress fractures: the amount of the load; the number of repetitions; and the frequency of the loading (Oliver, 1985; Chaffin & Andersson, 1991). However, Bruns and Yngve (1989) were more specific with their description of the injury. According to these authors, there were five common reasons for stress fractures:

1. An increase in the number of repetitions.
2. Initiation of a new strenuous activity.
3. A change in speed or gait.
4. Resumption of an activity following a period of absence.
5. A change in equipment or running surface. (p. 203)

As can be noted in point number one above, one cause of stress fractures that is often overlooked is the number of repetitions that are performed. Figure 2-14 is a graphical representation of the relationship between the number of repetitions and the impact load. It is obvious that from this graph that the athlete is in considerable danger when the impact load is large, however, if the impact forces are repeated often enough the athlete may be in the same amount of danger.

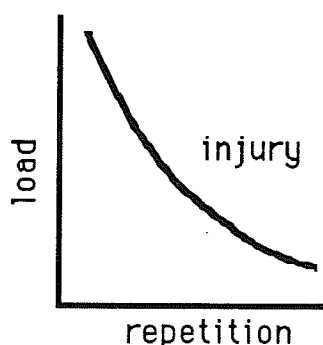


Figure 2-14 - The relationship between the load and the number of repetitions required to cause failure (Nordin and Frankel, 1989, p. 19).

Martin and McCulloch (1987) showed that a runner places  $10^6$  cycles on the bones of the leg during a period of 100 days. In figure skating the athlete performs 20 - 100 jumps every day. Therefore, the number of days required to reach  $10^6$  cycles would be 1000 days. However, if the impact forces were greater than those of the previous running studies, then the number of repetitions required for fracture to occur would be decreased.

Muscle fatigue is another major cause of stress fractures in bones. According to a number of authors (Sprague & Mann, 1983; Martin & McCulloch, 1987; Nigg, 1988; Bruns & Yngve, 1989; Chaffin & Andersson, 1992), the muscles are the main shock absorbing structures in the body, and

when they become fatigued the forces are transferred to the bones. An example of the fatigue effect was described by Dickinson et al. (1985). According to the author, the magnitude of the force transferred to the body increases from 186 % BW to 203 % BW after the muscles became fatigued in running. Furthermore, it has been suggested that muscle fatigue also leads to altered gait, which may increase and/or alter the load placed on the bones and induce stress fractures (Hughes, 1985; Bruns & Yngve, 1989). Figure 2-15 represents the general progression from muscle fatigue to the initiation of stress fractures.

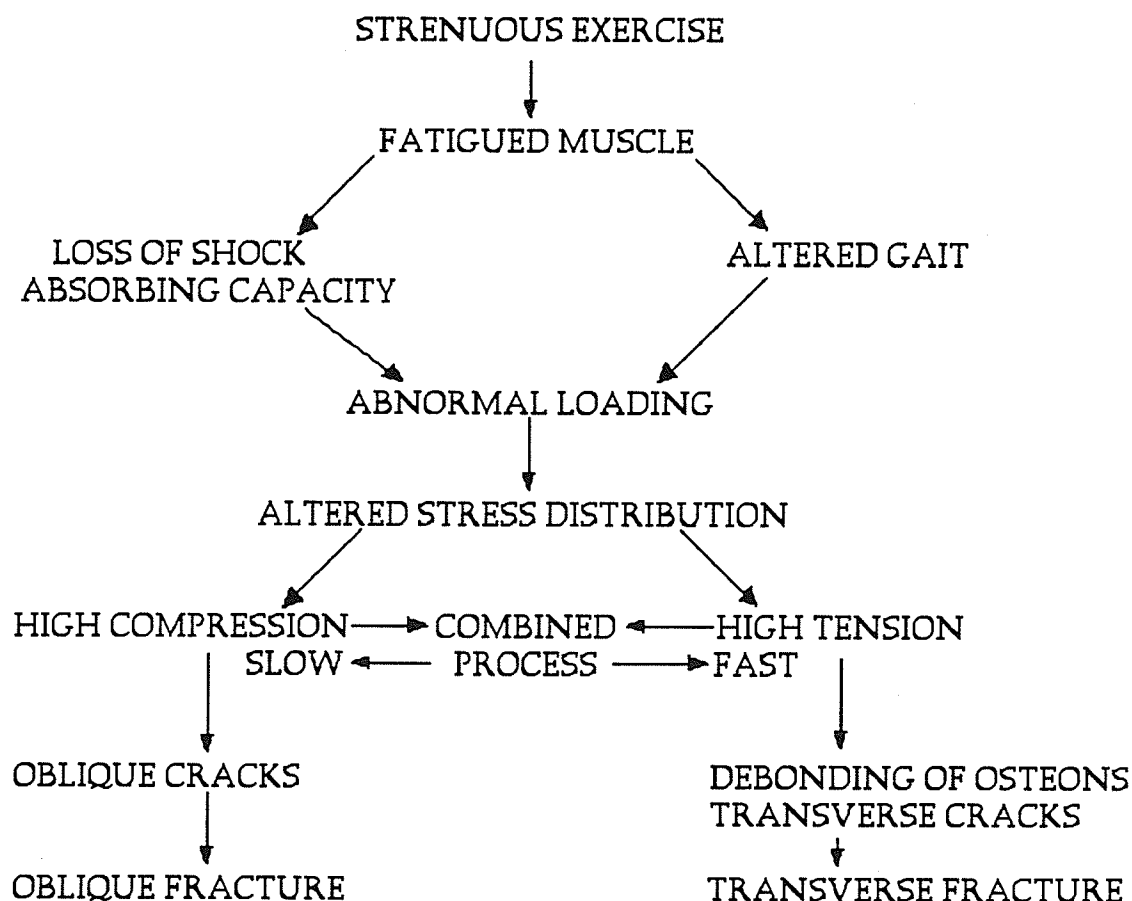


Figure 2-15 - The theory of muscle fatigue as a cause of fatigue fracture in the lower extremities. (Nordin & Frankel, 1989, p. 19)

Another cause of stress fractures could be related to the combination of the GRF and the forces exerted by the muscles. The bones of the lower limb are not straight, and they do not support all of the body's weight directly down their longitudinal axis. Figure 5-16 shows the weight bearing line for both of the major weight bearing bones of the lower limb. In each case, the force line does not follow directly in line with the bones, but instead passes outside the actual structure of the bone. As a result, normal loading from impact causes the bones to bend, and this bending is intensified by the contraction of muscles. According to Figure 5-16, the tibial bending forces cause compression on the posterior surface of the tibia, while the anterior surface is placed under tension. As a result, the tibia is susceptible to anterior tibial stress fractures (Bruns & Yngve, 1989) because the bone is weaker in tension than compression (Le Veau, 1992). The femur has a bending force in the medial - lateral direction, and this creates tension laterally and compressive forces medially (See Figure 2-16b).

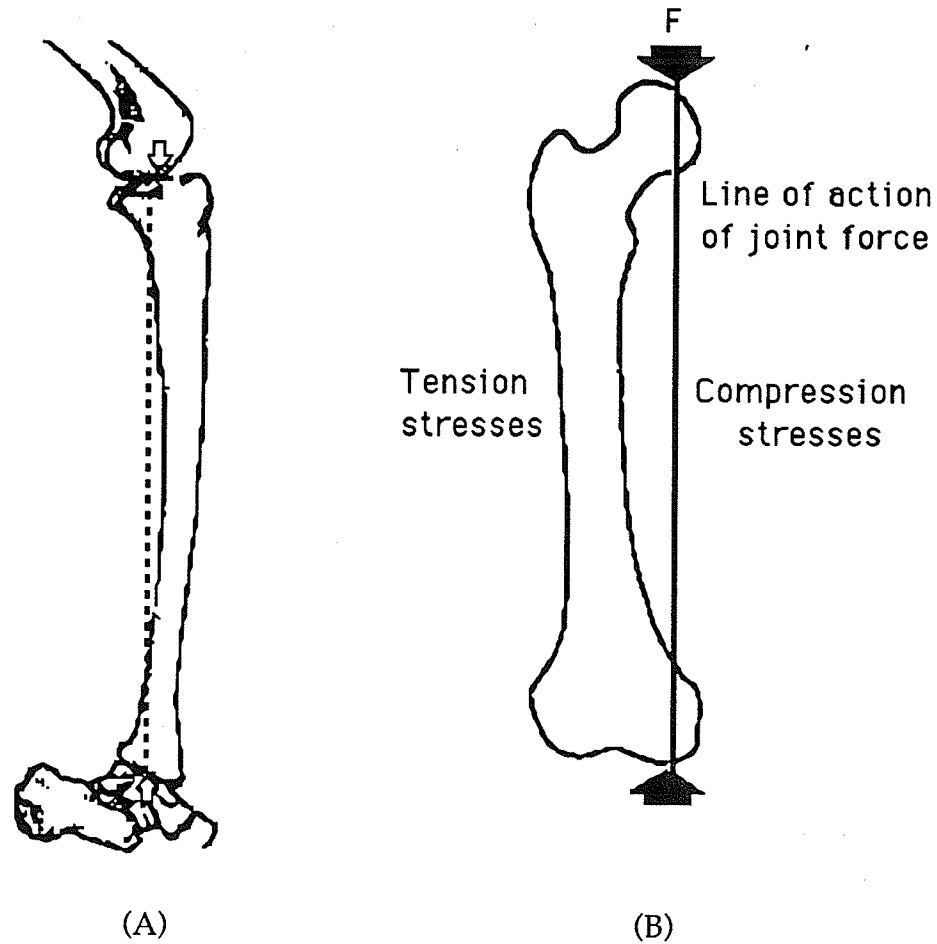


Figure 2-16 - (A) The line of force on the tibia places compression forces on the posterior surface of the tibia, and tension forces on the anterior surface (modified from Bruns and Yngve, 1989, p. 209); (B) The line of force for the femur, which places compressive forces medially and tension forces laterally (modified from Harrington, 1982, p. 41).

While these are the general factors that produce stress fractures, Cramer and McQueen (1990) presented other factors that may specifically predispose the figure skater to stress fractures.

- I. The need to be on deep edges, especially inside edges.
- II. Position Requirements
  - A. Hyperlordotic back
  - B. Extended knee and pointed toe, free leg
  - C. Extended knee, spinning

- D. Flexed knee, spinning
  - E. Abducted hip, camel spin
  - F. Stroking position
  - G. Hyperflexed ankle, spinning
- III. Jumps
- A. Use of picks puts pressure on ankle, foot, toes, knee.
  - B. Speed, height, and revolutions make both good landings stressful.
- IV. Skating programs are maximally aerobic. Anaerobic bursts are frequently superimposed. Fine psychomotor skills must be maintained when skater is maximally fatigued. (Cramer & McQueen, 1990, p. 255)

Finally, osteoporosis may be another cause of stress fractures found in figure skaters. Osteoporosis is the reduction in the amount of bone that is present in a body (Nordin, 1983), which increase in the susceptibility of the athlete to stress fractures due to this reduction of bone. Cramer and McQueen (1990) believe that the requirement for the female athlete to be thin and the exercise induced amenorrhea increases their potential for osteoporosis. While this may be true, there are also other causes for osteoporosis that are not directly related to females. Included in these causes are calcium deficiency; chronic acid base imbalance; calcium loss due to nocturnal fasting; a defect of the intestinal absorption of calcium; and an imbalance of calcium to phosphorus (Spencer, Kramer, Gatza, & Lender, 1978). As a result, all figure skaters are susceptible to bony overuse injuries because of any of these characteristics which result in the weakening of bone.

Therefore, since there are a large number of causes for stress fractures, it seems likely that any athlete that sustains repeated impact forces is in danger of becoming a victim of stress fractures.

### Cartilage

While impact forces are transmitted up the body the bones, muscles,

and cartilage are subject to the same forces. The joints of the body are separated by cartilage, and its purpose is to distribute loads over a greater area and to decrease stress between adjacent bones (Nordin & Frankel, 1989).

However, Radin and Paul (1970), found that the shock absorbing characteristics of cartilage and the synovial fluid are very small.

Damage to the cartilage is believed to occur in two different situations. Radin and Paul (1970) believed that the damage was the result of the changes that occur to the underlying bone tissue during impact situations and normal temporal changes. The second method by which cartilage can be damaged occurs from normal temporal changes of the surfaces. There are two types of wear, interfacial and fatigue wear. The first can be subdivided into adhesive and abrasive wear (Nordin & Frankel, 1989). Adhesive wear occurs when the two surfaces stick together, and are torn apart during motion. Abrasive wear is the scratching of a soft surface by a harder one. However, Nordin and Frankel (1989), believe that these two types of wear are rare in the human body.

Fatigue wear on the other hand, occurs by "... the accumulation of microscopic damage within the bearing material under repetitive stressing" (Nordin & Frankel, 1989, p. 51). This stress can occur by high loads being applied over short periods of time or light loads applied over extended periods of time (similar to the cause and occurrence of stress fractures). Repetitive, high loads have been shown to cause the surface of the cartilage to split, and/or show signs of increased cartilage layer erosion (Nordin & Frankel, 1989).

Overuse injuries to bone at the joints has already been covered in the previous section, however, overuse of the cartilage and the damage that results must be explored. During repetitive loading, the water that is held

within the cartilage's matrix is slowly extruded. As a result, the cartilage becomes more susceptible to injury because the viscous component of damping is reduced, and the matrix of the cartilage becomes exposed. This exposure makes the cartilage matrix susceptible to mechanical deformation and degradation (Serink, Nachemson, & Hansson, 1977). Once minor damage has been done to these structures, they become stress raisers and accelerate the rate at which the damage occurs. Furthermore, a damaged matrix allows the interstitial fluid to escape quicker than usual and further increases the chance of injury (Armstrong, Mow, & Wirth, 1985). Finally, once the muscles become fatigued due to repetitive loading, more force is transmitted to the joints, increasing the compressive forces on the cartilage and increasing the chance of damage (Armstrong et al., 1985).

Finally, once an injury has occurred at one joint, there is a considerable difference in the load at the joints that are proximal and distal to the injured one. The pathological damage at one joint changes the acceleration of the limb segments, increases the joint forces, and decreases the injured joint's ability to attenuate these forces. Furthermore, abnormalities at one joint caused increased forces to the proximal and distal joints making them more susceptible to injury (Chu et al., 1986). Therefore, it is important to recognize joint injuries as soon as possible in order to initiate the appropriate rehabilitation and to minimize any further damage.

#### Ligament and Tendon Injuries

In sporting activities, the main cause of injury to the ankle ligaments is the result of sudden inversion usually causing damage to the anterior talofibular ligament (Arnheim, 1985). At the knee, the major cause of damage is a combination of axial loading, abduction/adduction, and

internal/external rotation (Harrington, 1982; Andriacchi et al., 1987). The ligaments of the hip are generally damaged as the result of a violent twist caused by another participant or from impact forces (Arnheim, 1985).

Injury to soft tissue can occur by stressing or stretching the membranes past their limits. Muscles are most susceptible to rupture during eccentric contractions. This type of muscle activity is caused by an external force acting against the force generated by the muscle, and the muscle, in turn, acts to control the movement (Chaffin & Andersson, 1991). According to Garrett, Safran, Seaber, Glisson, and Ribbeck (1987), eccentric muscle contraction opposes a stretch, and therefore the stimulated muscle can obtain a greater force to failure. Furthermore, injuries occur because fibers near the myotendinous junction are less deformable (Chaffin & Andersson, 1991). Therefore, the portions of the muscle fibers that are less deformable are more susceptible to injury.

Table 2-9 - The ultimate stress capability of the Ligaments and tendons of the lower limb.

Author	Tendon/Ligament	Ultimate Stress (MPa)
Smith (1975)	Patellar Tendon	49.1 - 98.1
Burdett (1982)	General	34 - 147
Le Veau (1992)	Various Achilles	19.1 - 150 34 - 55

### Training Effect

Bone geometry also plays an important role in the prevention of injury due to impact. The geometrical configurations that are important to bone are the cross sectional area, length, and distribution of the mass about a neutral axis (Nordin & Frankel, 1989). A large cross-sectional area, and an extensive mass distribution about the neutral axis increases the strength of the bone. Furthermore, a short bone tends to be stronger than a long bone. Optimizing all three of these factors will reduce the risk of injury because of the increased force required to cause a disruption of the tissue.

All studies that have been mentioned previously deal with the ultimate stress levels calculated from cadaver tissues or animal tissues. It is generally agreed that with physical activity, tissues become stronger, and the cross sectional area increases (Churches et al., 1979; Martin & McCulloch, 1987; Nordin & Frankel, 1989; Tipton & Vailas, 1990; MacDougall et al., 1992). For example, Churches et al. (1979) noticed that the cross sectional area of sheep bone increased by 1.3 - 17 % when a force was applied over a period of time. Another example of increased bone cross sectional area was presented by MacDougall et al. (1992). In this study the cross sectional area of the bone was normalized to body weight, and the results showed that with increased running mileage, the cross sectional area increased. Tipton and Vailas (1990) found increases in rat ligaments, tendons, and cartilage as the result of chronic physical activity. The increase in strength for the ligaments ranged between 12 - 56 % and that of the tendon ranged between 25 - 62 %. The cartilage, on the other hand, increased in thickness by 10 %. Therefore, with this information, it is obvious that there will be a decrease in the calculated stress of the tissues because the area is increased and the force is distributed over a larger area.

While loading rate is not a training effect, the fact that figure skaters become more successful at landing complicated jumps with practice justifies its inclusion. A second reason that loading rate can be included in this section is the fact that with increased training, the height of the jumps increased because of the increase of muscle strength (Tipton & Vailas, 1990).

According to McElhaney (1966), the ultimate compressive strength of an embalmed human femur ranged from an average of 21,800 - 46,000 psi as the rate of loading increased from 0.001 - 1,500 inches per second. These same findings were found by a number of other authors and is known as the viscoelastic property of tissues (Evans, 1973; Butler, Grood, Noyes, & Zernicke, 1978; Churches et al., 1979; Currey, 1984; Soderberg, 1986; Nordin & Frankel, 1989). Therefore, the increased strength of the tissue, as the result of training and loading rate, further decreases the chances that the figure skater will injure themselves during the landing of a Triple Toe Loop.

#### Landing Strategies and Injury Reduction

As mentioned previously, exercise increases the size of biological tissues, which decreases the stress on the tissue, and thereby decrease the chance for injury. Dufek and Bates (1990) describe another method of attenuating forces

The ability of the performer to attenuate impact forces and absorb energy through technique modification becomes an important issue relative to safe and successful performances.  
p.55

The most important method of modifying the landing technique would be to increase the range of motion of the joints (Keohane, 1978;

Mizrahi & Susak, 1982; Panzer et al., 1988 McNitt - Gray, 1991). Landing with a large range of motion at the joints requires more time than a short, limited range of motion landing which imparts larger forces (Lees, 1981). Therefore, using the impulse - momentum relationship, to change the velocity ( $v_i$ ) from a given value to zero ( $v_f$ ), an impulse must be applied. However, since the impulse is equal to the product of force (F) and time (t), the longer the force is applied, the smaller the force will need to be to stop the downward motion. In other words,

$$F \cdot t = mv_f - mv_i \quad (2-1)$$

According to this equation, if the initial velocity was to remain constant and the final velocity was to be zero, then by increasing the time through which the force was applied, there would be an identical drop in the magnitude of the applied force. Therefore, by increasing the range of motion, the time over which the force works can be increased and the force on the human tissues would be reduced. Thus the landing technique influences the impact loads as well as the tension in muscles and tendons. (Stacoff et al., 1988).

Of all the joints in the body, the knee was the main force absorber when landing in a sporting event (Winter, 1983; Panzer et al., 1988). According to Keohane (1978), in figure skating the knee is also very important in absorbing forces. However, when landing in figure skating, not only does the knee flex but there is limited flexion at the ankle (Smith, 1990), and considerable flexion at the hip. McNitt - Gray (1991) described the flexion of the hip, knee and ankle as a way to absorb forces, however, she qualified the force absorbing capacity of each joint. The study showed that hip and knee

flexion play a major role in force absorption, while the ankle plays only a minor role. Stacoff et al (1988) and McNitt - Gray (1991) concluded that by altering the landing technique, GRF and joint angular velocity could be reduced, which in turn would reduce the chance of injury.

In other sports, the landing is just as essential to a good performance as it is in figure skating. For example, the landing in gymnastics must include a straight back, and as little flexion in the knees as possible, if a good score is to be achieved (McNitt - Gray, 1991). This type of landing could seriously injure an athlete because the force applied would need to be so large since the time through which the force acts is so short. For this reason, the landing technique is very important to the health of the athlete. With the large range of motion at the joints in figure skating, the landing seems to be acceptable to the judges, and yet still supplies the range of motion necessary to significantly reduce the forces on the body. Future studies should consider the landing of other sports skills and recommend changes to the governing body that may reduce the chance of injury to their athletes.

A second method, presented by Dickinson et al (1985) and Gross and Nelson (1991), was landing on the toe and not allowing the heel to come into contact with the ground. As a result the investigators found a significant decrease in the vertical GRF. Furthermore, this type of landing increased the time to peak impact, thereby reducing the force exerted by the muscles per unit time. As a result, Dickinson et al (1985) stated that this method of landing requires further research to decide if it is less dangerous for the body than landings with heel contact.

Modifying the activity of the non-reflex muscles, and pre-programming the muscles during the early phase of impact (Mizrahi & Susak, 1982) performs two functions, it prevents heel contact (Mizrahi &

Susak, 1982; Dickinson et al, 1985; Gross & Nelson, 1988) and reduces the passive forces. If the subject actively concentrates on preventing the heel from contacting the ground, the resulting GRF sustained by the body has only one force peak which is smaller than an impact with the heel (Bobbert et al., 1987; Gross & Nelson, 1988). If this same procedure were used at the knee and hip, the muscles would be ready to absorb the impact forces. Furthermore, this type of landing would reduce the passive impact forces because the muscles would already be active, and the reflex mechanism would not be needed to initiate the contraction of the muscles (Mizrahi & Susak, 1982).

The fourth way to reduce injury would be to alter the heel height of the footwear. The major reason cited for a raised heel is to prevent over stretching of the soft tissue, and stress to the gastrocnemius - soleus complex and the Achilles tendon (Drez, 1980; Frey & Shereff, 1988; Cook, Brinker, & Poche, 1990). In other words, the heel is stopped before the Achilles tendon has reached its maximum length, thereby preventing the rupture of the tendon by means of undue tension during landing. Steele and Milburn (1987) studied netball shoes, and believed the raised heel was advantageous in reducing stress, but they also believed that the heel should have some degree of cushioning. A cushioned heel is not possible in figure skating due to the attachment of the blade, however, the two inch raised heel is the norm on figure skates (Fassi, 1980). Therefore, the raised heel will act to reduce stretch and stress placed on the tendon, and may reduce the chance of injury.

Finally, by altering the technique of the landing, the athlete could use all the body's segments to aid in the absorption of the impact forces. According to Lees (1981), each segment contributes to the absorption of forces by controlling their acceleration, which is directly related to the acceleration of the whole body's CG and is related to the force. Figure 2-17 is a simple

example of how the segments work together to absorb the impact forces of a landing from a jump.

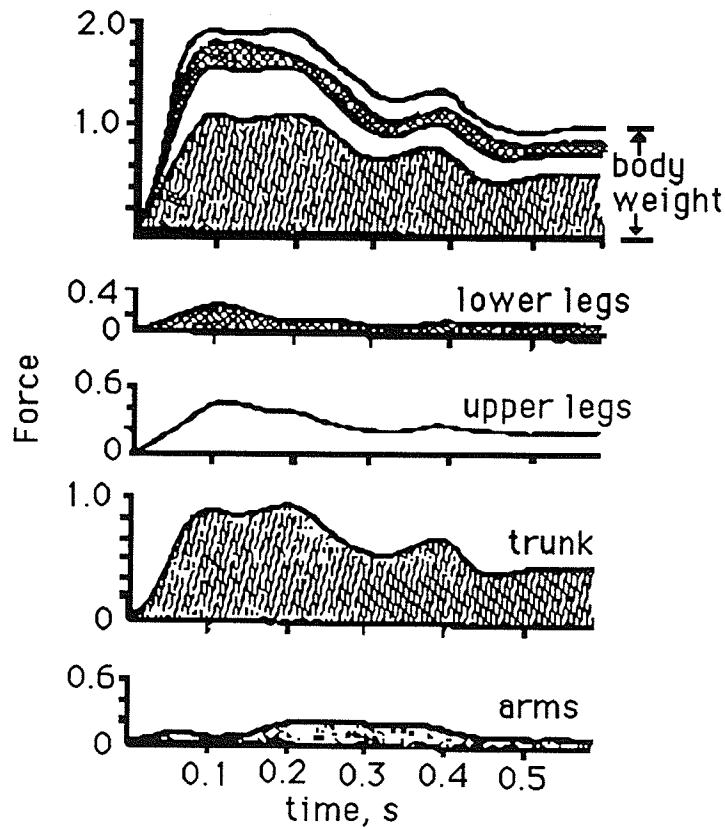


Figure 2-17 - Segmental contribution to the landing from a jump with the top graph being the representation of how all segments work together to absorb the forces (Lees, 1981, p. 209).

### Mechanical Aspects of Figure Skating

#### Force

There are three laws that apply to the concept of forces, and they were all presented by Newton (Dyson, 1978). The first law states that " a body remains in a state of rest or of uniform motion unless it is acted upon by some other body." (Rasch & Burke, 1978, p. 115). This is known as the law of

inertia, and the inertia or resistance to change in motion is proportional to the mass of a body (Dyson, 1978). In other words, the heavier an object is, the greater the force required to change the body's motion.

According to Kreighbaum & Barthels (1985), "... a force is something that causes or tends to cause a change in the motion or shape of an object of body" (p. 68). To further detail their explanation, Kreighbaum & Barthels (1985) list four characteristics that are unique to forces: magnitude, direction, point of application, and line of action.

The units that are used to record the force are  $\text{kg}\cdot\text{m}/\text{s}^2$  or Newtons (N). The equation used to calculate force is:

$$F = m \cdot a \quad (2-2)$$

where, 'm' is the mass of the body in (kg), and 'a' (in  $\text{m}/\text{s}^2$ ) is the linear acceleration (Hay, 1985).

In sport, forces are used to slow down, stop, or increase the speed of a body or implement (Dyson, 1978). According to Dyson (1978), a force cannot be seen directly, instead only the effect a force has can be seen, felt and measured. Therefore, all motions produced in athletics are the result of forces, which are produced by muscle tension, gravity, friction, GRF and air resistance (Dyson, 1978).

The third Newtonian law of motion, states that for "every action there is an equal and opposite reaction; or the mutual actions of two bodies in contact are always equal and opposite in direction." (Dyson, 1978, p. 31). However, although the two forces are equal and opposite in direction, they do not necessarily cancel each other out because the forces occur in different bodies (Dyson, 1978). An example presented by Dyson (1978) was the firing of

a gun. The explosion caused by the bullet pushes back against the gun, while the gun pushes the bullet forward. The forces are equal and opposite, but they do not cancel each other because movement was present in both the bullet and gun. If a maximum force was to be exerted by a body, the athlete would have to be in firm contact with the ground or some non-moveable surface (Dyson, 1978).

In figure skating the athlete must first overcome Newton's first law of motion (inertia), by applying a force to the ground. In other words, the muscles produce a force, which is applied to the ice, and is returned to the skater according to Newton's third law of motion. As a result, the body will begin to accelerate linearly along the ice. When a jump is to be performed, the skater must again apply a force to the ice, this time in a more vertical direction, in order to overcome the force of gravity. The body will then accelerate vertically in proportion to the force applied to the ground.

### Torques

Moments (or torques) are the angular equivalent of linear forces. They have both magnitude, and direction and tend to cause rotation of a body around an axis (Kreighbaum & Barthels, 1985). Furthermore, both torques and forces cause a body to be accelerated (Nordin & Frankel, 1989). According to Dyson (1978) a torque is produced by the application of a force at some distance from an axis of rotation. As a result the force causes the body or segment to rotate about this axis.

...it is important to note that the distance from the line of action of the force to the axis - the lever arm, ... - must be measured along a perpendicular, i.e. at right angles to the direction of the force. (Dyson, 1978, p. 75).

In the human body torques are produced by the muscles. For each movement, the muscles must produce a force at a distance from the joint which they are trying to move or control (Kreighbaum & Barthels, 1985). In figure skating there are a number of torques that are produced, however the ones of interest for this study are those associated with a controlled landing of a jump (ie. the ability to decelerate and control the CG by eccentrically contracting the muscles).

A second situation in which torques are used in figure skating is the initiation of a rotation during jumping. A torque is applied at a distance  $d_{\perp}$  from the axis of rotation, which causes the body to rotate. In the diagram by Kreighbaum & Barthels (1985), torque is produced by the planting of the toe pick into the ice, and the subsequent flexion of the hip (Figure 2-18). As a result, the lower limb's action initiates the body's rotation about its longitudinal axis, and the skater performs the required number of rotations.

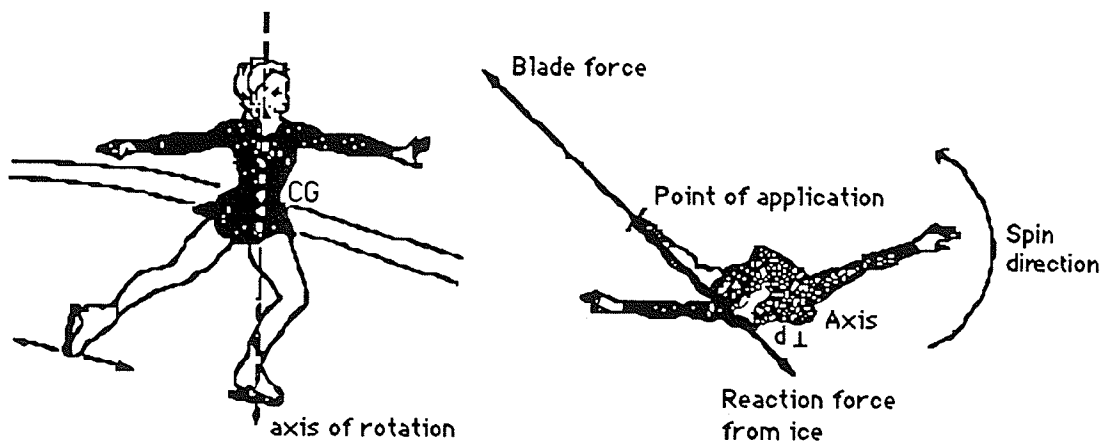


Figure 2-18- The production of torque by the use of a toe during the jumping motion. Note:  $d_{\perp}$  is represented by the solid white line from axis of rotation to the line of force (Kreighbaum & Barthels, 1985, p. 489)

## Frictional Forces

Friction is defined as the force created between two contacting surfaces that rub or slide past one another (Kreighbaum & Barthels, 1985). Friction always acts parallel to the surface and varies according to the nature of the surfaces, the force pushing the surfaces together, and the motion between the surfaces (Dyson, 1978). The area of contact between the surfaces has no bearing on the frictional forces present between the two surfaces (Dyson, 1978).

The equation for the frictional force is the product of the normal force ( $F_{\perp}$ ) and the coefficient of friction ( $\mu$ ) between the two surfaces (Kreighbaum & Barthels, 1985). In other words, the equation is

$$F_f = \mu F_{\perp} \quad (2-3)$$

The friction between two surfaces is necessary for stability and to allow movement across the ground (Dyson, 1978).

In speed skating the coefficient of friction between the ice and the blade ranges from 0.003 to 0.007 (Jobse, Schuurhof, Cserep, Schreurs, & Koning, 1990), while Kobayashi (1973) found a value of 0.005. Therefore, using the maximum coefficient of friction and the average weight for a male skater (mass of 66.5 kg, according to Brock & Striowski, 1986), results in a frictional force of  $[0.007 \times (66.5 \text{ kg} \times 9.81 \text{ m/s}^2)] = 4.57 \text{ N}$ . Therefore, since this value is so small, ice-blade frictional forces can be considered negligible in figure skating. Since kinetic friction is negligible (Jobse et al, 1990), and friction is required for stability (Dyson, 1978), skaters must use an alternative method to provide stability. According to Jobse et al (1990), the sharp edge of the blade cuts a groove in the ice, and it is this process that provides the stability for the

skaters and not the friction.

Frictional force also occurs between the joint surfaces. Nordin and Frankel (1989) reported an extremely low coefficient of friction of approximately 0.02 between joint surfaces. As a result, Zajac and Gordon (1989) believe that frictional forces are negligible and should not be included in the dynamic force and moment equations.

### Inertia and Moment of Inertia

As stated in Newton's first law of motion, inertia is the resistance of a body to motion or change in motion (Rasch and Burke, 1978). Moment of inertia (I) is the angular equivalent, and is determined by the product of the mass and the square of the distance that the mass is located away from the axis of rotation (Hay, 1985). The equation used to calculate a segments I is:

$$I = mr^2 \quad (2-4)$$

Therefore, in order to calculate the entire body's I, the mass and radius<sup>2</sup> of each segment must be calculated about an axis of rotation (Hay, 1985).

Changing the axis about which a body rotates, and calculating the body's new I can be performed by using the parallel-axis theorem. In other words, first the body must be divided into a large number of small particles, each with a mass (m) and a perpendicular distance (r) from the axis of rotation. Secondly, the moment of inertia of the entire body will equal the sum of all the products between each particles mass and the square of the perpendicular distance (Le Veau, 1992). The equation used to calculate I about any axis is:

$$I_a = I_{CG} + md^2 \quad (2-5)$$

where  $I_a$  is the I about the axis (a),  $I_{CG}$  is the I of any given segment, and  $md^2$  is the product of the mass and its squared distance to the axis of rotation. The body's total I is then calculated by the sum of the segmental I (Hay, 1985).

In figure skating, the  $I_a$  of the skater is continually changing. While airborne, the skater has his/her arms tucked in tight to the trunk, thereby reducing the  $I_{CG}$  by decreasing the distance of the segments from the axis and reducing the  $md^2$  term. However, prior to landing the skater spreads out the upper and lower limbs, increasing the body's total I and therefore decreasing the angular velocity. The increase in I prior to landing corresponds directly to an equal decrease, by exactly the same factor, in the angular velocity of the body resulting in an appropriate landing (Aleshinsky, 1986; Podolsky et al, 1990).

### Impulse - Momentum

According to Kreighbaum and Barthels (1985), momentum is the measure of the relationship between a body's resistance to change in motion and its velocity. Linear momentum can be measured by finding the product between the mass of the body and the velocity with which this body is moving. Because momentum is the product of a scalar (mass) and a vector quantity (velocity), momentum is a vector quantity (Kreighbaum and Barthels, 1985). Furthermore, the total momentum of a body will remain unchanged unless an external force was applied to the body. This is known as the Law of Conservation of Momentum (Hay, 1985).

Linear impulse, on the other hand, is the product of a force and the time through which the force is applied (Kreighbaum and Barthels, 1985). As a result, a force applied over time causes the body receiving the force to

change velocity. In any sporting event, an impulse can be obtained by producing a small force over a long period of time, or a very large force acting for a very short time (Dyson, 1978).

While an impulse creates a change in a body's velocity, and momentum is the resistance to change in motion of a body, these two concepts are closely related. According to Dyson (1978), Rasch and Burke (1978), Hay (1978), and Kreighbaum and Barthels (1985), the impulse and momentum are so closely related that an impulse is equal to the change in momentum of a body. In order to better understand this concept, Kreighbaum and Barthels (1985), reported the alteration of Newton's second law of motion to obtain the impulse-momentum relationship. The step shown below resembles those followed by Kreighbaum and Barthels (1985). First, Newton's second law of motion was identified.

$$F = ma$$

However, acceleration (a) is equal to the change in velocity of a body per unit time

$$a = \frac{(v_f - v_i)}{t}$$

When this was substituted back into the force - acceleration relationship the equation became

$$F = m \frac{(v_f - v_i)}{t} \quad (2-6)$$

rearrangement of the equation produced the impulse-momentum relationship

$$F \cdot t = mv_f - mv_i \quad (2-7)$$

In other words, since  $F \cdot t$  is the impulse, and  $mv_f$  and  $mv_i$  are the final and initial momentums respectively, the total impulse imparted by a body is equal to the change in momentum of the body.

Figure skaters are required to use this relationship when taking off and landing jumps. In order to produce and reduce the vertical velocity of the body's CG at take-off and landing respectively, the muscles exert a force over a given time. Upon landing "... the skater must absorb the force of the landing using a well bent knee so the edge continues to flow and balance is maintained." (Keohane, 1978). Podolsky et al (1990), found that it took one second to reduce the velocity of the CG upon landing of the jump. The optimal landing situation includes minimized forces, and maximal time of force application. This can be accomplished by flexing the limbs over longer periods of time and thereby minimizing the muscular force required (Kreighbaum & Barthels, 1985).

The linear impulse and momentum relationship just described can also be expressed in angular terms. The angular impulse -momentum equation can be expressed as

$$T \cdot t = I\omega_f - I\omega_i \quad (2-8)$$

The angular impulse is the product of a torque (T) and time (t), and the change in angular momentum is the difference between the products of the

moment of inertia of the body and its angular velocity ( $I\omega$ ) (Hay, 1985).

Similar to linear momentum, angular momentum is conserved unless an external force is applied to the body (Hay, 1985). The exception to angular momentum is that a change in the position of body segments results in a change of the overall moment of inertia. However, in order to maintain a constant momentum the angular velocity of the body changes according to the change in the body's  $I$ . This can be applied to motion of a skater during the phase of a jump. According to Keohane (1978), skaters are unable to initiate rotations while they are in the air, but they can alter the speed of rotation by altering the position of the upper and lower limbs to the the axis of rotation.

#### Projectile Motion

When a body is projected through the air, the CG follows a perfect parabolic path. Furthermore, when the body is free of support, the movement of body segments will have no effect on the parabolic path of the CG (Dyson, 1978).

The path followed by a projectile depends on three factors, the speed, angle and height of release (Hay, 1985). The angle of projection is of importance if the horizontal distance of a jump is to be maximized. For any projectile analysis, the optimal angle of release is  $45^\circ$  for maximum distance, regardless of the magnitude of the velocity at take-off (Kreighbaum & Barthels, 1985). According to the authors, this take-off angle will maximize the distance a body will remain in the air.

The velocity at take-off can be broken down into vertical and horizontal components. The horizontal component is relatively unaltered during flight due to the small air resistance, so this velocity should be the

same at take-off and touchdown (Hay, 1985). Since this value is relatively unchanged, the greater the horizontal take-off velocity, the further the athlete will jump. Vertical velocity is the key to the time a projectile spends in the air. When a body is projected into the air, and lands at the same height, the time of flight is equal to twice the time required for the force of gravity to bring the projectile's velocity to zero (Hay, 1985). Therefore, the greater the vertical velocity, the greater the time spent in the air, and the longer the jump will be.

The height of the CG at take-off is important because a higher CG at this instant increases the peak height obtained by the CG above the ground (Kreighbaum & Barthels, 1985). The location of the CG depends on the height and stature of the athlete. However, the height of the CG can be altered by simply moving the body's segments (Kreighbaum & Barthels, 1985). Thus at take-off, the CG can be raised within the body by simply raising the upper and lower limbs of the subject. By changing the body's CG at take-off, the peak vertical height of a jump can be raised by a few extra centimeters (Kreighbaum & Barthels, 1985) and subsequently results in a longer jump.

In figure skating, jumps are judged on the "... height, length, technique and whether there is a clean start and landing" (Keohane, 1978, p. 35). Therefore, maximizing the height reached during the jump increases the time of flight, which in turn increases the time available to complete the number of revolutions required for a jump. Aleshinsky (1986), found that by changing the absolute velocity of the skater from 5 m/s to 8 m/s, the height of the jump can be increased by 0.5 m and the length by 3 m. However, the increase in velocity requires a significantly greater amount of strength and body control, which may limit the number of athletes able to perform the harder jumps (Aleshinsky, 1986).

Although it would be advantageous to increase the velocity at take-off, Aleshinsky (1986) found that the time of flight for double and triple jumps did not significantly differ from each other. Therefore, there are other aspects of the figure skater's jump that are more important, namely, control of the body while jumping (Aleshinsky, 1986).

## Skating

### Equipment

The only pieces of equipment necessary in figure skating are the skates and the appropriate clothing (Petkevich, 1989). The object of this section is to describe the type of skates used by elite skaters, and their purpose.

#### The Boot

The boot "... is perhaps the most crucial element in a skater's performance." (Fassi, 1980, p. 2-3). According to Petkevich (1984), the degree of support required is directly related to the "... weight of the skater, and how vigorous the skater is." (p. 31). Furthermore, the key positions of support in the boot, are: 1) the toe, to protect against spiking one toe with the heel of the other skate; 2) the instep, to provide arch support; 3) the heel, to prevent breakdown of the boot; and 4) the ankle, which is the most important because it prevents the ankle from flopping from side to side. Fassi (1980), on the other hand, was more general with his explanation, stating that the boot should be snug enough to prevent heel movement and provide support to the instep of the foot.

The other functional characteristics of skate design which are important according to Fassi (1980), Petkevich (1984), and Smith, (1985) are as

follows:

- 1) the height of the boot - the usual height of a boot ranges between  $4\frac{1}{2}$  - 7 inches, and its main purpose is to provide adequate support to the ankle while not limiting the range of motion or muscular action.
- 2) the thickness of the tongue - this provides comfort by blocking the laces and eyelets from the skaters foot. However, the tongue thickness should not restrict the movement of the ankle or buckle when the ankle is moved.
- 3) internal padding - this feature provides comfort to the bony surfaces of the foot that come in direct contact with the skate and reduces minor injuries such as bursa inflammation, and tendinitis (Smith, 1985).
- 4) Metal eyelets - this feature prevents the leather from breaking down prematurely due to the repeated loosening and tightening of the laces.
- 5) Sole of the boot - for proper mounting of the blade, the sole of the skate must be flush with the heel of the skate. The flush heel allows the blade to be properly mounted and balanced on the boot.
- 6) height of the heel - on average the heel height should be two inches. The authors believed this is done to tip the body forward, and thereby shift the weight forward to improve balance. As previously mentioned by Cook et al (1990) and Steele and Milburn (1987), during rapid movements the heel height stops the ankle from being over stretched and thereby reduces the risk of injuries.

#### The Blade

The figure skating blade, unlike the boot, has less variability. There are three types of blades common to figure skating, they are the dance blade (the thinnest, under  $\frac{1}{8}$  inch, and the shortest to protect the skater's partner), the

figure blade, and the free-style blade. The latter two differ from each other by the amount of curvature that occurs from heel to toe. The heel-toe curvature is the greatest on the figure blade, while the freestyle blade has some curvature for the spins, but is flat enough to enhance speed and stability (Petkevich, 1984). Since jumps are not performed on figure blades or dance blades, they will not be described in this paper.

According to Petkevich (1984), the skate blade consist of three parts: the boot plate, which is the attachment of the blade to the boot; the stanchions, the upright structures between the boot plate and the body of the blade; and the body of the blade, which is that part of the blade in contact with the ice. Of these three parts, only the body of the blade varies significantly. This portion of the blade has four distinct features: "... the toe pick; the width; the lengthwise curvature, known as the radius [or rocker, (Smith, 1981)], and the length." (Petkevich, 1984, p. 37), each of which can be altered according to the preference of the particular athlete.

The toe picks, for free-style skaters, are large and angled down close to the ice (Fassi, 1980). Petkevich (1984) described these spikes as stabilizers that help prevent the skater from rotating forward during spins, and while skating backward. Furthermore, the picks provide a pole-vaulting action during "... forward-edge jumps." (p. 37). Finally, the upper portion of the toe picks were used for "... toe jumps, pivots, certain stops, and footwork ..." (p. 37).

The freestyle blade is  $\frac{1}{8}$  of an inch thick, and  $\frac{1}{2}$  inch longer than the boot (Jackson, 1981), and has a radius, from heel to toe, which is determined by the skater (Fassi, 1980). However, according to Petkevich (1984) the rocker must be small enough to allow the skater to maintain stability after jumping, and to enhance speed.

One further design aspect that is important to skaters is the depth of the

hollow of the blades. The deeper this groove is, the more the blade will dig into the ice, and therefore, provide more stability when landing a jump (Petkevich, 1984).

#### Attachment of the Blade to the Boot

Once the boot and blade have been selected, the blade must be attached to the boot. Initially the blade was fixed to the boot so that the blade was placed just medial to the centre line of the boot (Jackson, 1981; Petkevich, 1984). According to these authors, the placement of the blade medially allows the skater to maintain better balance while skating.

When testing the placement, if the ankle rolled out, the blade was placed too far medially, and if the ankle rolled in, the blade was too far laterally (Fassi, 1980; Jackson, 1981; Petkevich, 1984). The problem that may present itself is the fact that landing on a blade 1/8 of an inch thick, placed slightly medial, may predispose the skater to injuries on the medial side of the ankle. Muscles and ligaments may be damaged due to the rapid stretching upon landing jumps, like the toe loop, which land on a back outside edge (Petkevich, 1989).

Another problem with the blade placement is best described by Travers (1980)

Most biomechanical insufficiencies in skaters are approached by modifying the position of the blade on the boot in a non-quantified, rather haphazard, trial-and-error manner by well-meaning coaches and skaters" (Travers, 1980, p. 129).

In other words, the coaches blame the skater's inability to perform a jump on the placement of the blade, and randomly try different positions, hoping to

find a better position. This random assignment of the position of the blade may predispose the skater to injuries. Furthermore, Travers (1980) does not provide a solution to this problem.

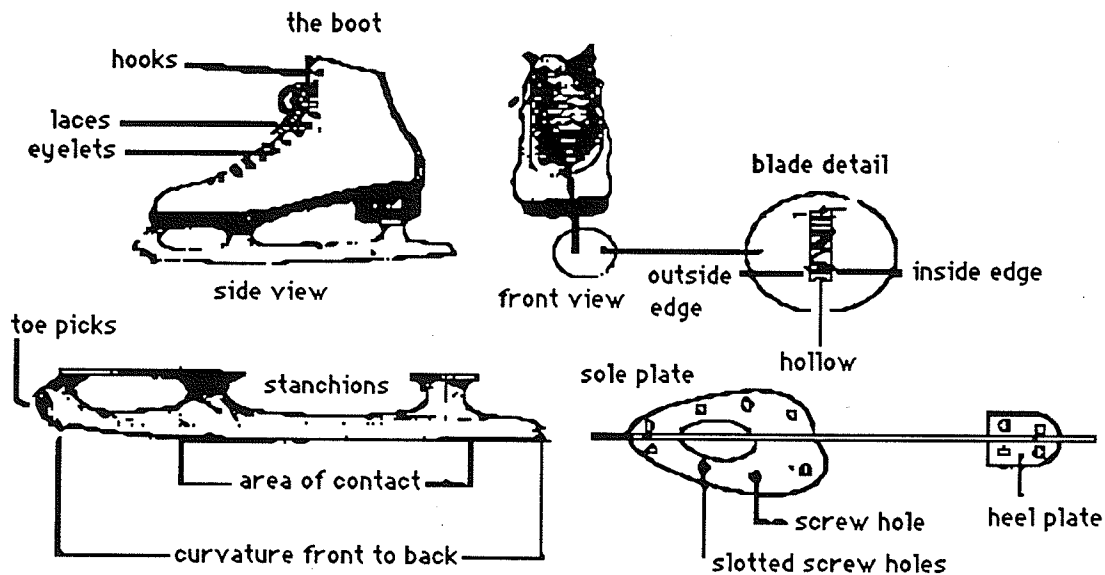


Figure 2-19 - the side and anterior view of the skate and blade and all the individual parts that make up the figure skate. (Fassi, 1980, p. 3).

### Figure Skating Injuries

Hage (1982), Smith (1985), Comper (1990), and Smith (1990), all agreed that a majority of these injuries that occur in the lower limb can be divided into overuse and acute mechanisms. The types of injuries that figure skaters acquire include calluses, bunions, bone spurs, hammertoe, stress fractures (Comper, 1990; Pecina et al, 1990), avulsion fractures (Brock & Striowski, 1986), compartment syndrome, and soft tissue injuries (Smith, 1985). In addition to these injuries, other injury sites include the upper extremity, head, and back (Smith & Micheli, 1982; Smith, 1985).

While both acute and overuse injuries can be detrimental to the

skater's training, it was found that skaters returned to skating sooner when they suffered an acute injury, as opposed to an overuse injury (Brock & Striowski, 1986). Smith & Micheli (1982) also showed that in competitive skaters the average acute injury rate was 18-22% while the overuse injury rate was 61-78%.

### Overuse Injuries

The minor injuries are calluses, bunions, bone spurs and hammertoes. These injuries will not require reduced training time and can be corrected by modifying the boot. Modifications can be made by simply adding insoles or orthotics to the boot (Smith, 1985).

The more severe overuse injuries include stress fractures. These injuries are the result of repetitive microtrauma caused by skating, and repeated jumps, from 20-100 times a day (Smith, 1985). The particular site distribution of stress fractures was found to be similar to those of runners (Pecina et al, 1990). Therefore, the most common sites of stress fractures occur in the tibia and fibula, while some occur in the metatarsals, femur, pelvic girdle (Sullivan et al., 1984; Hulkko & Orava, 1987; Markey, 1987;), and navicular (Pecina et al., 1990).

As mentioned, the cause of many of the stress fractures is due to repetitive microtrauma sustained by the bones of the lower limb and pelvis (Smith, 1985). In figure skating, Smith (1990) provided two possible reasons for the high incidence of stress fractures: first, the skate provides little or no cushioning ability to assist in the absorption of forces and second, the stiff boot restricts the amount of dorsiflexion and knee flexion. As a result, the metatarsals absorb most of the impact forces that result from landing a jump (Smith, 1990). Tibial stress fractures, on the other hand, occur because of the

tensile forces caused by the muscles during take-offs (Pecina et al, 1990).

Four other overuse injuries have been identified: tendinitis, chondromalacia patellae (Brock and Striowski, 1986), vertebral fractures and growth plate fractures (Smith & Micheli, 1982).

Smith (1985) found that the Achilles tendon was a common site of tendinitis, while Smith & Micheli (1982) found cases of peroneal tendinitis. These problems can be avoided by making alterations to the boot and relieving the pressure placed on the tendon (Smith & Micheli, 1982). The final type of tendinitis found in figure skaters occurs in the patellar tendon (Smith, 1985).

Chondromalacia patellae is a process that results in the premature degeneration of the patellar cartilage. This problem is thought to be caused by excessive muscular force exerted by the quadriceps during activities, which brings the patella tightly against the femur (Magee, 1987). A second reason cited by the author for premature degeneration was excessive tibial torsion. The result was abnormal stretching of the cartilage, causing damage to the cartilage and an acceleration of the normal degenerative process. Both of these causes of patellar injury can be a result of landing jumps in figure skating.

Back injuries present in figure skating tend to be the result of the hyperlordotic posture required to make figure skating aesthetically pleasing (Smith, 1985). According to Smith and Micheli (1982), back pain is associated with the "repeated hyperextension of the low back and frequent jumping and landing..." (p. 44). The frequent positioning of the body in hyperlordosis results in the overuse injuries of spondylolysis and spondylolisthesis (Smith and Micheli, 1982).

According to Smith & Micheli (1982), children go through a rapid

growth period in which they lose flexibility. As a result, this can lead to overuse injuries, due to the weak bone formation, which occurs during rapid growth. This can be further magnified by repeated microtrauma to the growth plates cause by repeated jumps.

#### Acute Injuries

Acute injuries include lacerations, contusions, concussions, sprains, strains and fractures (Smith, 1985). According to Smith (1985), there are probably no reasonable preventive measures that can reduce the number of lacerations, contusions, concussions or upper extremity fractures. On the other hand, sprains, strains and ankle fractures may be reduced by the appropriate equipment, training, and conditioning.

The boot must be strong enough to prevent excessive motion at the ankle joint (Podolsky et al, 1990), however, according to Smith (1985), the ankle is sprained regardless of the boot strength. Therefore, training becomes important if the skater wishes to avoid injury. Learning how to fall correctly (Smith, 1985) is important in the prevention of upper and lower body injuries that occur as the skater tries to prevent or cushion the fall (Petkevich, 1984). The skater must also be patient and learn the skills in a stepwise manner (Smith, 1985). Conditioning is important so that the the body is not subjected to the forces that may exceed the limits of the tissue and result in injury (Smith, 1985).

#### Toe Loop

#### Jumping

As previously mentioned, in 1990 the International Skating Union eliminated compulsory figures from the requirements of free style skating.

This increased the time the skater had to devote to jumps. Furthermore, the removal of compulsory figures has made figure skating "...more athletic, artistic, and from the spectator's perspective, appealing aspect of singles skating." (Petkevich, 1989, p. 21).

According to McPherson and Bothwell-Myers (1986), "Jumping is the most important and exciting element in free-skating today." (p. 56). From a judge's perspective, correctly performed jumps have three characteristics that are important: height, speed and length of jump. Furthermore, the judges consider whether the take-off and landing were smooth, and how well the jumps flowed in the overall program (Keohane, 1978; McPherson & Bothwell-Myers, 1986).

In figure skating there are 14 different types of jumps that include rotations (Keohane, 1978; Brauckmann & Power, 1980), of which the toe loop is the easiest toe assisted jump (Petkevich, 1989). When analyzing a jump, it can be broken down into four parts, the preparation, the take-off, the flight, and the landing (Keohane, 1978).

### Preparation

The preparation is vital to a properly executed jump. This phase is important because it provides the much needed speed and body position necessary for a successful jump (Keohane, 1978; Brauckmann & Power, 1980; Folk, 1982). Several extra points that were believed to be important to this phase were proper positioning of the body weight over the edge, keeping the head up, and maintaining a straight back, upper limbs and lower limbs (Folk, 1982; Petkevich, 1989). If the weight is positioned properly over the skate edge during the preparation, the skate will follow an arc on the ice. As a result, angular momentum will be produced, which will help create enough

rotation to successfully complete the required number of rotations (Petkevich, 1989). The proper positioning of the head, back, upper limbs and lower limb is to aid in balance and the production of momentum and force (Petkevich, 1989).

When performing the toe loop, the athlete approaches the jump by moving forward, on a left front inside edge. At the same time, the right lower limb is extended in front of the body with the foot slightly turned out (Folk, 1982) as outlined in Figure 2-20a. Prior to jumping the weight is transferred from the left front inside edge to a right front inside edge (Figure 2-20b). The skater then pivots on the foot and glides on a right back outside edge. At this point, the left upper limb extends up in front of the skater and the right upper limb is extended to the side and slightly backward (Figure 2-20c) (Petkevich, 1989).

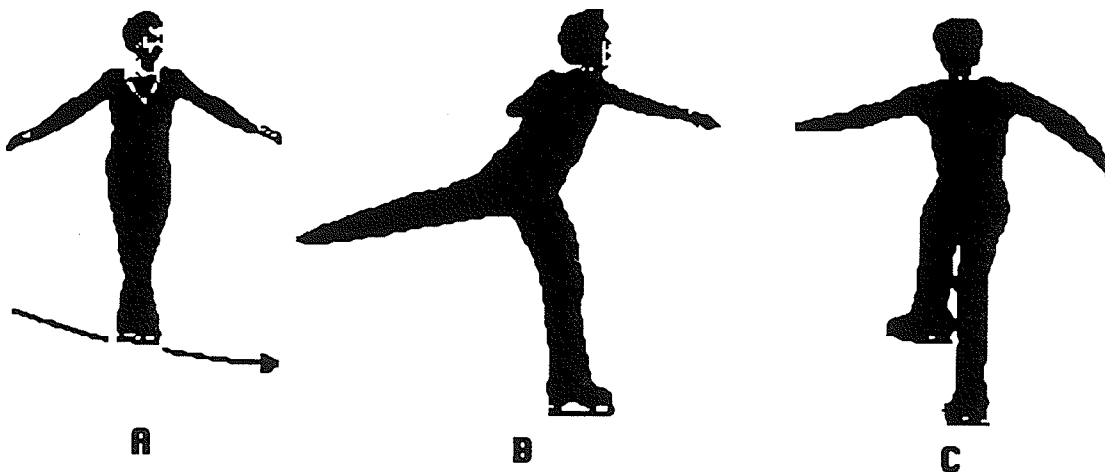


Figure 2-20 - (A) the approach into the jump prior to weight transfer to the right lower limb, weight is on a front left inside edge, (B) transfer of weight from the left front inside edge to a right front inside edge, (C) pivot on right foot to a back outside edge (Petkevich, 1989, p. 238).

The transfer of weight onto the take-off foot (right) should take place approximately two feet in front of the support limb (left). In order to shift the weight and be in position to take-off, the right foot must be placed onto the ice so that the right front inside edge is the edge that makes contact with the ice. In order to complete the transfer, the left lower limb must be extended directly behind the skater. If the lower limb is abducted and extended, unwanted angular momentum will be created and the jump may not be successfully completed (Petkevich, 1989).

According to Petkevich (1989), once the transfer of weight has taken place, the body begins to wind up and move into position for the take-off. The windup includes a gentle rotation of the upper limbs and shoulders in the counter clockwise direction (for a right foot take-off). The left lower limb should be moved behind the right lower limb, and the skater will rotate onto a right back outside edge. Petkevich (1989), also stated that the support of the skater on the front inside edge should be very short (approximately five feet), depending on the speed of the skater.

After completing the pivot onto a back outside edge, the skater extends the free lower limb behind the support skate, and slightly to the side. At this instant the shoulder rotation and upper limb movement are checked, and the left upper limb and shoulder are in front of the skater, while the right upper limb is back and to the side (Petkevich, 1989).

### Take-Off

In order to produce the best jump, the skater must jump as high as possible, without compromising too much of his/her horizontal velocity. The take-off angle is the resultant of the horizontal and vertical velocity components of the skater at the instant of take-off (Hay, 1985; Keohane, 1978;

Brauckmann & Power, 1980; Folk, 1982). Therefore, in order to optimize the horizontal distance, the take-off angle should be as close as possible to 45 degrees (Kreighbaum & Barthels, 1985).

During the take-off, the upper limbs are lowered and rotated clockwise. From this position the upper limbs are swung more vigorously around the body as well as up into the rotational position (Petkevich, 1989). While the rotational position is not described by the author, by looking at Figure 2-21, it is obvious that the position is such that the hands and elbows being moved down and toward the body, as compared to the preparatory phase.

While the upper limbs are moving through their desired motion, the left lower limb is also being positioned for take-off. The left toe pick is placed into the ice behind the right foot and off to the side. Petkevich (1989), made one cautionary note associated with toe assisted take-offs: the left lower limb should not cross the midline of the body because if the foot does cross this line, the right lower limb will skid across the ice and some of the horizontal and vertical forces will be lost.

The problem associated with jumping for distance is the need to transfer horizontal velocity into vertical velocity (Dyson, 1978; McWatt, 1989; Hay, 1985). According to McWatt (1989) and Dyson (1978), the athlete can change the horizontal velocity of the body into angular velocity around a fixed point. The authors described how a pole vaulter converts horizontal velocity, to angular velocity, by creating a pendulum with the pole in the box. In figure skating, the left foot is used to produce this pole-vaulting action and thereby converts linear motion at take-off into angular motion. The problem with this action is the increased strength and control that are required to successfully complete the jump (Folk, 1982).

Folk (1982) suggested swinging the upper limbs and free lower limbs

through a large range of motion just prior to take-off in order to increase the angular momentum of the body. By performing this action, the GRF are increased and the result is a greater height and length of the jump (Hay, Dapena, Wilson, Andrews, & Woodworth 1975; Hay, Vaughan, & Woodworth, 1981; Miller, 1990).

A second way to produce a rotation depends on the path followed by the skate during the take-off phase. The skater follows an arc, which causes the body to lean toward the centre of this arc, and as a result, rotation is initiated (Folk, 1982). Since the GRF are being applied at distance from the axis of rotation, the radius of the arc, which is the body, has a rotation about this axis proportional to the radius of the arc (Kreighbaum & Barthels, 1985). Therefore, the arc of the approach and the pole vaulting effect work together to produce the rotation and lift necessary to complete a jump.

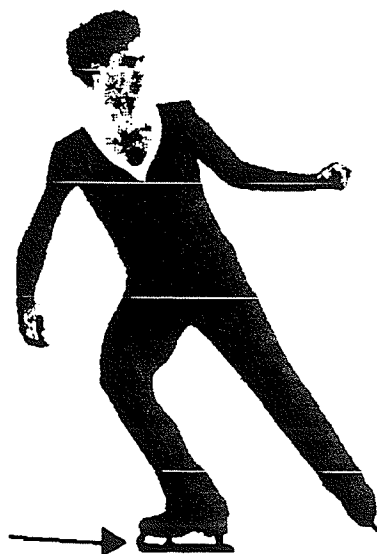


Figure 2-21 - (adapted from Petkevich, 1989, p. 239) the position of the skater just prior to take-off. Notice that the arms have begun their rotation and the extension and position of the rear foot producing the pole vault action.

In order to create a rotation about the longitudinal axis of the skater's body, a force is applied at a distance from the axis of rotation. The force is applied by a concentric contraction of the hip flexors of the skater's "pole-vaulting" limb (Petkevich , 1989).

The motion of a body can be checked by the placement of the foot on the ground. The consequence of checking the motion of the body is the production of a rotation about an axis located in the segment that checked the motion. The rotation occurs because the inertial properties of the CG, cause the CG to continue at the previous linear velocity (Dyson, 1978). The rotation that occurs depends on the placement of the foot, and the desired axis of rotation. In figure skating, the placement of the foot behind the athlete and slightly to the side (Petkevich, 1989) causes rotation to occur about the longitudinal axis of the body, which increases the angular momentum at take-off.

### The Flight

Once the skater leaves the ice, angular momentum cannot be created or increased according to the Law of Conservation of Angular Momentum (Dyson, 1978; Hay, 1985; Kreighbaum & Barthels, 1985). However, while in the air, the speed of rotation can be altered by changing the position of the upper limbs and lower limbs. By bringing the upper limbs close to the body, the speed of rotation is increased, while moving the upper limbs further from the trunk will decrease the speed of rotation (Dyson, 1978; Hay, 1985; Kreighbaum & Barthels, 1985; Brauckmann & Power, 1980). For jumps that require multiple rotations, it becomes evident that the moment of inertia must be as small as possible in order for the angular velocity to be as large as possible. Therefore, the closer the body segments are to the longitudinal axis

the more success the skater will have completing the more difficult jumps requiring three or more rotations.

According to Petkevich (1989), the length of time that an average jumper spends in the air was approximately one second while Aleshinsky (1986) found that the time of flight was between 0.59 and 0.61 seconds for the triple toe loop. As mentioned previously, the path followed by a projectile, in this case the human body, is a parabola. To maximize the time of the airborne phase and the distance travelled, the optimal angle of take-off is  $45^{\circ}$  (Kreighbaum & Barthels, 1985).



Figure 2-22 - starting from the right, the skater has just taken off and the diagrams show the position of the skater at the end of  $1\frac{1}{4}$ , 2 and 3 revolutions (Petkevich, 1989, p. 242-243)

### The Landing

Just prior to landing, the rotation of the jump must be slowed or checked (McPherson & Bothwell-Myers, 1986; Podolsky et al, 1990).

According to the Law of Conservation of Angular Momentum (Dyson, 1978; Hay, 1985; Kreighbaum & Barthels, 1985) this requires the athlete to extend the upper limbs to the side, increasing the moment of inertia, and slowing the angular velocity. Once the rotation begins to slow, the right foot is plantarflexed and reaches for the ice, while at the same time the left knee is flexed slightly, and the left foot is moved up and away from the right foot (Petkevich, 1989).

First contact with the ice is made by the toe and subsequently casting down the blade. Immediately after contact, the knee bends in order to help absorb the forces and to allow the speed and flow of the skater to be maintained (McPherson & Bothwell-Myers, 1986).

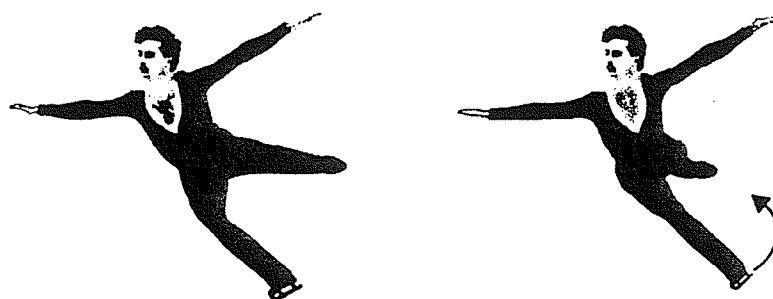


Figure 2-23 - The extension of the limbs, and style of landing for the triple toe loop (Petkevich, 1989, p. 238)

In addition to the landing pattern described above, Petkevich (1989) found that as the height of the jump increased, so did the knee flexion. Furthermore, Petkevich (1989) found an increased chance of successful landing when the time of landing was short and controlled. The problem with a short landing is the increased forces exerted on the body, according to the Impulse Momentum relationship,

$$F \cdot t = m \cdot v_f - m \cdot v_i \quad (2-9)$$

if time to control the momentum ( $m \cdot v_f - m \cdot v_i$ ) was small, the force per unit time produced would be vary large (Hay, 1985).

The landing of a toe loop of any degree takes place on a right back outside edge (Petkevich, 1989). Over the entire skill, the path followed by the skate follows an arc similar to Figure 2-24.

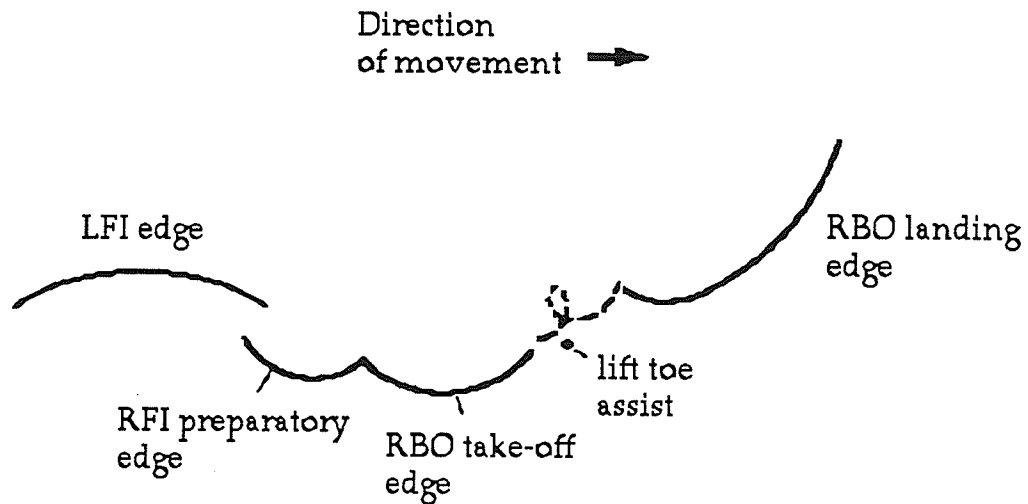


Figure 2-24 -The path for the left and right skate during the preparation, take-off and landing of a toe loop jump (Petkevich, 1989, p. 239).

## CHAPTER 3

### METHODS AND PROCEDURES

#### Subjects

The subjects used in this experiment were competitors from a divisional meet that was held in Brandon, Manitoba by the Manitoba Figure Skating Association in January, 1993. National and international calibre subjects were also selected during the month of February from a club in southern Ontario. This level of competitor was selected because they possessed the skills necessary to perform the triple toe loop.

A member of the Manitoba Figure Skating Association (MFSA) contacted all the Brandon competitors' coaches and informed them of the test that was to be performed. This provided each coach, and competitor, with prior knowledge of the test, and time to consider taking part in the analysis. A brief description of the experiment was provided, along with the reassurance that withdrawing from the study may occur at any time, without repercussions. A consent form (Appendix A) was distributed to the competitors which contained the same information, and was signed by the competitor or the parent/guardian (if under 18 yrs. old) prior to participation in the study. In Ontario the same procedure was carried out by the investigator, who individually contacted the coaches and subjects.

There was a total of nine subjects used in the experiment, with each subject agreeing to perform five triple toe loop jumps. This was supposed to provide for 45 triple toe loops.

The subjects that participated were weighed on a portable weigh scale,

prior to filming, with their skates on. This allowed the force calculations to be represented as a percentage of total body weight and also allowed between - subjects comparisons. The height of the subjects with their skates on was also recorded. This measurement allowed the limb lengths to be estimated using tables of limb lengths provided by Kreighbaum and Barthels (1985, p. 655).

## Data Collection

### Camera Setup

The first step in setting up the cameras included placing the cameras at approximately right angles to each other, and far enough away from the athlete to encompass the entire skill. The first camera, either the Panasonic OmniMovie VHS camcorder (PV-460-K) or the Panasonic OmniMovie VHS camcorder (PV-520D-K), was placed on the ice behind the subject. The second camera, a Panasonic Digital 5100, was placed at approximately 90° to the first camera and recorded a view from the side boards. The wires connecting the cameras were kept close to the boards so that they did not interfere with the performance of the skill. Both cameras film the skill at a rate of 60 frames per second (fps).

As mentioned above, the two video cameras were placed at right angles to one another, and they were linked together by a time code generator. This piece of equipment was used to synchronize the video cameras and placed identical time codes on each video tape. This allowed the user to start digitizing each subject at the same position on the film, which was essential for accurate three dimensional representation of the motion of the athlete.

The Panasonic Digital 5100 camera was linked to a portable video cassette recorder and both units were powered by a 12 volt car battery. The

Panasonic OmniMovie VHS (PV-460-K) or (PV-520D-K) cameras used their own internal battery pack as a power source. The time code generator was linked to the car battery. The entire system was set up as shown in Figure 3-1.

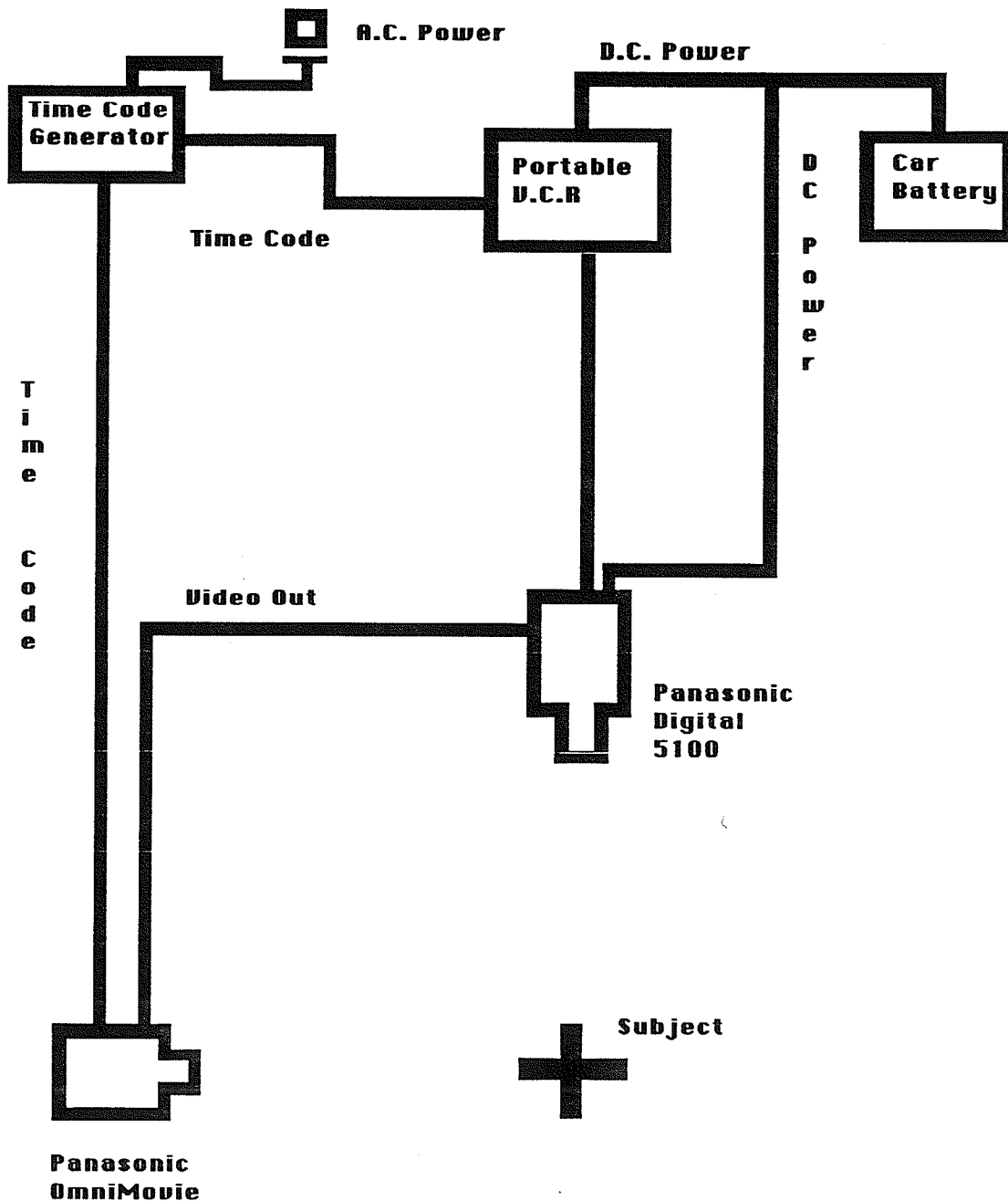


Figure 3-1 - the camera set-up that was used in this experiment to record the subjects performing a triple toe loop.

## Pilot Study

A pilot study was conducted in March 1992, and one skater performed a double toe loop. While this jump was different from the one to be studied in this research, it served the original purpose of the pilot, to check the digitizing reliability of the investigator.

The jump was digitized twice, on separate days, and the results were compared by correlation. In other words, the tendency of the two sets of data to vary between days was tested (Hassard, 1991). An adequate correlation with a  $p < 0.05$  was obtained between the two trials for the right knee, in the horizontal direction  $r = 1$  and for the vertical direction,  $r = 0.963$ . These values indicated that there was a strong relationship between the two testing procedures and that the digitizing skill of the investigator was reliable.

In this first pilot study, the data was smoothed using a second order Butterworth filter, at a frequency of 8 Hz. This frequency was chosen for the accuracy and smoothness that the graph provided. This pilot was also performed using one camera view, and was not representative of the filming procedure to be used in the study.

A second pilot was performed, in October 1992, with the purpose of testing the investigator's ability to calculate the vertical forces and moments that occurred during the skill. This study was performed using the equations that are outlined below. The two cameras were positioned at right angles to each other, the spatial tree was digitized, the film was digitized, and the forces were calculated. The spatial tree for this study is located in Appendix B. The raw data for this pilot were smoothed using a fast Fourier analysis, with a frequency of 6 Hz, which seemed to provide an adequate representation of the acceleration terms, without compromising the trends of the data. The Fourier analysis was chosen for a second reason, after smoothing the data

with the Butterworth, Spline, and Fourier methods at a number of different frequencies, the raw data was best represented by the Fourier method at a frequency of 6 Hz.

### Test Procedure

From the pilot study that was conducted, it was noted that during digitization the skate blades and certain body parts were difficult to identify because of the lack of contrast between the ice and blade. Therefore, pieces of black tape were placed on the skate blade to act as a contrast against the ice and the white boards. The athletes were asked to wear clothes that were tight fitting in order to make joint location predictions easier. Furthermore, white bands were placed around the right lower and upper limbs to make the left and right sides of the body distinguishable from each other during digitizing. Finally, two pylons were placed in the field of view of both cameras and acted as reference points.

The cameras were set up as described in the section above. Once the cameras had been set up, and recording had begun, the cameras remained in the record mode until the entire testing session had been completed.

The subjects took as much time as they felt was necessary to warm up, and while they were warming up, the calibration cube was videotaped. Once the subjects had warmed up and felt they were ready, the testing began. The subjects built up speed at one end of the ice and when the required velocity had been obtained, the subject moved toward the centre of the ice surface. The jump was initiated on the centre dot of the hockey arena. This position was used so that the cameras were allowed to remain stationary for the entire jump, and so that the preparation, take-off, and landing were all in the cameras' field of view. For the camera recording the side view, the take-off

started at the left side of the camera image, and traveled across to the right side of the frame. This view contained the section of ice between the red line and blue line which provided an area large enough to perform the jump, and maintain the largest possible subject image.

During all the jumps, the two pylons remained on the ice, in the field of view of both cameras. The pylons were used as reference markers for the digitizing process and the starting point of the skaters take-off.

Finally, each subject was asked to perform five jumps. Therefore, with the nine subjects, the total number of jumps recorded should have been 45.

## Data Reduction

### Setup Before Digitizing

The first step in digitizing includes the set-up of the digitizing equipment which was developed as a complete analysis system by Peak Performance Technologies (1992). The system consists of a specialized Panasonic AG-7300 video cassette recorder, a Sony Trinitron monitor, an IBM compatible personal computer supplied by Peak Performance Technologies, a MultiSync 2A computer monitor, a Hewlett Packard LaserJet series II printer, and a Hewlett Packard 7475A plotter. The Panasonic AG-7300 video cassette recorder is unique because it has the capability of reading the time code that is placed on the video tapes during the filming of the subjects. All of the above hardware was linked by a series of software programs produced by Peak Performance Technologies (1992).

The second step includes the set up of a spatial model. A spatial model is a stick figure that the computer uses to represent the subject performing a

skill. The spatial model for figure skating consisted of 21 individual points which produced a 12 segment model. The 12 segments included in the digitizing process correspond to the left side of Figure 3-2, while the right side of Figure 3-2 displays the points that were digitized during the analysis. Note: the stick figure only contains 19 points, the other two points digitized were the reference points.

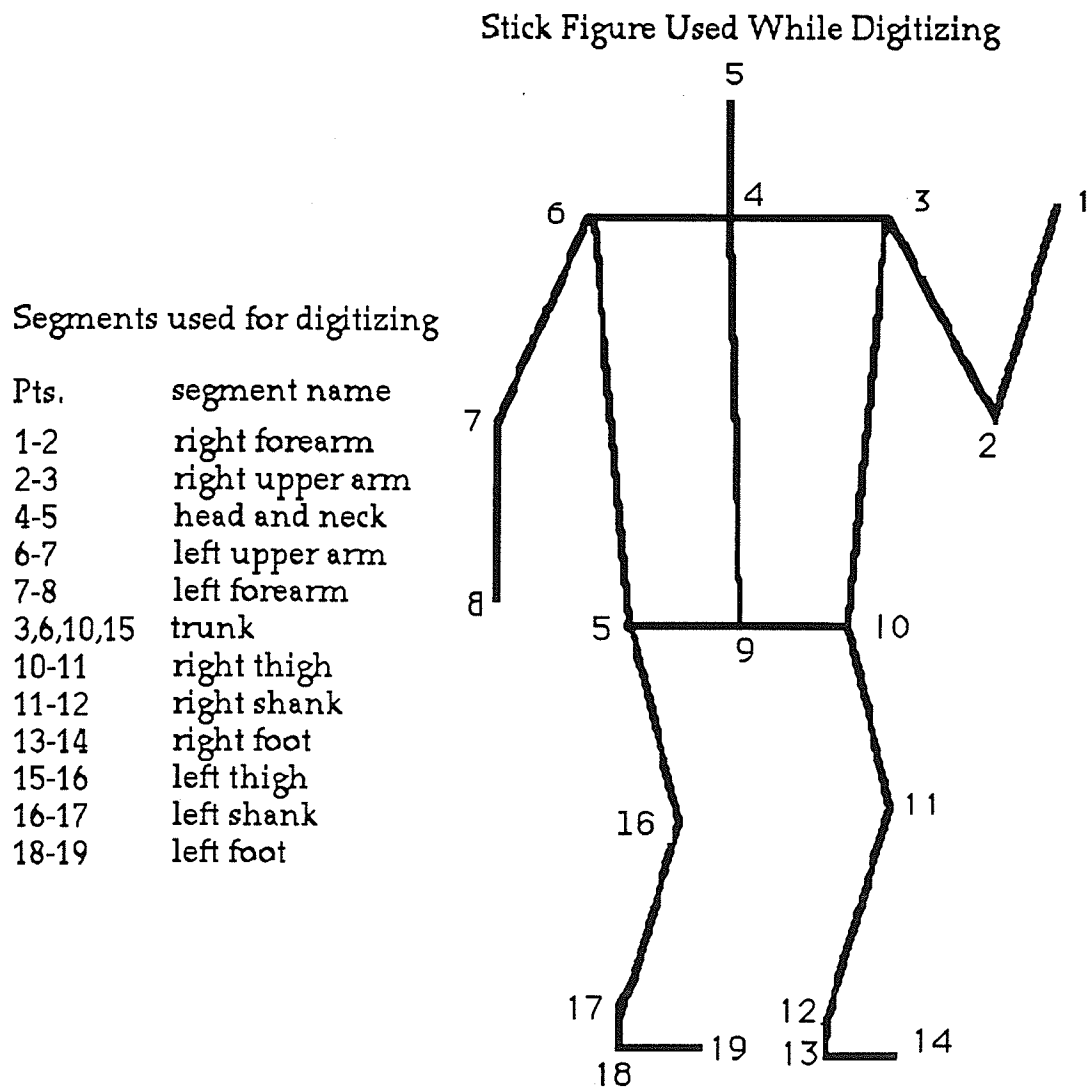


Figure 3-2 - The segmental sections used for the digitizing process (left); a graphical representation of the points that were digitized and the stick figure representing the spatial model (right).

The spatial model file also contains the segmental centres of gravity, the average weights of each segment, and distance of the segment's CG from the proximal joint. The values for the segmental masses were adapted from Humanscale (Diffrient, Tilley & Bardagjy, 1978) while the centre of gravity distance values were adapted from Hinrichs (1988).

### Digitizing Process

The digitizing process was quite simple. First, the digitizer played the video tape until the activity to be digitized or the spatial model tree was found. Once this had been done, the exact point at which digitizing was to begin was selected. The starting point was any distinguishable action performed by the athlete that was visible in both cameras, or any frame containing the spatial model tree. Once the starting point had been selected, the number appearing on the computer represented the number of the frame chosen. This number was recorded in a record book and used to select the exact starting point when digitizing the second view.

With the starting frame selected, and the frame number recorded, digitizing could begin. The computer used the recorded number to "grab" a series of video images and store them in the computer's memory. After grabbing the images, each set of two consecutive frames were then sent through an image processing technique set up in the Peak 5 software. This process splits the two frames and places a computer generated frame between the original frames, changing a film that was recorded at 30 fps into a film with a frequency of 60 fps (Peak Performance Technologies, 1990).

"Once the video frame is grabbed, split, and enhanced, the operator is presented with a firm, clear image with a moveable cursor superimposed on it." (Peak Performance Technologies, 1990, p. 1-4). The image and the

superimposed cursor were played back by the computer onto the attached television screen. The experimenter then moved the cursor to any position on the athlete, and by depressing the left mouse button, digitized that point for future analysis. Once an entire frame had been digitized, the values were automatically stored to the hard drive of the computer. This process was continued until the skill had been completely digitized.

As mentioned above, the points digitized were automatically stored on the hard drive of the computer. These values were representations of the individual pixels in the television screen. For the x co-ordinate value, the pixel value was stored directly, while the y co-ordinate value was the product of the y pixel value and the aspect ratio (T. Moore, personal communication, May 13, 1993). These values were then converted into real life numbers by multiplying them by the scaling factor which was calculated in the 3D project file.

The scaling factor was calculated by digitizing a spatial tree. This tree, as shown in Appendix B, had 24 white balls, each equivalent to the size of a ping pong ball. These balls were positioned at exact distances from each other, and these distances were taken from the Peak 5 manual and entered into the project file. The tree was digitized, starting with the camera view recorded by the Panasonic Digital 5100, and the balls were digitized in alphabetical order. When the Panasonic OmniMovie VHS (PV-460-K) or (PV-520D-K) camera view of the tree was digitized, the order of digitizing the balls had to be the same as that for the first camera so that the DLT parameter calculations were accurate. Once the tree had been digitized from both views, the computer used these values to produce three dimensional data via DLT parameters.

Once the spatial model and project file had been set up, digitizing began. For each skater, the side and rear views were digitized to produce a

three dimensional computer reconstruction. Each frame consists of 21 digitized points. Nineteen of these points were part of a stick figure, the other two points were used by the computer as points of reference. According to Aleshinsky (1986) the airborne and landing phases require just over 1.5 seconds with 0.59 seconds in the air, while Podolsky et al (1990) believed that one second was needed for a controlled landing (Podolsky et al, 1990). Since the skill was recorded at 60 fps the required 1.5 seconds resulted in approximately 90 digitized frames per skater. However, digitizing did not cease at 90 frames but continued until the subject had landed the jump and the vertical velocity of the CG had reached zero or began to move in the positive y-direction.

Peak5 allows the user to translate and rotate the reference frame. The first translation, for this study, was to move the reference axes to the position of the toe at the instant of take-off. This translation gave the toe the coordinates of (0,0,0) and allowed the maximum height of the CG during the jump to be obtained. The second translation was at the instant of touchdown. At the same time, the axes were rotated so that the x-axis remained in constant alignment with the toe and heel and parallel to the horizontal. By repeatedly rotating the reference axes, for each successive frame of film, the investigator was continually presented with a sagittal view of the athlete, thereby eliminating any any parallax errors introduced by the use of a single camera. Therefore, regardless of the path followed by the skater, there was an accurate two dimensional, sagittal, representation of the skill.

## Legend

s, h, a, k, hp, e	where - the subscripts are used to represent the joints of interest. The joints are the shoulder, head, ankle, knee, hips, and elbow respectively
H, UA, FA, TK, T, S, F	where - the subscripts are used to represent the segments of interest. The segments are the head, upper arm, forearm, trunk, thigh, shank, and foot.
R <sub>y</sub> , R <sub>x</sub>	where - R is the joint reaction force; - x, y, are the principal axes
W	where - W is the weight (mass x acceleration of gravity) of the segment
M <sub>z</sub>	where - M is the moment applied at a joint about the z - axis of rotation
$\theta$	where - $\theta$ is the angle between the horizontal and the limb segment.
m <sub>a<sub>y</sub></sub> m <sub>a<sub>x</sub></sub>	where - m is the mass of the segment - a is the linear acceleration of the segment - x, y, are the directions of the linear acceleration
I	where - I is the moment of inertia of the segment - z is the axis about which the moment of inertia was obtained
L1 L2	where - L1 is the distance from the proximal joint to the CG of the segment, and L2 is the distance from the distal joint to the CG segment.
$\alpha$	where - $\alpha$ is the angular acceleration of the segment - z is the axis about which the acceleration is occurring

## Force Calculations

As previously described, the coordinate system was moved to the position of the right toe at touchdown, and rotated, in varying amounts, so that the x-axis of the co-ordinate system remained in alignment with the line connecting the toe to the heel of the right foot. As a result, the x- z plane remained parallel to the horizontal, the x-axis remained parallel to the sagittal plane, and the z-axis remained parallel to the frontal plane. From these positions, all the joint angles and angular accelerations were calculated relative to the proximal segment. (Brüggemann, 1985).

Although the Peak5 software calculates the acceleration of each point it can also calculate the acceleration of each segment CG. In order to calculate the acceleration for each segment CG, a separate spatial model file and project file had to be created. The spatial model file was reduced from 21 points to 12, with one point representing the CG for each segment. Secondly, the project file was changed so that the new spatial model file, the 12 segment model, was used instead of the original. Since the new project file was an identical copy of the original, with only the line containing the spatial model file name being changed, the same scaling factor was being used for each project file. Finally, the file that contained the information on which project file and data files were to be used, was changed so that the correct project file was called during the acceleration calculations (J. Porter, personal communication, June 3, 1993). Once the values for the accelerations were calculated, the force calculations were performed.

The force calculations were performed on a 12 segment model of the human body, similar to the nine hinge model presented by Ramey (1973). The extra three segments of this model correspond to the head, and the feet.

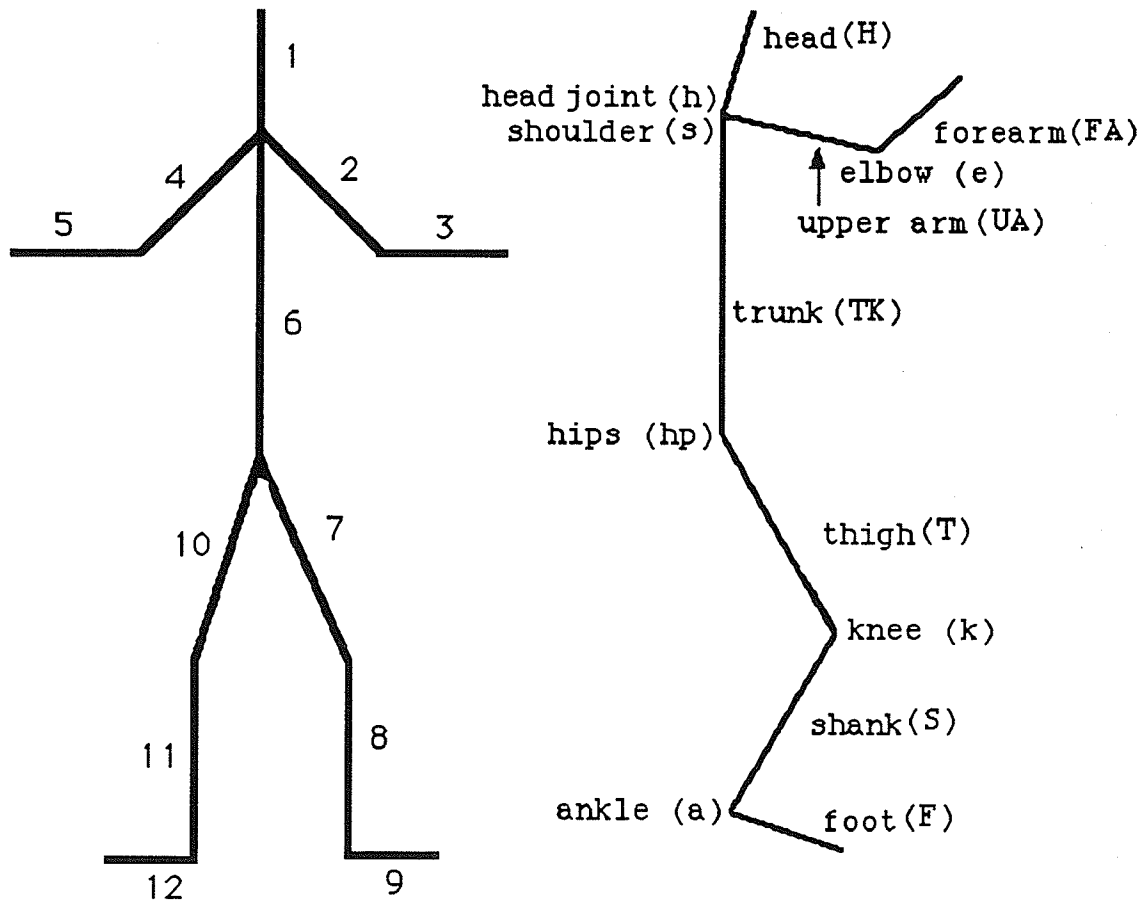


Figure 3-3 - A stick figure representation of the free body diagram used to calculate the forces and moments for the triple toe loop. The left diagram shows the twelve segment model, and how the segments are attached. The right diagram represents the segments and joints, with the letter(s) in brackets representing the subscripts used in the force and moment equations.

The calculation of forces and moments began at the segments furthest from the support limb, and proceeded, link by link, until reaching the segment that was in contact with the ground (Chaffin & Andersson, 1991). For the figure skater, there were four segments that were unsupported and attached to the trunk; the head, both upper limbs, and the left lower limb. Therefore, the force calculation started at the right forearm-hand segment, and proceeded to the shoulder. The same steps were followed for the left

upper limb. Force calculations for the left lower limb began at the left toe and proceeded to the left hip. The forces and moments found at the shoulders and hip were then added to those of the trunk, and subsequently passed down the support limb to the ground.

The reference frame for the force calculation was oriented so that forces causing movement vertically upward, and horizontally to the right, were considered positive. Moments acting in a counterclockwise direction were also denoted as positive.

As shown in Figure 3-3, the forearm-hand segment has only the upper arm segment attached to it, therefore there was only one set of forces to calculate. On the other hand, the upper arm segment must incorporate the forces and moments calculated at the elbow joint in order to obtain accurate force and moment values at the shoulder joints. The free body diagram used to represent the forearm and upper arm segments was identical for both the right and left sides of the body and was represented by Figure 3-4.

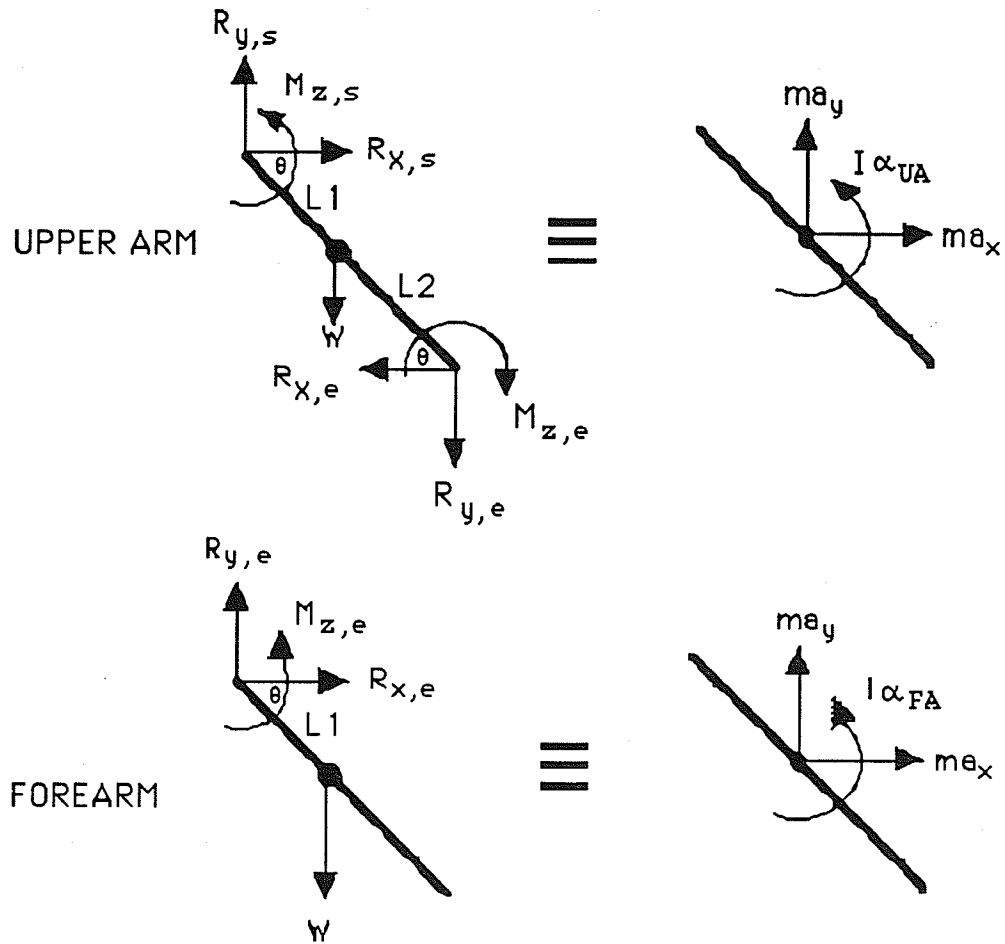


Figure 3-4 - free body diagram of the forearm-hand complex and upper arm, with the forces and moments being calculated at the elbow (e), and shoulder (s) joints.

Using the equation presented by Nordin and Frankel (1989), where the sum of the forces in any direction is equal to the product of the mass and the linear acceleration in the required direction,

$$\Sigma F_x = ma_x \quad (\text{Nordin \& Frankel, 1989}) \quad (3-1)$$

the resulting equation for the forces present in the x-direction for the elbow was:

$$R_{x,e} = ma_x \quad (3-2)$$

The force calculation in the y-direction, for the same segments resulted in the following equations:

$$R_y - W = ma_y \quad (\text{Miller \& Nelson, 1976}) \quad (3-3)$$

$$R_{y,e} - W_{FA} = ma_y \quad (3-4)$$

The equation that represents the forces for the upper arms were:

$$\text{in the x-direction} \quad R_{x,s} - R_{x,e} = ma_x \quad (3-5)$$

$$\text{in the y-direction} \quad R_{y,s} - R_{y,e} - W_{UA} = ma_y \quad (3-6)$$

The head had a slightly different free body diagram. In the previous free body diagram, the proximal joint was at the top of the diagram, however, with the head the proximal joint is at the bottom of the diagram. Therefore, the free body diagram for this segment of the body was:

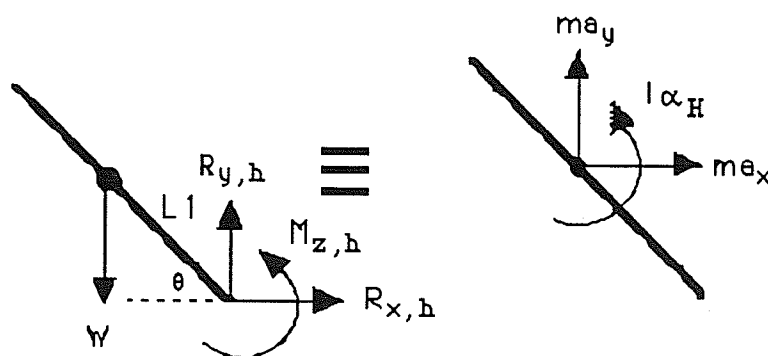


Figure 3-5 - the free body diagram of the head, along with its associated forces and moments

$$\text{and the force equations in the x direction} \quad R_{x,h} = ma_x \quad (3-7)$$

$$\text{while in the y direction the forces were} \quad R_{y,h} - W_H = ma_y \quad (3-8)$$

The force and moment calculations for the left leg were similar to those of the forearm and upper arm calculations, with the exception that there was an additional segment attached to the system.

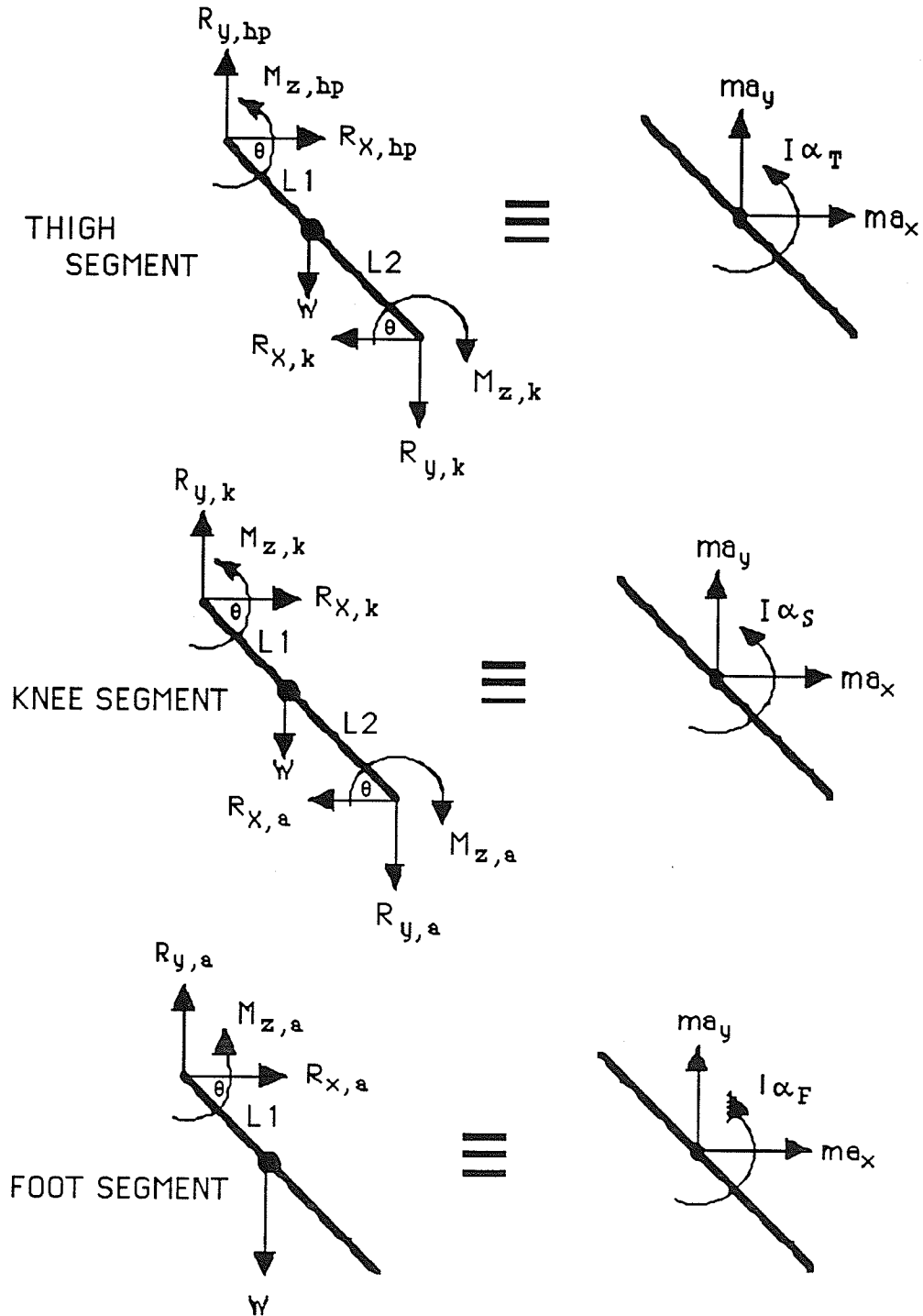


Figure 3-6 - The free body diagrams of the left lower limb. Subscripts (a), (k), and (hp) are the ankle, knee and hip respectively.

As mentioned, the force equations for the left lower limb are similar to those of the upper limbs. The distal segment had one other segment attached to it, and therefore, the force calculations were:

The force in the x - direction  $R_{x,a} = ma_x$  (3-9)

The force in the y - direction  $R_{y,a} - W_F = ma_y$  (3-10)

At the knee, the calculations became more complex and the values from the ankle had to be factored into the equations. The equations for the knee were:

The force in the x-direction at the knee was  $R_{x,k} - R_{x,a} = ma_x$  (3-11)

and the force in the y-direction  $R_{y,k} - R_{y,a} - W_S = ma_y$  (3-12)

Finally, the left hip force calculations used the values found at the knee to calculate the forces at the hip.

The force in the x-direction  $R_{x,hp} - R_{x,k} = ma_x$  (3-13)

and in the y-direction  $R_{y,hp} - R_{y,k} - W_T = ma_y$  (3-14)

Once the forces were calculated for the left and right shoulder, the head, and the left hip, the forces at the right hip could be calculated. The free body diagram for the trunk was considerably more difficult to draw and represent by a series of equations. With the forces and moments from both

upper limbs, the head, and the left lower limb, the number of variables was increased two fold in the y - direction and 2.5 times in the x - direction. The free body diagram of the trunk, the associated forces, and the moments is illustrated in Figure 3-7.

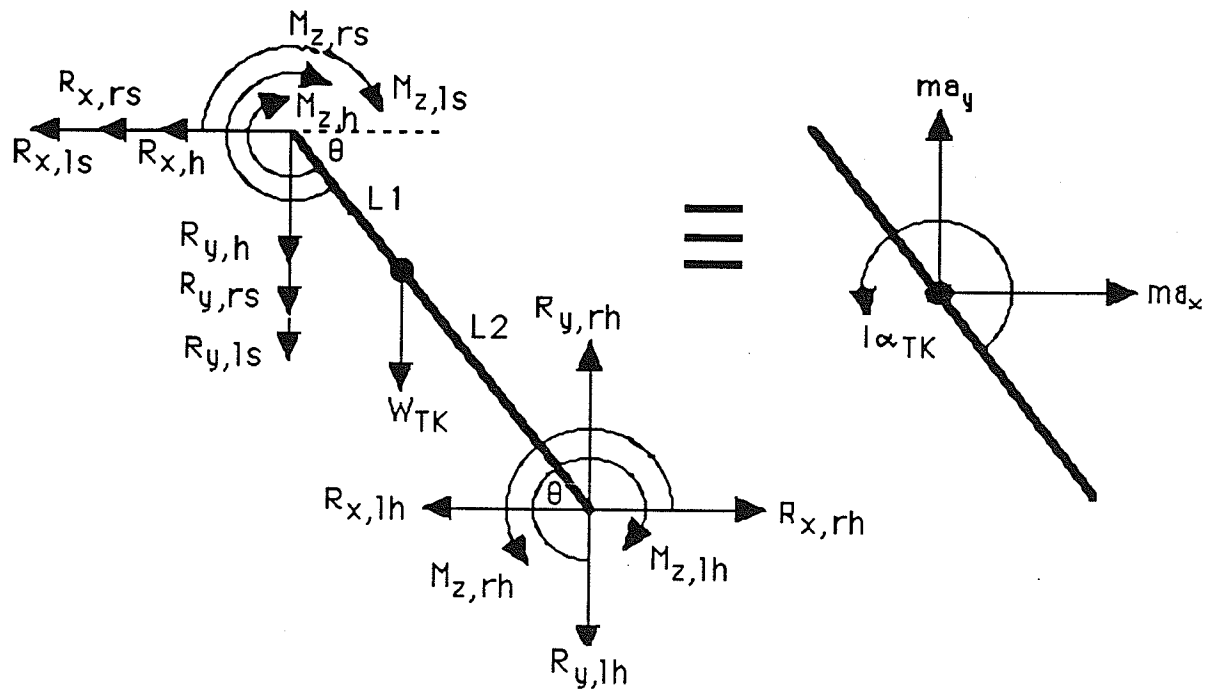


Figure 3-7 - free body diagram of the trunk. For each of the variables, the (ls) and (rs) were the left and right shoulders respectively, (h) represented the head, (lh) and (rh) were the left and right hips respectively .

The force in the x-direction for the trunk, at the right hip was

$$- R_{x,ls} - R_{x,rs} - R_{x,h} - R_{x,lh} + R_{x,rh} = ma_x \quad (3-15)$$

The force in the y-direction for the trunk, at the right hip was

$$- R_{y,ls} - R_{y,rs} - R_{y,h} - W_{TK} - R_{y,lh} + R_{y,rh} = ma_y \quad (3-16)$$

The forces and moments at the right hip are opposite to those of the left lower limb. The values calculated in the left lower limb were calculated moving proximally from the foot to the left hip, whereas the values for the right lower limb were calculated from proximal to distal. As a result, the forces in the femur are opposite to those of the right hip, and the result was the diagram presented in Figure 3-8.

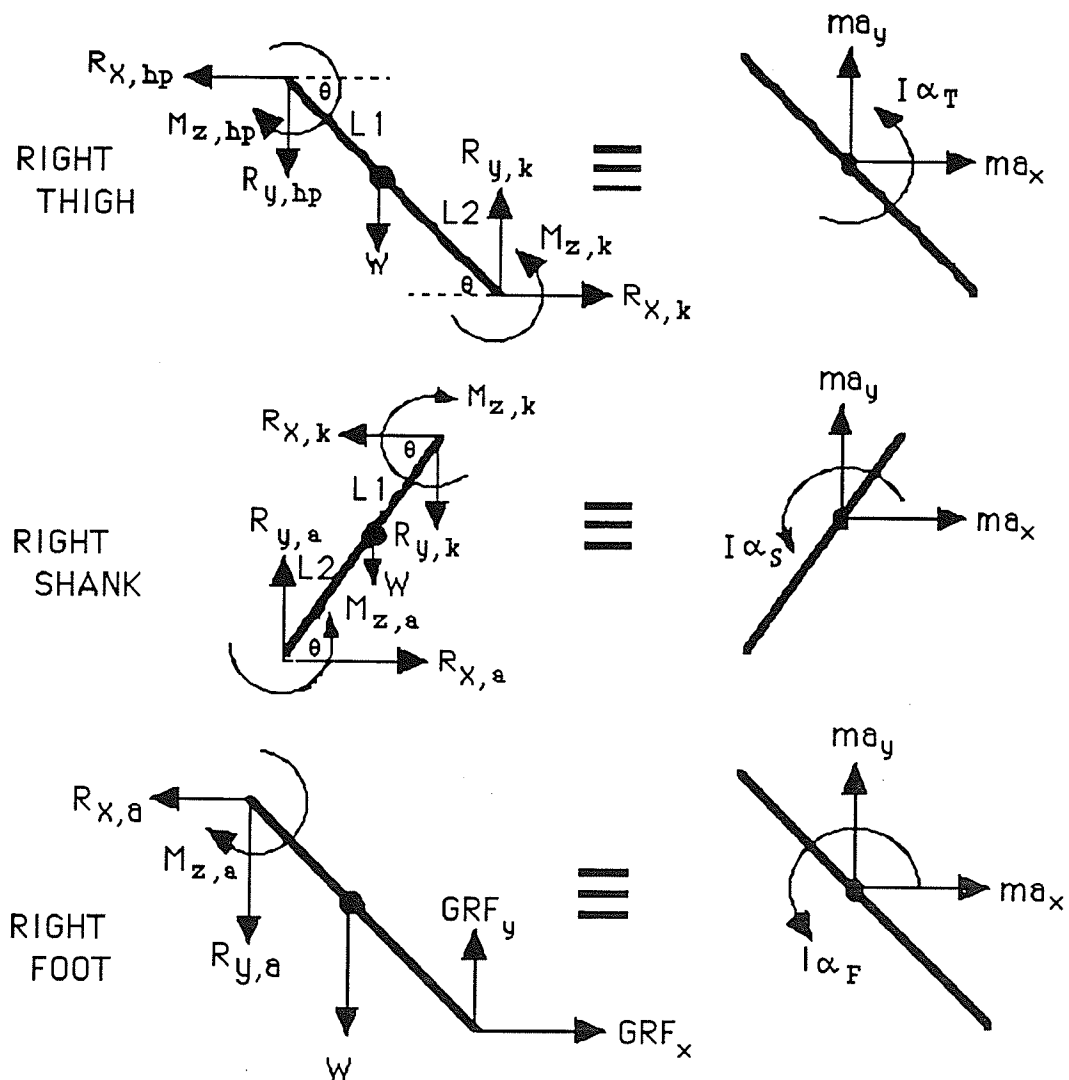


Figure 3-8 - FBD of the right lower limb. Notice that the direction of the forces and moments are opposite of the values for the left lower limb found in Figure 3-6.

The equations used to represent the three segments of the right lower limb were:

The force in the x - direction at the right knee:  $R_{x,k} - R_{x,hp} = ma_x$  (3-17)

and the force in the y-direction  $R_{y,k} - R_{y,hp} - W_T = ma_y$  (3-18)

The right shank, like the right thigh, was calculated differently than the left shank. Again the proximal joint had been calculated, and the distal joint (the ankle) was the joint in question.

The force in the x-direction for the right ankle  $R_{x,a} - R_{x,k} = ma_x$  (3-19)

and the force in the y-direction  $R_{y,a} - R_{y,k} - W_S = ma_y$  (3-20)

Finally, the GRF of the support foot was calculated using the following equations:

The GRF in the x-direction was  $-R_{x,a} + GRF_x = ma_x$  (3-21)

and the GRF in the y-direction was  $-R_{y,a} + GRF_y - W_F = ma_y$  (3-22)

The values found using equations #15 and #16 are representative of the impact forces found from the landing of a triple toe loop. These same values were also used later in the study, and compared to an alternative method of calculating forces using the entire body's CG.

### Calculation of Moments

For these calculations the length of the limbs, percent distance of the CG to the proximal joint, and the angle of the joint relative to the horizontal must all be known. Therefore, the moment equations for each limb segment about an axis parallel to the z-axis were as follows:

$$\Sigma M_z = I\alpha_z \quad (\text{Nordin \& Frankel, 1989}) \quad (3-23)$$

however, when calculating the equation about the CG, for the forearm-hand complex, and the free foot, the equation became:

$$M_{z,e} - R_{x,e}(L_1)(\sin \theta^*) - R_{y,e}(L_1)(\cos \theta) = I\alpha_{FA} \quad (3-24)$$

For the moment calculation at the foot the subscript (e) would be replaced by an (a). For the head, the moment equation was:

$$M_{z,h} + R_{x,h}(L_1)(\sin \theta) + R_{y,h}(L_1)(\cos \theta) = I\alpha_H \quad (3-25)$$

The moments found at the left shoulder and right shoulder were calculated using the formula that follows, with the exception that the subscripts would be changed to represent the joint in question.

$$M_{z,s} - M_{z,e} - R_{x,e}(L_2)(\sin \theta) - R_{x,s}(L_1)(\sin \theta) - R_{y,e}(L_2)(\cos \theta) - R_{y,s}(L_1)(\cos \theta) = I\alpha_{UA} \quad (3-26)$$

There are three moment equations that need to be calculated in the left leg. The moment at the left ankle has already been referenced above, however, the two remaining equations need to be addressed. At the knee, the equation was:

$$\begin{aligned}
M_{z,k} - M_{z,a} - R_{x,a}(L2)(\sin \theta) - R_{x,k}(L1)(\sin \theta) - R_{y,a}(L2)(\cos \theta) \\
- R_{y,k}(L1)(\cos \theta) = I\alpha_S
\end{aligned} \tag{3-27}$$

And at the left hip, the equation was:

$$\begin{aligned}
M_{z,hp} - M_{z,k} - R_{x,k}(L2)(\sin \theta) - R_{x,hp}(L1)(\sin \theta) - R_{y,k}(L2)(\cos \theta) \\
- R_{y,hp}(L1)(\cos \theta) = I\alpha_T
\end{aligned} \tag{3-28}$$

The trunk's moment equation was considerably more difficult. There were a large number of unknowns that had to be calculated in the free limbs before the trunk calculations could begin. However, the equation for the moment at the right hip, from all body segments above this joint was:

$$\begin{aligned}
- M_{z,ls} - M_{z,rs} - M_{z,h} + R_{x,ls}(L1)(\sin \theta) + R_{x,rs}(L1)(\sin \theta) + R_{x,h}(L1)(\sin \theta) + \\
R_{y,ls}(L1)(\cos \theta) + R_{y,rs}(L1)(\cos \theta) + R_{y,h}(L1)(\cos \theta) - M_{z,lh} + M_{z,rh} - \\
R_{x,lh}(L2)(\sin \theta) + R_{x,rh}(L2)(\sin \theta) - R_{y,lh}(L2)(\cos \theta) + \\
R_{y,rh}(L2)(\cos \theta) = I\alpha_{TK}
\end{aligned} \tag{3-29}$$

For each of the variables, the subscripts of (lh), (rh) were markers for the left and right hips respectively, (ls), (rs) were markers for the left and right shoulders respectively, while (h) represented the force and moments at the head.

Moving down the right leg to the support foot, the moment equation at the right knee was:

$$\begin{aligned}
M_{z,k} - M_{z,rh} + R_{x,rh}(L1)(\sin \theta) + R_{x,k}(L2)(\sin \theta) + R_{y,rh}(L1)(\cos \theta) \\
+ R_{y,k}(L2)(\cos \theta) = I\alpha_T
\end{aligned} \tag{3-30}$$

and at the ankle the equation was:

$$M_{z,a} - M_{z,k} + R_{x,k}(L1)(\sin \theta) + R_{x,a}(L2)(\sin \theta) - R_{y,k}(L1)(\cos \theta) - R_{y,a}(L2)(\cos \theta) = I\alpha_S \quad (3-31)$$

\*Note: the angle  $\theta$  was calculated as the internal angle between the plane and the segment in question. Therefore, for forces acting in the x-direction, the length of the moment arm was equal to the distance from the CG to the line of force (L1 or L2), times the sine of the angle between the horizontal and the limb segment. Similarly, for forces acting in the y-direction, the length of moment arm was equal to the distance from the CG to the line of force (L1 or L2), times the cosine of the angle between the horizontal and the limb segment.

The acceleration values, taken from double differentiation of the positional data, were substituted into these equations and the moment and force calculations were performed for each frame of the landing.

While the moments were calculated at the same time as the joint forces, the resulting values in the lower support limb were too large and too erratic. As a result, the positional data was smoothed at 12 Hz and subjected to the calculation procedure again. This provided smoother angular acceleration graphs without detracting from the shape of the original curves. However, during the second pass through the calculations the moment calculation started at the distal end of the support foot and moved proximally to the hip. In this calculation the following moment equations were used.

The moments at the ankle, knee, and hip were

$$M_{z,a} + GRF_x(L1)(\sin \theta) - R_{x,a}(L2)(\sin \theta) + GRF_y(L1)(\cos \theta) - R_{y,a}(L2)(\cos \theta) = I\alpha_F \quad (3-32)$$

$$M_{z,k} - M_{z,ra} + R_{x,ra}(L1)(\sin \theta) - R_{x,k}(L2)(\sin \theta) + R_{y,ra}(L1)(\cos \theta) - R_{y,k}(L2)(\cos \theta) = I\alpha_S \quad (3-33)$$

$$M_{z,h} - M_{z,k} - R_{x,h}(L1)(\sin \theta) - R_{y,h}(L1)(\cos \theta) + R_{y,k}(L2)(\cos \theta) + R_{x,k}(L2)(\cos \theta) = I\alpha_{TK} \quad (3-34)$$

The JRF and GRF values were calculated using a Pascal program written on the IBM compatible computer (Appendix E). The program read the required data files from the computer memory, into the program in order to calculate the GRF, JRF, and moment forces. The moment of inertia, mass, and length of each segment were incorporated in the computer program as percentages of the whole body values. The user of this program was prompted to enter the mass and height of each subject in order for the program to output the required forces. The resulting files were then stored back onto the computer hard drive in a format readable by Lotus 1-2-3. Lotus 1-2-3 was used so that Lap Link Mac (1988) could convert the information into a language readable by a Macintosh computer.

The data was then entered into a Macintosh statistical program, Statview, in order to find the peak GRF, peak moment and peak JRF for each subject. The mean peak values for all skaters, for each variable, were then calculated, irrespective of the time to peak impact "because averaging curves of different durations and with asynchronous peaks tends to attenuate peak values considerably" (Cavanagh & LaFortune, 1980, p. 399). Furthermore, for all the subjects, the average time to peak force was also calculated, in order to give a better understanding of the skill.

Furthermore, the GRF was calculated by a second method, which was then compared with the method above. The second method included the

weight of the subject, the acceleration of entire mass of the subject. The weight of the subject was the product of the mass and the acceleration due to gravity, while the second term was the product of the mass of the body and the vertical acceleration of the CG at each instant in time. The equation, presented by Miller and Nelson (1976),

$$R_y = W + ma_y \quad (3-35)$$

was used to calculate the GRF of the subject from the time of impact, to the time of zero acceleration of the CG. The results of the GRF calculations using the segmental method and the CG method were compared using a repeated measures ANOVA. This test compared the force values calculated by each method at each time interval. It was expected that there would not be a statistically significant difference ( $p < 0.05$ ) between the two GRF calculations. This same method of statistical comparison was used to compare the JRF and moments at the ankle, knee, and hip.

Finally, to allow comparison between the present study and previous studies the JRF was be divided by the cross - sectional area of bone in order to produce the pressure (MPa or MN/m<sup>2</sup> ) on the tissues. As for the moments, they were first divided by their respective moment arms, and then divided by the cross - sectional area in order to produce the pressure values.

## CHAPTER 4

## RESULTS

## Subjects

The subjects in the study consisted of seven males, and two females. The average height and weight of the subjects are reported in Table 4-1

Table 4-1 - The height and weight of subjects.

	Mean	$\pm$ s. d.	Minimum	Maximum
Height (cm)				
(male)	174.68	$\pm$ 5.73	170.0	185.4
(female)	167.65	$\pm$ 8.98	161.3	174.0
Weight (kg)				
(male)	69.13	$\pm$ 6.69	61.0	81.0
(female)	60.75	$\pm$ 3.88	58.0	63.5

Although there were originally to be nine subjects at five jumps each, for a total of 45 jumps, the final number of digitized jumps was 18. There were two reasons for the decrease in the number of jumps analyzed. The first reason was related to the failure of the Panasonic (PV-460-K) camcorder during the Brandon filming session. The three subjects at this filming session performed five triple jumps each, however, none of the trials were captured on film. This reduced the possible number of jumps from 45, down to 30 analyzable jumps, all of which came from the southern Ontario filming session. The second reason for the decrease in the number of jumps was the inability of the subjects to land the jumps successfully, and because some of

the subjects performed different jumps. The most commonly substituted jump was the triple flip. As a result, a total of 18 jumps were useable and the number of jumps recorded by each subject is reported in Table 4-2.

Table 4-2 - The subjects, number of acceptable jumps recorded, date of filming, and location of filming

SUBJECT	JUMPS LANDED	DATE	LOCATION
subject # 1	0	JAN. 7, 1993	Brandon, MN
subject # 2	6	FEB. 19, 1993	Barrie, ON
subject # 3	2	FEB. 19, 1993	Barrie, ON
subject # 4	3	FEB. 19, 1993	Barrie, ON
subject # 5	4	FEB. 19, 1993	Barrie, ON
subject # 6	2	FEB. 19, 1993	Barrie, ON
subject # 7	0	JAN. 7, 1993	Brandon, MN
subject # 8	1	FEB. 19, 1993	Barrie, ON
subject # 9	0	JAN. 7, 1993	Brandon, MN

#### Time Intervals of the Triple Toe Loop

The average time spent in the air for the subjects was  $0.638 \pm .037$  seconds while the minimum and maximum times spent in the air were 0.578 seconds and 0.714 seconds respectively. There was an interesting trend in the amount of time spent in the air, in that all subjects had their own unique amount of time that they spent in the air. For example, Subject #8 and Subject #6 consistently had trouble landing the Triple Toe Loop and their time in the air was under 0.6 seconds. The remainder of the athletes were in the air longer than 0.6 seconds, and as a result, they successfully landed their jumps. Furthermore, the most successful skaters, all of which competed at the national level or higher spent over 0.65 seconds in the air. Time intervals for each subject, during the airborne phase, are located in Table 4-3.

Table 4-3 - The mean, maximum, and minimum values for time of airborne phase of the Triple Toe Loop.

AIRBORNE PHASE					
Subject	Number of Jumps	Mean (seconds)	± S.D. (seconds)	Maximum (seconds)	Minimum (seconds)
2	6	0.652	± 0.023	0.680	0.629
3	2	0.689	± 0.036	0.714	0.663
4	3	0.606	± 0.010	0.612	0.595
5	4	0.654	± 0.022	0.680	0.629
6	2	0.586	± 0.012	0.595	0.578
8	1	0.595**			

\*\* This subject successfully landed only one jump, therefore, there were no standard deviation, maximum, or minimum values available.

The landing of the triple Toe Loop commenced at initial toe contact with the ice, and continued until the CG reached its lowest point. The time required to land this jump took an average of  $0.431 \pm 0.121$  seconds. The maximum time required was 0.731 seconds and the least amount of time was 0.272 seconds. The skaters with the most experience have the shortest time interval from initial contact to the lowest displacement of their CG. Subject #6, again required the most time ( $0.705 \pm 0.036$  seconds) to control the downward movement of the body's CG. The time intervals for each subject during the landing phase are presented in Table 4-4.

Table 4-4 - The mean, maximum, and minimum values for time spent during the landing of the Triple Toe Loop. \*\* This subject had no standard deviation, maximum, or minimum values as only one jump was completed.

LANDING PHASE					
Subject	# Jumps	Mean (s)	± SD (s)	Maximum (s)	Minimum (s)
2	6	0.431	± 0.050	0.493	0.374
3	2	0.357	± 0.048	0.391	0.323
4	3	0.419	± 0.109	0.544	0.340
5	4	0.348	± 0.082	0.459	0.272
6	2	0.705	± 0.036	0.731	0.680
8	1	0.391**			

#### Ground Reaction Forces (GRF)

A typical GRF curve for the figure skaters in this study is located in Figure 4-1. The first interval, between 0 - 0.05 seconds, is the impact peak force and the remainder of the graph is the force required to bring the body's CG to rest. The undulations in the curve after 0.05 seconds can be associated with the movement of the upper limbs, the free lower limb, the head, and the trunk.

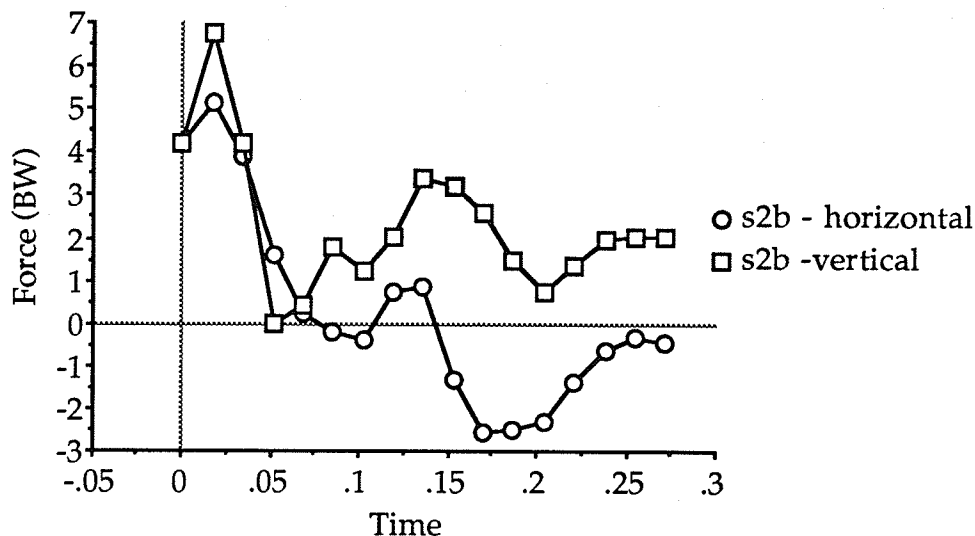


Figure 4-1 - A landing for one subject and the ground reaction force curves for the vertical and horizontal directions.

To interpret Figure 4-1, all vertically directed forces are greater than zero because a subject cannot have negative weight, however, the GRF and JRF values can be less than one body weight when the subject flexes their joints to absorb some of the forces. In addition, the horizontal force curve may have both positive and negative values for the GRF and JRF. A positive force value implies that a force is acting anteriorly on the proximal surface of the distal segment or ground, while a negative force acts posteriorly on the proximal surface of the distal segment or ground. In other words, the forces have the same magnitude but work in opposite directions on the ground or at the joints.

#### Subject GRF Differences

The vertical GRF for each subject was different from jump to jump, and from subject to subject. The peak vertical force had an average value of  $6.482 \pm 1.953$  BW, a maximum of 9.119 BW, and a minimum of 4.501 BW.

After performing a repeated measures analysis of variance it was found that there was a statistical difference ( $p < 0.0001$ ) between the subjects.

Furthermore, it was found that there was a statistical difference ( $p < 0.0001$ ) from jump to jump of the same subject. Subsequently, each individual subject's jumps were pooled to produce one set of data and then subjected to the same analysis. Again it was found that there was a statistically significant difference ( $p < 0.0309$ ) between subjects.

The graph for the horizontal GRF was considerably different than the one found for the vertical GRF. The mean and maximum horizontal GRF values were higher than the vertical GRF values, while the minimum value for the horizontal GRF was less than the vertical GRF. This is a unique finding, however, subject #6 and subject #8 skewed the horizontal values in the upper range. The mean, maximum, and minimum values for the horizontal GRFs for the Triple Toe Loop, were  $7.013 \pm 3.446$  BW, 14.260 BW, and 3.879 BW respectively. However, after removing subject #6 and #8 from the calculation of the mean values, the revised peak GRF in the horizontal direction became  $5.596 \pm 1.233$  BW, 8.265 BW, and 3.879 BW for the mean, maximum and minimum values.

As mentioned previously, subject #6 and #8 had a great deal of difficulty successfully landing the Triple Toe Loop. As a result, they spent the least amount of time in the air and experienced the greatest horizontal GRF. The average peak horizontal GRF for subject #6 was  $14.012 \pm 0.055$  BW and the horizontal GRF for subject #8 was 14.260 BW. These values were approximately 2.5 times larger than the values found for the overall mean of subjects # 2 - 5.

### Segmental vs. CG Methods of Force Calculations

The segmental and CG methods of calculating GRF provided similar curves, however, there were distinct differences between the peak force values and the minimum force values. From the vertical force curve in Figure 4-2, it is evident that the two methods of calculation were very similar. In other words, as one curve ascended or descended the second curve followed in the same direction. For each subject the segmental method of force calculation generally attained higher peak GRF and lower minimum values. However, a repeated measures ANOVA, determined that there was no significant difference ( $p < 0.2456$ ) between the two methods of force calculation regardless of the direction of force calculation. A typical curve for both the horizontal and vertical GRF using both methods of calculation is included in Figure 4-2.

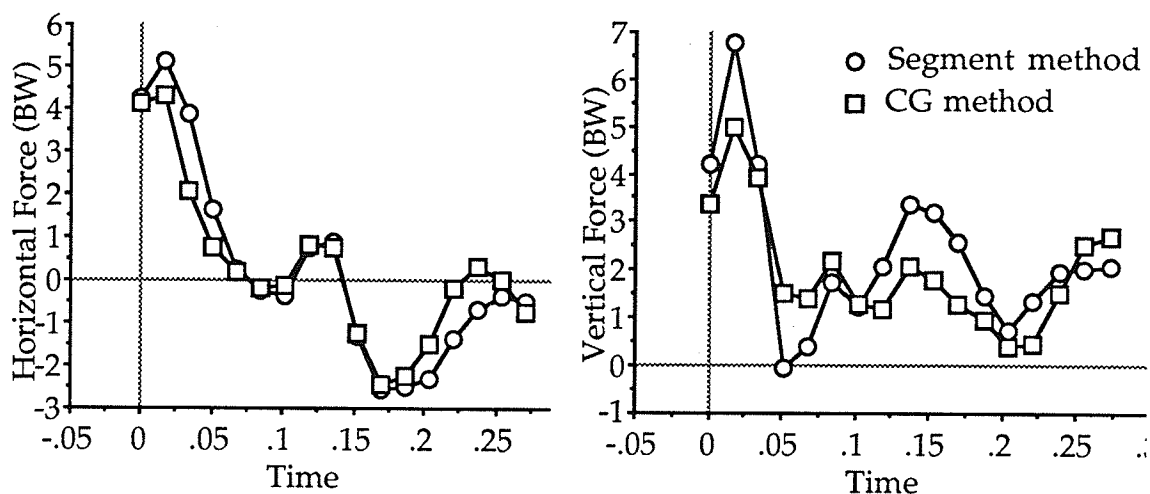


Figure 4-2 - The curves that compare the segmental and CG methods of horizontal and vertical GRF calculations for one subject.

The final finding of the statistical analysis was that when comparing the forces calculated in the x and y directions, there was a significant difference ( $p < 0.0001$ ) between the directions of the force calculation. Furthermore, when the direction and method of force calculation interaction was considered, there was no significant difference ( $p < 0.1988$ ) found between the methods regardless of the direction of the force calculation.

### Joint Reaction Forces

In general, the joint reaction forces calculated in this study resulted in the smallest force being located at the hip, a gradual increase at the knee, and a further increase at the ankle. Figure 4-3 reveals the close similarity between the vertical knee and ankle joint reaction force values, and a noticeable difference between these forces and the forces at the hip throughout the graphs, especially in the later stages of the landing.

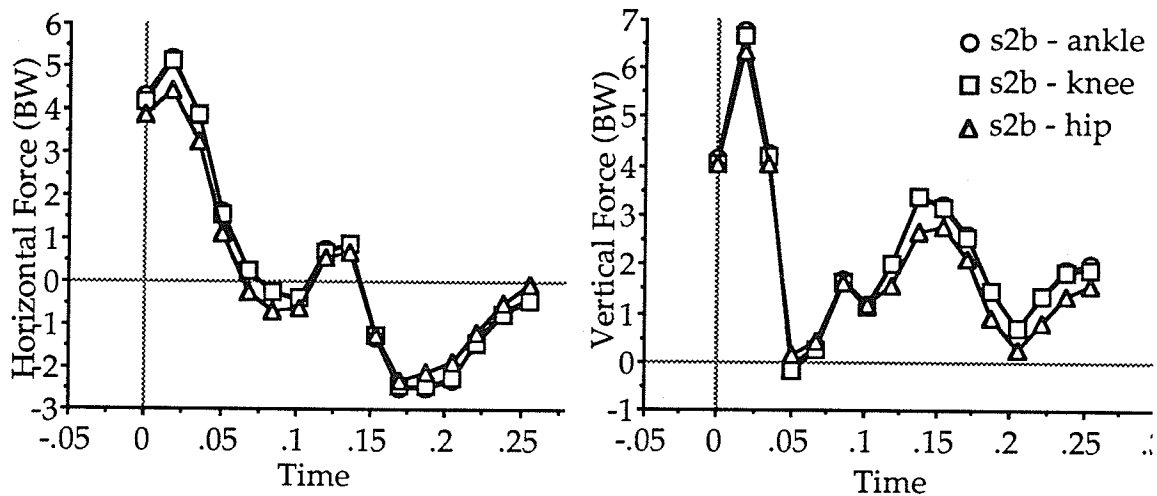


Figure 4-3- The horizontal and vertical JRF for one subject performing the Triple Toe Loop.

After a repeated measures ANOVA was performed on the data, the results showed that there was no difference ( $p < 1.000$ ) between the hip, knee, and ankle JRF. Table 4-5 contains the mean values for the peak JRF for all the subjects. It is important to note that the force values in the table are lowest at the hip, increase at the knee, and are highest at the ankle. This trend holds for both the horizontal and vertical directions.

Table 4-5 - Means, minimums, and maximum values calculated for the JRF at each of the hip, knee, and ankle for all subjects.

	HORIZONTAL				VERTICAL			
	mean	$\pm$ s. d.	Min.	Max.	mean	$\pm$ s. d.	Min.	Max.
Hip (BW)	6.465	$\pm$ 3.348	3.449	13.954	5.703	$\pm$ 1.292	3.789	8.663
Knee (BW)	6.970	$\pm$ 3.419	3.921	14.191	6.337	$\pm$ 1.354	4.439	8.978
Ankle (BW)	7.040	$\pm$ 3.452	3.910	14.319	6.501	$\pm$ 1.398	4.511	9.165

When comparing the vertical and horizontal GRF to the JRF values for the same subject, it is obvious that they follow the same trends. In fact, the curves were very similar, with the exception that the values for the JRF were lower than the GRF values. For example, in Figure 4-4 there is a graphical representation of the GRF and the joint reaction for the hip, knee, and ankle. From this diagram it is clear that the curves are identical in shape and the only differences are the magnitude of the forces.

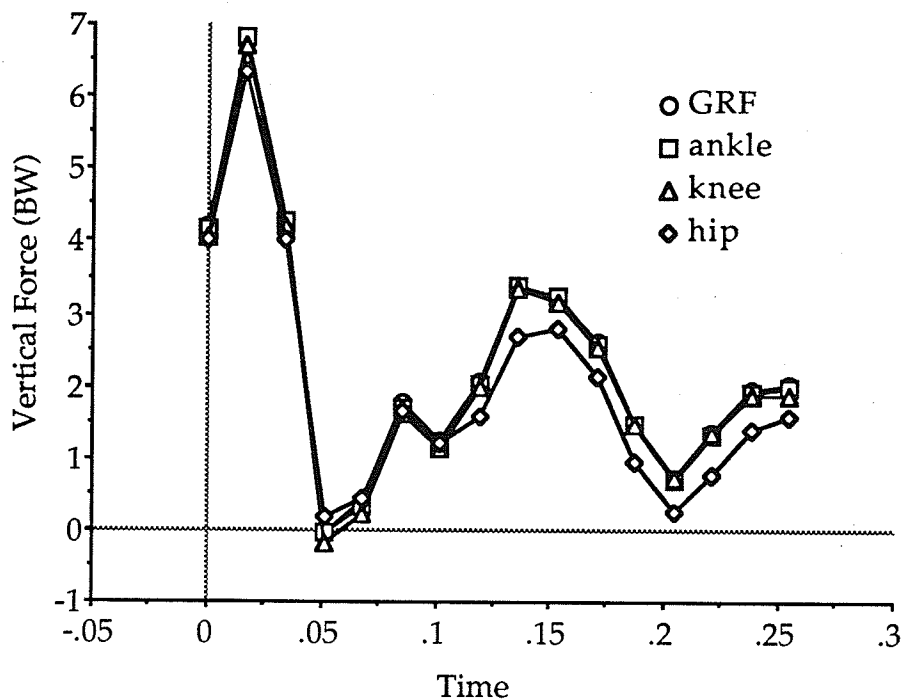


Figure 4-4 - A comparison of the vertical GRF and JRF for a single jump. In this diagram the values for the GRF are hidden by the ankle values except between 0.075 s. and 0.1 s. and from 0.225 s until the end of the jump.

In Figure 4-4, it is almost impossible to see the GRF curve. The reason for this is that the ankle value is almost identical. The mean peak GRF for this study was 6.482 BW, while the mean peak JRF for the ankle was 5.703 BW, resulting in a difference of 0.779 BW between the two forces. This difference can be associated with the mass of the foot, and the angular acceleration of this limb segment.

As mentioned previously, subjects #6 and #8 tended to skew the average horizontal JRF values. As a result, these values were considerably greater than the peak values found for the remaining subjects and Table 4-6 represents the peak horizontal forces for these two subjects.

Table 4-6 - Peak horizontal force values found for subject #6 and #8.

	Subject #6 Jump #1	Subject #6 Jump #2	Subject #8 Jump #1
Hip (BW)	12.819	13.200	13.954
Knee (BW)	13.772	13.934	14.191
Ankle (BW)	19.353	14.082	14.319

### Moments

Unlike the peak JRF and GRF which occurred within the first .05 seconds, the mean peak moment occurred after 0.05 seconds (s). The average time to peak moment for the hip, knee, and ankle was  $0.094 \pm 0.076$  s.,  $0.074 \pm 0.053$  s.,  $0.073 \pm 0.071$  s. respectively. The mean, minimum, and maximum moments found at each of the joints can be found below in Table 4-7.

Table 4-7 - The mean, minimum, and maximum peak moments found in the joints of the support limb during the landing of a Triple Toe Loop.

	MOMENT (N· m)			
	mean	$\pm$ s. d.	Min.	Max.
Hip	501.731	$\pm 145.612$	245.677	726.299
Knee	388.077	$\pm 121.495$	161.939	604.446
Ankle	76.513	$\pm 35.336$	39.611	170.621

The size of the moment at the hip is large, but the trend of having a smaller moment from joint to joint the more proximal the joint, still holds true. By looking at Figure 4-5, a representation of the moment at each of the joints, it is obvious that there was a difference between the curves.

Furthermore, throughout the graph the value of the ankle moment was less than the knee, and the value of the knee moment was less than the hip.

After a repeated measures ANOVA test, the results showed that there was no difference ( $p > 0.5576$ ) between the moment values at the three joints.

Furthermore, after pooling the jump values for each subject, the statistical analysis showed that there was still no difference ( $p > 0.5963$ ) between the moment values at each joint.

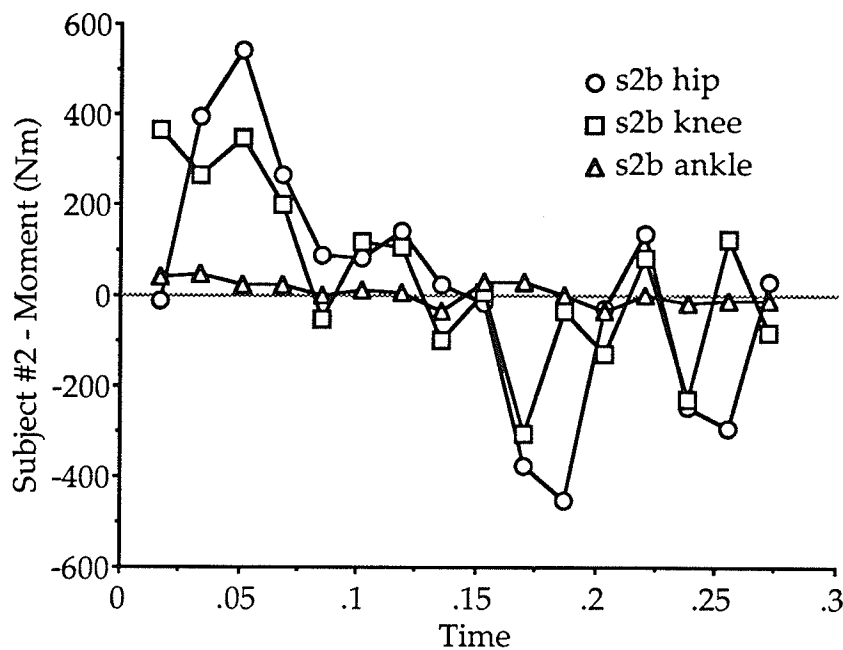


Figure 4-5 - A single representation of the moments found at the hip, knee, and ankle of one subject.

#### Accelerations and Angles of Support Limb

The difference between the angular acceleration of the support limbs of all the subjects was very minimal. With the exception of the first two frames of subject #8, all subjects have similar angular accelerations for the trunk, thigh, shank, and foot segments. The difference between subject #8 and the rest of the subjects occurred within the first 0.085 seconds and occurred at the

shank. The original angular acceleration for subject #8's shank for this time interval peaked at  $13586.675 \text{ deg/sec}^2$  ( $237.14 \text{ rad/sec}^2$ ). The remainder of the subjects had shank accelerations of between  $1384.676 - 4664.884 \text{ deg/sec}^2$  ( $24.17 - 81.42 \text{ rad/sec}^2$ ). However after resmoothing the data the values were  $10403.30 \text{ deg/sec}^2$  ( $181.56 \text{ rad/sec}^2$ ) for subject #8 and between  $194.57 - 7806.20 \text{ deg/sec}^2$  ( $3.40 - 136.23 \text{ rad/sec}^2$ ) for the remainder of the subjects.

Another finding that may relate to the differences between subjects #6, #8 and the remainder of the subjects, was the angle of the limb segments throughout the landing of the jump. By looking at Figure 4-6, it is evident that these two subjects have a completely different landing pattern than the remainder of the subjects. This graph represents the angle of the right shank and the horizontal axis. The landing angle between the horizontal and subject #6's shank was  $106.921$  degrees, while subject #8's shank was at an angle of  $92.880$  degrees. The angle of the other subject's shanks ranged from  $84.990 - 87.484$  degrees.

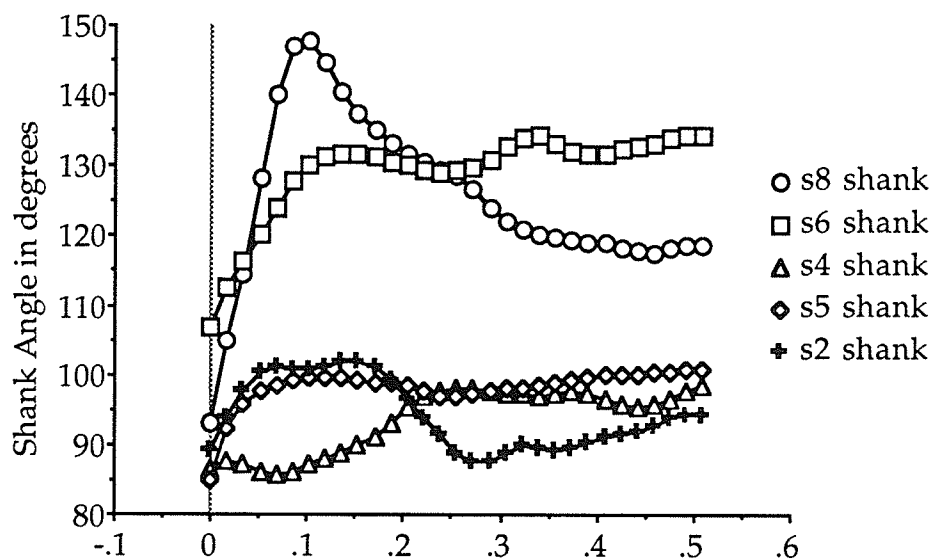


Figure 4-6 - The angle found between the posterior surface of the shank and the horizontal axis of the reference frame.

The first set of diagrams, Figure 4-7, are stick figure representations of the landing positions of three different subjects. For this set of diagrams, the first and third subjects are the more skilled subjects, while the second diagram is subject #8, the less skilled subject. The next page, Figure 4-8, contains three different subjects, however, this time the two jumps of subject #6 are located in pictures numbered one and three, while the more skilled subject is located in the middle.

Figure 4-7 - Touchdown Position of Subjects #4, #8, and #5

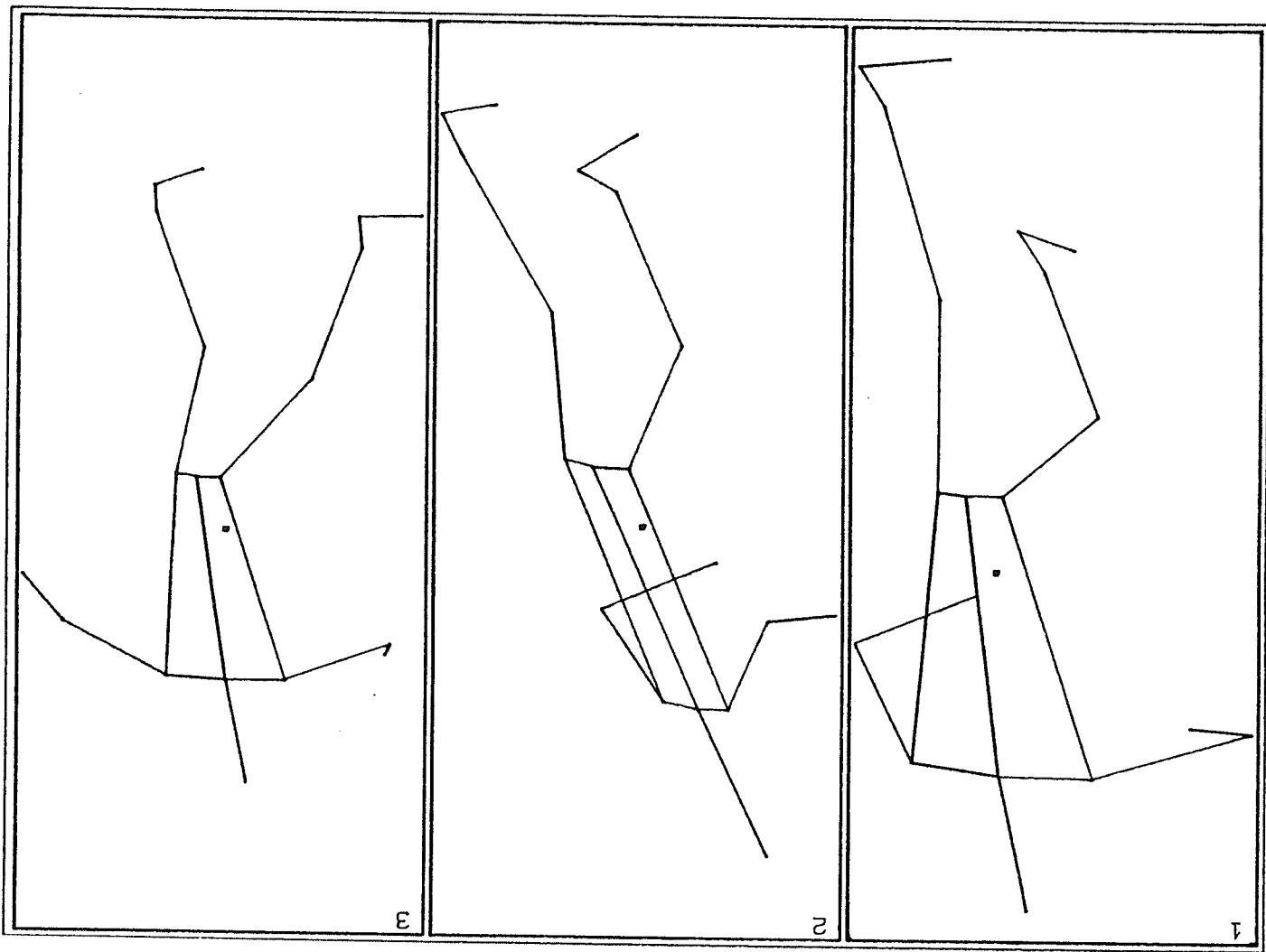
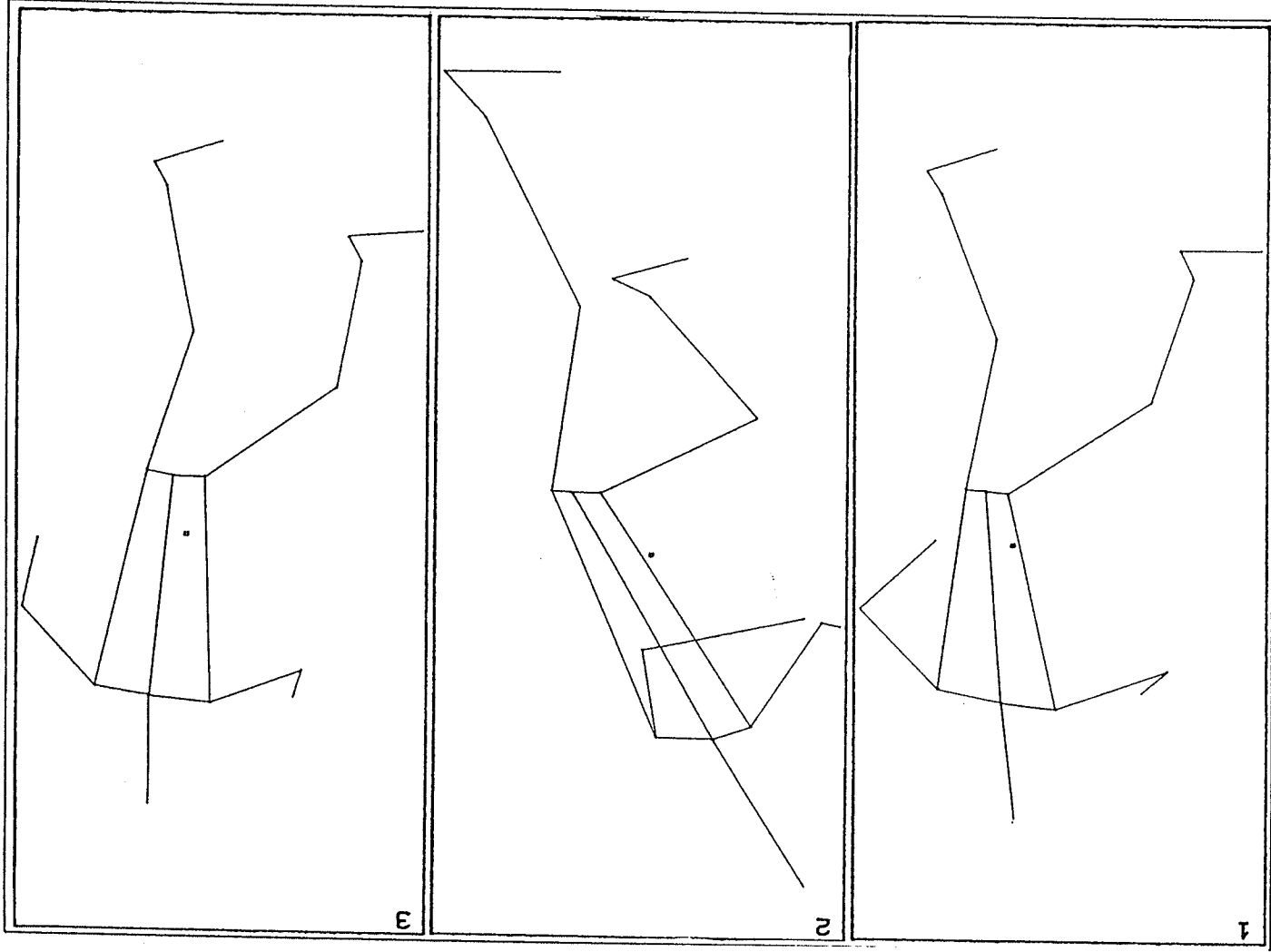


Figure 4-8 - Touchdown Position of Subject #6a, #2, and #6b



## CHAPTER 5

## DISCUSSION

## Time - Airborne Phase

In order to be successful in the performance of jumps there are only two variables that need to be considered during the airborne phase. The first is the time spent in the air, the second is the average angular velocity that the skater can obtain (Aleshinsky, 1986). According to this theory, the following equation was devised in order to find out how many revolutions could be completed

$$N = \text{TIME OF FLIGHT (T)} \times \text{AVERAGE ANGULAR VELOCITY (W)} \quad (\text{p. 13}) \quad (5-1)$$

where N was the number of revolutions to be performed. Aleshinsky (1986), believed that to increase the number of revolutions, the time in the air, and the average angular velocity had to be maximized. However, he was quick to point out that the time spent in the air did not change significantly from jump to jump, and that the only thing that could be increased was the angular velocity. While the increase in angular velocity will increase the number of rotations, the control of the body, and the precision of the jumping procedure must also be increased (Aleshinsky, 1986).

All of the subjects performing in this experiment produced similar airborne time intervals for the Triple Toe Loop. Moreover, what was intriguing was the small size of the standard deviation produced throughout the 18 jumps. The subjects that jumped with a mean airborne time of greater than 0.6 seconds had a standard deviation of 0.036 seconds, while those with

airborne times of less than 0.6 seconds had a standard deviation of 0.012 seconds. These results were consistent with the findings of Aleshinsky (1986), where his skaters were airborne for 0.59 - 0.61 seconds for the same jump. One notable finding of the present study, and that of Aleshinsky (1986), was that all skaters tended to perform jumps using the same time pattern for the airborne phase of the Triple Toe Loop. Furthermore, the small deviation within each subject showed that individually, the subject sets a specific framework for the amount of time he/she spend in the air.

Aleshinsky (1986) also found that the air time required for the Triple Toe Loop was the same as the time required for the Double Toe Loop. The times spent in the air for all double and triple jumps were between 0.55 - 0.61 seconds. Therefore, according to Aleshinsky (1986), because the time spent in the air for both the double and triple jumps were similar, the skater should place more emphasis on creating a greater average angular velocity than trying to jump higher. Furthermore, the result of the present study, and that of Aleshinsky (1986) further enforce the idea that elite figure skaters try to perform jumps with the same airborne time, regardless of whether it is a double or triple jump being performing.

Finally, from the present study, the time spent in the air may provide one possible explanation to the limited number of jumps that were landed. Aleshinsky (1986) found that his subjects successfully landed the Triple Toe Loop when the time interval ranged from 0.59 - 0.61 seconds. In the present study, the figure skaters that successfully landed their jumps had airborne time of greater than 0.6 seconds, while the subjects that had more difficulty landing the jumps had air time of less than 0.6 seconds. For example, subject #6 had an average time in the air of 0.586 seconds and subject #8 had an airborne time of 0.595 seconds. While these values were close to 0.6 second,

and/or close to those set by Aleshinsky (1986), these subjects landed only three jumps out of a total of ten trials. From these findings it was evident that these subjects were less skilled and need to improve their time spent in the air, or increase their average angular velocity. According to equation 5-1, by increasing the time spent in the air, the skater would be able to complete more rotations. Furthermore, by applying the law of conservation of angular momentum, by decreasing the rotational inertia of the body about its longitudinal axis, the rotational velocity about the same axis would be increased. As a result, the chance of successfully landing a jump would significantly increase.

It should be noted that there was one exception to this finding, and that was associated with subject #3. This subject landed a total of seven jumps, however, five of these jumps were more difficult than the Triple Toe Loop, and did not apply to this study. The jumps that subject #3 attempted were, three Triple Flips, two Triple Axles, and a Quadruple Toe Loop. While the Quadruple Toe Loop would have aided in the understanding of the GRF and JRF that occur when landing a jump in figure skating, the attempt was unsuccessful.

#### Landing Pattern

In the present study, the landing started with the initial contact of the toe pick with the ice and ended when the CG reached its lowest point. Similar to the time spent in the air, the skilled athletes have an established time pattern for landing. Aleshinsky (1986) found that the average time for a landing in figure skating took approximately 0.91 seconds (1.5 seconds for the airborne and landing, but the airborne phase takes a minimum of 0.59 seconds for the Triple Toe Loop). Podolsky et al. (1990), described the landing

time as taking 1 second, while Petkevich (1989) believed that the landing should be kept as short as possible for a successful landing. The current study showed that the average time to the lowest point of the CG took between 0.348 - 0.431 seconds. While this value is considerably lower than those of Aleshinsky (1986) and Podolsky et al. (1990), they meet Petkevich's (1989) standard of keeping the landing as short as possible. The most interesting finding, was the relationship between the skaters and an experiment that used gymnasts. McNitt - Gray's (1991) subjects jumped down from a height of 0.72 m, and stopped the downward motion of their CG between 0.259 - 0.285 seconds. While these values were smaller than those of the present study, they were considerably closer than those of the former studies.

The reason for the large difference between the times for the landing phase of this study and the previous ones could be the definition used for landing. In this study the definition of landing was understood to be the time from contact until the CG reaches its lowest vertical position. McNitt - Gray (1991) used this method on gymnasts and recreational athletes in order to standardize the end of the downward movements of the athletes. In this study, it was considered to continue the landing phase until the subject had begun to perform a new task, however, if a subject over exaggerated the landing, and another subject under exaggerated the landing, the times would be significantly different from each other. Therefore, the lowest point of the subject CG marked the difference between the landing and the rest of the landing movements, namely those that tend to lift the CG up from its lowest point. In the studies by Aleshinsky (1986), Petkevich (1989), and Podolsky et al. (1990), the timing of the landings was not explained, and no definite end point was defined, as a result, the times are considerably different from those of the present study. It was assumed that the landing phase in the studies

above concluded when the subject's motion reached a predefined minimal value.

The time required for the landing phase was not as stable as the airborne phase. Most subjects were fairly consistent with their landing procedure, however, the standard deviation between jumps was considerably different. In the landing phase, the largest standard deviation was 0.109 seconds, and the smallest was 0.036 seconds. The smallest standard deviation in the landing phase was equal to the largest in the airborne phase, indicating the differences that take place in the landing patterns. It should also be noted here that subject #6 again had a significantly different landing time than the rest of the subjects, requiring a mean of 0.705 second to control the downward and forward movement of the body's CG.

Relating the results of the McNitt - Gray (1991) study to those of of this study, is reasonable. The elite skaters in the present study were similar to the gymnasts of the former study, in that they tended to have a constant landing pattern, with little deviation from this pattern. The weaker subject, namely subject #6 had a considerably longer landing pattern, similar to those of the recreational athletes in McNitt - Gray's (1991) study. Therefore, the more elite the athlete is, the greater is the chance that the landing pattern will become more uniform.

One additional note that should be made was that since subject #6 had a very large mean landing time ( $0.705 \pm 0.036$  second) with a small standard deviation, implies that this subject favoured a longer landing pattern. The only problem that might arise from this pattern is the fact that during a competition the transfer from a jump to another maneuver may take longer than other skaters, and it may appear as if the skater was having trouble landing the jumps.

### Force Interpretation

In the literature there is disagreement about the time that is required for muscles to react to impact forces (Cavanagh and LaFortune, 1980; Valiant & Cavanagh, 1985; Steele & Milburn, 1987; Bobbert et al., 1987; Ricard and Veatch, 1990; Dufek & Bates, 1991). According to Nigg et al. (1981), the forces that occur from impact until the muscles become active, are known as passive forces. The importance of passive forces and the time through which they occur, is the lack of muscle control (Nigg et al., 1981). During this time period the forces occur faster than the neuromuscular system can respond, and as a result, the method of force absorption is inefficient (Nigg et al., 1981) because the force must be absorbed by the bones, soft tissue, and through passive flexion of the ankle, knee, and hip joints (Ricard & Veatch, 1990).

At the lower end of the scale, Nigg et al. (1981) found passive forces occur through times as low as 10 milliseconds (ms), while McNitt - Gray (1991) found passive forces occur through times as high as 61 ms. Although there is a noticeable differences between the length of time through which passive forces occur, these forces do not appear to occur any later than 61 ms.

The peak forces in both the x and y directions for this study occurred during the passive stage of the landing. In the x and y directions, the time from the instant of toe touchdown to the peak impact force was  $0.044 \pm 0.019$  and  $0.045 \pm 0.014$  seconds respectively. These were within the normal time frame of passive forces, and therefore, all the forces during this time must be absorbed by the bones, cartilage, and by flexion of the supporting limb.

Once the musculoskeletal system has had time to respond to the initial impact, the passive forces become active forces and the muscles are used to slow the body's downward motion (Nigg et al., 1981). While Nigg et al. (1981), suggested the active forces begin 30 ms after impact, Miller (1990), suggested

that these active forces occur between 80 - 120 ms after touchdown. Furthermore, Cavanagh and LaFortune (1980) found the peak active force occurred 83 ms after contact. While the present study was unable to record the start of muscular activity, the graph showed a significant drop in the force after 0.05 s, and the subsequent lower forces after this time may be an indication of the start of the muscular activity. Furthermore, after the large drop in the vertical force, any forces present were an indication of the forces exerted by the body to halt its downward movements. The undulations found in the graph following the peak GRF can be related to the movements and forces required to bring the head, trunk, and upper limbs to rest.

#### Vertical Ground Reaction Forces

As noted in the results, each subject in this study had a unique landing pattern because the GRF curves were statistically different from each other. These same findings were reported in a number of other studies (Cavanagh and LaFortune, 1980; Bates et al., 1983; Valiant & Cavanagh, 1985), and according to Dufek & Bates (1990), subjects were different from trial to trial, and a between subject analysis was only useful if all subjects performed in a similar manner. However, since this was not the case, a comparison of the peak force values could provide information that might relate to the occurrence of injuries present in figure skaters.

The peak vertical forces found in this analysis were consistent with other studies in which the subjects jumped from similar heights (Bobbert et al., 1987; Stacoff et al, 1988; McNitt - Gray, 1991). The subjects in this study jumped an average of 0.452 m into the air (0.371 - 0.655 m), while those in previous studies jumped from heights between 0.32 - 0.72 m (Bobbert et al., 1987; Stacoff et al, 1988; McNitt - Gray, 1991). The findings of the Bobbert et al.

(1987) study showed GRF values of  $3,515 \pm 964$  N for 0.4 m jumps and  $4,496 \pm 693$  N for jumps of 0.6 m. On the other hand, McNitt - Gray (1991) found peak GRF values of  $3.93 \pm 1.3$  BW and  $6.26 \pm 1.9$  BW for heights of 0.32 and 0.72 m respectively. Finally, the study by Stacoff et al. (1988) was the closest to the present study because the subjects performed their jumps while trying to block shots in volleyball. The height of the jumps varied between 35 - 65 cm, producing vertical GRF values between 1000 - 6500 N. Therefore, the average peak impact force values of  $4,395.8 \pm 128.2$  N ( $6.48 \pm 1.95$  BW) found in the present study were similar to other impact studies.

Furthermore, Steele and Milburn (1987), studied the forces in netball landings and found the mean force values were in the range of 3.9 - 4.3 BW. During this study however, the height of the jumps was not reported, instead the subject simply performed a jump that is required in the sport of netball. Therefore, as mentioned above, the forces found in this study of the figure skater seem to be within the same range as previous studies.

An interesting finding of the present study was the shape of the force curve that resulted from the impact landing. The impact force curve did not contain the two force peaks that is typical of other landing curves, instead there was only one impact peak. Other studies that have found single impact peaks when landing from jumps were reported by Bobbert et al. (1987), and Gross and Nelson (1988). Both of these studies found that a single force peak was evident upon metatarsal contact, but the second force peak was absent. Gross and Nelson (1988) explained the lack of a second peak as a result of not allowing the heel to contact the ground. As a result, the impact peak was rounded, the landing was more controlled, and there was a significant decrease (22%) in the peak vertical force (Gross and Nelson, 1988). However, Bobbert et al (1987) found that subjects were only able to control the landing

for jumps that were performed from heights of under 0.6 m. If the jump was greater than 0.6 m, the heel of the subject would strike the floor creating a second force peak.

In this study, there were no vertical force curves that contained two peak force values, and according to Gross and Nelson (1988),

non-heel contact landers avoided the second transient associated with heel contact by playing a more active role in the cushioning process. The cessation of downward motion of the heel was a product of controlled joint motion rather than the collision with the landing surface displayed by heel strike landers. (p. 513)

Two other reasons for the lack of two peak force values are the skate and the anatomical structures of the lower limb. The skate prevents the typical two peaked force curve because of the blunt shape of the skate's blade (see Figure 2-15, pg. 89). If the skaters were to rock too far backward onto the heel of the skate, the heel of the skate blade would dig into the ice causing the skater to lose his/her balance, resulting in an unsuccessful jump attempt. In addition, the stiffness of the boot provides very little flexion (Smith, 1990), and therefore, any flexion occurring at the knee would cause the heel to be lifted off of the ice preventing the heel from contacting the ground. As a result, in this study the vertical GRF curves contain only one vertical force peak in the landing of a Triple Toe Loop.

The second explanation is related to the anatomical structures of the support limb. Upon landing from a jump, the downward movement of the body is suddenly stopped, and the angular acceleration of the lower limb rises to aid in the absorption of the vertical forces (Bobbert et al., 1987). As a result, the increasing angular velocity of the shank, and the stretch placed on the

Achilles tendon and triceps surae increases the load on these structures. In order to prevent over-stretching and injury to these structures, the skater rocks slightly forward preventing the heel from contacting the ground, which also helps to eliminate the second force peak. This action also helps maintain the skater's balance and prevents falling by keeping the CG over the base of support, the landing foot.

#### Horizontal Ground Reaction Forces

Typically the force curve for the anterior - posterior direction has two peak forces. The first peak is known as the braking force, while the second is the propulsive force (Munro, Miller, & Fuglevand, 1987; Miller, 1990). Of the two forces, the braking force tends to be larger than the propulsive forces (Munro et al. 1987).

From the literature review, the general consensus is that for any given subject, the braking pattern is reasonably consistent, however, across subjects there is a considerable difference (Miller, 1990). In the present study this was true for the between subject differences, however, there was also a difference between the individual subject's landing patterns as can be noted in Figure 5-1.

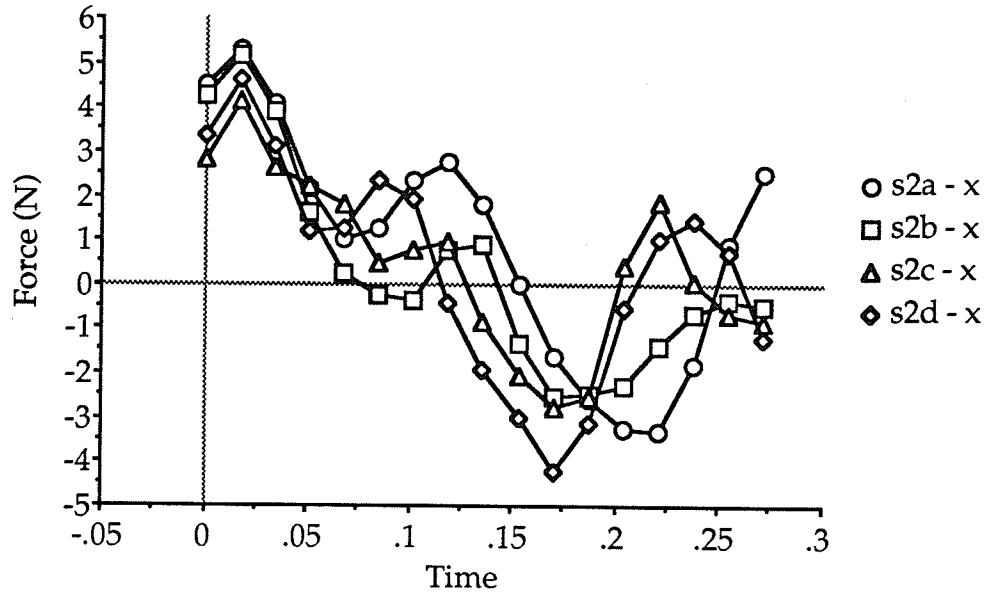


Figure 5-1 - A typical horizontal GRF curve for one subject, and the large degree of variability that is present.

In order to explain the differences found in the initial force value, the velocity of the subject must be considered. By comparing the velocities and the forces, it was found that the largest velocity at touchdown, from the graph above, was directly related to the horizontal velocity of the subjects CG. In other words, the velocity of Subject 2a at touchdown was  $-2.379$  m/s, which corresponds to the largest horizontal GRF. Furthermore, the velocity of the other trials for this subject were  $-1.816$ ,  $-1.487$ , and  $-1.237$  m/s for the jumps labeled s2b, s2d, and s2c respectively. By ranking the velocities and forces from smallest to largest, it was found that as the velocity increased so did the impact force. From this, it is evident that the variability found in the force values is the result of the large horizontal accelerations caused by stopping the larger horizontal velocity with which the subject contacted the ice.

The initial braking force in figure skating starts at toe contact. However, because the reference frame was rotated in order to provide a purely sagittal view of the skater at all times, the skater was initially moving

through the air in a negative horizontal direction. As a result, the skater's horizontal velocity was constant, but negative. At touchdown the ankle was slightly plantarflexed and the toe pick became the first part of the blade to contact the ice. The shape of the toe pick caused the foot to dig into the ice and produced a large acceleration in the positive direction. Therefore, according to Newton's Third Law of Equal and Opposite forces (Hall, 1991), the skater applied a force in the negative direction to the ground and the GRF applied to the skater was in the positive direction. After the initial force was applied by the ground, the skater began to dorsiflex the ankle, moving the weight down the length of the blade and the acceleration of the foot became negative, which produced the negative force. Therefore, similar to other studies (Cavanagh & LaFortune, 1980; McNitt - Gray, 1991) the anterior - posterior GRF curve is bimodal, with an original braking component, followed by a propulsive component. However, due to the fact that the reference frame was rotated 180°, the forces in the horizontal direction for this study were 180° out of phase with previous studies. In other words, what is positive in this study would be negative in other studies, and what was negative in this study would have been positive in previous studies (Munro al., 1987; Miller, 1990).

In previous studies, the horizontal GRF was found to vary between 0.43 - 13 BW (Cavanagh & LaFortune, 1980; Panzer et al., 1987; Steele & Milburn, 1987; McNitt - Gray, 1991). While a majority of the athletes in this study were within these limits, subjects #6 and #8 exceeded the upper limit of these studies by one times body weight. The mean value of  $7.013 \pm 3.446$  BW is almost exactly in the middle of the range found in the previous studies, indicating that it is a reasonable finding. While the large values of 13 BW found by Panzer et al. (1987) were the result of the somersaulting rotation, the

figure skater's anterior - posterior force may be largely the result of the braking force caused by the toe pick halting the horizontal and rotational velocity of the foot.

### Joint Reaction Forces (JRF)

According to a number of sources ( Radin, Parker, Pugh, Steinberg, Paul, & Rose, 1973; Soderberg, 1986; Nigg, 1986; Stacoff et al., 1988) the forces that occur at the joints are due to external forces, muscular forces, and to a small extent from the body's weight. The maximum JRF found in the literature for each of the joints, and those calculated in this study are located in Table 5-1.

Table 5-1 - The JRF values for the three joints of the lower limb from previous studies.

Author	Activity	Joint	Vertical JRF (BW)	Shear JRF (BW)
Skelly & DeVita (1990)	Jump Landing	Ankle	15.8	
Harrison, Lees, McCullagh, & Rowe (1986)	Running	Knee	33.0	
Crowninshield, Johnston, Andrews, & Brand (1978)	Walking	Hip	7.0	
Burdett (1982)	Running	Ankle		5.5
Panzer et al (1988)	Gymnastics	Knee		2.8
		Hip		1.7
Present Study	Landing of a Triple Toe Loop	Hip	6.5	7.1
		Knee	6.3	6.9
		Ankle	5.7	6.5

While it is obvious that the vertical JRF values are well below the maximum values reported by Harrison, Lees, McCullagh, and Rowe (1986), the values are still within the range of previous studies. On the other hand, the forces in the horizontal direction are somewhat higher than a majority of the studies presented. The only JRF values that were similar to those found in this study were presented by Burdett (1982) and Crowninshield, Johnston, and Andrews (1978).

The JRF pattern with regards to time, in both the x and y direction, follow the same pattern set by the GRF which is in agreement with Zarrugh (1981). Furthermore, according to Denoth et al (1984), the GRF "...acts nearly unreduced at the joints" (p. 668). While the GRF is the main contributor to the magnitude of the forces at the joints, the JRF become less and less similar to the original GRF because of the force of gravity, inertia, and muscular forces (Zarrugh, 1981). In the present study, both of these findings existed, and by looking at Figure 5-2, it is obvious that these findings were similar to those of Zarrugh (1981) and Denoth, Gruber, Ruder, and Keppler (1984). In other words, the JRF at the ankle and knee were basically unchanged from the GRF values, however, as the hip JRF follows the GRF pattern, the trend becomes less similar than the previous joints.

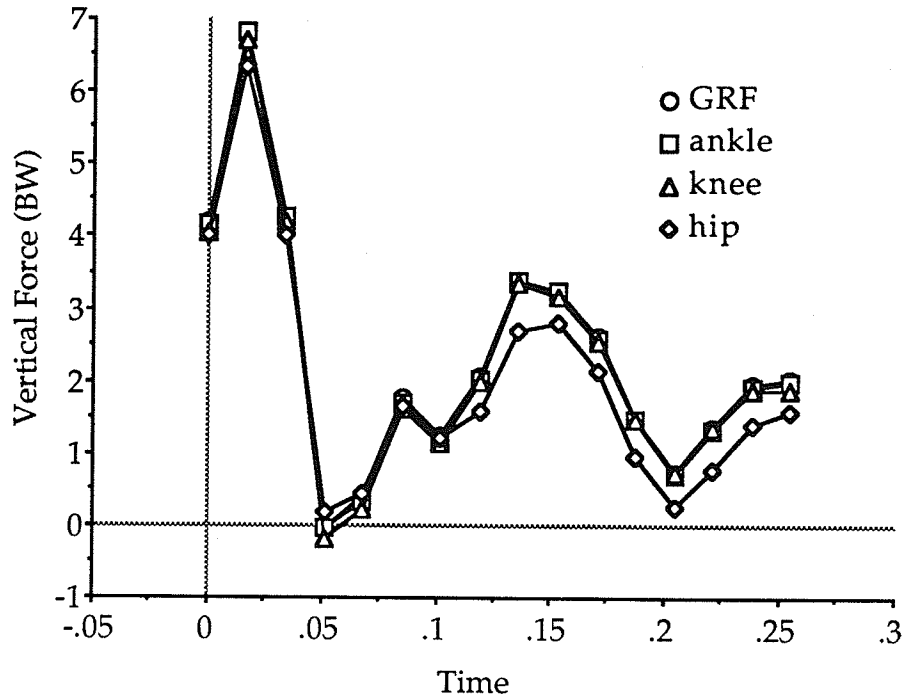


Figure 5-2 - A comparison of the GRF and JRF for a single jump. In this diagram the values for the GRF are hidden by the ankle values except between 0.075 s. and 0.1 s. and from 0.225 s until the end of the jump.

Brown, Abani, and Usman (1986), studied the joint reaction forces for weight lifters and noted that the joint forces decrease as the joints were located further away from the point of application of the force. In the present study, force values at the ankle, knee, and hip for the figure skaters followed the same trend. The figure skater's mean vertical peak JRF at the ankle, knee, and hip were 6.501, 6.337, and 5.703 BW respectively. In the horizontal direction, these same joint forces were 7.070, 6.970, and 6.465 BW respectively.

In the present study, the JRF values decreased both vertically and horizontally as the joints were located further from the point of application of the force, which support the findings of Zarrugh (1981) and Brown et al. (1986). This decrease in JRF can be explained by the ability of the joints to

attenuate the forces (Valiant, 1990). In addition, impact forces are a function of the body's mass, impact velocity, and distance through which the mass is decelerated (Kaelin et al., 1988). Therefore, by increasing the amount of flexion of the support limb, the athlete reduces the magnitude of the forces in the joints by increasing the distance through which the body's mass is decelerated (Stacoff et al, 1988; McNitt - Gray, 1991).

In all studies to date the general consensus has been that the knee joint is the prime force absorber (Cappozzo, Figura, & Marchetti, 1976; Winter, 1983; Dickinson, Cook, and Leinhardt, 1985; White & Winter, 1985; Chu, Yazdani - Ardakani, Gradisar, & Askew, 1986; Dufek & Bates, 1990; Valiant, 1990; Ounpuu, Gage, & Davis, 1991). In the present study, the fact that the knee absorbs a great deal of the force can be seen in Figure 5-3. In this diagram, it is obvious that the ankle does not play an important role in the absorption of impact forces. Figure 5-3 shows the similarity between the force curves for the ankle, knee, and hip. The two lines for the ankle and knee are almost indistinguishable, therefore, the ankle cannot play a very active role in the damping of the forces. Furthermore, the visual difference between the former two JRF values and the JRF curve for the hip is significant in the first three and last eight frames. Therefore, the knee must perform a greater role in the damping of the forces passed from the ankle to the hip.

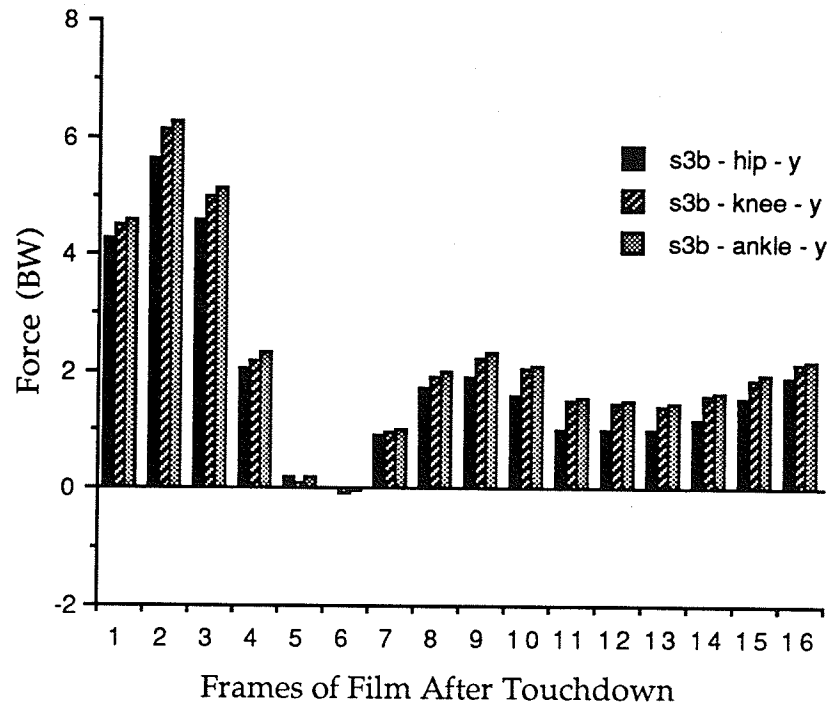


Figure 5-3 - This bar graph provides a comparison of the JRF for a single jump of subject #3. In this diagram the value for the JRF at the knee and ankle are almost identical, however, the JRF at the hip was somewhat smaller.

The large range of motion present in the landing of a jump also occurred in phase. In other words, moving proximally, the most distal segments were brought to rest one at a time (McNitt - Gray, 1991). As a result, the foot segment was stopped very quickly and did not have time to absorb a great deal of force. Therefore, the JRF at the ankle should resemble the GRF curve. Furthermore, because the ankle was stopped so quickly, almost all the force at the ankle was transferred to the knee. At the knee the JRF were similar to those of the ankle, however, the flexion of the knee was used to absorb these forces by eccentric muscle contraction and the resulting forces

passed to the hip were somewhat smaller. These differences can be seen initially at times of less than 0.1 seconds and after 0.15 seconds in Figure 5-3.

The high shear forces present in the joints can be related to the fact that upon landing, the downward movement of the thigh and upper body forces the knee to flex (Stacoff et al., 1988). The faster the forced flexion, the larger the shear force will become.

### Moments

The number of studies that have reported moments of force at the joints in the lower limb is considerably fewer than those reporting JRF values. Table 5-2 contains the maximum moments of force as reported in the literature from a number of these studies. Also included are the values from the present study.

Table 5-2 - The maximum moments from a number of studies and those calculated in this study.

Author	Activity	Joint	Moment (N·m)
Brüggemann (1985)	Gymnast	Ankle	345
Zernicke, Garhammer, & Jobe (1977)	Jumping	Knee	550 - 560
Bobbert et al (1986)	Counter Movement Jump	Hip	366
Present Study	Landing of a Triple Toe Loop	Hip	501.731
		Knee	388.077
		Ankle	76.513

The largest moment values, when divided by moment arm length and average body weight, produced muscular forces of 2.47, 9.80, and 8.45 BW at the ankle, knee, and hip respectively. While these values were relatively small, according to Smith (1975), the moment of force, from positional data, can be misrepresented by as much as  $\pm 50\%$ . If this were the case, and the values were off by the maximum of 50%, then the values at the ankle, knee and hip would still be within the acceptable range.

One reason for these small values may be the filming rate of the cameras. The time between frames was 0.017 seconds, and according to Denoth et al (1984), when accelerations reach values that are very large, for example  $600 \text{ m/s}^2$  or  $10^5 \text{ deg/s}^2$ , video tape recording devices are not as accurate as high speed photography. In the present study the angular accelerations of the support limb was as high as  $10403.30 \text{ deg/s}^2$  ( $181.56 \text{ rad/s}^2$ ). As a result, these moment values may have been too fast for the video taping method, and should have been performed using high speed cameras to produce more accurate values.

Figure 5-4 shows the moment curve for one subject, and the large differences between successive film frames. During the time interval of 0.187 - 0.204, the moment value jumps from - 452.081 to - 27.676 N·m. This produces a difference of 424.405 N·m between successive frames. However, if more frames were recorded between the two frames mentioned, then possibly the angular accelerations would be smaller, and the moments lower and more accurate.

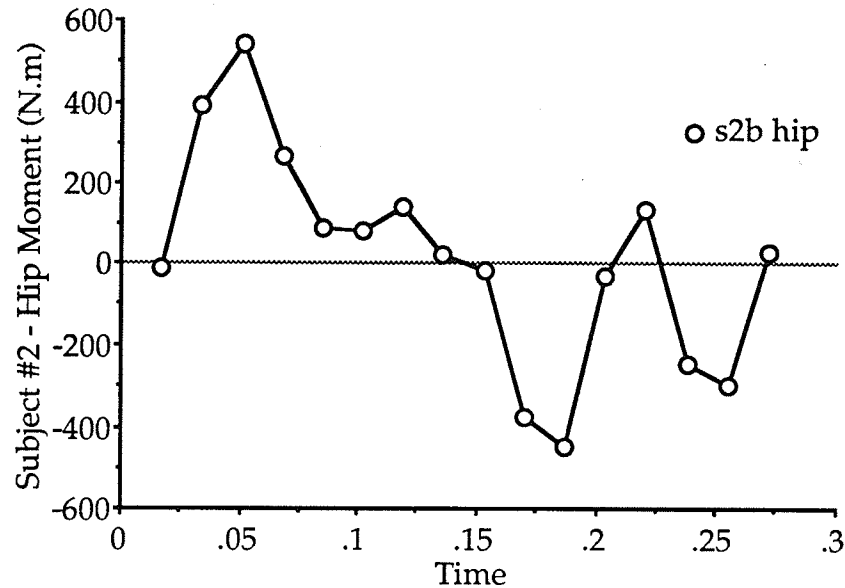


Figure 5-4 - A single subject representation of the moments produced by the second calculation procedure. From this diagram it is important to note the large moment values and the difference between successive film frames.

#### Acceleration and Angles of the Lower Extremity

In order to understand why the original horizontal forces of subjects #6 and #8 were so much different than the other subjects, the angular acceleration and angles of the segments at touchdown were considered. This information was included at this point due to the contribution of these values to the forces and moments at the joints and may help shed light on the values presented above.

The angular acceleration of the segments of the support limb was compared across subjects, and the only segmental difference was found at the shank. Subject #6 had acceleration values within the limits set by the other subjects (194.57 - 7806.20 deg/s<sup>2</sup> or 3.4 - 136.23 rad/s<sup>2</sup>), while subject #8 had values that were considerably larger (10403.30 deg/s<sup>2</sup> or 181.56 rad/s<sup>2</sup>).

Since acceleration is directly related to the force produced (Hall, 1991), the speed at which the angle between the bones at the joints changes will have a significant effect on the force. According to Stacoff et al. (1988), the downward movements of the thigh and upper body force the knee into flexion. Furthermore, the greater the impact force, the greater the flexion acceleration will be at the knee. As a result, the moment at the joints is greatly increased. Therefore, the high angular acceleration of subject #8's shank causes the knee moment to be significantly increased. In this study, the largest moment at the knee for subject #8 (504.731 N·m) corresponded with the subject's high angular acceleration (10403.30 deg/s<sup>2</sup>).

In order to arrest this acceleration, the muscles around the knee were forced to eccentrically contract and absorb the force. Therefore, a method of slowing down the shank's acceleration would be to place emphasis on a conditioning program. This would build up the strength of the quadriceps and Achilles complexes so that they will be stronger and able to absorb more force and reduce the angular acceleration.

The segment angles at touchdown for Subject #6 and #8 were different than the remainder of the subjects. As noted in Figure 4-6, the angle between the posterior surface of the shank and the horizontal was considerably greater for these subjects than that of the remaining subjects. Two possible reasons for these increased horizontal joint forces are described below.

The first reason may be related to the skate's toe pick. If the boot of the skate is as stiff as indicated by Smith (1990), then very little flexion is allowed. The increased angle of the shank at touchdown may position the skater such that more of the toe pick digs into the ice, increasing the time the toe pick is in contact with the ice. As a result, the foot becomes fixed for a brief period of time longer than the other subjects, and the horizontal force may be

increased. Furthermore, the stiffness of the boot, and the large shank angle may prevent the toe picks from being completely freed from the ice. Toe picks may be scraped across the ice surface, increasing the resistance, and result in a larger forces being exerted by the ground, and at the joints.

The second cause of the large horizontal force, as related to segment angle, could be due to the initial impact force. Because the segments were flexed further than the other subjects, this in itself may create a greater shear force. The normal subject has a shank angle close to the vertical which causes most of the force to be applied axially to the tibia. As the knee was flexed, the initial force was still applied axially, but the horizontal component of the force would be increased. Figure 5-5 is an example of how the angle can influence the forces.

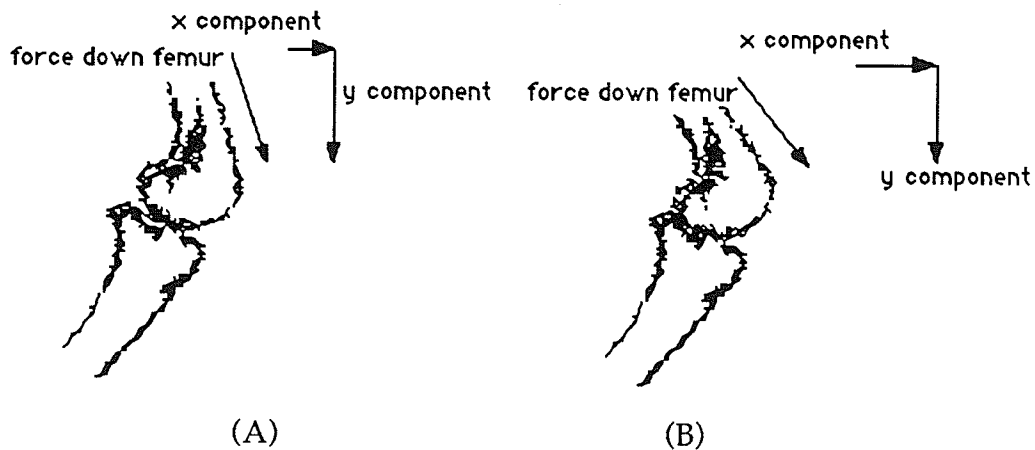


Figure 5-5 - This diagram shows how the increased angle of a segment can alter the horizontal component of force. In this case the femur angle was altered, but the result would be the same if the shank angle was altered. In order to resolve the original force vector, the x component of force was larger in (B) than in (A), indicating a larger shear force (diagram modified from Bruns & Yngve, 1989, p. 209).

As shown in the modified diagram by Bruns and Yngve (1989, p. 209), the larger the angle at touchdown the greater is the shear force placed on the joints. In turn, this larger force will cause a greater chance of injury since tissues are weaker in shear than in compression (Frost, 1967; Evans, 1973; Le Veau, 1992).

In order to reduce the shear forces, more emphasis should be placed on eccentric strength training and proper landing technique. The strength training would be key in increasing the skater's strength, which indirectly increases the height and time spent in the air, allowing for a greater chance of a successful landing. The landing technique should be practiced further so that the shank angle is straighter at touchdown to reduce the shear force. For example, gymnasts have a greater degree of extension of the joints at impact than recreational athletes. The gymnasts had knee angles of  $160.6^{\circ}$  -  $160.2^{\circ}$ , while the recreational athlete had knee angles of  $154.8^{\circ}$  -  $156.4^{\circ}$  (McNitt - Gray, 1991). Subject #6 and #8 both have greater knee flexion angles at impact than the other subjects and they were  $126^{\circ}$  and  $140^{\circ}$  respectively. The remainder of the subjects ranged from  $150^{\circ}$  to  $168^{\circ}$  of knee flexion at impact. From these measurements, subjects #6 and #8 tend to be similar to those of the recreational athletes while the remainder are similar to the gymnasts of McNitt - Gray (1991). The increased extension of the knees of the gymnasts and subjects #2 - #5 in this study allow themselves a greater range of motion upon landing, which will help decrease the maximum forces of landing.

#### Implications - Bone

The following table shows the resulting pressure in the bones using the cross - sectional values from previous studies and the maximum force of

pressure calculated using force of 3890.26 N for the shank, and 3792.12 N for the femur in this study. These were the maximum force values at the distal end of the respective bones, and it was assumed that these forces would be passed, unchanged, up the entire length of the bone.

Table 5-3 - The pressure found in the femur and tibia of the present study using the cross-sectional area from the authors listed.

Study	Location of Measurement	Cross - Sectional Area (cm <sup>2</sup> )	Calculated Pressure (MPa)
Chu et al(1986)	Tibia (average)	9.62	4.044
Ackland et al (1988)	Knee Joint	53.98	0.721
	Mid - Tibial Shaft	7.05	5.518
	Ankle	21.45	1.814
Mungiole & Martin (1990)	Knee Joint	45.77	0.850
	Mid - Tibial Shaft	7.75	5.020
	Ankle	17.16	2.267
Overend et al (1993)	Femur	8.50	4.461

By comparing the results found in Table 5-3 with the values required to cause an acute fracture (Table 2-8), it is obvious that the calculated force values were well within the acute fracture limits of bone. The largest value in Table 5-3 for the tibia was 5.518 MPa which is only 1.53 % of the value required to fracture the tibia in compression. Bending causes both tension and compression, therefore, the force of 5.518 MPa represents only 3.99 % of the value in tension. The fracture limit of the femur in compression has a minimum of 170 MPa, and the largest value for this study was 4.461 MPa, which was only 2.62 % and 2.59 % of the bone's fracture limit in compression

and tension respectively. Therefore, with the values calculated in this study, it is unlikely that the figure skater will sustain an acute fracture to the lower extremity bones during the correct landing of a Triple Toe Loop.

Fatigue fractures depend on the number of repetitions and the magnitude of the load applied. The load on the bone for these figure skaters was very small, and hence, the number of repetitions required would need to be very large. Since the maximum calculated stress in the bones was 5.518 MPa, it is unlikely that repeated landing from jumps is the sole contributor to the large number of stress fractures in figure skating.

The other factors that may influence the number of stress fractures in figure skating are the limb positions, the limb angles, and length of practices (Cramer & McQueen, 1990). Therefore, since the athlete is continually skating, stresses are regularly being applied to the bone in both tension and compression. This repeated loading may be all that is required to decrease the number of cycles that produce stress fractures. According to Martin and McCulloch (1987), a person that runs at a pace of 2 steps per second would place the bone through  $10^6$  cycles after about 100 days of running. Figure skaters attempt between 20 - 100 jumps per practice session (Smith, 1985) and while this may not be enough cycles to create stress fractures, continual skating in between jumps may contribute significantly to the initiation of stress fractures. Since the number of stress fractures in figure skating represents 69 % of all the injuries (Smith & Micheli, 1982), and the jumping, skating, off ice training, and long hours may be more than the bones of the support limb can withstand.

While stress fractures can occur from a variety of directions, the results of the present study suggests that the fractures are the result of bending forces. Figure 2-16 shows the line of action of the joint forces and the tensile and

compressive sides of the bones. Since bone is weaker in tension than compression (Frost, 1967; Le Veau, 1992), it would seem likely that stress fractures would occur on the tensile side of the bone.

One further possibility in the cause of stress fractures could be the torque placed on the bones about their longitudinal axes during the rotation occurring during landing. The forces and moments that produce these torques were not calculated because the nature of the study was two dimensional. Since bone is weakest under torsional loading (Frost, 1967; Le Veau, 1992), it is important in the future to calculate these values and relate them to injuries. At the present time there have been no studies located which identify the type of stress fractures that occur in figure skating, and for this reason, further studies should be performed to identify whether stress fractures to figure skaters are compression, tension, or spiral in nature.

#### Joint Related Injuries

The most common joint injuries in figure skating occur most frequently at the knee, but are followed closely by the ankle. The injuries at the joints occasionally result in damage to the ligaments and cartilage, however, most of the injuries are the result of overuse of the extensor mechanism of the knee (Smith, 1985). The JRF provide little chance of acute injury to the tissues of the support limb joints. Table 5-4 represents the values for this experiment, and the pressures found at each of the joints. Comparing these values to the ultimate stresses (columns 6 and 7) reveals the large difference between the calculated value and the total pressure required to fracture these tissues.

Table 5-4 - Calculated stress for the present study (column 5) and ultimate stresses (column 6 and 7).

Joint	Direction	Maximum Force (N)	Cross - Sectional Area (cm <sup>2</sup> )	Calculated Stress (MPa)	Ultimate Stress †† (Bone)	Ultimate Stress (Cartilage)
Ankle	Horiz.	9710.65	21.45 †	4.53	132-180 MPa (Bending)	10-40 MPa* (Tension)
	Vertical	6215.39		2.90		
Knee	Hori.	9623.84	53.98 †	1.78	100-280 MPa (Compress)	7-23 MPa †† (Compress)
	Vertical	6088.57		1.13		
Hip	Horiz.	9453.62	9.0 †††	10.51	50-100 MPa (Shear)	unknown** (Shear)
	Vertical	5874.95		6.53		

\* Kempson (1979); \*\* Frost (1967); † Ackland et al., (1988); †† Le Veau, (1992) - These values were for the bones or cartilage, but they are independent of the joints located at the left of the table; ††† Aiken (1988) - the femur and acetabular surface area.

The vertical compressive forces in the bones at the ankle, knee, and hip joints represent only 2.90, 1.13, and 13.06 % of the pressure required to cause damage. In shear, these same values were 9.06, 3.56, and 42.04 %. Cartilage appears to be more susceptible to acute damage because of the lower values of ultimate tissue strength. Furthermore, cartilage, like bone, is more susceptible to injury under tension than any other type of loading (Weightman & Kempson, 1979). At the ankle, knee, and hip the calculated forces from the present study represent approximately 41, 16, and between 28 - 93 % of the ultimate stress of cartilage in compression. In tension, these cartilage values for the same joints were 45, 17, and 105 % respectively. The large value for the hip can be explained by the fact that the contact surface area of the femoral head was used, and the cross sectional area may be considerably larger. Therefore, while cartilage at the ankle and knee seem to be in little

danger of injury from compression or tension, the value at the hip may cause degeneration of the cartilage from overuse, or fracture from a single loading response.

Since the ultimate stress placed on the cartilage is larger than bone, the chance of an overuse injury is greater than that of bone. While the forces on the cartilage were lower than the force required to cause an acute fracture, repetitive loading of the joints within the physiological limits may result in joint degradation (Radin et al., 1973). Therefore, the long hours of practice, repetitive jumping, and continual skating of the figure skater may be significant enough to stress the cartilage beyond its limits, and result in damage to the tissue.

According to a number of authors (Smith & Micheli, 1982; Smith, 1985; and Crammer and McQueen, 1990), low back pain also has a high rate of occurrence in figure skaters. The present study did not consider this aspect since the study was directed at calculating the forces and moments in the lower extremity. Furthermore, the studies to date that have reported lower back injuries relate the injuries to the repeated jumps, repeated hyperextension, tight lumbodorsal fascia, and low back inflexibility (Smith & Micheli, 1982; Smith, 1985; and Crammer and McQueen, 1990). However, the force and moment values at the L5 - S1 joint can easily be calculated by including another digitized point at this joint and by breaking the trunk section into two rigid bodies during the force calculation.

#### Ligament Injuries

Ligaments play an important role in the prevention of abnormal joint motion and work to stabilize the joint (Le Veau, 1992). Therefore, according

to the JRF calculated in this study, the ligaments are not stressed to the point of an acute injury when the Triple Toe Loop is landed correctly.

During pure axial compression the ligaments do not support any force, instead they simply collapse, and therefore, they are unstressed (Le Veau, 1992). As the GRF initiates joint flexion, there is an increasing force placed on the ligaments in both the mediolateral direction and anteroposterior directions. However, since the present study was performed in only two dimensions, the forces in the medial - lateral direction were not calculated. The result is that the forces on the ligaments preventing medial/lateral motion at the joints were not calculated.

In the anterior - posterior direction the peak stresses at the ankle, knee, and hip were 4.53, 1.78, and 10.51 respectively. The ultimate stress for ligaments ranges between 37.8 and 100 MPa depending on the amount of elastic fibres present in the tissue (Le Veau, 1992). From this information it is evident that there is very little chance of injury to the ligaments if the Triple Toe Loop is landed correctly. Furthermore, Cramer and McQueen (1990) believed that there is very little chance of ligament damage from the from jumps in figure skating. However, it is important to stress that the chance of injury may be considerably larger if the forces and moments were considered for all three cardinal planes.

### Strain Injuries

Table 5-5 contains the calculated values and the ultimate stress values of a number of tissues in the support limb. The calculated values of this table were found by dividing the moment by the moment arm, and then dividing this answer by the cross - sectional area of the tissue in question.

The calculated stress in the Achilles, quadriceps, biceps femoris, and gluteal muscles, indicates that the forces were within the limits of the tissue's ultimate stress. Therefore, it is unlikely that damage will be done to these structures as the result of eccentric contraction during the landing of a Triple Toe Loop. One thing that should be considered while making this assumption is that the calculated moments are net moments. In other words, the calculated moment assumes that the antagonistic muscle group is inactive and that the force exerted does not have to provide force against the antagonistic muscles (Gagnon et al, 1987). Furthermore, according to Smith (1975), the moments only provide an estimate of the forces present in the body, and are subject to errors of up to  $\pm 50\%$ .

Table 5-5 - Calculated stresses for the tissues of the lower limb.

Author	Muscle/ Tendon	Moment (N· m)	Cross - Sectional Area (cm <sup>2</sup> )	Calculated Stress (MPa)
Present Study (Test #2)	Achilles	76.513	2.0	8.140
	Quadriceps	388.077	0.85	76.094
	Gluteal	501.731	60.0	0.929
	Biceps Femoris	(501.731)	15.8	3.528
	Hamstrings	(501.731)	50.0	1.115

The calculated moment values of the lower limb are within the limits outlined in Table 2-9. The largest value in the present study would place a stress of 76.094 MPa on the quadriceps tendon, and the maximum value expressed in Table 2-9 for the same tendon was 98.1 MPa. Therefore, this represents approximately 77% of the maximum stress capable for the tissue. While this may be considerably large, the value was produced by the small

cross - sectional area provided for the patellar ligament. For example, the cross - sectional area for the Achilles tendon was  $2 \text{ cm}^2$  (Nigg, 1985), however the only source of the patellar cross - sectional area was provided by Smith (1975) at  $0.85 \text{ cm}^2$ . It is assumed that the patellar tendon is larger than the Achilles tendon, and if other cross - sectional values were to be obtained for the patellar tendon, the stress on this tissue would be considerably smaller.

### Limitations and Future Considerations

The first limitation of the study was the fact that the force calculations was performed in only two dimensions, and the calculation of moments were about a single axis. Because it is a single plane analysis, the mediolateral forces were not calculated, and the moments about the y and z axes were not calculated. These values may have been substantial, and might have been greater than the estimated injury threshold. If the moments are great enough to cause the femur to fracture (Wright, 1987), it is important that these forces be known. Therefore, that is one area that might be considered for future studies.

Another aspect that might be related to the use of three dimensional studies is the anatomical alignment of the support limb. Because the anatomical alignment of the lower limb is important to the prevention or initiation of injuries (Hughes, 1985; Bruns & Yngve, 1989), a three dimensional study would be able to identify any abnormal joint movements and technique flaws that may lead to injuries.

Another drawback was the lack of variety of jumps, and the lack of randomization when selecting subjects. First, the lack of variety between jumps provides little insight as to what the forces would be for other jumps. There are still eight double jumps, seven triple jumps, and the Quadruple

Toe Loop that have not been quantified. Furthermore, the lack of variability provides no comparison between the different levels of jumps. As for the lack of randomization of subject selection, this further narrows the generalization to only subjects capable of performing the Triple Toe Loop successfully.

Finally, the recording rate of the cameras reduces the chance of exactly catching the passive force peaks on camera. With only three frames of film being recorded in the first 61 ms (McNitt - Gray, 1991), it is unlikely that the passive peak force is accurately captured because this is the longest time through which passive forces occur. By using cameras with faster filming rates, the number of frames from touchdown to occurrence of the passive peak would increase, and there would be a better chance of catching the exact passive force peak. Furthermore, there would be more frames over which to calculate the force and the force - time curve would have a smoother appearance and be a more accurate curve, because of the increased number of frames used to calculate the forces and draw the graphs.

## CHAPTER 6

### SUMMARY

This study was designed to calculate the joint reaction forces and the ground reaction forces at impact during a Triple Toe Loop. It was hypothesized that the force values would be very high, and in the range to cause tissue breakdown.

Using the method of inverse dynamics, the maximum GRF values found in this study were 14.260 BW in the horizontal direction, and 9.119 BW in the vertical direction. These values were similar to the maximum values of 13 BW (Panzer et al., 1987) and 11 BW (McNitt - Gray, 1991) for jump landings in the horizontal and vertical directions respectively. Furthermore, the two methods used to calculate the GRF, CG and segmental methods, were not statistically different from each other.

The JRF for the ankle, knee, and hip in the horizontal directions were 14.319, 14.191, and 13.954 BW respectively. In the vertical directions these same values were 9.165, 8.978, and 8.663 BW respectively. As shown by these values, the trend of the JRF was to decrease in magnitude the more proximal the joint became. Finally, the vertical and horizontal JRF values found in this study were within the range of previous sports related studies.

On the other hand the joint moment values that were calculated for the ankle, knee, and hip were less than the values from previous studies. However, unlike the JRF, the moments did not decrease as the joints became more proximal. One explanation could be the restricted movement at the ankle prevented a large moment from occurring. Secondly, the large flexion

at the knee and hip caused the surrounding muscles to contract in order to slow the body's downward movement, which resulted in the large moments.

After calculating the forces and moments, it was found that the forces and moments in all of the tissues of the lower limb were within acute fracture limits. However, some of the tissues were found to be more susceptible to injury than others. For example the cartilage values were within their ultimate fracture limits, however, the forces represented 28 - 93 % of the fracture limit. A second example was the patellar tendon and was found to be exposed to a stress of as high as 77 % of its maximum limit. The problem associated with these calculations was the estimated cross - sectional area of the tissue. With only one source for each of these values, it is unlikely that the values represent those of the highly skilled athletes used in this study. Therefore, if more sources of the cross - sectional area were available for comparison, the calculated stresses in these tissues may be considerably less.

In most cases the forces produced in the tissues of the lower limb are so small that it seems unlikely that stress fractures will occur to any of the tissues as a result of landing from a Triple Toe Loop. However, the long hours, jumps, skating between jumps, and off ice training may be the cause of the overuse type of injuries.

It was also found that the angular acceleration of the lower limb, namely the shank, plays a significant role in increasing the JRF that were present. Furthermore, the greater the angle at the knee joint upon contact, the greater the JRF by increasing the forces that are present in the horizontal direction.

## CONCLUSION

On the basis of the present study, the following conclusions appear to be justified:

1. Calculation of the GRF using the segmental method and the CG method are not statistically different from each other.
2. For its simplicity and accuracy, the CG method of force calculation produces accurate numbers. However, the segmental method should be used wherever possible because it is likely more accurate. For example, the segmental method obtains higher peaks and lower troughs which may more closely resemble the true values.
3. The vertical JRF were lower than most other studies reviewed, whereas the horizontal JRF were larger than all studies except the checking of the rotational motion of the gymnast in the study by Panzer et al (1988).
4. Unlike the JRF, the moments values increased as the joints became further from the ground. However, the stress caused by these values were not great enough to cause an acute injury to the tendons or ligaments, and is unlikely to cause overuse injuries unless there is a problem with the anatomical alignment of the lower limb.
5. The forces and moments are not large enough to cause acute fractures, and may be too low to be the sole cause of stress fractures, except following a very high number of repetitions. However, this assumes that the forces in the frontal plane and moments about the longitudinal axes of the segments are insignificant, which may not be the case.
6. The GRF and JRF force values were considerably less than expected, and are in fact, less than the values from other skills, like running, that visually would seem to produce lower forces.

7. The information obtained from this study may be below the forces that cause injury, however, by applying these results to those of future studies, appropriate conditioning and training programs for the competitive figure skater may be developed. These new conditioning and training programs may then reduce the percentage of injuries found using the present conditions.

### RECOMMENDATIONS

On the basis of the present study, the following recommendations are made for future studies with the same methodology.

1. The filming rate use in this study was too slow. A faster filming rate would be required to obtain more accurate force values. The faster filming rate would provide more frames to digitize, more accurate angular acceleration values, and force curves with smoother transitions from one value to the next.
2. A more detailed stick figure representation of the human body may be considered during the force calculations. In other words, the shoulder and hips could be taken into consideration during the force calculations. Furthermore, individualized anthropometric measurements could be taken for each subject instead of using values from tables.
3. Since the number of injuries significantly increases with the performance of triple jumps, and the triple toe loop force values do not seem to be large enough to cause injury, the other aspects of figure skating must be considered, such as the forces during skating, jump take-offs, and spinning.

4. Individual force or pressure measuring devices that could be placed in the skate may provide the information required to accurately measure the GRF and JRF. However, this device must be wireless, otherwise the skater will become entangled in the wires and possibly be injured.

## REFERENCES

- Abraham, L. D. (1987). An inexpensive technique for digitizing spacial [sic] coordinates from videotape. In, B. Jonsson (Ed.) Biomechanics X-B. (pp. 1107-1110). Champaign: Human Kinetics Publishers.
- Ackland, T. R., Henson, P. W., & Bailey, D. A. (1988). The uniform density assumption: its effect upon the estimation of body segment inertial parameters. International Journal of Biomechanics, 4, 146 - 155.
- Aiken, N. (1988). Biomechanics of the Hip. Unpublished notes, Orthopaedic biomechanics class. Faculty of Medicine, University of Manitoba.
- Aleshinsky, S. Y. (1986). What biomechanics can do for figure skating. Part two. Sports Medicine, 63, 11-15.
- Alexander, R. McN., & Vernon, A. (1975). The dimensions of knee and ankle muscles and the forces they exert. Journal of Human Movement Studies, 1, 115 - 123.
- Allard, P., Nagata, S. D., Duhaime, M., & Labelle, H. (1987). Application of stereophotogrammetry and mathematical modeling in the study of ankle kinematics. In, B. Jonsson (Ed.) Biomechanics X-B. (pp. 1111-1115). Champaign: Human Kinetics Publishers.
- Andriacchi, T., Sabiston, P., DeHaven, K., Dahners, L., Woo, S., Frank, C., Oakes, B., Brand, R., & Lewis, J. (1987). Ligament: injury and repair. In, S. L-Y. Woo, & J. A. Buckwalter (Eds.) Injury and Repair of the Musculoskeletal Soft Tissues. Park Ridge, Ill.: American Academy of Orthopaedic Surgeons.
- Armstrong, C. G., Mow, V. C., & Wirth, C. R. (1985). Biomechanics of impact-induced microdamage to articular cartilage: a possible genesis for

- chondromalacia patella. In, G. Finerman (Ed.) Symposium on Sports Medicine: The Knee. (pp. 70 - 84). St. Louis: Mosby Company.
- Arnheim, D. D. (1985). Modern Principles of Athletic Training (6th Ed.), St. Louis: Times Mirror/Mosby College Publishing.
- Bartee, H. & Dowell, L. (1982). A cinematographical analysis of twisting about the longitudinal axis when performers are free of support. Journal of Human Movement Studies, 8, 41-54.
- Basmajian, J. V. & De Luca, C. J. (1985). Muscles Alive: Their Function Revealed by Electromyography (5th Ed.). Baltimore: Williams & Wilkins.
- Bates, B. T., Osternig, L. R., Sawhill, J. A., & James, S. L. (1983). An assessment of subject variability, subject-shoe interaction, and the elevation of running shoes using ground reaction force data. Journal of Biomechanics, 16, 181-191.
- Benedik, G. B., & Villars, F. M. H. (1973) Physics with Illustrated Examples from Medicine and Biology, Volume 1, Mechanics. Reading: Addison-Wesley.
- Bobbert, M. F., Huijing, P. A. & van Ingen Schenau, G. J. (1986). A model of the human triceps surae muscle-tendon complex applied to jumping. Journal of Biomechanics, 19, 887-898.
- Bobbert, M. F., Huijing, P. A. & van Ingen Schenau, G. J. (1987). Drop jumping. II. The influence of dropping height on the biomechanics of drop jumping. Medicine and Science in Sports and Exercise, 19, 339-338.
- Bobbert, M. F., Schamhardt, H. C., & Nigg, B. M. (1991). Calculation of vertical ground reaction force estimates during running from positional data. Journal of Biomechanics, 24, 1095-1105.

- Brauckmann, L., & Power, B. (1980). Free skating. In, A. Mason (ed.) Figure Skating Coaching Certification Program Level I. (pp. 69-109). Ottawa: Canadian Figure Skating Association.
- Brock, R. M. & Striowski, C. C. (1986). Injuries in elite figure skaters. The Physician and Sportsmedicine, 14, 111-115.
- Brown, E. W., Abani, K., & Usman, M. (1986). Comparison between a static and dynamic model for the calculation of joint reaction forces and intersegmental resultant moments in the dead lift. In, Adrian, M., & Deutsch, H. (eds.) Biomechanics: The 1984 Olympic Scientific Congress Proceedings. Eugene: Microform Publications.
- Brüggemann, P. (1985). Mechanical load on the Achilles tendon during rapid dynamic sport movements. In, S. M. Perren, & E. Schneider (ed.) Biomechanics: Current Interdisciplinary Research, Dordrecht: Kluwer Academic Publishers Group.
- Bruns, B. R., & Yngve, D. (1989). Stress reaction and stress fracture. Advances in Sports Medicine and Fitness 2, 201-222.
- Brussatis, F., Dupuis, H., Hartung, E., & Steeger, D. (1976). Distribution of load forces in the hip under different parameters. In, P. V. Komi (Ed.) Biomechanics V-B. Baltimore: University Park Press.
- Burdett, R. G. (1982). Forces predicted at the ankle during running. Medicine and Science in Sports and Exercise, 14, 308 - 316.
- Butler, D. L., Grood, E. S., Noyes, F. R., & Zernicke, R. F. (1978). Biomechanics of ligaments and tendons. In, R. Hutton (Ed.) Exercise and Sport Sciences Reviews (vol 6). Indianapolis: The Franklin Institute Press.
- Cairns, M. A., Burdett, R. G., Pisciotta, J. C., & Simon, S. R. (1986). A biomechanical analysis of racewalking gait. Medicine and Science in Sports and Exercise, 18, 446 - 453.

- Cappozzo, A., Figura, F., & Marchetti, M. (1976). The interplay of muscular and external forces in human ambulation. Journal of Biomechanics, 9, 35 - 43.
- Carter, D. R. & Hayes, W. C. (1977a). Compact bone fatigue damage - I. Residual strength and stiffness. Journal of Biomechanics, 10, 325 - 337.
- Carter, D. R. & Hayes, W. C. (1977b). The compressive behaviour of bone as a two - phase porous structure. Journal of Bone Joint Surgery, 59A, 954 - 962.
- Cavanagh, P. R. & LaFortune, M. A. (1980). Ground reaction forces in distance running. Journal of Biomechanics, 13, 397-406.
- Chaffin, D. B., & Andersson, G. B. J. (1984). Occupational Biomechanics. New York: Wiley.
- Chaffin, D. B., & Andersson, G. B. J. (1991). Occupational Biomechanics (2nd. ed.) New York: John Wiley & Sons.
- Challis, J. & Kerwin, D. (1988). An evaluation of splines in biomechanical data analysis. In, G. de Groot, A. P. Hollander, P. A. Huijing, & G. J. van Ingen Schenau (eds.) Biomechanics XI-B, (1057-1062), Amsterdam: Free University Press.
- Chao, E. Y. & Rim, K. (1973). Application of optimization principles in determining the applied moments in human leg joints during gait. Journal of Biomechanics, 6, 497-510.
- Chu, M. L., Yazdani - Ardakani, S., Gradisar, I. A., & Askew, M. J. (1986). An in vitro simulation study of impulsive force transmission along the lower skeletal extremity. Journal of Biomechanics, 19, 979 - 987.
- Churches, A. E., Howlett, C. R., Waldron, K. J., & Ward, G. W. (1979). The response of living bone to controlled time-varying loading: method and preliminary results. Journal of Biomechanics, 12, 35 - 45.

- Comper, P. (1990). Foot problems in figure skating. Coach to Coach, Fall 1990, 7.
- Cook, S. D., Brinker, M. R., & Poche, M. (1990). Running shoes: their relationship to running injuries. Sports Medicine, 10, 1-8.
- Cramer, L. M., & McQueen (1990). Overuse injuries in figure skating. In, M. J. Casey, C. Foster, & E. G. Hixson (Eds.), Winter Sports Medicine, (pp. 254 - 268). Philadelphia: F. A. Davis Company.
- Crowninshield, R. D., Johnston, R. C., Andrews, J. G., & Brand, R. A. (1978). A biomechanical investigation of the human hip. Journal of Biomechanics, 11, 75 - 85.
- Currey, J. (1984). The Mechanical Adaptations of Bones. Princeton: Princeton University Press.
- Dainty, D. A, Cotton, C. E., & Morrison, W. E. (1978). An Evaluation of Selected Figure Skates. Unpublished manuscript, University of Ottawa, School of Human Kinetics, Department of Kinanthropology.
- Davis, M. W., & Litman, T. (1979). Figure skater's foot. Minnesota Medicine, 62, 647-648.
- Demak, R. (1987). The pain that won't go away. Sports Illustrated, 66(17), 60-62, 64, 66, 71.
- Denoth, J., Gruber, K., Ruder, H., & Keppler, M. (1984). Forces and torques during sports activities with high accelerations. In, S. M. Perren & E. Schneider (Eds.) Biomechanics: Current Interdisciplinary Research. (663-668). Dordrecht: Martinus Nijhoff Publishers.
- Dickinson, J. A., Cook, S. D., & Leinhardt, T. M. (1985). The measure of shock waves following heel strike while running. Journal of Biomechanics 18, 415-422.

- Diffrient, N., Tilley, A. R., & Bardagjy, J. C. (1978). Humanscale 1/2/3. Cambridge: MIT press.
- Drez, D. (1980). Running footwear: examination of the training shoe, the foot and functional orthotic devices. American Journal of Sports Medicine 8, 141-142.
- Dufek, J. S., & Bates, B. T. (1990). Regression models for predicting impact forces and knee joint moments and powers during landing. Proceedings of 6th Biennial Conference of the Canadian Society for Biomechanics. 55 - 56.
- Dufek, J. S., & Bates, B. T. (1991). Biomechanical factors associated with injury during landing in sports jumps. Sports Medicine, 15, 326-337.
- Dye, S. F., & Cannon, W. D. (1988). Anatomy and biomechanics of the anterior cruciate ligament. Clinics in Sports Medicine, 7, 715-725.
- Dyson, G. H. G. (1978). The Mechanics of Athletics. London: Hodder and Stoughton.
- Ericson, M. O., & Brand, R. (1986). Tibiofemoral joint forces during ergometer cycling. American Journal of Sports Medicine, 14, 285 - 290.
- Evans, (1973). Mechanical Properties of Bone. Springfield: Charles c. Thomas.
- Fassi, C. (1980). Figure Skating with Carlo Fassi. New York: Charles Scribner's Sons
- Folk, G. (1982). Free skating. In, A. Mason & T. Villiers (Eds.) Figure Skating Coaching Certification Program Level II. (pp. 67-128). Ottawa: Canadian Figure Skating Association.
- Frey, C. C., & Shereff, M. J., (1988). Tendon injuries about the ankle in athletes. Clinics in Sports Medicine, 7, 103-118.

- Frost, H. M. (1967). An Introduction to Biomechanics. Springfield, Ill: Charles C. Thomas Publisher.
- Fukashiro, S., & Komi, P. V. (1987). Joint moment and mechanical power flow of the lower limb during vertical jump. International Journal of Sports Medicine, 8 (supplement) 15-21.
- Fukuda, H. (1988). Biomechanical analysis of landing on surfaces with different stiffnesses. In, G. de Groot, A. P. Hollander, P. A. Huijing, & G. J. van Ingen Schenau (eds.) Biomechanics XI-B, (679-684), Amsterdam: Free University Press.
- Gagnon, M., Robertson, G., & Norman, R. (1987). Kinetics. In, D. A. Dainty & R. W. Norman (eds.) Standardizing Biomechanical Testing in Sport, (21-58) Champaign: Human Kinetics Publishers.
- Garrett, W. E., Safran, M. R., Seaber, A. V., Glisson, R. R., & Ribbeck, B. M. (1987). Biomechanical comparison of stimulated and nonstimulated skeletal muscle pulled to failure. The American Journal of Sports Medicine, 15, 448-453.
- Gozna, E. R., & Harrington, I. J. (1982). Biomechanics of Musculoskeletal Injuries, Baltimore: Williams & Wilkins.
- Groh, H., & Baumann, W. (1975). Joint and muscle forces acting in the leg during gait. In, P. V. Komi (Ed.), Biomechanics V, (pp. 328 - 333). Baltimore: University Park Press.
- Gross, T. S. & Nelson, R. C. (1988). The shock attenuation role of the ankle during landing from a vertical jump. Medicine and Science in Sports and Exercise, 20, 506-514.
- Hage, P. (1982). Injuries common among national figure skaters. The Physician and Sportsmedicine, 10, 202.
- Hall, S. J. (1991). Basic Biomechanics. St. Louis: Mosby - Year Book.

- Hanks, G. A., Kalenak, A., Bowman, L. S., & Sebastianelli, W. J. (1989). Stress fractures of the carpal scaphoid. The Journal of Bone and Joint Surgery, 71-A, 938-941.
- Harrington, I. J. (1982). Biomechanics of joint injuries. In, E. R. Gozna, & I. J. Harrington (Eds.), Biomechanics of Musculoskeletal Injury, (31 - 85). Baltimore: Williams & Wilkins.
- Harris, R. (1981). Exercises for strengthening and conditioning jumps. Canadian Skater, 8 (2), 30-31.
- Harrison, R. N., Lees, A., McCullagh, P. J. J., & Rowe, W. B. (1986). A bioengineering analysis of human muscle and joint forces in the lower limbs during running. Journal of Sports Sciences, 4, 201 - 218.
- Hassard, T. H. (1991). Understanding Biostatistics. St. Louis: Mosby-Year Book Inc.
- Hawkins, D. (1992). Software for determining lower extremity muscle-tendon kinematics and moment arm lengths during flexion/extension movements. Computers in Biology and Medicine, 22, 59 - 71.
- Hay, J. G. (1985). The Biomechanics of Sports Techniques (3rd ed.). Englewood Cliffs: Prentice-Hall.
- Hay, J. G., Dapena, J., Wilson, B. D., & Andrews, J. G. (1977). An Analysis of Joint Contribution to the Performance of a Gross Motor Skill. Unpublished Manuscript, University of Iowa.
- Hay, J. G., Vaughan, C. L., & Woodworth, G. G. (1981). Technique and performance: Identifying the limiting factors. In, A. Morecki, K. Fidelus, & A. Wit, (Eds.) Biomechanics VII-B. (511-520) Baltimore: University Park Press.
- Higgs, C. (1984). Cinematographic techniques in biomechanical analysis. In, M. Alexander, C. Higgs, G. Robertson, & J. Stevenson (eds.) Technology

- for Biomechanical Analysis of Athletes, (3-22). Ottawa:  
CAHPER/ASCEPL.
- Hinrichs, R. N. (1988, September). Adjustments to the Segment Center of Mass Proportions of Clauser et al (1969). Paper presented at the twelfth Annual Meeting of the American Society of Biomechanics, Urbana, Il.
- Holden, J. P. (1984). The Free Moment of Ground Reaction in Distance Running and its Change with Pronation. Unpublished master's thesis, Pennsylvania State University, University Park, Pa. Cited by Miller, D. I. (1990). Ground reaction forces in distance running. In, P. Cavanagh, (Ed.), Biomechanics of Distance Running. (203-224). Champaign, Il: Human Kinetics Publishers.
- Hughes, L. Y. (1985). Biomechanical analysis of the foot and ankle for predisposition to developing stress fractures. The Journal of Orthopaedic and Sports Physical Therapy, 7 (3), 96-101.
- Hulkko, A., & Orava, S. (1987). Stress fractures in athletes. International Journal of Sports Medicine, 8, 221-226.
- Inman, V. T. (1976). The Joints of the Ankle. Baltimore: Williams and Wilkins.
- Jackson, D. (1980). Don Jackson's skating tips: Shape of the blade and how to utilize it. Canadian Skater, 7, 46.
- Jackson, D. (1981). Don Jackson's skating tips: Preparation of the boot for mounting. Canadian Skater, 7 (5), 46-47.
- Jobse, H., Schuurhof, R., Cserep, F., Schreurs, A. W., & de Koning, J. J. (1990). Measurement of push-off force and ice friction during speed skating. International Journal of Biomechanics, 6, 92-100.
- Kaelin, X., Stacoff, A., Denoth, J., & Stuessi, E. (1988). Shock absorption during landing after a jump. In, G. de Groot, A. P. Hollander, P. A. Huijling, &

- G. J. van Ingen Schenau (eds.) Biomechanics XI-B, (685-688),  
Amsterdam: Free University Press.
- Kapandji, I. A. (1987). The physiology of the Joints: Volume 2 Lower Limb  
(5th ed.) (L. H. Honoré, Trans.). Edinburgh: Churchill Livingstone.  
(Original work published 1970).
- Kaufman, K. R., An, K., Litchy, W. J., Morrey, B. F., & Chao, E. Y. S. (1991).  
Dynamic joint forces during knee isokinetic exercise. *American  
Journal of Sports Medicine*, 19, 305-316.
- Kempson, G. E. (1979). Mechanical properties of articular cartilage. In, M. A.  
R. Freeman (Ed.) Adult Articular Cartilage (2nd Ed.), (pp. 333 - 414).  
Kent, England: Pitman Medical Publishing.
- Kennedy, P. W. J, Wright, D. L. & Smith, G. A. (1989). Comparison of film  
and video techniques for three-dimensional DLT repredictions.  
International Journal of Sport Biomechanics, 5, 457-460.
- Keohane, A. (1978). Perfecting your jumps. Canadian Skater, February-April,  
35-41.
- Kobayashi, T. (1973). Studies of the properties of the ice in speed skating  
rinks. Ashrae Journal, 50, (51-56). Cited by de Boer, R. W.,  
Schermerhorn, P., Gademan, J., de Groot, G, & van Ingen Schenau, G. J.  
(1986). Characteristics stroke mechanics of elite and trained male speed  
skaters. International Journal of Biomechanics, 2, (175-185).
- Kreighbaum, E., & Barthels, K. M. (1985). Biomechanics: a Qualitative  
Approach for Studying Human Movement. (2nd. ed.). New York:  
MacMillen Publishing Company.
- Lamb, H. F., & Stothart, P. (1978). A comparison of cinematographic and force  
platform techniques for determining take-off velocity in the vertical

- jump. In E. Asmussen, & K. Jorgensen (Eds.) Biomechanics VI-A. (387-391). Baltimore: University Press.
- Lap Link Mac (1988). [computer program]. Bothel, WA: Traveling Software, Inc.
- Lees, A. (1981). Methods of impact absorption when landing from a jump. Engineering in Medicine, 10, 207 - 211.
- Le Veau, B. F. (1992). Williams and Lissner's Biomechanics of Human Motion. (3rd ed.) Philadelphia: W. B. Saunders Company.
- Lundberg, A., Svensson, O. K., Nemeth, G., & Selvik, G. (1989). The axis of rotation of the ankle joint. Journal of Bone and Joint Surgery [Br.], 71-B, 94-99.
- MacDougall, J. D., Webber, C. E., Martin, J., Ormerod, S., Chesley, A., Younlai, E. V., Gordon, C. L., & Blimkie, C. J. R. (1992). Relationship among running mileage, bone density, and serum testosterone in male runners. Journal of Applied Physiology, 73, 1165 - 1170.
- Magee, D. J. (1987). Orthopedic Physical Assessment. Philadelphia: W. B. Saunders Company.
- Markey, K. L. (1987). Stress fractures. Clinics in Sports Medicine, 6, 402-425.
- Marshall, R. N., Jensen, R. K., & Wood, G. A. (1985). A general Newtonian simulation of an n-segment open chain model. Journal of Biomechanics, 18, (359-367).
- Martin, A. D., & McCulloch, R. G. (1987). Bone dynamics: stress, strain and fracture. Journal of Sports Sciences, 5, 155 - 163.
- May, H. (1980). Figures. In, A. Mason (Ed.) Figure Skating Coaching Certification Program Level I. Ottawa: Canadian Figure Skating Association.

- McElhaney, J. H. (1966). Dynamic response of bone and muscle tissue. Journal of Applied Physiology, 21, 1231 - 1236.
- McNitt-Gray, J. L. (1991). Kinematics and impulse characteristics of drop landings from three heights. International Journal of Sport Biomechanics, 7, 201-224.
- McPherson, M. N., & Bothwell-Myers, C. (1986). The waltz jump. Coaching Review, March/April, 55-57.
- McPoil, T. G., & Knecht, H. G. (1985). Biomechanics of the foot in walking: A function approach. The Journal of Orthopaedic and Sports Physical Therapy, 7, 69-72.
- McWatt, B. (1989). The mechanics of the take-off in jumping. Modern Athlete and Coach. 27, (2), 7-10.
- Miller, D. I. (1990). Ground reaction forces in distance running. In, P. Cavanagh, (Ed.), Biomechanics of Distance Running. (203-224). Champaign, Il: Human Kinetics Publishers.
- Miller, D. I. & Nelson, R. C. (1976). Biomechanics of Sport: A Research Approach. Philadelphia: Lea & Febiger.
- Mizrahi, J. & Susak, Z. (1982). Analysis of parameters affecting impact force attenuation during landing in human vertical free fall. Engineering in Medicine, 11, 141 - 147.
- Moore, K. L. (1985). Clinically Oriented Anatomy (2nd ed.) (pp. 396-564). Baltimore: Williams & Wilkins.
- Morrison, J. B. (1970). The mechanics of the knee joint in relation to normal walking. Journal of Biomechanics, 3, 51-61.
- Moyle, D. D., & Bowden, R. W. (1984). Fracture of human femoral bone. Journal of Biomechanics, 17, 203 - 213.

- Mungiole, M., & Martin, P. E. (1990). Estimating segment inertial properties: comparison of magnetic resonance imaging with existing methods. Journal of Biomechanics, 23, 1039 - 1046.
- Munro, C. F., Miller, D. I., & Fuglevand, A. J. (1987). Ground reaction forces in running: a reexamination. Journal of Biomechanics, 20, 147-155.
- Muraki, Y., Sakamoto, T., Asito, S. & Shibukawa, K. (1982). A 3-dimensional cinematographical analysis of foot deformations during the takeoff phase of the fosbury flop. Track and Field Quarterly Review, 82 (4), 33-36.
- Nelson, R. C. & Martin, P. E. (1985). Effects of gender and load on vertical jump performance. In, D. A. Winter, R. W. Norman, R. P. Wells, K. C. Hayes, & A. E. Patla (Eds.) Biomechanics IX-B. (429-433). Champaign: Human Kinetics Publishers.
- Netter, F. H. (1989). Atlas of Human Anatomy. Summit: Ciba-Geigy Corporation.
- Nigg, B. M. (1985). Loads in Selected Sport Activities -- An Overview. In, Winter, D. A., Norman, R. W., Wells, R. P., Hayes, K. C., Patla, A. E., (Eds.) Biomechanics IX-B. (91-96). Champaign: Human Kinetics Publishers.
- Nigg, B. M. (1986). Assessment of load effects in the reduction and treatment of injuries. In, J. S. Skinner, C. B. Corbin, D. M. Landres, P. E. Martin, & C. L. Wells (Eds.) Future Directions in Exercise and Sport Science Research. (p. 181-193). Champaign: Human Kinetic Books.
- Nigg, B. M. (1988). Causes of injuries. In, A. Dirix, H. G. Knuttgen, & K. Tittel (Ed), Encyclopedia of Sports Medicine I: The Olympic Book of Sports Medicine (363-375). London: Blackwell Scientific Publications.

- Nigg, B. M., Denoth, J., & Neukomm, P. A. (1981). Quantifying the load on the human body: Problems and some possible solutions. In, A. Morecki, K. Fidelus, K. Kedzior, & A Wit (Ed), Biomechanics VII-B. (88-99). Baltimore: University Park Press.
- Nigg, B. M., & Morlock, M. (1987). The influence of lateral heel flare of running shoes on pronation and impact forces. Medicine and Science in Sports and Exercise, 19, 294-302.
- Niinimaa, V. (1982). Figure skating: What do we know about it? The Physician and Sportsmedicine, 10, 51-53; 56.
- Nordin, N. & Frankel, V. H. (1989). Basic Biomechanics of the Musculoskeletal System, (2nd. ed.). Philadelphia: Lea & Febiger.
- Oakes, B. W. & Parker, A. W. (1990). Discussion: Bone and connective tissue adaptations to physical activity. In, C. Bouchard, R. J. Shephard, T. Stephens, J. R. Sutton, & B. D. McPherson (eds.) Exercise, Fitness & Health: a Consensus of Current Knowledge. Champaign: Human Kinetic Publishers.
- Oliver (1985). Stress fractures of the lower extremity. In, R. P. Welsh and R. J. Shephard (Eds.), Current Therapy in Sports Medicine 1985-1986. (pp. 257 - 259). Toronto: C. V. Mosby.
- Ounpuu, S., Gage, J. R., & Davis, R. B. (1991). Three-dimensional lower extremity joint kinetics in normal pediatric gait. Journal of Pediatric Orthopaedics, 11, 341 - 349.
- Overend, T. J., Cunningham, D. A., Paterson, D. H., & Lefcoe, M. S. (1993). Anthropometric and computed tomographic assessment of the thigh in young and old men. Canadian Journal of Applied Physiology, 18, 263 - 273.

- Panzer, V., Wood, G., Bates, B., & Mason, B. (1988). Lower extremity loads in landing of elite gymnasts. In, G. de Groot, A. P. Hollander, P. A. Huijing, & G. J. van Ingen Schenau (eds.) Biomechanics XI-B, (679-684), Amsterdam: Free University Press.
- Peak Performance Technologies (1990). Peak5 User's Reference Manual. (Manual version 4.2.0.0 for Software Version 4.2.0.) Englewood, Co.
- Peak Performance Technologies (1992). Peak5 User's Reference Manual. (Manual version 1.0.0 for Software Version 5.0.0.) Englewood, Co.
- Pecina, M., Bojanic, I. & Dubravacic, S. (1990). Stress fractures in figure skaters. The American Journal of Sports Medicine, 18, 277-279.
- Pedotti, A., Krishnan, V. V., & Stark, L. (1978). Optimization of muscle-force sequencing in human locomotion. Mathematical Biosciences, 38, 57 - 76.
- Peterson, L. & Frankel, V. H. (1986). Biomechanics of the knee in athletes. In, J. A. Nicholas & E. B. Hershman (Eds.), The Lower Extremity and Spine in Sports Medicine (pp. 695 - 727). St. Louis: C. V. Mosby Company.
- Petkevich, J. M. (1984). The Skater's Handbook. New York: Charles Scribner's Sons.
- Petkevich, J. M. (1989). Sports Illustrated Figure Skating: Championship Techniques. New York: Winner's Circle Books.
- Pick, T. P., & Howden, R. (Eds.) (1974). Gray's Anatomy. Philadelphia: Running Press.
- Podolsky, A., Kaufman, K. R., Cahalan, T. D., Aleshinsky, S. Y. & Chao, E. Y. S. (1990). The relationship of strength and jump height in figure skaters. The American Journal of Sports Medicine, 18, 400-405.
- Procter, P., & Paul, J. P. (1982). Ankle joint Biomechanics. Journal of Biomechanics, 15, 627-634.

- Radin, E. L. & Paul, I. L. (1970). Does cartilage compliance reduce skeletal impact loads? Arthritis and Rheumatism, 13, 139-144.
- Radin, E. L., Parker, H. G., Pugh, J. W., Steinberg, R. S., Paul, I. L., & Rose, R. M. (1973). Response of joints to impact loading. III. Relationship between trabecular microfractures and cartilage degeneration. Journal of Biomechanics, 6, 51-57.
- Ramey, M. R. (1973). A simulation of the running long jump. The Winter Annual Meeting of The American Society of Mechanical Engineers, 4, 101-112.
- Rasch, P. J., & Burke, R. K. (1978). Kinesiology and Applied Anatomy: The Science of Human Movement. (6th ed.) Philadelphia: Lea & Febiger.
- Read, L., & Herzog, W. (1992). External loading at the knee joint for landing movements in alpine skiing. International Journal of Sport Biomechanics, 8, 62 - 80.
- Renstrom, P. & Johnson, R. J. (1990). Anatomy and biomechanics of the menisci. Clinics in Sports Medicine, 9, 523 - 538.
- Ricard, M. D., & Veatch, S. (1990). Comparison of impact forces in high and low impact aerobic dance movements. International Journal of Sport Biomechanics, 6, 67-77.
- Robbins, S. E., & Gouw, G. J. (1990). Athletic footwear and chronic overloading: a brief review. Sports Medicine, 9, 76-85.
- Roberts, E. M. (1970). Cinematography in biomechanical investigation. In, J. M. Cooper (Ed.) Selected Topics in Biomechanics: Proceedings of the C. I. C. Symposium on Biomechanics, (41-50), Chicago: The Athletic Institute.

- Robertson, G., & Springings, E. (1987). Kinematics. In, D. A. Dainty, & R. W. Norman (Eds.) Standardizing Biomechanics Testing in Sport. (9-20) Champaign: Human Kinetics Publishers.
- Rodgers, M. M., & Cavanagh, P. R. (1984). Glossary of Biomechanical terms, concepts, and units. Physical Therapy, 64, 1886-1900.
- Romanes, G. J. (1986). Cunningham's Manual of Practical Anatomy: Volume One Upper and Lower Limbs (15th ed.). Oxford : Oxford University Press.
- Ruby, P., Hull, M. L., & Hawkins, D. (1992). Three - dimensional knee joint loading during seated cycling. Journal of Biomechanics, 25, 41 - 53.
- Rugg, S. G., Gregor, R. J., Mandelbaum, B. R. & Chiu, L (1990). In vivo moment arm calculations at the ankle using magnetic resonance imaging (MRI). Journal of Biomechanics, 23, 495-501.
- Sammarco, G. J., Burstein, A. H., & Frankel, V. H. (1973). Biomechanics of the ankle: A kinematic study. Orthopedic Clinics of North America, 4, 75-96.
- Seireg, A & Arvikar, R. J. (1975). The prediction of muscular load sharing and joint forces in the lower extremities during walking. Journal of Biomechanics, 8, 89- 102.
- Serink, M. T., Nachemson, A., & Hansson, G. (1977). The effect of impact loading on rabbit knee joints. Acta Orthopaedics Scandinavia, 48, 250 - 262.
- Shapiro, R. (1976). Direct linear transformation method for three-dimensional cinematography. The Research Quarterly, 49, 197-205.
- Simon, S. R., Radin, E. L., Paul, I. L., Rose, R. M. (1972). The response of joints to impact loading - II. In vivo behavior of subchondral bone. Journal of Biomechanics, 5, 267 - 272.

- Skelly, W. A., & DeVita, P. (1990). Compressive and shear forces on the tibia and knee during landing. Proceedings of 6th Biennial Conference of the Canadian Society for Biomechanics. 59 - 60.
- Smith, A. (1985). Figure skating. In R. C. Schneider, J. C. Kennedy, & M. L. Plant (Eds.) Sports injuries: Mechanisms, Prevention, and Treatment, (516-531). Baltimore: Williams & Wilkins.
- Smith, A. D. (1990). Foot and ankle injuries in figure skating. The Physician and Sportsmedicine, 18, 73-74; 76; 80; 85-86.
- Smith, A. D., & Micheli, L. J. (1982). Injuries in competitive figure skaters. The Physician and Sportsmedicine. 10. 36-42; 44-45; 47.
- Smith, A. J. (1975). Estimates of muscle and joint forces at the knee and ankle during a jumping activity. Journal of Human Movement Studies, 1, 78 - 86.
- Soderberg, G. L. (1986). Kinesiology Application to Pathological Motion. Baltimore: Williams & Wilkins.
- Spencer, H., Kramer, L., Gatza, C. A., & Lender, M. (1978). Calcium loss, calcium absorption, and calcium requirement in osteoporosis. In, U. S. Barzel (Ed.) Osteoporosis II (pp. 65 - 89). New York: Grune & Stratton.
- Sprague, P., & Mann, R. V. (1983). The effect of muscular fatigue on the kinematics of sprint running. Research Quarterly for Exercise and Sport, 54, 60 - 66.
- Stacoff, A., Kaelin, X., & Stuessi, E. (1988). The impact in landing after a volleyball block. In, G. de Groot, A. P. Hollander, P. A. Huijijng & G. J. van Ingen Schenau (Eds.) Biomechanics XI-B (694-700). Amsterdam: Free University Press.
- Steele, J. R. & Milburn, P. D. (1987). Ground reaction forces on landing in netball. Journal of Human Movement Studies, 13, 399-410.

- Sullivan, D., Warren, R. F., Pavlov, H., & Kelman, G. (1984). Stress fractures in 51 runners. Clinical Orthopaedics and Related Research, 187, 188-192.
- Taunton, J. E., Clement, D. B., & Webber, D. (1981). Lower extremity stress fractures in athletes. The Physician and Sportsmedicine, 9, 77 - 83.
- Ting, A., King, W., Yocum, L., Antonelli, D., Moynes, D., Kerlin, R., Jobe, F., Wong, L., & Bertolli, J. (1988). Stress fractures of the tarsal navicular in long-distance runners. Clinics in Sports Medicine, 7, 89-101.
- Tipton, C. M., & Vailas, A. C. (1990). Bone and connective tissue adaptations to physical activity. In, C. Bouchard, R. J. Shephard, T. Stephens, J. R. Sutton, & B. D. McPherson (Eds.) Exercise Fitness and Health. Champaign: Human Kinetic Books.
- Travers, G. R. (1980). Evolution of the ice skate. In, R. R. Rinaldi & M. L. Sabia (Eds.) Sports Medicine '80, Part II. A Review by Members of the American Academy of Podiatric Sports Medicine. Mount Kisco, NY: Futura Publishing Company.
- Valiant, G. A., (1990). Transmission and attenuation of heelstrike accelerations. In, P. R. Cavanagh (Ed.) Biomechanics of Distance Running. Champaign: Human Kinetics Publishers.
- Valiant, G. A. & Cavanagh, P. R. (1985). A study of landing from a jump: implications for the design of a basketball shoe. In, D. A. Winter, R. W. Norman, R. P. Wells, K. C. Hayes, & A. E. Patla (Eds.) Biomechanics IX-B. (117-122). Champaign: Human Kinetics Publishers.
- Van Dommelen, B. A., & Fowler, P. J. (1989). Anatomy of the posterior cruciate ligament. A review. American Journal of Sports Medicine, 17, 24-29.

- Van Heuvelen, A (1982). Physics: A General Introduction. Boston: Little, Brown and Company.
- Viano, D. C. (1986). Biomechanics of bone and tissue: a review of material properties and failure characteristics. In, D. C. Viano, & R. S. Levine (Eds.) Biomechanics and Medical Aspects of Lower Limb Injuries. (33 - 64) Warrendale, Pa: Society of Automotive Engineers, Inc.
- Walker, P. S., & Hajek, J. V. (1972). The load-bearing area in the knee joint. Journal of Biomechanics, 5, 581 - 589.
- Warfel, J. H. (1985). The Extremities (5th ed.). Philadelphia: Lea & Febiger.
- Waters, P. M., & Millis, M. B. (1988). Hip and pelvic injuries in the young athlete. Clinics in Sports Medicine, 7, 513 - 526.
- Weightman, B., & Kempson, G. E. (1979). Load carriage. In, M. A. R. Freeman (Ed.) Adult Articular Cartilage (2nd Ed.), (pp. 291 - 331). Kent, England: Pitman Medical Publishing.
- Wells, K. F., & Luttgens, K., (1976). Kinesiology: Scientific Basis of Human Motion (6th ed.). Philadelphia: W. B. Saunders Company.
- White, S. C., & Winter, D., (1985). Mechanical power analysis of the lower limb musculature in race walking. International Journal of Sport Biomechanics, 1, 15 - 24.
- Williams, P. L., Warwick, R., Dyson, M., & Bannister, L. H. (1989). Gray's Anatomy, (37th Ed.). London: Churchill Livingstone.
- Winter, D. A. (1983). Moments of force and mechanical power in jogging. Journal of Biomechanics, 16, 91 -97.
- Winter, D. A. (1990). Biomechanics and Motor Control of Human Movement. (2nd. ed.) New York: John Wiley & Sons, Inc.
- Wood, G. A. (1982). Data smoothing and differentiation procedures in biomechanics. Exercise and Sport Science Reviews, 10, 308-362.

- Wood, G. A. & Marshall, R. N. (1986). Technical note: The accuracy of DLT extrapolation in three-dimensional film analysis. Journal of Biomechanics, 19, 781-785.
- Wright, R. (1987). Blade Spinner. Saturday Night, 102 (7), 43-46.
- Zajac, F. E. & Gordon, M. E. (1989). Determining muscle's force and action in multi-articular movement. Exercise and Sport Sciences Review, 17, 187-230.
- Zarrugh, M. Y., (1981). Kinematic prediction of intersegment loads and power at the joints of the leg in walking. Journal of Biomechanics, 14, 713 - 725.
- Zatsiorsky, V. M. & Prilutsky, B. I. (1987). Soft and stiff landing. In, B. Jonsson (Eds.) Biomechanics X-B. (739-743). Champaign: Human Kinetics Publishers.
- Zatziorsky, V. M. & Aleshinsky, S. Y. (1975). Simulation of human locomotion in space. in, P. V. Komi (ed.) Biomechanics V-B, (387-394). Baltimore: University Park Press.
- Zernicke, R. F., Garhammer, J., & Jobe, F. W. (1977). Human patellar - tendon rupture. Journal of Bone and Joint Surgery, 59 - A, 179 - 183.

APPENDIX A

Personal Consent Form,  
Location and Subject Record

## PERSONAL CONSENT FORM

You have been selected to participate in a study entitled The Descriptive Analysis of the Ground Reaction Force, Joint Moments, and Joint Reaction Forces During the Landing of a Triple Toe Loop.

The purpose of this study is to calculate the the forces absorbed by the body upon contact with the ice, and the force that is absorbed in the lower limb when landing the triple toe loop. These values will then be related to the number and type of injuries that occur in figure skating.

In the following study, you will first be weighed on a portable scale, and then have their height measured. You will then skate around one end of the arena building up speed. Once the required speed has been obtained, you will be asked to proceed toward the hockey face-off dot, at the centre of the ice rink. Preparation for the jump will occur prior to this point with the triple toe loop take-off occurring at this point. This procedure will be repeated five times.

During the jump, two cameras will film your performance, and the video tapes will then be used for force calculations. Your name, height, and weight, will be recorded for identification by the investigator, however, your identity will remain confidential. The recorded films will not be redistributed or used for any purpose other than this biomechanical research study.

As an elite figure skater it is assumed that your are capable of performing the triple toe loop, and the risk of injury is low.

I, \_\_\_\_\_, have read the above information and understand the testing procedure, the risks involved and I agree to participate at my own risk. I acknowledge that a triple toe loop is well within my capability and I can successfully perform this maneuver on a regular basis. I also understand that I have the right to withdraw at any time I feel appropriate. In the case of injury, I relieve the University of Manitoba, the Western Ontario Figure Skating Association, and the Investigator of any liability that may arise as the result of my participation.

\_\_\_\_\_  
Signature of Investigator

\_\_\_\_\_  
Date

\_\_\_\_\_  
Signature of Subject (Parent/Guardian)

\_\_\_\_\_  
Date

\_\_\_\_\_  
Witness

\_\_\_\_\_  
Date

## LOCATION RECORD

Location:	<u>Brandon, MB</u>	camera	shutter
Date:	<u>January 9, 1993</u>	#1 <u>Digital</u>	<u>1/500</u>
Investigator:	<u>Daryl Boldt</u>	#2 <u>Panasonic PV-460-K</u>	<u>1/500</u>
Project Name:	<u>Skater</u>	#3 _____	_____
Spatial Model:	<u>Skater2</u>		

Location:	<u>Barrie, Ontario</u>	camera	shutter
Date:	<u>February 18, 1993</u>	#1 <u>Digital</u>	<u>1/500</u>
Investigator:	<u>Daryl Boldt</u>	#2 <u>Panasonic PV-520D-K</u>	<u>1/500</u>
Project Name:	<u>Skater2</u>	#3 _____	_____
Spatial Model:	<u>Skater2</u>		

## SUBJECT RECORD

NAME: Subject #1  
 HEIGHT: 1.78 m  
 MASS: 62.6 Kg  
 WEIGHT: 614.11 Kg · m/s<sup>2</sup>  
 LOCATION: Brandon, Manitoba

## NO DATA

NAME: Subject #2  
 HEIGHT: 1.765 m  
 MASS: 68 Kg  
 WEIGHT: 667.08 Kg · m/s<sup>2</sup>  
 LOCATION: Barrie, Ontario

Name: <u>Sub2-1.3r1</u>	Name: <u>Sub2-1.3r2</u>	Name: <u>Sub2-1.3td</u>
1 <sup>st</sup> Frame Digitized: 10076	1 <sup>st</sup> Frame Digitized: 17057	Take Off ( E1): 19
Take Off ( E1): 19	Take Off ( E1): 24	Touchdown (E2): 57
Touchdown (E2): 59	Touchdown (E2): 62	T. Frames Digitized: 98
T. Frames Digitized: 98	T. Frames Digitized: 101	Total Frames in Air: 22

Name: <u>Sub2-2.3r1</u>	Name: <u>Sub2-2.3r2</u>	Name: <u>Sub2-2.3td</u>
1 <sup>st</sup> Frame Digitized: 11581	1 <sup>st</sup> Frame Digitized: 18565	Take Off ( E1): 33
Take Off ( E1): 36	Take Off ( E1): 33	Touchdown (E2): 70
Touchdown (E2): 73	Touchdown (E2): 70	T. Frames Digitized: 101
T. Frames Digitized: 104	T. Frames Digitized: 105	Total Frames in Air: 29

Name: <u>Sub2-3.3r1</u>	Name: <u>Sub2-3.3r2</u>	Name: <u>Sub2-3.3td</u>
1 <sup>st</sup> Frame Digitized: 13014	1 <sup>st</sup> Frame Digitized: 19998	Take Off (E1): 24
Take Off (E1): 26	Take Off (E1): 24	Touchdown (E2): 64
Touchdown (E2): 66	Touchdown (E2): 64	T. Frames Digitized: 91
T. Frames Digitized: 93	T. Frames Digitized: 94	Total Frames in Air: 25

Name: <u>Sub2-4.3r1</u>	Name: <u>Sub2-4.3r2</u>	Name: <u>Sub2-4.3td</u>
1 <sup>st</sup> Frame Digitized: 14192	1 <sup>st</sup> Frame Digitized: 21176	Take Off (E1): 24
Take Off (E1): 26	Take Off (E1): 24	Touchdown (E2): 62
Touchdown (E2): 64	Touchdown (E2): 62	T. Frames Digitized: 91
T. Frames Digitized: 93	T. Frames Digitized: 94	Total Frames in Air: 26

Name: <u>Sub2-5.3r1</u>	Name: <u>Sub2-5.3r2</u>	Name: <u>Sub2-5.3td</u>
1 <sup>st</sup> Frame Digitized: 15568	1 <sup>st</sup> Frame Digitized: 22552	Take Off (E1): 22
Take Off (E1): 25	Take Off (E1): 23	Touchdown (E2): 59
Touchdown (E2): 63	Touchdown (E2): 60	T. Frames Digitized: 91
T. Frames Digitized: 94	T. Frames Digitized: 95	Total Frames in Air: 28

Name: <u>Sub2-6.3r1</u>	Name: <u>Sub2-6.3r2</u>	Name: <u>Sub2-6.3td</u>
1 <sup>st</sup> Frame Digitized: 18298	1 <sup>st</sup> Frame Digitized: 25282	Take Off (E1): 23
Take Off (E1): 25	Take Off (E1): 23	Touchdown (E2): 60
Touchdown (E2): 62	Touchdown (E2): 60	T. Frames Digitized: 89
T. Frames Digitized: 91	T. Frames Digitized: 93	Total Frames in Air: 22

NAME: Subject #3

HEIGHT: 1.701 m

MASS: 73 Kg

WEIGHT: 716.13 Kg · m/s<sup>2</sup>

LOCATION: Barrie, Ontario

Name: <u>Sub3-1.3r1</u>	Name: <u>Sub3-1.3r2</u>	Name: <u>Sub3-1.3td</u>
1 <sup>st</sup> Frame Digitized: 12118	1 <sup>st</sup> Frame Digitized: 19102	Take Off (E1): 13
Take Off (E1): 13	Take Off (E1): 13	Touchdown (E2): 53
Touchdown (E2): 55	Touchdown (E2): 55	T. Frames Digitized: 76
T. Frames Digitized: 76	T. Frames Digitized: 82	Total Frames in Air: 23

Name: <u>Sub3-2.3r1</u>	Name: <u>Sub3-2.3r2</u>	Name: <u>Sub3-2.3td</u>
1 <sup>st</sup> Frame Digitized: 13278	1 <sup>st</sup> Frame Digitized: 20262	Take Off ( E1): 19
Take Off ( E1): 21	Take Off ( E1): 19	Touchdown (E2): 58
Touchdown (E2): 60	Touchdown (E2): 58	T. Frames Digitized: 94
T. Frames Digitized: 96	T. Frames Digitized: 98	Total Frames in Air: 19

Name: <u>Sub3-3.3r1</u>	Name:	
1 <sup>st</sup> Frame Digitized: 16460	1 <sup>st</sup> Frame Digitized: 23444	
Take Off ( E1):	Take Off ( E1):	<b>TRIPLE FLIP</b>
Touchdown (E2):	Touchdown (E2):	
T. Frames Digitized: 96	T. Frames Digitized:	

Name: <u>Sub3-4.3r1</u>	Name:	
1 <sup>st</sup> Frame Digitized: 17954	1 <sup>st</sup> Frame Digitized: 24938	
Take Off ( E1):	Take Off ( E1):	<b>TRIPLE LUTZ</b>
Touchdown (E2):	Touchdown (E2):	
T. Frames Digitized:	T. Frames Digitized:	

Name: <u>Sub3-5.3r1</u>	Name: <u>Sub3-5.3r2</u>	Name: <u>Sub3-5.3td</u>
1 <sup>st</sup> Frame Digitized: 20402	1 <sup>st</sup> Frame Digitized: 27386	Take Off ( E1): 23
Take Off ( E1): 27	Take Off ( E1): 24	Touchdown (E2): 65
Touchdown (E2): 71	Touchdown (E2): 67	T. Frames Digitized: 94
T. Frames Digitized: 98	T. Frames Digitized: 94	Total Frames in Air: 29
		<b>TRIPLE AXLE</b>

NAME: Subject #4

HEIGHT: 1.701 m

MASS: 61 Kg

WEIGHT: 598.41 Kg · m/s<sup>2</sup>

LOCATION: Barrie, Ontario

Name: <u>Sub4-1.3r1</u>	Name: <u>Sub4-1.3r2</u>	Name: <u>Sub4-1.3td</u>
1 <sup>st</sup> Frame Digitized: 13507	1 <sup>st</sup> Frame Digitized: 20491	Take Off ( E1): 17
Take Off ( E1): 18	Take Off ( E1): 18	Touchdown (E2): 53
Touchdown (E2): 54	Touchdown (E2): 53	T. Frames Digitized: 106
T. Frames Digitized: 107	T. Frames Digitized: 106	Total Frames in Air: 32

Name: <u>Sub4-2.3r1</u>	Name: <u>Sub4-2.3r2</u>	Name: <u>Sub4-2.3td</u>
1 <sup>st</sup> Frame Digitized: 15799	1 <sup>st</sup> Frame Digitized: 22783	Take Off ( E1): 22
Take Off ( E1): 24	Take Off ( E1): 22	Touchdown (E2): 58
Touchdown (E2): 60	Touchdown (E2): 58	T. Frames Digitized: 97
T. Frames Digitized: 99	T. Frames Digitized: 102	Total Frames in Air: 22

Name: <u>Sub4-3.3r1</u>	Name: <u>Sub4-3.3r2</u>	Name: <u>Sub4-3.3td</u>
1 <sup>st</sup> Frame Digitized: 17167	1 <sup>st</sup> Frame Digitized: 24151	Take Off ( E1): 16
Take Off ( E1): 19	Take Off ( E1): 17	Touchdown (E2): 51
Touchdown (E2): 54	Touchdown (E2): 51	T. Frames Digitized: 97
T. Frames Digitized: 100	T. Frames Digitized: 101	Total Frames in Air: 20

NAME: Subject #5

HEIGHT: 1.854 m

MASS: 81 Kg

WEIGHT: 794.61 Kg · m/s<sup>2</sup>

LOCATION: Barrie, Ontario

Name: <u>Sub5-1.3r1</u>	Name: <u>Sub5-1.3r2</u>	Name: <u>Sub5-1.3td</u>
1 <sup>st</sup> Frame Digitized: 13970	1 <sup>st</sup> Frame Digitized: 20954	Take Off ( E1): 19
Take Off ( E1): 20	Take Off ( E1): 21	Touchdown (E2): 59
Touchdown (E2): 60	Touchdown (E2): 59	T. Frames Digitized: 98
T. Frames Digitized: 99	T. Frames Digitized: 100	Total Frames in Air: 27

Name: <u>Sub5-2.3r1</u>	Name: <u>Sub5-2.3r2</u>	Name: <u>Sub5-2.3td</u>
1 <sup>st</sup> Frame Digitized: 15121	1 <sup>st</sup> Frame Digitized: 22105	Take Off ( E1): 17
Take Off ( E1): 19	Take Off ( E1): 17	Touchdown (E2): 55
Touchdown (E2): 57	Touchdown (E2): 55	T. Frames Digitized: 93
T. Frames Digitized: 95	T. Frames Digitized: 97	Total Frames in Air: 18

Name: <u>Sub5-3.3r1</u>	Name: <u>Sub5-3.3r2</u>	Name: <u>Sub5-3.3td</u>
1 <sup>st</sup> Frame Digitized: 16305	1 <sup>st</sup> Frame Digitized: 23289	Take Off ( E1): 16
Take Off ( E1): 18	Take Off ( E1): 16	Touchdown (E2): 55
Touchdown (E2): 57	Touchdown (E2): 55	T. Frames Digitized: 88
T. Frames Digitized: 90	T. Frames Digitized: 92	Total Frames in Air: 16

Name: <u>Sub5-4.3r1</u>	Name: <u>Sub5-4.3r2</u>	Name: <u>Sub5-4.3td</u>
1 <sup>st</sup> Frame Digitized: 17374	1 <sup>st</sup> Frame Digitized: 24358	Take Off ( E1): 16
Take Off ( E1): 18	Take Off ( E1): 16	Touchdown (E2): 53
Touchdown (E2): 55	Touchdown (E2): 53	T. Frames Digitized: 88
T. Frames Digitized: 90	T. Frames Digitized:	Total Frames in Air: 21

Name: <u>Sub5-5.3r1</u>	Name:	
1 <sup>st</sup> Frame Digitized: 18730	1 <sup>st</sup> Frame Digitized: 25714	
Take Off ( E1):	Take Off ( E1):	<b>TRIPLE FLIP</b>
Touchdown (E2):	Touchdown (E2):	
T. Frames Digitized:	T. Frames Digitized:	

NAME: Subject #6

HEIGHT: 1.727 m

MASS: 68 Kg

WEIGHT: 667.08 Kg · m/s<sup>2</sup>

LOCATION: Barrie, Ontario

Name: <u>Sub6-1.3r1</u>	Name: <u>Sub6-1.3r2</u>	Name: <u>Sub6-1.3td</u>
1 <sup>st</sup> Frame Digitized: 16696	1 <sup>st</sup> Frame Digitized: 23680	Take Off ( E1): 15
Take Off ( E1): 17	Take Off ( E1): 14	Touchdown (E2): 49
Touchdown (E2): 51	Touchdown (E2): 49	T. Frames Digitized: 95
T. Frames Digitized: 97	T. Frames Digitized: 105	Total Frames in Air: 40

Name: <u>Sub6-2.3r1</u>	Name: <u>Sub6-2.3r2</u>	Name: <u>Sub6-2.3td</u>
1 <sup>st</sup> Frame Digitized: 20070	1 <sup>st</sup> Frame Digitized: 27054	Take Off ( E1): 9
Take Off ( E1): 12	Take Off ( E1): 10	Touchdown (E2): 44
Touchdown (E2): 47	Touchdown (E2): 44	T. Frames Digitized: 87
T. Frames Digitized: 90	T. Frames Digitized: 92	Total Frames in Air: 43

NAME: Subject #7  
 HEIGHT: 1.700 m  
 MASS: 70.3 Kg  
 WEIGHT: 689.64 Kg · m/s<sup>2</sup>  
 LOCATION: Brandon, Manitoba

NO DATA

NAME: Subject #8  
 HEIGHT: 1.613 m  
 MASS: 58 Kg  
 WEIGHT: 568.98 Kg · m/s<sup>2</sup>  
 LOCATION: Barrie, Ontario

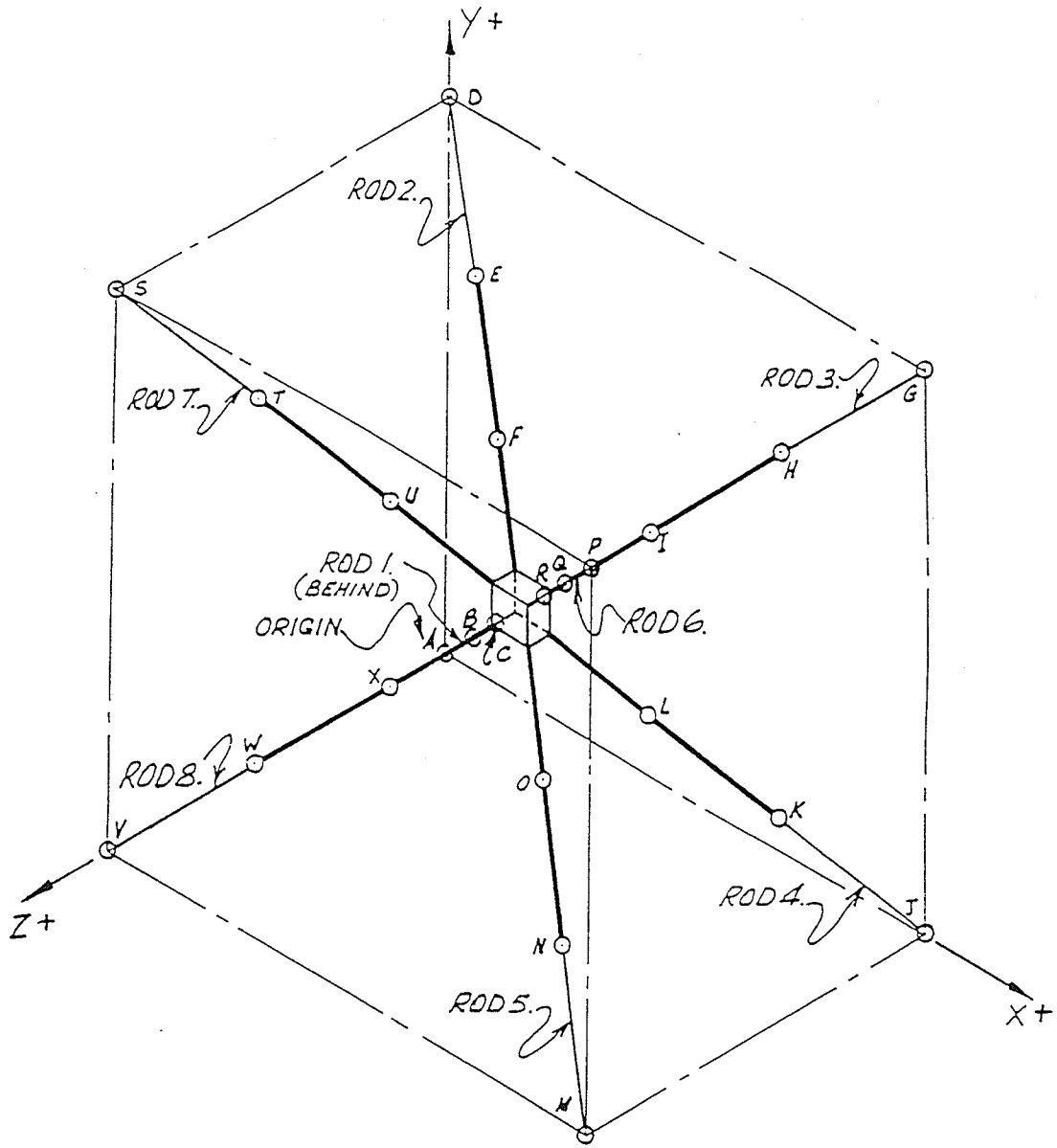
Name: <u>Sub8-1.3r1</u>	Name: <u>Sub8-1.3r2</u>	Name: <u>Sub8-1.3td</u>
1 <sup>st</sup> Frame Digitized: 17623	1 <sup>st</sup> Frame Digitized: 24607	Take Off ( E1): 16
Take Off ( E1): 19	Take Off ( E1): 16	Touchdown (E2): 51
Touchdown (E2): 54	Touchdown (E2): 51	T. Frames Digitized: 81
T. Frames Digitized: 84	T. Frames Digitized:	Total Frames in Air: 23

NAME: Subject #9  
 HEIGHT: 1.74 m  
 MASS: 63.5 Kg  
 WEIGHT: 622.94 Kg · m/s<sup>2</sup>  
 LOCATION: Brandon, Manitoba

NO DATA

## APPENDIX B

### Digitizing Reference Frame



## APPENDIX C

Single Subject Representation of the Linear Accelerations,  
Angular Accelerations, and Angles from  
the Digitized Information

Trial Name: JAN1A.3LA

subject 2a  
 March 1993  
 take off  
 toe touchdown  
 heel touchdown

Project: segmt\_cg  
 Spatial Model: segmt\_cg

Time Between Pictures: 0.017 s

	EVENTS
1 take off	19
2 toe touchdown	59
3 heel touchdown	60

Parameter #	1	:	right forearm	X acceleration (METERS/s/s)			
1	-3.7066	21	39.6814	41 -23.1250			
2	-6.6420	22	28.3947	42 -31.4387			
3	-9.3684	23	9.0328	43 -33.9032			
4	-11.6259	24	-18.3267	44 -29.7775			
5	-13.9524	25	-48.9634	45 -21.7431			
6	-16.7358	26	-74.0523	46 -12.9924			
7	-18.2768	27	-84.6910	47 -6.8093			
8	-17.4258	28	-77.1271	48 -3.5592			
9	-13.3698	29	-55.9673	49 -0.7171			
10	-4.8949	30	-30.4214	50 3.3302			
11	7.1386	31	-9.0954	51 9.4662			
12	21.8373	32	3.3242	52 16.7437			
13	37.2437	33	7.6548	53 22.2437			
14	50.3454	34	6.9439	54 22.3955			
15	58.8384	35	4.5947	55 15.4877			
16	62.0108	36	3.5415	56 3.6122			
17	60.8940	37	3.4846	57 -8.9693			
18	56.3850	38	2.2126	58 -17.2490			
E1	50.7965	39	-2.6158	E2 -18.1801			
20	45.8621	40	-12.0956	E3 -12.1716			
				80 11.4790			
Minimum:	-84.6910	Mean:	0.76438	Std. Dev.:	25.27915	Maximum:	62.0108

Parameter #	1	:	right forearm	Y acceleration (METERS/s/s)
1	-12.5167	21	-51.5245	41 0.0178
2	-12.3656	22	-61.6871	42 6.4451
3	-12.6208	23	-64.3404	43 9.4404
4	-12.8292	24	-55.8381	44 8.8554
5	-11.3717	25	-35.0295	45 5.8976
6	-7.8743	26	-5.3707	46 2.5229
7	-2.5837	27	24.0478	47 0.7506
8	4.5814	28	43.2181	48 -0.0554
9	12.6816	29	48.0559	49 -1.5410
10	20.7686	30	42.0361	50 -3.6594
11	28.3635	31	32.1565	51 -6.1341
12	34.5553	32	23.1167	52 -8.4888
13	38.0994	33	16.2047	53 -10.0133
14	38.0345	34	10.6130	54 -10.7593
15	34.1326	35	4.5983	55 -11.9571
16	25.3747	36	-2.4327	56 -14.7504
17	11.9335	37	-8.8920	57 -18.9392
18	-3.9258	38	-12.7827	58 -23.1036
E1	-20.7190	39	-12.5925	E2 -24.8281
				79 -0.0472

20 -37.1800 40 -7.5761 E3 -22.8912 80 0.7219  
 Minimum: -64.3404 Mean: 0.28964 Std. Dev.: 20.08525 Maximum: 48.0559

Parameter # 1 : right forearm Z acceleration (METERS/s/s)

1	11.55	21	61.60	41	72.85	61	-38.48	81	6.66
2	10.97	22	81.18	42	46.67	62	-55.30	82	5.72
3	10.12	23	93.29	43	12.43	63	-63.37	83	3.91
4	8.26	24	95.04	44	-22.56	64	-64.00	84	1.63
5	5.41	25	82.93	45	-51.29	65	-57.85	85	-0.77
6	2.58	26	55.12	46	-69.52	66	-47.07	86	-3.26
7	-1.84	27	14.62	47	-75.74	67	-34.27	87	-5.16
8	-9.38	28	-30.75	48	-69.81	68	-20.83	88	-6.38
9	-18.04	29	-70.84	49	-53.35	69	-8.19	89	-7.08
10	-27.26	30	-97.42	50	-28.79	70	1.33	90	-6.60
11	-36.42	31	-108.29	51	1.67	71	7.60	91	-5.61
12	-43.85	32	-103.80	52	35.25	72	11.60	92	-4.89
13	-48.99	33	-86.68	53	67.92	73	12.91	93	-3.45
14	-51.29	34	-61.00	54	93.94	74	12.50	94	-1.32
15	-50.28	35	-28.76	55	108.36	75	11.49	95	0.25
16	-45.07	36	5.92	56	107.40	76	10.07	96	1.52
17	-33.80	37	38.01	57	89.34	77	8.93	97	2.77
18	-15.49	38	64.11	58	58.69	78	8.02	98	-3.74
E1	9.15	39	80.65	E2	22.71	79	7.59		
20	36.56	40	84.54	E3	-11.68	80	7.29		

Minimum: -108.29 Mean: -1.010 Std. Dev.: 48.254 Maximum: 108.36

Parameter # 1 : right forearm R acceleration (METERS/s/s)

1	17.4285	21	89.5794	41	76.4329	61	42.4562	81	11.9880
2	17.8154	22	105.8379	42	56.6416	62	56.7191	82	10.0944
3	18.6963	23	113.6889	43	37.3223	63	64.9013	83	7.6190
4	19.1845	24	111.7425	44	38.3933	64	66.2926	84	5.4665
5	18.7947	25	102.4747	45	56.0242	65	60.6145	85	4.5748
6	18.6752	26	92.4686	46	70.7698	66	50.2298	86	5.1510
7	18.5505	27	89.2445	47	76.0516	67	38.2672	87	6.1382
8	20.3117	28	93.6055	48	69.9016	68	26.5709	88	6.9706
9	25.7897	29	102.2769	49	53.3723	69	17.8627	89	7.4204
10	34.6142	30	110.3802	50	29.2153	70	14.9143	90	6.7592
11	46.7142	31	113.3260	51	11.4028	71	14.8758	91	5.6584
12	59.9465	32	106.3973	52	39.9394	72	15.4375	92	4.9204
13	72.3810	33	88.5160	53	72.1658	73	14.9394	93	3.6473
14	81.3150	34	62.3053	54	97.1670	74	13.9414	94	2.7983
15	84.5863	35	29.4883	55	110.1123	75	13.7095	95	3.7410
16	80.7517	36	7.3135	56	108.4702	76	14.0239	96	5.5184
17	70.6616	37	39.1951	57	91.7623	77	14.6376	97	7.5754
18	58.6044	38	65.4140	58	65.3871	78	14.9939	98	9.2198
E1	55.6179	39	81.6701	E2	38.2429	79	14.7930		
20	69.4423	40	85.7318	E3	28.4337	80	13.6177		

Minimum: 2.7983 Mean: 45.98781 Std. Dev.: 35.15621 Maximum: 113.6889

Parameter # 2 : left forearm X acceleration (METERS/s/s)

1	5.6665	21	19.6175	41	-15.5318	61	40.0634	81	4.6506
2	5.5273	22	0.3395	42	-12.5216	62	37.5138	82	5.4607
3	5.9005	23	-18.6309	43	-8.5996	63	32.3827	83	6.1229
4	6.8219	24	-36.0644	44	-4.4280	64	25.4356	84	6.7407
5	6.7946	25	-49.5766	45	-1.8489	65	17.1018	85	7.2414
6	4.9801	26	-55.9199	46	-1.7877	66	9.1661	86	7.5496
7	2.5084	27	-52.7314	47	-4.9997	67	2.5049	87	7.6513
8	-0.2301	28	-40.6492	48	-10.2829	68	-2.3701	88	7.4142
9	-2.8401	29	-24.6631	49	-15.4575	69	-5.2493	89	6.7155

10	-3.6054	30	-10.7032	50	-19.8767	70	-6.5263	90	5.7018
11	-1.7504	31	-2.7384	51	-22.4629	71	-6.3860	91	4.4055
12	3.6472	32	-1.6110	52	-22.7249	72	-5.4144	92	3.0742
13	13.5301	33	-5.0878	53	-20.8133	73	-4.3897	93	1.4338
14	27.3594	34	-10.7402	54	-17.0151	74	-3.2976	94	-0.6380
15	42.2115	35	-16.2239	55	-10.7106	75	-1.7449	95	-2.5780
16	54.8178	36	-19.4231	56	-1.3921	76	-0.1636	96	-4.4765
17	62.5009	37	-20.1447	57	9.8583	77	1.0250	97	-5.6601
18	61.7060	38	-19.3443	58	21.7106	78	2.1135	98	6.0751
E1	52.2939	39	-18.1489	E2	31.8184	79	3.1546		
20	37.5210	40	-17.2562	E3	38.2204	80	3.8923		

Minimum: -55.9199 Mean: 1.04604 Std. Dev.: 21.47310 Maximum: 62.5009

Parameter #	2	left forearm		Y acceleration (METERS/s/s)					
1	-3.0805	21	-39.8310	41	2.7390	61	-12.1631	81	0.6374
2	-2.6230	22	-40.9409	42	3.1335	62	-5.4886	82	0.5403
3	-2.4969	23	-36.0227	43	2.0689	63	0.3169	83	0.6871
4	-2.7246	24	-24.1737	44	0.0646	64	4.8739	84	0.7552
5	-2.2523	25	-6.6895	45	-1.9478	65	8.3492	85	1.0228
6	-0.6748	26	12.8855	46	-3.0632	66	10.9986	86	1.5898
7	1.4793	27	28.5348	47	-2.6667	67	12.9008	87	1.8681
8	4.5109	28	34.6909	48	-1.7503	68	13.8976	88	1.9887
9	8.2797	29	31.5572	49	-1.6239	69	14.0933	89	2.1376
10	11.8925	30	23.5372	50	-2.4879	70	13.8315	90	2.1524
11	15.1705	31	15.6914	51	-4.4037	71	13.1010	91	1.8335
12	17.6494	32	10.6522	52	-7.1270	72	11.8248	92	1.2478
13	18.2667	33	7.9696	53	-10.5979	73	10.1183	93	0.6115
14	16.7258	34	6.5457	54	-14.7086	74	8.3818	94	-0.2874
15	13.1897	35	5.0811	55	-19.1765	75	6.8074	95	-1.2337
16	6.6815	36	2.7286	56	-23.7193	76	5.2490	96	-1.9578
17	-2.9076	37	0.3695	57	-26.7912	77	3.8210	97	-2.6492
18	-13.8245	38	-1.0516	58	-27.0674	78	2.5977	98	3.3697
E1	-24.5890	39	-1.0387	E2	-24.2240	79	1.7196		
20	-33.8750	40	0.8120	E3	-18.7901	80	1.0925		

Minimum: -40.9409 Mean: 0.14901 Std. Dev.: 13.83500 Maximum: 34.6909

Parameter #	2	left forearm		Z acceleration (METERS/s/s)					
1	-13.6656	21	31.4444	41	26.6729	61	-34.3911	81	6.7474
2	-10.7215	22	41.7301	42	12.7812	62	-37.5608	82	3.9395
3	-8.1117	23	45.4542	43	-1.4018	63	-37.6886	83	0.6243
4	-5.3881	24	40.8431	44	-13.8898	64	-35.9725	84	-2.2006
5	-0.9717	25	28.3765	45	-22.0937	65	-31.8004	85	-3.9559
6	5.2123	26	8.4022	46	-24.7479	66	-25.5824	86	-5.2183
7	10.6867	27	-15.6655	47	-22.1137	67	-17.9732	87	-6.1959
8	14.1553	28	-37.8774	48	-14.6779	68	-9.4810	88	-6.9945
9	16.2911	29	-53.6155	49	-3.6636	69	-1.1031	89	-7.4595
10	15.3522	30	-60.7663	50	9.5574	70	5.8501	90	-6.8349
11	10.4282	31	-60.0840	51	23.3861	71	11.1998	91	-6.1034
12	3.4900	32	-52.5496	52	35.7757	72	15.1955	92	-5.9036
13	-4.5892	33	-40.0197	53	44.6380	73	18.1171	93	-5.0419
14	-12.8401	34	-24.4997	54	47.5967	74	19.8642	94	-3.4537
15	-19.3794	35	-6.7902	55	43.7424	75	19.8678	95	-2.1390
16	-22.6660	36	10.7419	56	33.2367	76	18.8552	96	-0.7784
17	-20.8782	37	25.1115	57	17.4618	77	17.3307	97	1.0579
18	-13.1482	38	34.3684	58	0.1057	78	15.1959	98	-2.9800
E1	0.3791	39	38.2266	E2	-15.2556	79	12.3850		
20	16.9121	40	36.1040	E3	-26.8373	80	9.3627		

Minimum: -60.7663 Mean: -0.21902 Std. Dev.: 24.03030 Maximum: 47.5967

Parameter #	2	left forearm		R acceleration (METERS/s/s)					
-------------	---	--------------	--	-----------------------------	--	--	--	--	--

1	15.111	21 54.407	41 30.987	61 54.183	81 8.220
2	12.344	22 58.461	42 18.165	62 53.369	82 6.755
3	10.337	23 60.917	43 8.955	63 49.691	83 6.193
4	9.110	24 59.608	44 14.579	64 44.325	84 7.131
5	7.224	25 57.514	45 22.256	65 37.060	85 8.315
6	7.241	26 57.997	46 25.001	66 29.316	86 9.314
7	11.076	27 61.970	47 22.828	67 22.265	87 10.021
8	14.858	28 65.502	48 18.007	68 16.990	88 10.385
9	18.494	29 66.923	49 15.968	69 15.080	89 10.262
10	19.751	30 66.039	50 22.195	70 16.375	90 9.157
11	18.492	31 62.159	51 32.724	71 18.381	91 7.747
12	18.357	32 53.643	52 42.978	72 20.001	92 6.772
13	23.190	33 41.122	53 50.379	73 21.210	93 5.277
14	34.542	34 27.540	54 52.643	74 21.811	94 3.524
15	48.284	35 18.307	55 48.947	75 21.074	95 3.570
16	59.694	36 22.363	56 40.856	76 19.573	96 4.948
17	65.960	37 32.195	57 33.464	77 17.777	97 6.338
18	64.588	38 39.452	58 34.699	78 15.561	98 7.559
E1	57.788	39 42.329	E2 42.801	79 12.896	
20	53.304	40 40.024	E3 50.340	80 10.198	
Minimum: 3.524 Mean: 28.9348 Std. Dev.: 19.6285 Maximum: 66.923					

Parameter # 3 : right upper arm X acceleration (METERS/s/s)

1	16.9996	21 -5.2788	41 -32.0000	61 85.0748	81 -10.2279
2	24.2893	22 -48.0789	42 -15.8327	62 80.5276	82 -5.4692
3	31.7302	23 -82.9343	43 1.8161	63 69.2272	83 -0.8871
4	38.6049	24 -99.9096	44 16.0344	64 55.2200	84 3.6619
5	43.3153	25 -94.2300	45 23.3010	65 40.9257	85 7.3628
6	45.2337	26 -66.7592	46 23.3345	66 28.5011	86 10.2434
7	43.5977	27 -25.7073	47 17.0578	67 18.5190	87 12.7011
8	36.7187	28 16.1110	48 7.1023	68 10.3742	88 13.9898
9	24.0348	29 46.1824	49 -4.0217	69 3.2463	89 14.3627
10	6.4665	30 58.3207	50 -16.1713	70 -3.5480	90 13.8425
11	-13.6640	31 54.1056	51 -29.4807	71 -10.3420	91 12.4937
12	-31.8349	32 39.0809	52 -43.5686	72 -16.9848	92 10.4383
13	-41.6407	33 19.9854	53 -55.8969	73 -22.4513	93 7.6519
14	-38.2671	34 1.3867	54 -62.3929	74 -26.1484	94 4.7294
15	-21.3302	35 -14.7266	55 -58.1474	75 -28.2930	95 1.5919
16	6.0296	36 -27.7824	56 -39.7121	76 -28.5907	96 -1.3353
17	35.5549	37 -37.7497	57 -9.5068	77 -26.8476	97 -3.4178
18	54.6745	38 -44.1029	58 26.0087	78 -23.6172	98 5.1262
E1	54.1448	39 -46.1915	E2 57.6309	79 -19.5223	
20	32.3927	40 -42.6486	E3 78.0028	80 -14.9878	
Minimum: -99.9096 Mean: 0.98797 Std. Dev.: 37.38509 Maximum: 85.0748					

Parameter # 3 : right upper arm Y acceleration (METERS/s/s)

1	-7.0068	21 -64.8247	41 14.4932	61 1.3114	81 4.2987
2	-5.0604	22 -50.4952	42 11.1940	62 11.3069	82 3.3476
3	-2.8468	23 -25.7439	43 5.3918	63 18.0920	83 2.0950
4	0.1561	24 5.7151	44 -0.4816	64 21.8453	84 0.4725
5	4.2283	25 35.9434	45 -4.3149	65 23.3619	85 -1.1611
6	9.4133	26 55.2324	46 -5.6250	66 23.2467	86 -2.7003
7	15.2468	27 57.8736	47 -4.9497	67 22.0501	87 -4.1100
8	21.2054	28 44.6352	48 -3.6711	68 19.8702	88 -5.1436
9	26.4693	29 23.6754	49 -3.0473	69 17.1909	89 -5.8623
10	29.9584	30 5.1008	50 -3.0868	70 14.6195	90 -6.3176
11	31.1872	31 -6.0252	51 -3.9824	71 11.9456	91 -6.4137
12	28.9386	32 -10.0174	52 -6.0456	72 9.3423	92 -6.1786
13	21.9853	33 -9.7576	53 -9.8481	73 7.3093	93 -5.8022

14	10.8024	34	-7.7807	54	-15.8708	74	5.8971	94	-5.5418
15	-3.1384	35	-5.5345	55	-23.4340	75	5.0216	95	-5.1405
16	-18.9901	36	-3.2808	56	-30.7127	76	4.6956	96	-4.6283
17	-35.5511	37	0.0708	57	-34.1882	77	4.7081	97	-4.9979
18	-50.4955	38	4.7171	58	-31.4575	78	4.7973	98	6.0588
E1	-61.9453	39	9.5836	E2	-22.9345	79	4.8694		
20	-67.8511	40	13.6003	E3	-10.8804	80	4.7982		

Minimum: -67.8511 Mean: 0.24996 Std. Dev.: 21.61034 Maximum: 57.8736

Parameter # 3 : right upper arm Z acceleration (METERS/s/s)

1	-52.93	21	22.37	41	-14.18	61	-90.26	81	6.57
2	-49.41	22	11.26	42	-34.06	62	-71.40	82	5.75
3	-44.53	23	-7.76	43	-44.66	63	-51.26	83	5.04
4	-35.99	24	-35.26	44	-44.71	64	-30.78	84	3.95
5	-22.66	25	-67.05	45	-34.34	65	-10.42	85	3.47
6	-4.60	26	-96.18	46	-16.24	66	8.19	86	2.41
7	16.58	27	-113.84	47	5.34	67	24.68	87	0.37
8	38.72	28	-113.71	48	27.46	68	38.92	88	-1.50
9	59.31	29	-96.29	49	47.84	69	49.24	89	-3.56
10	74.14	30	-67.39	50	64.11	70	54.59	90	-5.71
11	80.79	31	-35.54	51	73.18	71	55.55	91	-7.76
12	79.04	32	-6.00	52	72.63	72	52.46	92	-10.24
13	70.26	33	19.41	53	60.90	73	46.79	93	-11.82
14	57.76	34	38.80	54	36.54	74	39.74	94	-11.77
15	45.74	35	52.08	55	2.11	75	31.63	95	-11.98
16	37.46	36	59.05	56	-36.26	76	24.11	96	-11.59
17	32.30	37	58.00	57	-71.81	77	18.30	97	-9.54
18	29.36	38	48.26	58	-96.69	78	13.97	98	7.00
E1	28.85	39	31.41	E2	-106.50	79	10.40		
20	27.75	40	9.66	E3	-103.28	80	8.02		

Minimum: -113.84 Mean: 1.410 Std. Dev.: 48.075 Maximum: 80.79

Parameter # 3 : right upper arm R acceleration (METERS/s/s)

1	56.0282	21	68.7803	41	37.8812	61	124.0447	81	12.8950
2	55.2852	22	70.6269	42	39.1916	62	108.2170	82	8.6114
3	54.7551	23	87.1845	43	45.0186	63	88.0213	83	5.5334
4	52.7809	24	106.1016	44	47.4974	64	66.8876	84	5.4060
5	49.0684	25	121.1048	45	41.7209	65	48.2621	85	8.2204
6	46.4309	26	129.4517	46	28.9782	66	37.6796	86	10.8632
7	49.0715	27	130.2709	47	18.5478	67	37.9240	87	13.3548
8	57.4226	28	123.2142	48	28.5998	68	44.9115	88	14.9809
9	69.2508	29	109.3888	49	48.1056	69	52.2535	89	15.9169
10	80.2270	30	89.2710	50	66.1882	70	56.6255	90	16.2528
11	87.6697	31	65.0116	51	78.9969	71	57.7521	91	16.0429
12	89.9876	32	40.7883	52	84.9150	72	55.9226	92	15.8744
13	84.5798	33	29.5220	53	83.2514	73	52.4133	93	15.2257
14	70.1246	34	39.5983	54	74.0277	74	47.9382	94	13.8423
15	50.5687	35	54.4058	55	62.7273	75	42.7335	95	13.1336
16	42.4278	36	65.3428	56	61.9310	76	37.6900	96	12.5544
17	59.7623	37	69.2058	57	80.0963	77	32.8323	97	11.3010
18	80.0070	38	65.5494	58	104.9522	78	27.8555	98	10.5846
E1	87.1835	39	56.6774	E2	123.2467	79	22.6490		
20	80.1456	40	45.7948	E3	129.8864	80	17.6606		

Minimum: 5.4060 Mean: 55.47648 Std. Dev.: 32.70327 Maximum: 130.2709

Parameter # 4 : left upper arm X acceleration (METERS/s/s)

1	24.5510	21	36.3478	41	-7.7388	61	-6.9968	81	-20.3550
2	22.3338	22	27.2942	42	-15.6586	62	12.5929	82	-19.3145
3	19.2551	23	15.3897	43	-20.9755	63	27.4954	83	-17.7304

4	14.1813	24	3.7665	44	-21.9587	64	37.0407	84	-15.7100
5	7.0341	25	-4.4385	45	-18.6226	65	42.0640	85	-13.6600
6	-1.5467	26	-6.7749	46	-12.7043	66	45.1417	86	-11.3533
7	-13.0914	27	-2.8552	47	-6.1144	67	47.9411	87	-8.3286
8	-28.0751	28	5.6468	48	0.4495	68	50.0730	88	-5.6524
9	-43.6243	29	14.8484	49	6.9744	69	50.5773	89	-3.5465
10	-57.8977	30	20.4543	50	13.3794	70	48.1104	90	-1.7007
11	-67.4437	31	20.8352	51	19.1652	71	41.3059	91	-0.5306
12	-69.2987	32	16.2840	52	22.0956	72	30.3563	92	-0.2820
13	-62.6418	33	8.8656	53	18.6679	73	17.9071	93	-0.7019
14	-48.1098	34	1.8517	54	6.8837	74	5.9127	94	-1.2130
15	-28.7470	35	-2.2502	55	-12.4902	75	-4.9984	95	-1.8378
16	-7.8890	36	-2.5241	56	-34.5415	76	-13.2637	96	-2.6241
17	11.2440	37	-0.1004	57	-51.3319	77	-18.0918	97	-3.2787
18	26.6794	38	2.7846	58	-56.4309	78	-19.9970	98	3.8383
E1	36.6936	39	3.3754	E2	-47.7888	79	-20.4847		
20	39.9073	40	-0.3727	E3	-28.9700	80	-20.6640		

Minimum: -69.2987 Mean: -0.89518 Std. Dev.: 26.46379 Maximum: 50.5773

Parameter # 4 : left upper arm Y acceleration (METERS/s/s)

1	6.8322	21	-4.9595	41	-7.3023	61	-52.7701	81	-2.9039
2	2.6695	22	-5.8062	42	-1.7023	62	-43.3694	82	-2.5843
3	-2.0431	23	-4.0684	43	2.4628	63	-30.4476	83	-2.1280
4	-7.5291	24	1.6271	44	4.6168	64	-16.2853	84	-1.8708
5	-12.7031	25	10.9039	45	5.3352	65	-2.0849	85	-1.8135
6	-16.5367	26	21.1655	46	6.3216	66	10.8639	86	-2.1639
7	-18.6113	27	28.3755	47	8.9632	67	21.4593	87	-2.8414
8	-18.2118	28	29.2624	48	12.6446	68	28.7904	88	-3.3573
9	-15.5853	29	24.1617	49	16.2976	69	32.7485	89	-3.8948
10	-11.7606	30	16.4962	50	19.4774	70	33.7119	90	-4.3390
11	-7.0851	31	9.8143	51	21.4191	71	31.8022	91	-4.6925
12	-2.8511	32	5.6708	52	21.9327	72	27.5664	92	-4.8076
13	-0.5224	33	3.6861	53	20.6561	73	21.9271	93	-4.5679
14	0.1156	34	2.0617	54	16.3643	74	15.7889	94	-4.5572
15	0.2089	35	-1.0406	55	7.6100	75	9.9069	95	-4.1715
16	-0.4760	36	-5.8006	56	-6.2743	76	4.8905	96	-3.3774
17	-1.6870	37	-10.7042	57	-23.5523	77	1.0494	97	-3.5639
18	-2.0506	38	-14.2870	58	-40.3788	78	-1.6527	98	4.5164
E1	-2.2483	39	-15.4873	E2	-52.0343	79	-3.0662		
20	-3.3245	40	-12.8226	E3	-56.0590	80	-3.1999		

Minimum: -56.0590 Mean: -0.24329 Std. Dev.: 17.26493 Maximum: 33.7119

Parameter # 4 : left upper arm Z acceleration (METERS/s/s)

1	-25.94	21	30.10	41	61.34	61	-128.11	81	34.17
2	-12.26	22	33.43	42	41.46	62	-151.41	82	24.37
3	2.03	23	31.94	43	15.08	63	-161.18	83	16.13
4	17.76	24	25.14	44	-12.61	64	-158.20	84	10.51
5	34.52	25	12.50	45	-34.60	65	-143.04	85	7.14
6	51.20	26	-6.63	46	-47.18	66	-116.97	86	3.98
7	63.50	27	-30.58	47	-49.41	67	-82.96	87	1.36
8	67.90	28	-54.08	48	-41.18	68	-44.10	88	-0.80
9	64.05	29	-72.22	49	-24.19	69	-3.42	89	-3.52
10	49.74	30	-82.39	50	-0.00	70	34.89	90	-7.22
11	26.82	31	-83.51	51	28.64	71	67.58	91	-11.33
12	0.41	32	-75.75	52	57.87	72	91.86	92	-16.10
13	-24.31	33	-60.64	53	84.20	73	107.00	93	-20.84
14	-42.07	34	-39.94	54	102.13	74	113.60	94	-24.36
15	-49.31	35	-14.82	55	105.22	75	111.61	95	-27.68
16	-44.11	36	11.75	56	89.56	76	103.11	96	-29.21
17	-30.14	37	35.90	57	55.43	77	90.14	97	-28.49

18	-12.35	38	55.23	58	8.02	78	75.54	98	27.48
E1	6.34	39	67.95	E2	-43.84	79	60.87		
20	21.39	40	70.82	E3	-91.28	80	46.43		
Minimum:	-161.18	Mean:	1.968	Std. Dev.:	61.812	Maximum:	113.60		

Parameter # 4 : left upper arm R acceleration (METERS/s/s)

1	36.3671	21	47.4516	41	62.2516	61	138.7254	81	39.8756
2	25.6193	22	43.5480	42	44.3481	62	157.9995	82	31.2031
3	19.4696	23	35.6913	43	25.9496	63	166.3209	83	24.0652
4	23.9437	24	25.4759	44	25.7403	64	163.2933	84	18.9922
5	37.4534	25	17.1711	45	39.6555	65	149.1108	85	15.5181
6	53.8304	26	23.1921	46	49.2668	66	125.8517	86	12.2230
7	67.4573	27	41.8141	47	50.5848	67	98.1860	87	8.9037
8	75.6989	28	61.7444	48	43.0822	68	72.6691	88	6.6230
9	79.0473	29	77.5900	49	29.9899	69	60.3506	89	6.3329
10	77.2310	30	86.4820	50	23.6300	70	68.3241	90	8.5933
11	72.9267	31	86.6319	51	40.5778	71	85.3518	91	12.2764
12	69.3585	32	77.6875	52	65.7110	72	100.5989	92	16.8071
13	67.1972	33	61.4000	53	88.6803	73	110.6863	93	21.3457
14	63.9098	34	40.0374	54	103.6606	74	114.8413	94	24.8074
15	57.0770	35	15.0242	55	106.2347	75	112.1649	95	28.0516
16	44.8102	36	13.3418	56	96.1934	76	104.0777	96	29.5200
17	32.2173	37	37.4600	57	79.1354	77	91.9416	97	28.9020
18	29.4697	38	57.1117	58	69.8510	78	78.1633	98	28.1097
E1	37.3056	39	69.7721	E2	83.1440	79	64.2972		
20	45.3993	40	71.9761	E3	110.9716	80	50.9195		
Minimum:	6.3329	Mean:	58.37833	Std. Dev.:	37.15768	Maximum:	166.3209		

Parameter # 5 : head and neck X acceleration (METERS/s/s)

1	-4.4692	21	42.6810	41	-25.0174	61	-5.8868	81	10.7452
2	-8.4105	22	30.6052	42	-33.6979	62	4.2589	82	8.6885
3	-11.9722	23	9.4068	43	-36.0190	63	12.0229	83	6.3655
4	-14.7697	24	-20.4187	44	-31.2977	64	16.0369	84	4.3260
5	-17.4920	25	-53.4573	45	-22.4382	65	15.3885	85	2.8076
6	-20.4395	26	-79.9966	46	-12.8269	66	11.9444	86	1.8238
7	-21.6341	27	-90.6206	47	-5.8376	67	7.7446	87	1.1190
8	-19.8680	28	-81.7315	48	-1.9138	68	3.7509	88	0.6364
9	-14.3707	29	-58.3698	49	1.4657	69	0.4304	89	0.2443
10	-4.1131	30	-30.4863	50	5.9432	70	-1.3042	90	0.0606
11	9.7005	31	-7.2981	51	12.4274	71	-0.9316	91	-0.2579
12	25.6508	32	6.2866	52	19.8674	72	0.6490	92	-0.6071
13	41.3518	33	11.1123	53	25.1296	73	2.7287	93	-1.0269
14	53.8877	34	10.4263	54	24.4512	74	5.3637	94	-2.0503
15	61.2565	35	7.7676	55	16.1210	75	8.4166	95	-3.1113
16	63.2429	36	6.1860	56	2.4940	76	11.1468	96	-4.6110
17	61.5308	37	5.4014	57	-11.7818	77	13.0449	97	-6.0657
18	57.3089	38	3.1883	58	-21.2400	78	14.0359	98	6.9077
E1	52.6274	39	-2.6808	E2	-22.5789	79	13.9284		
20	48.6011	40	-13.1812	E3	-16.3232	80	12.5673		
Minimum:	-90.6206	Mean:	0.72141	Std. Dev.:	26.93304	Maximum:	63.2429		

Parameter # 5 : head and neck Y acceleration (METERS/s/s)

1	-14.0265	21	-54.8326	41	-0.0370	61	-18.5454	81	1.2095
2	-14.1797	22	-66.1717	42	6.6913	62	-11.2193	82	1.9596
3	-14.6450	23	-69.3368	43	9.8925	63	-3.4036	83	2.7492
4	-14.8807	24	-60.3928	44	9.3761	64	3.8320	84	3.1808
5	-13.3062	25	-38.1741	45	6.3735	65	9.6199	85	3.3755
6	-9.4968	26	-6.6020	46	2.9173	66	13.7388	86	3.2446
7	-3.6114	27	24.6489	47	1.0884	67	16.3654	87	2.6604

8	4.3593	28	45.0811	48	0.2693	68	17.3040	88	2.0794
9	13.3518	29	50.3462	49	-1.2420	69	16.9582	89	1.4497
10	22.3769	30	44.1288	50	-3.4149	70	15.5731	90	0.5484
11	30.9323	31	33.8213	51	-5.9075	71	13.2297	91	-0.3333
12	37.9158	32	24.3428	52	-8.2174	72	10.4352	92	-0.9157
13	41.9893	33	17.0297	53	-9.6310	73	7.3144	93	-1.4305
14	42.1824	34	11.0347	54	-10.2461	74	4.3255	94	-2.0917
15	38.1137	35	4.6160	55	-11.3879	75	2.1186	95	-2.4660
16	28.7588	36	-2.7795	56	-14.2873	76	0.5501	96	-2.6830
17	14.3776	37	-9.5563	57	-18.7678	77	-0.5107	97	-3.2895
18	-2.6888	38	-13.5910	58	-23.3705	78	-0.9228	98	4.1272
E1	-20.9164	39	-13.2808	E2	-25.5017	79	-0.5644		
20	-38.9646	40	-7.9700	E3	-23.7374	80	0.3740		

Minimum: -69.3368 Mean: 0.31440 Std. Dev.: 21.47392 Maximum: 50.3462

Parameter # 5 : head and neck Z acceleration (METERS/s/s)

1	16.32	21	67.06	41	74.57	61	-39.32	81	6.75
2	14.86	22	86.81	42	47.07	62	-56.99	82	5.73
3	12.82	23	98.86	43	11.36	63	-65.52	83	3.73
4	9.28	24	99.96	44	-24.95	64	-66.31	84	1.40
5	4.49	25	86.47	45	-54.55	65	-60.08	85	-0.97
6	-0.52	26	56.46	46	-72.97	66	-49.15	86	-3.42
7	-7.20	27	13.45	47	-78.88	67	-36.16	87	-5.26
8	-16.78	28	-34.23	48	-72.36	68	-22.60	88	-6.36
9	-26.91	29	-75.93	49	-54.97	69	-9.75	89	-6.84
10	-36.54	30	-102.93	50	-29.32	70	0.06	90	-6.23
11	-45.21	31	-113.11	51	2.38	71	6.49	91	-5.15
12	-51.17	32	-107.40	52	37.33	72	10.68	92	-4.47
13	-54.09	33	-88.87	53	71.37	73	12.20	93	-3.08
14	-53.99	34	-61.84	54	98.58	74	12.09	94	-1.01
15	-50.63	35	-28.39	55	113.81	75	11.34	95	0.33
16	-43.42	36	7.47	56	113.05	76	10.02	96	1.44
17	-30.65	37	40.54	57	94.33	77	8.97	97	2.48
18	-11.30	38	67.16	58	62.28	78	8.18	98	-3.13
E1	14.02	39	83.81	E2	24.70	79	7.78		
20	41.84	40	87.28	E3	-11.19	80	7.41		

Minimum: -113.11 Mean: -1.176 Std. Dev.: 50.685 Maximum: 113.81

Parameter # 5 : head and neck R acceleration (METERS/s/s)

1	21.9787	21	96.5666	41	78.6576	61	43.8680	81	12.7458
2	22.1965	22	113.3630	42	58.2720	62	58.2440	82	10.5891
3	22.8491	23	121.1165	43	39.0414	63	66.6974	83	7.8737
4	22.9279	24	118.5600	44	41.1083	64	68.3279	84	5.5496
5	22.4326	25	108.5876	45	59.3245	65	62.7625	85	4.4971
6	22.5440	26	98.1385	46	74.1473	66	52.4116	86	5.0556
7	23.0844	27	94.8716	47	79.1002	67	40.4357	87	6.0022
8	26.3692	28	99.4186	48	72.3817	68	28.7100	88	6.7216
9	33.2973	29	108.1999	49	55.0066	69	19.5644	89	6.9996
10	43.0430	30	116.0657	50	30.1095	70	15.6277	90	6.2582
11	55.6303	31	118.2879	51	13.9646	71	14.7656	91	5.1719
12	68.6548	32	110.3045	52	43.0755	72	14.9430	92	4.6051
13	79.9915	33	91.1700	53	76.2746	73	14.4870	93	3.5465
14	87.1667	34	63.6750	54	102.0816	74	13.9116	94	3.0983
15	88.1389	35	29.7886	55	115.5068	75	14.2783	95	3.9840
16	81.9291	36	10.0913	56	113.9806	76	14.9967	96	5.5270
17	70.2313	37	41.9969	57	96.8937	77	15.8377	97	7.3338
18	58.4741	38	68.5975	58	69.8297	78	16.2712	98	8.6329
E1	58.3423	39	84.8964	E2	42.0767	79	15.9638		
20	75.0377	40	88.6293	E3	30.9051	80	14.5962		

Minimum: 3.0983 Mean: 48.76811 Std. Dev.: 36.80543 Maximum: 121.1165

Parameter # 6 : trunk

				X acceleration (METERS/s/s)					
1	12.3448	21	-4.3012	41	-19.6658	61	69.0940	81	-1.7951
2	15.1907	22	-35.9847	42	-3.7656	62	59.1753	82	1.1389
3	18.4201	23	-60.5280	43	10.5165	63	46.0946	83	4.0004
4	21.4552	24	-71.8687	44	19.6760	64	32.3781	84	6.7271
5	22.9905	25	-67.1331	45	21.7919	65	19.5291	85	8.5360
6	22.5592	26	-47.4388	46	17.6572	66	9.1328	86	9.5545
7	20.0879	27	-18.8728	47	8.6030	67	1.6498	87	10.1821
8	15.4052	28	9.6675	48	-3.0042	68	-3.4270	88	9.9978
9	8.5655	29	29.4525	49	-14.9154	69	-6.6828	89	9.2388
10	0.4045	30	36.2226	50	-26.7983	70	-8.5999	90	7.9678
11	-7.7427	31	31.2075	51	-38.1073	71	-9.8465	91	6.1890
12	-13.1172	32	18.5623	52	-47.5449	72	-10.9717	92	4.4185
13	-12.4075	33	3.2539	53	-52.2576	73	-11.9310	93	2.5388
14	-3.9677	34	-11.5839	54	-49.2206	74	-12.7021	94	0.3766
15	11.2011	35	-24.5844	55	-36.1510	75	-13.1302	95	-1.6527
16	30.1466	36	-34.7318	56	-13.0661	76	-12.7982	96	-3.3951
17	47.3168	37	-41.2975	57	15.4536	77	-11.5980	97	-4.8722
18	54.6814	38	-43.4868	58	43.0172	78	-9.8192	98	6.1931
E1	47.3283	39	-40.7793	E2	62.9151	79	-7.5493		
20	26.0500	40	-32.9057	E3	71.4193	80	-4.7783		

Minimum: -71.8687 Mean: 0.86631 Std. Dev.: 28.66952 Maximum: 71.4193

Parameter # 6 : trunk

				Y acceleration (METERS/s/s)					
1	-0.5025	21	-43.3663	41	10.4769	61	-2.6994	81	1.2317
2	0.3330	22	-34.6361	42	6.3336	62	3.0169	82	1.0242
3	1.0468	23	-18.5709	43	1.0981	63	6.6055	83	0.8182
4	1.6308	24	2.5615	44	-3.2715	64	8.7768	84	0.6356
5	2.6404	25	23.1589	45	-5.6583	65	10.0742	85	0.6017
6	4.3568	26	36.6261	46	-6.0267	66	10.7157	86	0.5519
7	6.5902	27	38.7838	47	-4.6786	67	11.1851	87	0.4721
8	9.5428	28	29.7616	48	-2.9510	68	11.2315	88	0.5068
9	12.5248	29	15.4708	49	-2.0076	69	10.9516	89	0.5023
10	14.8414	30	3.0480	50	-1.6600	70	10.5738	90	0.4096
11	16.6131	31	-4.0341	51	-2.2370	71	9.6768	91	0.1736
12	16.8338	32	-5.8558	52	-4.0615	72	8.5000	92	-0.1429
13	14.2153	33	-4.4538	53	-7.4563	73	7.2839	93	-0.4422
14	8.8598	34	-2.0183	54	-12.7373	74	5.9702	94	-1.0788
15	1.6835	35	0.2706	55	-18.8497	75	4.7971	95	-1.7489
16	-7.6285	36	2.4286	56	-24.0890	76	3.8356	96	-2.1947
17	-18.8141	37	5.0989	57	-26.2263	77	3.0136	97	-3.0277
18	-29.7519	38	7.9804	58	-23.8147	78	2.2577	98	4.1958
E1	-38.8634	39	10.2545	E2	-17.6946	79	1.6969		
20	-44.3119	40	11.6118	E3	-10.0055	80	1.4250		

Minimum: -44.3119 Mean: 0.22265 Std. Dev.: 13.92496 Maximum: 38.7838

Parameter # 6 : trunk

				Z acceleration (METERS/s/s)					
1	-28.0996	21	20.1814	41	-17.3935	61	-40.7586	81	4.9516
2	-25.0455	22	14.3475	42	-26.9896	62	-30.1732	82	1.5793
3	-21.5971	23	1.4566	43	-28.9198	63	-21.6191	83	-1.4056
4	-16.2729	24	-18.7868	44	-23.6374	64	-15.0102	84	-3.8519
5	-8.1690	25	-42.2385	45	-12.3598	65	-8.2785	85	-4.5940
6	2.2389	26	-63.5999	46	2.4552	66	-1.7853	86	-4.6924
7	13.5327	27	-76.5863	47	17.3449	67	3.8363	87	-5.1490
8	24.5295	28	-76.2357	48	30.3349	68	9.6162	88	-5.3602
9	34.1807	29	-63.2497	49	40.5880	69	15.4194	89	-5.3272
10	39.9447	30	-42.3834	50	47.3142	70	20.3383	90	-5.0725
11	40.9670	31	-20.2129	51	48.5419	71	24.1584	91	-4.7967

12	37.3795	32	-0.2801	52	43.2715	72	26.5640	92	-5.5281
13	30.2680	33	16.2372	53	31.7760	73	28.0657	93	-5.9643
14	22.1372	34	27.8902	54	13.5723	74	28.6218	94	-4.9787
15	14.7136	35	35.0953	55	-8.9058	75	27.4425	95	-4.6802
16	10.1540	36	37.4515	56	-30.5677	76	25.0702	96	-4.4454
17	9.2564	37	34.1036	57	-47.6273	77	22.1135	97	-2.2061
18	11.1836	38	25.0505	58	-56.6861	78	18.4993	98	-1.0506
E1	15.5631	39	11.5316	E2	-56.4754	79	14.0315		
20	20.0422	40	-3.3931	E3	-50.2195	80	9.2545		

Minimum: -76.5863 Mean: 0.52590 Std. Dev.: 28.14798 Maximum: 48.5419

Parameter # 6 : trunk R acceleration (METERS/s/s)

1	30.696	21	48.025	41	28.267	61	80.265	81	5.409
2	29.294	22	51.965	42	27.977	62	66.492	82	2.200
3	28.405	23	63.330	43	30.792	63	51.339	83	4.318
4	26.978	24	74.328	44	30.929	64	36.752	84	7.778
5	24.541	25	82.627	45	25.684	65	23.482	85	9.712
6	23.085	26	87.389	46	18.818	66	14.192	86	10.659
7	25.102	27	87.897	47	19.919	67	11.939	87	11.420
8	30.497	28	82.408	48	30.626	68	15.178	88	11.355
9	37.397	29	71.465	49	43.288	69	20.059	89	10.676
10	42.615	30	55.837	50	54.402	70	24.483	90	9.454
11	44.880	31	37.400	51	61.753	71	27.825	91	7.832
12	43.043	32	19.466	52	64.416	72	29.971	92	7.078
13	35.668	33	17.149	53	61.613	73	31.354	93	6.497
14	24.172	34	30.268	54	52.622	74	31.878	94	5.108
15	18.569	35	42.850	55	41.732	75	30.798	95	5.263
16	32.713	36	51.135	56	41.053	76	28.408	96	6.009
17	51.755	37	53.801	57	56.524	77	25.152	97	6.146
18	63.248	38	50.816	58	75.040	78	21.065	98	7.554
E1	63.187	39	43.601	E2	86.376	79	16.024		
20	55.171	40	35.059	E3	87.880	80	10.512		

Minimum: 2.200 Mean: 35.6039 Std. Dev.: 22.9900 Maximum: 87.897

Parameter # 7 : right thigh X acceleration (METERS/s/s)

1	11.4500	21	34.3052	41	-16.4674	61	33.0609	81	-11.9530
2	10.3578	22	18.3369	42	-15.5245	62	42.5039	82	-12.0066
3	9.4919	23	-0.1654	43	-12.0633	63	45.3718	83	-11.5479
4	8.3765	24	-16.1773	44	-6.6944	64	43.4296	84	-10.8580
5	5.6799	25	-25.6537	45	-1.0365	65	38.5572	85	-9.7846
6	1.8302	26	-25.6824	46	3.6861	66	33.2674	86	-8.0038
7	-4.0146	27	-16.4667	47	6.3915	67	29.0757	87	-5.6949
8	-13.1995	28	-1.7745	48	7.5740	68	25.9784	88	-3.5434
9	-23.7705	29	12.4457	49	7.9550	69	23.4495	89	-1.5291
10	-34.0486	30	20.9992	50	6.9231	70	20.5124	90	0.1209
11	-41.8232	31	22.3772	51	3.7083	71	16.2099	91	1.0045
12	-44.6507	32	17.4086	52	-2.9134	72	10.6484	92	1.2238
13	-40.9828	33	9.1354	53	-13.6070	73	5.1628	93	0.8731
14	-30.5641	34	1.0362	54	-27.1970	74	0.1807	94	0.1456
15	-15.0239	35	-5.2796	55	-39.6502	75	-4.4067	95	-1.0240
16	3.6037	36	-8.8916	56	-45.7110	76	-7.7669	96	-2.3595
17	22.0460	37	-10.4257	57	-41.6176	77	-9.6923	97	-3.1577
18	36.7449	38	-11.5037	58	-26.8911	78	-10.4283	98	3.5560
E1	44.6276	39	-13.2041	E2	-5.5299	79	-10.6703		
20	43.7111	40	-15.3562	E3	16.2465	80	-11.2821		

Minimum: -45.7110 Mean: -0.29071 Std. Dev.: 20.85828 Maximum: 45.3718

Parameter # 7 : right thigh Y acceleration (METERS/s/s)

1	2.9400	21	-14.6047	41	0.6747	61	-31.7909	81	-1.7007
---	--------	----	----------	----	--------	----	----------	----	---------

2	-0.1595	22	-15.1570	42	3.4687	62	-25.7647	82	-2.8015
3	-3.3280	23	-11.5782	43	4.1537	63	-19.1982	83	-3.2534
4	-6.7082	24	-2.8757	44	3.3944	64	-12.6047	84	-3.6762
5	-9.7125	25	9.5160	45	2.5410	65	-6.1436	85	-3.6030
6	-11.3270	26	21.8023	46	2.6607	66	0.0864	86	-3.2934
7	-11.4946	27	29.1232	47	4.3028	67	6.0507	87	-3.3402
8	-9.9290	28	28.2221	48	6.8174	68	11.1588	88	-3.1875
9	-6.9677	29	20.8088	49	9.3276	69	15.2287	89	-2.9944
10	-3.4339	30	11.6100	50	11.7254	70	18.3463	90	-3.0928
11	0.6515	31	4.6258	51	13.6187	71	20.0683	91	-3.3346
12	3.9831	32	1.0563	52	14.5479	72	20.2976	92	-3.4759
13	5.3058	33	-0.2033	53	13.8606	73	19.2154	93	-3.5022
14	4.9728	34	-0.8872	54	10.3672	74	17.1239	94	-3.5456
15	3.7101	35	-2.4829	55	2.7632	75	14.3798	95	-3.3582
16	1.3093	36	-5.0458	56	-8.8026	76	11.2100	96	-2.7897
17	-1.8276	37	-7.2162	57	-21.2037	77	7.8554	97	-2.2013
18	-4.7446	38	-7.9435	58	-30.8821	78	4.6908	98	1.7430
E1	-7.8863	39	-6.7200	E2	-35.8753	79	2.1111		
20	-11.5597	40	-3.3883	E3	-35.7823	80	0.0596		

Minimum: -35.8753 Mean: -0.25401 Std. Dev.: 12.27113 Maximum: 29.1232

Parameter # 7 : right thigh				Z acceleration (METERS/s/s)					
1	-20.57	21	32.90	41	29.26	61	-108.41	81	30.48
2	-12.68	22	33.20	42	7.65	62	-107.41	82	25.94
3	-4.57	23	28.27	43	-12.95	63	-99.71	83	20.98
4	4.53	24	17.18	44	-28.58	64	-86.78	84	17.43
5	15.40	25	-0.78	45	-35.90	65	-69.41	85	14.57
6	27.32	26	-24.25	46	-33.46	66	-48.72	86	10.76
7	36.71	27	-48.88	47	-22.39	67	-26.67	87	7.63
8	41.45	28	-68.72	48	-5.33	68	-4.81	88	4.69
9	41.17	29	-79.61	49	15.26	69	15.82	89	0.97
10	33.41	30	-80.23	50	37.07	70	33.17	90	-3.36
11	19.22	31	-71.65	51	56.81	71	46.66	91	-7.93
12	2.48	32	-56.26	52	71.65	72	55.70	92	-13.04
13	-13.49	33	-36.03	53	78.87	73	60.36	93	-18.05
14	-24.92	34	-13.55	54	74.85	74	61.75	94	-21.23
15	-28.71	35	9.04	55	57.13	75	59.96	95	-23.77
16	-24.03	36	29.73	56	27.17	76	56.18	96	-25.08
17	-13.08	37	45.38	57	-10.50	77	51.32	97	-24.64
18	1.13	38	53.51	58	-48.36	78	45.88	98	24.05
E1	15.63	39	53.62	E2	-79.00	79	40.27		
20	27.06	40	45.74	E3	-99.40	80	34.99		

Minimum: -108.41 Mean: 1.046 Std. Dev.: 44.020 Maximum: 78.87

Parameter # 7 : right thigh				R acceleration (METERS/s/s)					
1	23.7230	21	49.7272	41	33.5837	61	117.7132	81	32.7851
2	16.3763	22	40.8439	42	17.6500	62	118.3508	82	28.7249
3	11.0489	23	30.5488	43	18.1756	63	111.2148	83	24.1718
4	11.6486	24	23.7750	44	29.5525	64	97.8588	84	20.8621
5	19.0712	25	27.3731	45	36.0089	65	79.6354	85	17.9149
6	29.6293	26	41.5103	46	33.7722	66	58.9943	86	13.8078
7	38.6732	27	59.2358	47	23.6794	67	39.9161	87	10.0922
8	44.6203	28	74.3124	48	11.5001	68	28.6797	88	6.6891
9	48.0517	29	83.2165	49	19.5710	69	32.1268	89	3.5004
10	47.8266	30	83.7431	50	39.4936	70	43.1033	90	4.5659
11	46.0315	31	75.2040	51	58.5365	71	53.3155	91	8.6642
12	44.8965	32	58.9008	52	73.1690	72	60.2326	92	13.5469
13	43.4707	33	37.1734	53	81.2232	73	63.5512	93	18.4117
14	39.7461	34	13.6196	54	80.3080	74	64.0843	94	21.5241
15	32.6120	35	10.7586	55	69.5993	75	61.8201	95	24.0292

16	24.3350	36	31.4350	56	53.9006	76	57.8112	96	25.3442
17	25.6991	37	47.1145	57	47.8736	77	52.8169	97	24.9409
18	37.0671	38	55.3106	58	63.3659	78	47.2811	98	24.3692
E1	47.9378	39	55.6317	E2	86.9366	79	41.7155		
20	52.6930	40	48.3643	E3	106.8829	80	36.7603		

Minimum: 3.5004 Mean: 42.94556 Std. Dev.: 25.71657 Maximum: 118.3508

Parameter # 8 : left thigh X acceleration (METERS/s/s)

1	5.2775	21	26.7916	41	-16.3767	61	47.9354	81	-0.8896
2	4.5997	22	6.2855	42	-9.6509	62	44.1006	82	-0.2709
3	4.6251	23	-14.5155	43	-2.1972	63	36.4640	83	0.3807
4	5.4824	24	-30.6682	44	4.3596	64	27.1496	84	1.0283
5	5.3384	25	-38.4037	45	8.2772	65	17.5865	85	1.5790
6	3.8245	26	-35.6233	46	8.9543	66	9.2544	86	2.1990
7	1.1223	27	-23.5067	47	6.2633	67	3.0400	87	2.8375
8	-3.7326	28	-6.4716	48	1.6027	68	-1.1271	88	3.0631
9	-9.8609	29	8.6980	49	-3.5527	69	-3.8249	89	3.1602
10	-15.9021	30	17.1992	50	-9.4929	70	-5.3154	90	3.0278
11	-20.7428	31	18.0863	51	-16.0360	71	-6.1498	91	2.3581
12	-22.5397	32	12.4636	52	-22.5292	72	-6.7352	92	1.4131
13	-19.3219	33	3.7557	53	-28.0287	73	-6.7063	93	0.4168
14	-10.5522	34	-5.0547	54	-30.6927	74	-6.2595	94	-0.7838
15	2.6202	35	-12.5858	55	-27.6567	75	-5.7343	95	-2.2570
16	18.7992	36	-17.8424	56	-17.3364	76	-5.0995	96	-3.6403
17	34.8360	37	-20.9915	57	-1.0220	77	-4.2387	97	-4.6387
18	46.0162	38	-22.5078	58	18.0546	78	-2.9799	98	5.4086
E1	48.7461	39	-22.6067	E2	34.8527	79	-1.8554		
20	41.9481	40	-20.8885	E3	45.2355	80	-1.3120		

Minimum: -38.4037 Mean: 0.28376 Std. Dev.: 18.50787 Maximum: 48.7461

Parameter # 8 : left thigh Y acceleration (METERS/s/s)

1	-2.4949	21	-23.7944	41	4.8389	61	-9.9192	81	0.5930
2	-2.7301	22	-23.1525	42	4.9372	62	-6.7104	82	-0.9655
3	-3.1069	23	-17.5140	43	3.3718	63	-4.8065	83	-2.0586
4	-3.7662	24	-6.4531	44	1.2735	64	-3.6910	84	-2.8495
5	-3.9837	25	7.6911	45	-0.3862	65	-2.8479	85	-3.0964
6	-3.1087	26	20.5159	46	-0.9383	66	-1.8424	86	-2.9281
7	-1.4973	27	27.3996	47	-0.0145	67	-0.3898	87	-2.8726
8	1.1253	28	25.7519	48	1.3928	68	1.2539	88	-2.5976
9	4.3178	29	17.6349	49	2.3859	69	3.2811	89	-2.0687
10	7.1949	30	8.2087	50	3.0958	70	5.6010	90	-1.7957
11	9.8855	31	1.7855	51	3.4588	71	7.6719	91	-1.7602
12	11.6072	32	-1.1099	52	3.1203	72	9.4049	92	-1.6542
13	11.3785	33	-1.7745	53	1.5165	73	10.4720	93	-1.6510
14	9.3096	34	-1.2941	54	-1.5473	74	10.8498	94	-1.8487
15	6.1240	35	-1.2567	55	-6.2778	75	10.7305	95	-1.6721
16	1.6400	36	-2.1096	56	-12.2152	76	9.8284	96	-1.3020
17	-4.1036	37	-2.4035	57	-16.8624	77	8.3065	97	-1.4529
18	-9.8313	38	-1.5621	58	-18.5475	78	6.5048	98	1.9475
E1	-15.3368	39	0.0982	E2	-17.3013	79	4.5359		
20	-20.5811	40	2.7204	E3	-13.9093	80	2.5175		

Minimum: -23.7944 Mean: -0.06599 Std. Dev.: 8.85360 Maximum: 27.3996

Parameter # 8 : left thigh Z acceleration (METERS/s/s)

1	-18.0164	21	30.4323	41	9.7249	61	-55.5502	81	16.7621
2	-13.1198	22	29.3335	42	-6.4940	62	-46.3460	82	13.8177
3	-8.6778	23	23.1473	43	-19.1850	63	-35.8461	83	10.3636
4	-4.4781	24	10.6692	44	-25.9959	64	-24.8934	84	7.4494
5	1.1895	25	-8.1310	45	-25.3242	65	-14.1833	85	5.2204

6	8.9613	26	-30.3167	46	-17.8688	66	-3.9421	86	2.8022
7	15.9293	27	-51.1169	47	-5.8182	67	5.0305	87	1.2765
8	20.3998	28	-65.4668	48	8.4428	68	12.4826	88	0.5257
9	22.2938	29	-70.0099	49	22.7233	69	18.3314	89	-0.8504
10	19.4820	30	-64.5203	50	35.4377	70	21.9028	90	-2.5072
11	12.8651	31	-52.4041	51	44.6375	71	23.8230	91	-3.8561
12	4.1654	32	-36.4515	52	48.0666	72	24.3462	92	-5.8915
13	-4.8383	33	-17.9602	53	44.5183	73	24.4999	93	-8.2684
14	-11.0759	34	0.3541	54	33.3286	74	24.8725	94	-9.5705
15	-13.0402	35	17.3098	55	14.3452	75	24.4287	95	-10.9387
16	-10.0039	36	30.8829	56	-8.8842	76	24.0039	96	-11.9245
17	-2.8470	37	38.7133	57	-31.8958	77	23.7432	97	-10.9894
18	6.7706	38	40.2428	58	-50.0621	78	22.8114	98	9.1610
E1	17.4463	39	35.2734	E2	-59.6359	79	21.2480		
20	26.3603	40	24.7800	E3	-60.9343	80	19.2187		

Minimum: -70.0099 Mean: 0.16548 Std. Dev.: 27.15696 Maximum: 48.0666

Parameter # 8 : left thigh R acceleration (METERS/s/s)

1	18.939	21	47.012	41	19.652	61	74.041	81	16.796
2	14.168	22	37.895	42	12.637	62	64.326	82	13.854
3	10.313	23	32.454	43	19.603	63	51.358	83	10.573
4	8.018	24	33.106	44	26.390	64	37.019	84	8.042
5	6.766	25	40.001	45	26.645	65	22.772	85	6.272
6	10.227	26	51.079	46	20.009	66	10.226	86	4.611
7	16.039	27	62.580	47	8.549	67	5.891	87	4.235
8	20.769	28	70.647	48	8.706	68	12.596	88	4.050
9	24.757	29	72.719	49	23.123	69	19.011	89	3.872
10	26.157	30	67.276	50	36.817	70	23.224	90	4.322
11	26.334	31	55.466	51	47.557	71	25.772	91	4.851
12	25.693	32	38.539	52	53.176	72	26.955	92	6.280
13	22.939	33	18.434	53	52.629	73	27.475	93	8.442
14	17.908	34	5.230	54	45.335	74	27.848	94	9.779
15	14.643	35	21.438	55	31.782	75	27.291	95	11.294
16	21.358	36	35.729	56	22.993	76	26.435	96	12.536
17	35.192	37	44.104	57	36.093	77	25.509	97	12.017
18	47.539	38	46.136	58	56.358	78	23.907	98	10.815
E1	53.998	39	41.896	E2	71.207	79	21.806		
20	53.648	40	32.524	E3	77.154	80	19.427		

Minimum: 3.872 Mean: 28.0777 Std. Dev.: 19.0279 Maximum: 77.154

Parameter # 9 : right shank X acceleration (METERS/s/s)

1	-1.8642	21	29.2589	41	-5.5487	61	15.3944	81	3.7490
2	-0.7489	22	23.9661	42	-8.9968	62	12.7562	82	4.2172
3	0.3917	23	13.7337	43	-11.1036	63	9.0672	83	4.8297
4	1.4512	24	-0.7855	44	-11.2757	64	4.8943	84	5.5053
5	1.8491	25	-16.6693	45	-10.4765	65	0.6991	85	6.1799
6	1.2568	26	-29.3715	46	-9.9050	66	-3.3981	86	6.9674
7	0.2424	27	-34.9646	47	-10.4563	67	-6.8213	87	7.5086
8	-1.2252	28	-32.2493	48	-11.6620	68	-8.9481	88	7.5738
9	-2.6903	29	-23.8717	49	-11.8544	69	-10.3157	89	7.2862
10	-2.8315	30	-14.5142	50	-10.3747	70	-10.7094	90	6.3616
11	-1.2416	31	-8.1104	51	-6.7787	71	-10.0129	91	5.0333
12	2.3329	32	-6.1798	52	-1.2321	72	-8.8052	92	3.5847
13	7.7964	33	-7.6145	53	4.8761	73	-6.9541	93	1.6460
14	14.2172	34	-10.0044	54	10.0588	74	-4.8337	94	-0.5722
15	20.0033	35	-11.0553	55	13.7313	75	-2.7614	95	-2.4053
16	24.3479	36	-9.6109	56	15.8985	76	-0.8527	96	-4.1109
17	27.4007	37	-6.2111	57	16.8515	77	0.7695	97	-5.9884
18	29.0968	38	-2.6351	58	17.3136	78	2.1728	98	7.8771

E1 30.0160 39 -1.0237 E2 17.3164 79 3.1142  
 20 30.5640 40 -2.3258 E3 16.7565 80 3.4931  
 Minimum: -34.9646 Mean: 0.78016 Std. Dev.: 12.65294 Maximum: 30.5640

Parameter # 9 : right shank Y acceleration (METERS/s/s)  
 1 -5.2835 21 -23.6696 41 -0.9173 61 -4.0935 81 2.0854  
 2 -3.9062 22 -26.9264 42 2.7755 62 -0.9983 82 1.4174  
 3 -2.8375 23 -27.3511 43 4.6054 63 1.3547 83 0.8120  
 4 -2.0706 24 -22.4015 44 4.5409 64 2.7869 84 0.2824  
 5 -0.9084 25 -11.1928 45 3.1495 65 3.7145 85 -0.2162  
 6 0.8774 26 4.0684 46 1.6713 66 3.9460 86 -0.7376  
 7 2.9882 27 18.6920 47 0.8844 67 3.6986 87 -1.1885  
 8 5.4931 28 27.1924 48 0.4148 68 3.2073 88 -1.2472  
 9 8.0581 29 27.5358 49 -0.4818 69 2.6339 89 -1.2596  
 10 10.1617 30 22.4538 50 -1.9350 70 2.2196 90 -1.3128  
 11 11.9806 31 16.3403 51 -3.7768 71 1.6501 91 -1.1825  
 12 13.0900 32 11.5378 52 -5.3617 72 1.2635 92 -0.9766  
 13 12.5839 33 8.1696 53 -6.2544 73 1.2933 93 -0.6332  
 14 10.6045 34 5.6076 54 -6.8224 74 1.3421 94 -0.4547  
 15 7.5657 35 2.6223 55 -7.4777 75 1.4611 95 -0.2943  
 16 2.7856 36 -1.5647 56 -8.5243 76 1.8477 96 0.0984  
 17 -3.1115 37 -5.6194 57 -9.6040 77 2.2539 97 0.0661  
 18 -8.7444 38 -8.0005 58 -10.0867 78 2.3150 98 0.3729  
 E1 -14.1127 39 -8.2328 E2 -9.3129 79 2.2974  
 20 -19.1891 40 -5.4776 E3 -7.0875 80 2.3718  
 Minimum: -27.3511 Mean: 0.02454 Std. Dev.: 9.13723 Maximum: 27.5358

Parameter # 9 : right shank Z acceleration (METERS/s/s)  
 1 -8.8246 21 46.8973 41 42.1715 61 -28.7838 81 6.5619  
 2 -6.3960 22 55.9626 42 24.9856 62 -30.7019 82 5.5715  
 3 -4.3027 23 59.0823 43 4.4404 63 -28.8556 83 3.3971  
 4 -2.3569 24 55.9102 44 -15.5450 64 -24.2607 84 1.3156  
 5 0.5705 25 44.9722 45 -30.5427 65 -16.8960 85 -0.2121  
 6 4.6252 26 25.5887 46 -37.9244 66 -8.2325 86 -2.2182  
 7 7.2036 27 -0.8888 47 -38.1792 67 -0.1991 87 -4.1534  
 8 7.1081 28 -29.7806 48 -31.4531 68 6.3545 88 -5.1608  
 9 5.1350 29 -54.2210 49 -19.0227 69 11.1479 89 -5.6112  
 10 -0.0184 30 -69.7014 50 -4.2061 70 13.4388 90 -5.5170  
 11 -7.9514 31 -75.1445 51 11.0587 71 13.0395 91 -5.1554  
 12 -17.1453 32 -69.8780 52 25.7550 72 10.9716 92 -5.2962  
 13 -26.3602 33 -55.7670 53 37.3878 73 8.7502 93 -5.1208  
 14 -33.4603 34 -36.6802 54 43.4630 74 7.4525 94 -3.8935  
 15 -36.1512 35 -13.9032 55 43.2502 75 6.1557 95 -3.0668  
 16 -31.9843 36 9.6267 56 36.1460 76 5.2849 96 -2.8221  
 17 -21.5091 37 29.5814 57 23.2798 77 5.5237 97 -2.3172  
 18 -5.9088 38 43.9927 58 7.4384 78 5.8652 98 1.7112  
 E1 13.5506 39 51.7600 E2 -8.5071 79 6.2939  
 20 32.3150 40 51.6413 E3 -21.3317 80 6.6514  
 Minimum: -75.1445 Mean: -0.33810 Std. Dev.: 27.68215 Maximum: 59.0823

Parameter # 9 : right shank R acceleration (METERS/s/s)  
 1 10.453 21 60.131 41 42.545 61 32.898 81 7.840  
 2 7.532 22 66.567 42 26.701 62 33.261 82 7.130  
 3 5.169 23 66.539 43 12.815 63 30.277 83 5.960  
 4 3.457 24 60.236 44 19.733 64 24.906 84 5.667  
 5 2.138 25 49.251 45 32.443 65 17.314 85 6.187  
 6 4.873 26 39.167 46 39.232 66 9.741 86 7.349  
 7 7.803 27 39.657 47 39.595 67 7.762 87 8.663  
 8 9.066 28 51.636 48 33.548 68 11.434 88 9.249  
 9 9.927 29 65.330 49 22.419 69 15.415 89 9.282

10 10.549	30 74.653	50 11.361	70 17.327	90 8.522
11 14.433	31 77.327	51 13.510	71 16.523	91 7.301
12 21.697	32 71.093	52 26.336	72 14.125	92 6.469
13 30.232	33 56.874	53 38.220	73 11.252	93 5.416
14 37.870	34 38.431	54 45.130	74 8.984	94 3.961
15 42.003	35 17.955	55 45.990	75 6.903	95 3.909
16 40.294	36 13.693	56 40.398	76 5.663	96 4.987
17 34.973	37 30.744	57 30.301	77 6.015	97 6.421
18 30.952	38 44.792	58 21.374	78 6.669	98 8.069
E1 35.829	39 52.421	E2 21.423	79 7.388	
20 48.442	40 51.983	E3 28.037	80 7.878	

Minimum: 2.138 Mean: 24.9123 Std. Dev.: 19.5857 Maximum: 77.327

Parameter # 10 : left shank X acceleration (METERS/s/s)

1 -2.6273	21 23.4435	41 -2.2356	61 5.4721	81 5.9328
2 -1.4832	22 21.2099	42 -4.1243	62 4.7219	82 6.8968
3 -0.2523	23 14.0315	43 -5.0633	63 3.3181	83 7.7372
4 0.8924	24 2.6323	44 -4.9278	64 1.6088	84 8.3488
5 1.4887	25 -10.4745	45 -4.4646	65 -0.2849	85 8.9060
6 1.5768	26 -21.3585	46 -4.4028	66 -2.1643	86 9.1597
7 1.6539	27 -26.6747	47 -5.4347	67 -3.6753	87 9.0650
8 1.9191	28 -25.4273	48 -6.8948	68 -4.7530	88 8.7022
9 2.9377	29 -19.7235	49 -7.5306	69 -5.4648	89 7.9034
10 5.2300	30 -13.2456	50 -7.2208	70 -5.4462	90 6.6859
11 8.4374	31 -8.7471	51 -5.4872	71 -4.9425	91 5.2205
12 12.2875	32 -7.6094	52 -2.3090	72 -4.2739	92 3.4726
13 16.1703	33 -8.8848	53 0.9719	73 -3.0806	93 1.3200
14 19.1243	34 -10.4388	54 3.5168	74 -1.8194	94 -1.0888
15 20.4285	35 -10.8558	55 4.8739	75 -0.7092	95 -3.2546
16 20.0671	36 -9.2519	56 4.9879	76 0.4701	96 -5.2847
17 19.1461	37 -5.9451	57 4.7668	77 1.7995	97 -7.4411
18 18.9165	38 -2.5980	58 4.8655	78 3.1502	98 9.6079
E1 20.1005	39 -0.6539	E2 5.2671	79 4.2837	
20 22.2314	40 -0.6640	E3 5.5799	80 5.1629	

Minimum: -26.6747 Mean: 1.19395 Std. Dev.: 9.69610 Maximum: 23.4435

Parameter # 10 : left shank Y acceleration (METERS/s/s)

1 -2.9269	21 -15.7717	41 -0.8844	61 -1.7468	81 0.3387
2 -1.7810	22 -19.1373	42 1.9428	62 0.7654	82 0.1104
3 -1.0278	23 -20.7028	43 3.1359	63 2.4778	83 -0.0526
4 -0.9053	24 -17.7363	44 2.7952	64 3.2951	84 -0.1866
5 -0.7134	25 -9.3558	45 1.3872	65 3.4878	85 -0.3049
6 -0.1069	26 2.7754	46 0.0216	66 3.0249	86 -0.3149
7 0.6247	27 14.9763	47 -0.5986	67 2.3859	87 -0.4035
8 1.7096	28 22.4675	48 -0.6723	68 1.4498	88 -0.2985
9 2.8150	29 23.0332	49 -0.7899	69 0.4877	89 -0.1321
10 3.7048	30 18.8188	50 -1.2090	70 -0.0701	90 -0.1235
11 4.9191	31 13.6079	51 -1.7314	71 -0.6487	91 -0.0881
12 5.9383	32 9.5384	52 -1.9402	72 -0.9790	92 0.0044
13 6.1035	33 6.6017	53 -1.6672	73 -0.8585	93 0.2107
14 5.5212	34 4.1101	54 -1.3575	74 -0.7998	94 0.1409
15 4.2169	35 1.3216	55 -1.6868	75 -0.6937	95 0.0408
16 1.6120	36 -2.1922	56 -2.9643	76 -0.2870	96 0.1911
17 -2.0154	37 -5.3874	57 -4.6191	77 0.0516	97 -0.1598
18 -5.4077	38 -7.0834	58 -5.7312	78 0.1600	98 0.9670
E1 -8.6140	39 -6.9954	E2 -5.5501	79 0.2160	
20 -12.1553	40 -4.5987	E3 -4.0463	80 0.3315	

Minimum: -20.7028 Mean: -0.04464 Std. Dev.: 6.58643 Maximum: 23.0332

Parameter # 10 : left shank

Z acceleration (METERS/s/s)			
1	-5.5921	21	45.4612
2	-3.0005	22	54.4346
3	-1.0701	23	58.3574
4	0.1611	24	56.1454
5	1.6619	25	45.8021
6	3.0411	26	27.3176
7	2.8842	27	2.6447
8	0.9217	28	-24.1603
9	-2.1489	29	-46.7672
10	-6.9698	30	-60.7534
11	-13.1564	31	-64.9860
12	-19.1587	32	-59.0854
13	-24.6048	33	-45.2226
14	-28.5760	34	-27.3441
15	-29.5566	35	-6.6191
16	-25.5875	36	13.8171
17	-16.1875	37	29.8843
18	-2.3547	38	40.5767
E1	14.9304	39	45.3382
20	32.0070	40	43.0741
41	32.5841	61	-27.2779
42	16.3139	62	-27.0644
43	-1.4877	63	-23.9547
44	-18.1806	64	-19.8197
45	-29.5828	65	-14.0576
46	-33.6021	66	-7.7293
47	-31.3976	67	-2.6656
48	-23.3790	68	1.2234
49	-10.9082	69	4.0782
50	3.2686	70	5.0482
51	17.1358	71	4.3674
52	29.7106	72	3.0240
53	38.6938	73	1.8163
54	42.0636	74	1.1760
55	39.5099	75	0.8568
56	30.1268	76	1.0309
57	16.0030	77	1.5674
58	0.8963	78	2.1024
E2	-12.6052	79	2.4690
E3	-22.3605	80	2.9229
81	3.0042		
82	2.2879		
83	1.2622		
84	0.0582		
85	-0.7652		
86	-1.7048		
87	-2.7983		
88	-3.0394		
89	-3.1145		
90	-3.1889		
91	-3.0954		
92	-3.3406		
93	-3.2570		
94	-2.3116		
95	-1.6832		
96	-1.0989		
97	0.8623		
98	-3.6050		

Minimum: -64.9860 Mean: -0.28625 Std. Dev.: 24.72084 Maximum: 58.3574

Parameter # 10 : left shank

R acceleration (METERS/s/s)			
1	6.837	21	53.526
2	3.791	22	61.475
3	1.505	23	63.491
4	1.281	24	58.939
5	2.342	25	47.907
6	3.427	26	34.787
7	3.383	27	30.705
8	2.730	28	41.654
9	4.601	29	55.738
10	9.469	30	64.966
11	16.385	31	66.969
12	23.522	32	60.332
13	30.069	33	46.558
14	34.825	34	29.556
15	36.176	35	12.783
16	32.558	36	16.773
17	25.153	37	30.943
18	19.815	38	41.272
E1	26.479	39	45.879
20	40.822	40	43.324
41	32.673	61	27.876
42	16.939	62	27.484
43	6.139	63	24.310
44	19.043	64	20.156
45	29.950	65	14.487
46	33.889	66	8.578
47	31.870	67	5.129
48	24.384	68	5.118
49	13.279	69	6.836
50	8.018	70	7.426
51	18.076	71	6.627
52	29.863	72	5.326
53	38.742	73	3.678
54	42.232	74	2.309
55	39.845	75	1.311
56	30.680	76	1.169
57	17.325	77	2.387
58	7.571	78	3.791
59	14.746	79	4.949
E3	23.399	80	5.942
81	6.659		
82	7.267		
83	7.840		
84	8.351		
85	8.944		
86	9.322		
87	9.496		
88	9.223		
89	8.496		
90	7.408		
91	6.070		
92	4.819		
93	3.521		
94	2.559		
95	3.664		
96	5.401		
97	7.493		
98	10.307		

Minimum: 1.169 Mean: 20.6443 Std. Dev.: 17.8735 Maximum: 66.969

Parameter # 11 : right foot

X acceleration (METERS/s/s)			
1	-4.4868	21	15.9373
2	-2.9577	22	12.8925
3	-1.7356	23	10.0121
4	-1.0680	24	6.9465
5	-0.8426	25	3.8944
6	-0.8492	26	0.9653
7	-0.8889	27	-1.8942
8	-0.6750	28	-4.5389
9	0.1936	29	-7.0020
10	1.7053	30	-9.2244
11	3.9206	31	-11.2788
12	6.8069	32	-13.3149
41	0.5782	61	0.9672
42	3.9560	62	-0.9295
43	6.1990	63	-2.7059
44	6.9700	64	-4.0041
45	6.2340	65	-5.0379
46	4.4557	66	-5.7665
47	1.8983	67	-5.8137
48	-1.2177	68	-5.3197
49	-4.0279	69	-4.8491
50	-6.1199	70	-4.1382
51	-7.1596	71	-3.0478
52	-6.8278	72	-1.8919
81	7.4400		
82	8.4796		
83	9.3946		
84	10.0126		
85	10.4549		
86	10.6042		
87	10.3175		
88	9.6375		
89	8.6398		
90	7.1647		
91	5.1134		
92	2.8348		

13	9.9778	33	-15.0057	53	-5.5725	73	-0.8129	93	0.3998
14	13.3090	34	-16.1253	54	-3.7140	74	0.0954	94	-2.1805
15	16.5330	35	-16.4195	55	-1.5720	75	1.0798	95	-4.6394
16	19.1545	36	-15.7012	56	0.2762	76	2.1275	96	-6.7870
17	20.9008	37	-13.9927	57	1.6873	77	3.0340	97	-8.6625
18	21.4405	38	-11.1359	58	2.7300	78	4.0113	98	10.4628
E1	20.6560	39	-7.3960	E2	2.9231	79	5.1917		
20	18.7722	40	-3.3623	E3	2.2552	80	6.3877		

Minimum: -16.4195 Mean: 1.17692 Std. Dev.: 8.39391 Maximum: 21.4405

Parameter # 11 : right foot Y acceleration (METERS/s/s)

1	-1.278	21	-6.504	41	2.864	61	-1.401	81	-1.106
2	-0.973	22	-8.424	42	3.555	62	-0.947	82	-1.420
3	-0.961	23	-9.704	43	3.048	63	-0.807	83	-1.466
4	-1.353	24	-9.305	44	1.552	64	-0.924	84	-1.263
5	-1.560	25	-6.427	45	-0.400	65	-1.264	85	-1.014
6	-1.423	26	-1.263	46	-1.951	66	-1.515	86	-0.755
7	-1.234	27	4.809	47	-2.804	67	-1.447	87	-0.433
8	-0.736	28	9.332	48	-3.059	68	-1.344	88	-0.010
9	-0.002	29	10.733	49	-2.747	69	-0.921	89	0.371
10	0.612	30	9.449	50	-1.980	70	-0.236	90	0.640
11	1.338	31	6.973	51	-0.908	71	0.384	91	0.714
12	2.182	32	4.453	52	0.638	72	0.945	92	0.747
13	2.684	33	2.209	53	2.312	73	1.324	93	0.878
14	2.714	34	0.340	54	3.502	74	1.510	94	0.728
15	2.443	35	-1.148	55	3.680	75	1.487	95	0.516
16	1.682	36	-2.363	56	2.520	76	1.298	96	0.430
17	0.292	37	-2.856	57	0.694	77	0.903	97	0.115
18	-1.357	38	-2.297	58	-1.052	78	0.245	98	0.361
E1	-2.871	39	-0.983	E2	-2.011	79	-0.411		
20	-4.514	40	0.995	E3	-1.918	80	-0.805		

Minimum: -9.704 Mean: -0.0679 Std. Dev.: 3.1604 Maximum: 10.733

Parameter # 11 : right foot Z acceleration (METERS/s/s)

1	-1.7647	21	15.6068	41	8.7377	61	-22.6304	81	0.1287
2	-0.5541	22	21.6626	42	-0.5216	62	-19.8248	82	-0.1484
3	0.5549	23	26.0429	43	-9.4982	63	-15.8773	83	-0.5367
4	1.3761	24	27.9619	44	-16.4862	64	-11.4337	84	-0.8770
5	1.9025	25	26.3805	45	-19.4870	65	-6.5217	85	-1.1742
6	2.4120	26	20.3120	46	-18.7030	66	-2.2726	86	-1.4396
7	2.0742	27	10.1837	47	-14.3091	67	0.8148	87	-1.3406
8	0.3602	28	-2.0145	48	-7.1463	68	2.8294	88	-1.1434
9	-2.0067	29	-13.1193	49	1.2012	69	3.7504	89	-0.8377
10	-5.1646	30	-20.4625	50	10.3166	70	3.6031	90	-0.4406
11	-8.6030	31	-23.1519	51	18.9879	71	2.4546	91	-0.0732
12	-11.6651	32	-21.1456	52	25.7933	72	0.7818	92	0.1187
13	-14.0916	33	-15.6534	53	29.4079	73	-0.3544	93	0.1505
14	-15.4221	34	-8.0836	54	28.7980	74	-0.8051	94	0.4292
15	-15.4816	35	0.7813	55	23.4864	75	-1.2110	95	0.5752
16	-13.9748	36	9.3958	56	13.9211	76	-1.2776	96	0.7329
17	-10.7674	37	15.8001	57	2.3739	77	-0.8874	97	0.9175
18	-5.6428	38	19.0480	58	-8.9273	78	-0.2373	98	-0.8629
E1	1.0795	39	19.3881	E2	-17.7508	79	0.2494		
20	8.4864	40	16.1518	E3	-22.3413	80	0.3057		

Minimum: -23.1519 Mean: -0.08490 Std. Dev.: 12.54048 Maximum: 29.4079

Parameter # 11 : right foot R acceleration (METERS/s/s)

1	4.988	21	23.235	41	9.213	61	22.694	81	7.523
2	3.163	22	26.579	42	5.344	62	19.869	82	8.599
3	2.060	23	29.541	43	11.745	63	16.126	83	9.523

4	2.206	24	30.277	44	17.966	64	12.150	84	10.130
5	2.601	25	27.430	45	20.464	65	8.337	85	10.569
6	2.926	26	20.374	46	19.325	66	6.381	86	10.728
7	2.572	27	11.420	47	14.704	67	6.046	87	10.413
8	1.062	28	10.571	48	7.868	68	6.173	88	9.705
9	2.016	29	18.339	49	5.021	69	6.199	89	8.688
10	5.473	30	24.353	50	12.158	70	5.492	90	7.207
11	9.548	31	26.680	51	20.313	71	3.932	91	5.164
12	13.681	32	25.382	52	26.689	72	2.255	92	2.934
13	17.474	33	21.796	53	30.020	73	1.594	93	0.977
14	20.551	34	18.041	54	29.247	74	1.714	94	2.338
15	22.781	35	16.478	55	23.825	75	2.201	95	4.703
16	23.770	36	18.450	56	14.150	76	2.801	96	6.840
17	23.513	37	21.298	57	2.994	77	3.287	97	8.712
18	22.212	38	22.183	58	9.394	78	4.026	98	10.504
E1	20.882	39	20.774	E2	18.102	79	5.214		
20	21.090	40	16.528	E3	22.537	80	6.446		

Minimum: 0.977 Mean: 12.7916 Std. Dev.: 8.5912 Maximum: 30.277

Parameter # 12 : left foot

X acceleration (METERS/s/s)			
1	3.0659	21	21.2782
2	3.3513	22	5.5641
3	3.8268	23	-10.3239
4	4.5138	24	-24.5482
5	4.5206	25	-34.7512
6	3.0745	26	-38.5460
7	0.7159	27	-34.7142
8	-2.3997	28	-24.4216
9	-5.8419	29	-12.2480
10	-8.1788	30	-2.7374
11	-8.6141	31	1.5248
12	-5.7901	32	0.1426
13	1.4277	33	-4.7420
14	12.2818	34	-10.7763
15	24.7896	35	-15.9825
16	36.9175	36	-18.6606
17	46.0285	37	-18.6453
18	48.8821	38	-16.8521
E1	44.6004	39	-14.6740
20	34.8198	40	-13.0057
41	-11.1113	61	31.7614
42	-8.7961	62	26.5768
43	-6.2631	63	20.1919
44	-3.7389	64	13.2243
45	-2.3837	65	6.1396
46	-2.9270	66	-0.1437
47	-5.9712	67	-5.0182
48	-10.5697	68	-8.2330
49	-14.7339	69	-10.1401
50	-17.6657	70	-10.7220
51	-18.4872	71	-10.0566
52	-16.6127	72	-8.9241
53	-12.0664	73	-7.4128
54	-5.4095	74	-5.5678
55	2.9411	75	-3.6124
56	12.3631	76	-1.6954
57	21.3533	77	-0.0354
58	28.7489	78	1.5211
E2	33.1785	79	2.7843
E3	34.1486	80	3.4816

Minimum: -38.5460 Mean: 0.64139 Std. Dev.: 16.55888 Maximum: 48.8821

Parameter # 12 : left foot

Y acceleration (METERS/s/s)			
1	-4.6786	21	-32.3133
2	-3.6184	22	-32.8882
3	-2.9273	23	-28.6580
4	-2.5956	24	-18.7743
5	-1.5945	25	-4.4245
6	0.3610	26	11.2474
7	2.8860	27	23.3002
8	6.2683	28	27.5935
9	9.9525	29	24.4076
10	13.1264	30	17.5451
11	15.8280	31	11.2897
12	17.5145	32	7.3147
13	17.1449	33	5.3303
14	14.6044	34	4.5024
15	10.5168	35	3.2849
16	4.2301	36	1.0325
41	2.3999	61	-6.8717
42	3.6430	62	-2.8051
43	3.3615	63	0.3128
44	2.0883	64	2.6621
45	0.4121	65	4.4555
46	-0.8571	66	5.6720
47	-0.8724	67	6.5608
48	-0.5628	68	7.0031
49	-0.9837	69	7.1982
50	-2.0162	70	7.2578
51	-3.7505	71	6.9042
52	-5.9212	72	6.4423
53	-8.3323	73	5.8400
54	-10.8871	74	5.0864
55	-13.4201	75	4.5157
56	-15.8313	76	3.9973
81	1.4273		
82	0.9637		
83	0.6579		
84	0.4554		
85	0.4235		
86	0.3572		
87	0.2478		
88	0.3363		
89	0.4172		
90	0.3226		
91	0.1229		
92	-0.0522		
93	-0.2502		
94	-0.6722		
95	-0.9246		
96	-0.9991		

17	-4.1281	37	-1.0431	57	-17.2623	77	3.3894	97	-1.5411
18	-12.8158	38	-2.1616	58	-16.9760	78	2.6963	98	2.4230
E1	-21.0403	39	-2.1444	E2	-14.7972	79	2.1735		
20	-28.0215	40	-0.1896	E3	-11.1487	80	1.8685		

Minimum: -32.8882 Mean: 0.11862 Std. Dev.: 10.67584 Maximum: 27.5935

Parameter # 12 : left foot Z acceleration (METERS/s/s)

1	-12.5028	21	30.9318	41	27.8167	61	-26.5085	81	6.6780
2	-9.5816	22	36.9226	42	14.9517	62	-28.2316	82	4.3671
3	-6.6995	23	37.4095	43	0.6051	63	-27.6376	83	1.6242
4	-3.6659	24	31.5574	44	-12.1226	64	-24.9934	84	-0.8682
5	0.4938	25	19.2768	45	-20.6421	65	-19.8073	85	-2.6818
6	6.5381	26	1.5161	46	-24.1013	66	-12.9030	86	-4.3467
7	11.9026	27	-19.1710	47	-22.8774	67	-5.6688	87	-5.5195
8	14.9537	28	-38.1438	48	-17.2036	68	1.5480	88	-6.0120
9	15.9914	29	-51.1294	49	-8.1897	69	7.9853	89	-6.3233
10	13.2148	30	-56.5741	50	2.5191	70	12.6492	90	-5.8985
11	7.2007	31	-55.6943	51	13.5836	71	15.5070	91	-5.0068
12	-1.0993	32	-48.7885	52	23.5112	72	16.6929	92	-4.7126
13	-10.4733	33	-36.8701	53	30.7558	73	17.0576	93	-4.2857
14	-18.1386	34	-22.3330	54	33.4822	74	17.1148	94	-3.0152
15	-22.8164	35	-5.6802	55	30.8106	75	16.1648	95	-2.1842
16	-22.9451	36	10.8224	56	23.4415	76	14.9611	96	-1.8590
17	-17.9463	37	24.2794	57	12.4226	77	13.9810	97	-0.7632
18	-8.2702	38	33.5674	58	-0.1662	78	12.5053	98	-0.8512
E1	5.3915	39	37.5033	E2	-11.9116	79	10.7572		
20	19.8403	40	35.7135	E3	-21.1328	80	8.8154		

Minimum: -56.5741 Mean: -0.20013 Std. Dev.: 20.89629 Maximum: 37.5033

Parameter # 12 : left foot R acceleration (METERS/s/s)

1	13.697	21	49.535	41	30.050	61	41.937	81	7.969
2	10.776	22	49.758	42	17.726	62	38.874	82	6.555
3	8.252	23	48.242	43	7.134	63	34.229	83	5.610
4	6.368	24	44.170	44	12.857	64	28.401	84	6.040
5	4.819	25	39.985	45	20.783	65	21.210	85	7.050
6	7.234	26	40.182	46	24.293	66	14.095	86	8.139
7	12.268	27	45.995	47	23.660	67	10.018	87	8.934
8	16.391	28	53.036	48	20.199	68	10.919	88	9.046
9	19.721	29	57.965	49	16.886	69	14.778	89	8.850
10	20.343	30	59.295	50	17.958	70	18.101	90	7.848
11	19.406	31	56.847	51	23.246	71	19.730	91	6.218
12	18.479	32	49.334	52	29.391	72	19.995	92	5.199
13	20.141	33	37.554	53	34.073	73	19.494	93	4.339
14	26.328	34	25.202	54	35.621	74	18.703	94	3.330
15	35.295	35	17.277	55	33.735	75	17.168	95	3.784
16	43.672	36	21.596	56	30.870	76	15.578	96	4.955
17	49.576	37	30.630	57	30.138	77	14.386	97	6.209
18	51.206	38	37.622	58	33.387	78	12.883	98	7.759
E1	49.608	39	40.329	E2	38.232	79	11.322		
20	48.901	40	38.008	E3	41.677	80	9.660		

Minimum: 3.330 Mean: 24.0436 Std. Dev.: 15.5319 Maximum: 59.295

Trial Name: JAN1.3AA

subject 2a  
 March 1993  
 take off  
 toe touchdown  
 heel touchdown

Project: skater2  
 Spatial Model: skater2

Time Between Pictures: 0.017 s

	EVENTS
1 take off	19
2 toe touchdown	59
3 heel touchdown	60

Parameter # 1 : RIGHT FOREARM angular acceleration (degrees/s/s)

1	-4805.9	21	-1281.9	41	-724.3	61	-5743.8	81	-916.8
2	-8148.4	22	19070.6	42	-4535.7	62	-4305.0	82	-760.3
3	-11485.3	23	33709.7	43	-8739.8	63	-2695.0	83	-516.6
4	16875.9	24	23995.9	44	-11681.7	64	-1286.9	84	-215.1
5	58680.7	25	6115.0	45	-10507.1	65	-177.3	85	168.1
6	40885.4	26	-2049.2	46	-6588.2	66	589.1	86	586.1
7	-495.3	27	-4175.3	47	-3934.3	67	1053.1	87	1001.8
8	-12924.8	28	-7332.4	48	-3939.0	68	1259.3	88	1321.6
9	-11937.4	29	-13454.8	49	-4656.1	69	1269.1	89	1400.2
10	-8885.7	30	-17036.1	50	-867.0	70	1116.0	90	1332.0
11	-6524.8	31	-12088.4	51	13187.1	71	781.4	91	1141.4
12	-5840.5	32	-4246.3	52	26794.7	72	353.1	92	829.6
13	-9581.8	33	-1207.7	53	21752.5	73	-45.1	93	476.2
14	-20183.2	34	-1500.2	54	5704.6	74	-369.2	94	205.9
15	-25937.9	35	-552.8	55	-3501.8	75	-658.3	95	30.8
16	-12673.1	36	4701.7	56	-5175.2	76	-903.5	96	-145.6
17	4411.8	37	13198.0	57	-5244.9	77	-1041.4	97	-238.7
18	6002.8	38	17640.7	58	-5715.4	78	-1044.2	98	252.1
E1	-1856.4	39	13208.2	E2	-6322.7	79	-1020.0		
20	-7262.2	40	5013.6	E3	-6461.1	80	-997.4		

Minimum: -25937.9 Mean: 214.01 Std. Dev.: 11650.67 Maximum: 58680.7

Parameter # 2 : LEFT FOREARM angular acceleration (degrees/s/s)

1	3417.8	21	-5405.3	41	1950.2	61	-21984.6	81	1079.9
2	3067.8	22	-6225.8	42	9969.4	62	-12705.6	82	659.5
3	2129.9	23	-6957.1	43	16445.6	63	-13973.4	83	343.3
4	-1682.4	24	-7310.5	44	15079.8	64	-15239.6	84	93.3
5	-11064.7	25	-4392.5	45	7813.3	65	-11058.6	85	-138.6
6	-21364.6	26	9544.7	46	1905.4	66	-4024.1	86	-326.0
7	-20965.1	27	30143.2	47	368.9	67	712.6	87	-504.8
8	-9086.4	28	32085.7	48	972.4	68	2050.5	88	-664.2
9	2438.8	29	11425.0	49	-466.9	69	1869.7	89	-748.4
10	7237.4	30	-5964.0	50	-6222.5	70	1496.4	90	-784.0
11	7817.0	31	-9918.9	51	-12129.3	71	1203.5	91	-754.5
12	7269.9	32	-8199.4	52	-12463.7	72	1181.8	92	-664.0
13	6678.3	33	-5760.7	53	-9199.4	73	1394.6	93	-518.7
14	6242.0	34	-4079.1	54	-7452.9	74	1657.4	94	-367.5
15	5476.2	35	-4063.6	55	-9272.7	75	1984.2	95	-231.1
16	3932.6	36	-6730.1	56	-15537.2	76	2279.3	96	-83.2
17	1734.0	37	-10431.6	57	14608.1	77	2393.9	97	56.1

18	-757.6	38	-10875.5	58	66145.7	78	2271.9	98	-187.5
E1	-2887.6	39	-7546.4	E2	41004.1	79	1955.9		
20	-4356.6	40	-3366.4	E3	-15940.0	80	1542.5		

Minimum: -21984.6 Mean: -101.08 Std. Dev.: 11874.65 Maximum: 66145.7

Parameter # 3 : RIGHT UPPER ARM angular acceleration (degrees/s/s)

1	-5381.5	21	-4713.6	41	3616.7	61	8787.3	81	-840.0
2	-8167.4	22	-4641.1	42	4310.5	62	3319.7	82	-529.0
3	-10292.6	23	-3326.2	43	4015.2	63	-292.2	83	-262.0
4	5880.7	24	-18.3	44	2833.0	64	-1917.0	84	67.8
5	41684.8	25	6616.4	45	1253.6	65	-2249.8	85	445.4
6	45128.7	26	15472.0	46	-359.2	66	-1981.4	86	723.1
7	10802.8	27	20280.0	47	-1896.4	67	-1644.3	87	928.8
8	-9321.8	28	15553.1	48	-3205.9	68	-1410.4	88	1110.6
9	-9778.1	29	4626.0	49	-4211.4	69	-1237.5	89	1206.4
10	-7988.0	30	-4184.8	50	-4858.8	70	-1157.8	90	1160.3
11	-6542.9	31	-7851.9	51	-5147.3	71	-1192.5	91	1051.5
12	-5892.8	32	-8443.9	52	-5142.6	72	-1322.7	92	810.7
13	-5663.0	33	-7906.8	53	-4835.1	73	-1420.2	93	537.2
14	-5678.0	34	-7093.3	54	-4131.1	74	-1485.1	94	312.7
15	-5324.8	35	-6061.7	55	-2823.0	75	-1587.8	95	54.0
16	-4133.2	36	-4766.4	56	-506.8	76	-1596.3	96	-106.6
17	-2787.8	37	-3271.0	57	3490.3	77	-1558.1	97	-261.9
18	-2320.2	38	-1560.6	58	8921.2	78	-1467.7	98	497.7
E1	-2918.2	39	293.3	E2	13259.8	79	-1294.5		
20	-3966.4	40	2137.3	E3	13276.3	80	-1103.4		

Minimum: -10292.6 Mean: 198.29 Std. Dev.: 8337.71 Maximum: 45128.7

Parameter # 4 : LEFT UPPER ARM angular acceleration (degrees/s/s)

1	2283.0	21	25802.3	41	4254.6	61	-9786.2	81	819.6
2	-810.4	22	16625.8	42	1896.6	62	-11753.2	82	620.9
3	-4271.9	23	4033.4	43	-1155.5	63	-8990.1	83	413.2
4	-8190.9	24	-73.5	44	-3957.4	64	-3884.8	84	213.4
5	-10909.6	25	461.7	45	-5656.9	65	-41.7	85	46.0
6	-10440.0	26	1696.3	46	-5829.0	66	1415.7	86	-105.9
7	-6820.7	27	2419.1	47	-4796.3	67	1497.7	87	-252.4
8	-2224.8	28	1130.9	48	-3464.4	68	1227.0	88	-369.0
9	1258.9	29	-5710.7	49	-2533.6	69	917.4	89	-483.4
10	3211.3	30	-18586.4	50	-1767.5	70	754.3	90	-563.5
11	3942.3	31	-25527.5	51	-99.1	71	858.5	91	-638.4
12	4103.1	32	-16800.4	52	3072.4	72	1080.5	92	-619.3
13	3959.8	33	-3025.7	53	6829.5	73	1285.5	93	-516.8
14	3265.0	34	3594.9	54	9161.9	74	1474.1	94	-439.4
15	1869.3	35	4102.1	55	8929.1	75	1627.8	95	-267.7
16	-539.9	36	3310.8	56	6858.2	76	1695.3	96	-107.0
17	-3701.4	37	3283.5	57	4385.1	77	1633.0	97	-51.8
18	-5385.7	38	4085.7	58	1892.6	78	1464.0	98	13.5
E1	689.5	39	5153.2	E2	-1148.8	79	1256.0		
20	16584.0	40	5397.7	E3	-5222.8	80	1028.8		

Minimum: -25527.5 Mean: -67.71 Std. Dev.: 6424.04 Maximum: 25802.3

Parameter # 5 : HEAD angular acceleration (degrees/s/s)

1	774.89	21	1089.12	41	-698.12	61	1194.06	81	-137.61
2	585.90	22	223.92	42	-592.71	62	1219.00	82	-145.09
3	530.87	23	-796.70	43	-418.19	63	1152.84	83	-133.55
4	577.10	24	-1903.71	44	-168.11	64	1081.87	84	-98.09
5	509.28	25	-2897.34	45	-32.77	65	1007.56	85	-93.82

6	337.16	26	-3463.12	46	15.81	66	944.09	86	-61.09
7	107.21	27	-3421.31	47	63.89	67	890.53	87	-23.05
8	-82.95	28	-2870.91	48	91.91	68	838.32	88	-44.24
9	-209.27	29	-2019.77	49	105.78	69	766.64	89	-18.91
10	-246.60	30	-1088.87	50	-16.24	70	715.50	90	25.21
11	-117.70	31	-437.12	51	-335.27	71	738.88	91	51.86
12	168.40	32	-109.75	52	-848.15	72	763.75	92	98.77
13	642.77	33	74.07	53	-1437.43	73	655.94	93	140.10
14	1229.24	34	160.67	54	-1889.85	74	522.66	94	150.28
15	1907.38	35	204.78	55	-1977.38	75	465.23	95	144.60
16	2519.58	36	178.89	56	-1654.12	76	320.04	96	124.93
17	2808.46	37	74.87	57	-1011.52	77	131.99	97	55.52
18	2821.91	38	-120.73	58	-188.26	78	-4.73	98	44.25
E1	2492.54	39	-377.30	E2	503.15	79	-121.86		
20	1839.32	40	-623.30	E3	950.74	80	-153.06		
Minimum: -3463.12 Mean: 48.411 Std. Dev.: 1111.690 Maximum: 2821.91									

Parameter # 6 : TRUNK angular acceleration (degrees/s/s)

1	-307.26	21	922.08	41	624.87	61	-998.64	81	11.65
2	-273.53	22	1135.89	42	488.61	62	-1379.11	82	1.24
3	-257.60	23	1201.34	43	280.60	63	-1497.59	83	19.57
4	-265.39	24	1314.61	44	30.90	64	-1362.15	84	10.89
5	-262.66	25	1535.76	45	-179.13	65	-1054.70	85	-50.77
6	-206.31	26	1846.24	46	-304.73	66	-718.55	86	-93.53
7	-181.62	27	2101.65	47	-288.28	67	-413.61	87	-105.32
8	-272.50	28	2041.25	48	-148.82	68	-223.65	88	-118.75
9	-474.84	29	1646.02	49	17.00	69	-170.94	89	-113.52
10	-814.48	30	1120.85	50	174.27	70	-172.62	90	-133.18
11	-1232.10	31	608.67	51	318.75	71	-243.02	91	-163.27
12	-1703.94	32	222.73	52	461.69	72	-353.07	92	-220.70
13	-2191.04	33	-11.14	53	657.22	73	-414.74	93	-242.39
14	-2599.32	34	-60.41	54	981.51	74	-425.73	94	-194.43
15	-2758.17	35	63.96	55	1363.58	75	-408.68	95	-168.28
16	-2552.62	36	206.76	56	1611.56	76	-344.37	96	-130.61
17	-2041.77	37	350.02	57	1576.52	77	-252.36	97	-152.71
18	-1191.78	38	492.52	58	1188.29	78	-149.75	98	250.98
E1	-251.33	39	601.98	E2	495.16	79	-51.19		
20	456.02	40	667.96	E3	-328.44	80	9.41		
Minimum: -2758.17 Mean: -46.639 Std. Dev.: 930.643 Maximum: 2101.65									

Parameter # 7 : RIGHT THIGH angular acceleration (degrees/s/s)

1	-461.32	21	-2083.52	41	-226.01	61	-1184.81	81	304.49
2	-292.48	22	-848.14	42	-418.62	62	68.46	82	561.10
3	-116.10	23	-239.19	43	-341.39	63	1002.51	83	798.62
4	26.54	24	-365.22	44	-42.18	64	1546.84	84	944.31
5	79.17	25	-962.44	45	354.45	65	1693.93	85	1083.73
6	15.26	26	-1662.48	46	734.06	66	1625.21	86	1066.55
7	-32.04	27	-2137.37	47	1048.14	67	1427.17	87	943.33
8	50.57	28	-2108.34	48	1272.22	68	1095.19	88	838.55
9	260.73	29	-1540.48	49	1402.51	69	754.75	89	642.22
10	698.25	30	-712.68	50	1412.56	70	468.48	90	488.10
11	1384.91	31	136.97	51	1270.20	71	183.44	91	398.69
12	2381.55	32	748.36	52	903.23	72	-28.87	92	263.80
13	3578.96	33	1057.74	53	181.23	73	-183.14	93	173.95
14	4705.28	34	1202.45	54	-891.83	74	-344.47	94	83.75
15	5333.74	35	1204.75	55	-2275.92	75	-425.39	95	7.10
16	4595.42	36	1142.96	56	-3709.53	76	-450.60	96	-57.22
17	2084.44	37	1049.65	57	-4638.36	77	-407.85	97	-281.61

18	-1168.22	38	812.20	58	-4714.03	78	-304.73	98	613.55
E1	-3218.99	39	475.81	E2	-3914.66	79	-157.70		
20	-3247.31	40	123.23	E3	-2598.31	80	76.48		

Minimum: -4714.03 Mean: 123.350 Std. Dev.: 1652.764 Maximum: 5333.74

Parameter # 8 : LEFT THIGH angular acceleration (degrees/s/s)

1	138.0	21	1886.8	41	-1714.3	61	1645.5	81	-1296.1
2	189.3	22	1874.5	42	-1906.8	62	1150.9	82	-1047.4
3	241.6	23	1344.8	43	-1497.1	63	638.5	83	-801.8
4	216.5	24	513.5	44	-584.5	64	743.3	84	-540.7
5	100.9	25	-385.8	45	529.9	65	2306.7	85	-269.9
6	75.8	26	-942.7	46	1560.0	66	6147.8	86	37.7
7	-7.5	27	-974.3	47	2333.6	67	11201.5	87	401.3
8	-350.7	28	-539.8	48	2886.7	68	13810.9	88	756.4
9	-795.4	29	300.8	49	3363.5	69	11504.6	89	1091.7
10	-1348.2	30	1205.1	50	3898.3	70	6299.4	90	1344.2
11	-1972.6	31	1908.1	51	4458.9	71	1748.9	91	1376.3
12	-2484.4	32	2342.1	52	4448.1	72	-823.5	92	1072.3
13	-2848.1	33	2445.2	53	2272.2	73	-1855.7	93	478.0
14	-2966.0	34	2281.0	54	-4163.4	74	-2189.9	94	-286.1
15	-2726.6	35	1926.1	55	-13428.8	75	-2321.6	95	-1208.7
16	-2216.0	36	1476.4	56	-18104.5	76	-2315.4	96	-1923.8
17	-1490.4	37	967.1	57	-13760.2	77	-2183.8	97	-2234.2
18	-531.6	38	388.6	58	-5777.1	78	-2002.3	98	2415.7
E1	508.8	39	-328.5	E2	-444.5	79	-1791.5		
20	1372.0	40	-1111.2	E3	1503.6	80	-1550.1		

Minimum: -18104.5 Mean: 51.90 Std. Dev.: 3979.31 Maximum: 13810.9

Parameter # 9 : RIGHT SHANK angular acceleration (degrees/s/s)

1	128.16	21	-1151.64	41	1881.46	61	-1431.96	81	177.02
2	-65.97	22	-2065.75	42	2687.89	62	-1970.97	82	98.26
3	-259.02	23	-1757.28	43	2785.87	63	-2173.67	83	41.42
4	-375.27	24	314.30	44	2213.04	64	-2110.04	84	19.78
5	-397.75	25	3660.87	45	1355.03	65	-1825.31	85	-20.99
6	-359.99	26	6634.39	46	614.97	66	-1397.83	86	-45.47
7	-339.60	27	7418.84	47	102.30	67	-932.81	87	-11.41
8	-386.47	28	5524.56	48	-201.31	68	-488.45	88	12.90
9	-475.34	29	2307.88	49	-498.69	69	-8.92	89	33.93
10	-735.14	30	-435.04	50	-931.74	70	423.34	90	64.44
11	-1143.15	31	-1987.22	51	-1376.97	71	731.02	91	49.92
12	-1635.86	32	-2489.53	52	-1616.14	72	916.38	92	33.54
13	-2141.55	33	-2272.25	53	-1481.51	73	993.62	93	6.84
14	-2405.77	34	-1713.06	54	-860.04	74	982.29	94	-40.76
15	-2210.34	35	-1178.57	55	124.13	75	892.60	95	-130.48
16	-1496.30	36	-921.69	56	1071.59	76	782.02	96	-232.34
17	-431.24	37	-901.15	57	1573.25	77	622.75	97	-250.57
18	584.19	38	-810.72	58	1356.45	78	459.01	98	221.73
E1	882.86	39	-320.00	E2	528.51	79	337.15		
20	127.88	40	687.24	E3	-527.23	80	241.88		

Minimum: -2489.53 Mean: -7.355 Std. Dev.: 1674.126 Maximum: 7418.84

Parameter # 10 : LEFT SHANK angular acceleration (degrees/s/s)

1	1456.6	21	1025.7	41	1921.5	61	-14118.8	81	565.9
2	1173.4	22	2370.8	42	264.9	62	-12172.4	82	439.3
3	816.7	23	3505.6	43	-1333.7	63	-6184.7	83	347.4
4	426.9	24	4205.2	44	-2570.9	64	-992.1	84	320.1
5	203.4	25	4343.8	45	-3241.2	65	1454.7	85	292.2

6	112.2	26	3802.1	46	-3290.6	66	2299.9	86	196.9
7	-63.5	27	2774.7	47	-2770.5	67	2829.2	87	28.5
8	-382.9	28	1572.6	48	-1879.8	68	3530.6	88	-297.0
9	-967.8	29	473.9	49	-745.2	69	4104.1	89	-716.5
10	-2013.4	30	-259.6	50	825.7	70	3938.4	90	-1223.3
11	-3392.2	31	-552.0	51	2864.3	71	3113.1	91	-1730.5
12	-4833.5	32	-604.2	52	4903.5	72	2155.6	92	-2010.0
13	-5867.2	33	-600.1	53	6291.9	73	1429.6	93	-2068.6
14	-5979.7	34	-441.3	54	6563.8	74	1009.3	94	-1875.2
15	-5149.1	35	13.7	55	5775.6	75	813.1	95	-1462.1
16	-3911.6	36	828.1	56	4384.8	76	766.6	96	-990.4
17	-2868.5	37	1979.8	57	2618.6	77	759.5	97	-690.1
18	-2051.9	38	3062.9	58	9.7	78	773.8	98	555.9
E1	-1207.6	39	3557.8	E2	-4420.4	79	771.2		
20	-198.8	40	3169.0	E3	-10324.4	80	691.3		

Minimum: -14118.8 Mean: -81.30 Std. Dev.: 3404.10 Maximum: 6563.8

Parameter # 11 : RIGHT FOOT angular acceleration (degrees/s/s)

1	-24.3	21	-611.1	41	-5647.9	61	5383.5	81	-300.8
2	12.9	22	-13803.1	42	-15667.2	62	4506.1	82	-437.9
3	90.8	23	-4705.8	43	-24033.2	63	3898.7	83	-537.9
4	175.2	24	-186.1	44	-21898.2	64	3375.8	84	-534.5
5	147.0	25	388.1	45	-12170.2	65	2778.9	85	-469.0
6	-66.3	26	-2912.4	46	4467.9	66	2096.3	86	-360.7
7	-377.1	27	-11419.8	47	32213.9	67	1337.4	87	-322.0
8	-674.0	28	-20997.9	48	43472.2	68	523.4	88	-269.6
9	-850.7	29	-21427.4	49	21468.6	69	-257.9	89	-165.6
10	-761.5	30	-11247.8	50	1243.7	70	-823.3	90	-94.9
11	-486.2	31	-527.1	51	2236.6	71	-1108.7	91	-34.1
12	-179.4	32	6529.7	52	14237.1	72	-1089.1	92	-4.6
13	-92.0	33	13105.3	53	23989.9	73	-873.6	93	59.3
14	-625.2	34	16957.0	54	-22689.3	74	-618.1	94	163.8
15	-2499.1	35	13922.9	55	-81186.4	75	-314.4	95	243.0
16	-7362.1	36	7193.3	56	-44059.4	76	-102.1	96	339.0
17	-15811.4	37	2581.8	57	10962.4	77	6.2	97	380.1
18	-1200.7	38	1146.3	58	15262.5	78	33.2	98	-350.9
E1	40405.7	39	792.8	E2	9471.0	79	-98.2		
20	40316.3	40	-531.3	E3	6726.3	80	-229.9		

Minimum: -81186.4 Mean: -15.18 Std. Dev.: 14719.18 Maximum: 43472.2

Parameter # 12 : LEFT FOOT angular acceleration (degrees/s/s)

1	-33126.2	21	5285.8	41	-8959.7	61	3281.3	81	-1020.5
2	-5407.2	22	6614.4	42	-9465.6	62	2025.9	82	-1062.0
3	22401.4	23	7985.6	43	-6585.8	63	1428.1	83	-966.3
4	33365.2	24	6650.4	44	-2328.4	64	1520.7	84	-831.1
5	15031.2	25	-1942.3	45	2160.5	65	2227.5	85	-711.6
6	-5991.7	26	-14382.0	46	7082.2	66	3358.7	86	-565.0
7	-11397.4	27	-18637.8	47	11225.3	67	4461.9	87	-446.9
8	-9909.8	28	-12393.7	48	11437.4	68	5207.6	88	-454.3
9	-7917.4	29	-5265.5	49	8037.1	69	5637.6	89	-458.4
10	-6586.5	30	-2461.7	50	5076.7	70	5758.6	90	-489.2
11	-5325.6	31	-2769.6	51	4906.2	71	5263.1	91	-530.5
12	-3665.4	32	-3212.0	52	7037.4	72	4006.0	92	-508.5
13	-1601.5	33	1737.5	53	9095.5	73	2520.4	93	-445.7
14	541.6	34	12664.4	54	2731.7	74	1227.0	94	-382.3
15	2414.5	35	16978.0	55	-21188.4	75	435.9	95	-348.9
16	3278.8	36	9388.3	56	-40511.3	76	224.1	96	-227.3
17	3144.5	37	1521.8	57	-27677.1	77	115.6	97	-203.2

18	3073.1	38	-1086.7	58	-3993.9	78	-47.1	98	348.6
E1	3395.3	39	-2546.6	E2	5181.4	79	-349.3		
20	4156.8	40	-5586.1	E3	4966.6	80	-762.9		
Minimum:	-40511.3	Mean:	-52.23	Std. Dev.:	9570.98	Maximum:	33365.2		

Trial Name: JAN1.3AD

subject 2a  
 March 1993  
 take off  
 toe touchdown  
 heel touchdown

Project: skater2  
 Spatial Model: skater2

Time Between Pictures: 0.017 s

	EVENTS
1 take off	19
2 toe touchdown	59
3 heel touchdown	60

Parameter # 1 : RIGHT FOREARM angles (degrees)

1	48.8854	21	54.2850	41	66.0773	61	114.1899	81	99.4320
2	41.9988	22	40.3762	42	74.1741	62	114.7309	82	97.5563
3	32.8488	23	31.5726	43	81.1734	63	114.0517	83	95.4601
4	20.5068	24	35.6235	44	85.7013	64	112.6651	84	93.2194
5	4.0507	25	46.3155	45	86.5586	65	110.9190	85	90.9143
6	17.7658	26	57.5328	46	84.2486	66	109.1695	86	88.6437
7	40.4535	27	67.8528	47	80.2694	67	107.5893	87	86.5552
8	60.4531	28	77.1652	48	75.4758	68	106.3284	88	84.7190
9	76.3059	29	84.7508	49	69.6087	69	105.4298	89	83.3093
10	88.7795	30	88.6505	50	62.3262	70	104.8865	90	82.2628
11	98.8945	31	86.6991	51	53.7746	71	104.6804	91	81.6192
12	107.2329	32	81.2067	52	48.2133	72	104.6847	92	81.2866
13	114.2334	33	75.2159	53	52.5928	73	104.7992	93	81.1973
14	119.1968	34	69.0447	54	63.8722	74	104.8752	94	81.2321
15	118.9259	35	62.3908	55	75.5805	75	104.8679	95	81.3045
16	108.7349	36	55.2160	56	85.8695	76	104.6555	96	81.4064
17	94.7985	37	48.9514	57	94.6772	77	104.2051	97	81.4458
18	84.1918	38	46.6113	58	102.1166	78	103.4320	98	81.4189
E1	75.5731	39	50.1764	E2	107.9462	79	102.3852		
20	66.3186	40	57.6074	E3	112.0133	80	101.0483		

Minimum: 4.0507 Mean: 80.53305 Std. Dev.: 25.23121 Maximum: 119.1968

Parameter # 2 : LEFT FOREARM angles (degrees)

1	127.7365	21	73.1303	41	70.4577	61	102.4195	81	70.9195
2	131.1725	22	70.0462	42	62.0728	62	111.9133	82	71.9942
3	135.4607	23	65.2452	43	56.4032	63	118.5729	83	73.2534
4	140.5039	24	58.4980	44	56.1632	64	121.3164	84	74.5924
5	145.5516	25	49.6299	45	60.6216	65	119.2002	85	75.9688
6	147.9660	26	38.8270	46	67.0089	66	113.7866	86	77.2941
7	143.3483	27	29.1342	47	73.5215	67	107.5402	87	78.5300
8	131.6895	28	29.7612	48	79.9718	68	101.7855	88	79.6337
9	117.8505	29	42.1309	49	86.8313	69	96.6721	89	80.5304
10	105.3170	30	56.3462	50	94.0152	70	92.0628	90	81.2353
11	95.0624	31	67.8220	51	99.6223	71	87.8814	91	81.6992
12	86.9861	32	76.3046	52	101.1446	72	84.0027	92	81.9658
13	80.9599	33	82.4921	53	98.9363	73	80.4279	93	82.0297
14	76.7328	34	87.1525	54	94.4254	74	77.2557	94	81.9585
15	74.2777	35	90.7614	55	88.0288	75	74.5240	95	81.7838
16	73.4150	36	93.4681	56	79.4252	76	72.3502	96	81.5429
17	73.6803	37	94.5156	57	66.8182	77	70.8248	97	81.2811

18	74.4669	38	92.3057	58	47.1615	78	69.9773	98	81.0349
E1	75.0095	39	86.6791	E2	61.8388	79	69.7855		
20	74.6769	40	79.0595	E3	88.3930	80	70.1288		

Minimum: 29.1342 Mean: 84.36439 Std. Dev.: 23.76180 Maximum: 147.9660

Parameter # 3 : RIGHT UPPER ARM angles (degrees)

1	51.2904	21	99.0917	41	106.9989	61	56.0997	81	98.7928
2	44.9282	22	94.7633	42	105.2479	62	61.2302	82	96.9489
3	36.2972	23	89.0613	43	104.7627	63	67.0779	83	94.9746
4	24.6236	24	82.3119	44	105.4694	64	72.7249	84	92.9205
5	9.8677	25	75.3350	45	106.9877	65	77.7314	85	90.8653
6	10.8531	26	69.8402	46	108.8388	66	82.0896	86	88.9673
7	29.7545	27	68.9603	47	110.6056	67	85.8852	87	87.2508
8	47.2256	28	74.5595	48	111.8090	68	89.2528	88	85.8176
9	61.6445	29	85.1189	49	112.1165	69	92.2120	89	84.6683
10	73.2406	30	96.5601	50	111.2171	70	94.8489	90	83.9018
11	82.6699	31	106.4175	51	108.9480	71	97.1638	91	83.4264
12	90.3800	32	113.9109	52	105.2265	72	99.1584	92	83.2753
13	96.4254	33	118.9918	53	100.0604	73	100.7907	93	83.3528
14	100.9718	34	121.8797	54	93.5220	74	101.9983	94	83.5496
15	103.8887	35	122.7807	55	85.8003	75	102.8396	95	83.8761
16	105.2548	36	121.9671	56	77.2273	76	103.1881	96	84.1714
17	105.4355	37	119.8345	57	68.4037	77	103.1243	97	84.4594
18	104.9453	38	116.7584	58	60.3695	78	102.6042	98	84.6746
E1	103.8848	39	113.2538	E2	54.8851	79	101.6777		
20	102.0579	40	109.8158	E3	53.4241	80	100.3896		

Minimum: 9.8677 Mean: 88.23219 Std. Dev.: 23.39902 Maximum: 122.7807

Parameter # 4 : LEFT UPPER ARM angles (degrees)

1	135.0138	21	34.1584	41	107.3085	61	118.5552	81	70.3084
2	137.3875	22	40.8763	42	109.9658	62	120.5910	82	70.8669
3	139.5361	23	51.8123	43	113.2332	63	118.8879	83	71.6008
4	140.6002	24	62.9868	44	116.1348	64	114.5275	84	72.4434
5	139.3118	25	73.9477	45	117.8739	65	109.2316	85	73.3523
6	134.7120	26	85.0157	46	117.9067	66	104.1476	86	74.2570
7	126.9657	27	96.5962	47	116.2292	67	99.5289	87	75.1549
8	117.2238	28	108.9293	48	113.2018	68	95.3407	88	75.9529
9	107.0411	29	121.9326	49	109.2552	69	91.4904	89	76.6770
10	97.2636	30	134.0994	50	104.6476	70	87.8971	90	77.2387
11	88.5152	31	140.9237	51	99.4661	71	84.4712	91	77.6620
12	80.8716	32	138.6180	52	94.1296	72	81.2918	92	77.8985
13	74.3696	33	131.5510	53	89.5669	73	78.4058	93	77.9377
14	69.0385	34	124.4695	54	87.0253	74	75.8869	94	77.8702
15	64.6239	35	118.8163	55	87.2560	75	73.7688	95	77.6392
16	60.8333	36	114.3154	56	90.1008	76	72.1200	96	77.3537
17	56.9551	37	110.6396	57	94.8664	77	70.9406	97	77.0432
18	52.0281	38	107.8400	58	100.7966	78	70.2368	98	76.7183
E1	45.1737	39	106.1112	E2	107.3490	79	69.9268		
20	37.2389	40	105.9042	E3	113.5954	80	69.9803		

Minimum: 34.1584 Mean: 93.56487 Std. Dev.: 25.53283 Maximum: 140.9237

Parameter # 5 : HEAD angles (degrees)

1	81.1636	21	94.7460	41	114.4685	61	75.4774	81	60.3650
2	80.4191	22	99.4766	42	113.5751	62	72.4933	82	60.6492
3	79.8373	23	104.2648	43	112.5496	63	69.8411	83	60.8955
4	79.3658	24	108.8534	44	111.3590	64	67.5136	84	61.0955
5	79.1008	25	112.8984	45	110.1661	65	65.4857	85	61.2776

6	78.9536	26	116.1149	46	108.9561	66	63.7360	86	61.4327
7	78.9302	27	118.3128	47	107.7461	67	62.2499	87	61.5555
8	78.9162	28	119.5285	48	106.5708	68	61.0073	88	61.7021
9	78.8787	29	119.9257	49	105.3972	69	60.0035	89	61.8077
10	78.7865	30	119.7522	50	104.2876	70	59.2101	90	61.9223
11	78.5947	31	119.2944	51	103.1657	71	58.6089	91	62.0390
12	78.3829	32	118.7660	52	101.9864	72	58.2079	92	62.1705
13	78.1799	33	118.1774	53	100.5618	73	58.0354	93	62.3278
14	78.1663	34	117.6579	54	98.7428	74	58.0544	94	62.5285
15	78.4793	35	117.1427	55	96.3607	75	58.1906	95	62.7724
16	79.3156	36	116.7283	56	93.3994	76	58.4815	96	63.0534
17	80.8980	37	116.3356	57	89.9625	77	58.8628	97	63.3776
18	83.2644	38	115.9975	58	86.2180	78	59.2643	98	63.7172
E1	86.4372	39	115.6116	E2	82.4404	79	59.6816		
20	90.3487	40	115.1326	E3	78.8275	80	60.0418		

Minimum: 58.0354 Mean: 84.45931 Std. Dev.: 21.90728 Maximum: 119.9257

Parameter # 6 : TRUNK angles (degrees)

1	98.9038	21	82.4810	41	67.1271	61	103.0965	81	128.8403
2	100.1247	22	78.6521	42	68.2373	62	106.2803	82	129.3336
3	101.2697	23	75.1480	43	69.4865	63	109.0590	83	129.8081
4	102.3481	24	71.9706	44	70.8236	64	111.4079	84	130.3065
5	103.3495	25	69.1498	45	72.1576	65	113.3574	85	130.7977
6	104.2766	26	66.7497	46	73.4443	66	115.0220	86	131.2914
7	105.1374	27	64.8580	47	74.6298	67	116.4840	87	131.7308
8	105.9759	28	63.5802	48	75.7264	68	117.8377	88	132.1725
9	106.7234	29	62.9014	49	76.7816	69	119.1511	89	132.5470
10	107.3723	30	62.6788	50	77.8432	70	120.4050	90	132.9216
11	107.7819	31	62.7737	51	78.9523	71	121.6282	91	133.2370
12	107.8639	32	63.0227	52	80.1536	72	122.7804	92	133.5228
13	107.4714	33	63.3223	53	81.4771	73	123.8353	93	133.7456
14	106.4621	34	63.6142	54	82.9770	74	124.7635	94	133.8787
15	104.7264	35	63.8586	55	84.7323	75	125.5815	95	133.9848
16	102.1722	36	64.1385	56	86.8909	76	126.2736	96	134.0185
17	98.9167	37	64.4658	57	89.5025	77	126.8737	97	134.0371
18	95.0461	38	64.8925	58	92.5955	78	127.4010	98	134.0133
E1	90.8385	39	65.4620	E2	96.0244	79	127.8854		
20	86.5957	40	66.1938	E3	99.6203	80	128.3621		

Minimum: 62.6788 Mean: 99.49108 Std. Dev.: 24.90006 Maximum: 134.0371

Parameter # 7 : RIGHT THIGH angles (degrees)

1	76.325	21	67.654	41	70.807	61	89.202	81	53.674
2	73.759	22	69.172	42	71.655	62	85.448	82	52.210
3	71.112	23	70.520	43	72.361	63	81.757	83	50.887
4	68.430	24	71.853	44	72.960	64	78.347	84	49.826
5	65.769	25	73.119	45	73.535	65	75.426	85	48.988
6	63.130	26	74.128	46	74.218	66	72.965	86	48.491
7	60.514	27	74.650	47	75.103	67	70.977	87	48.292
8	57.847	28	74.556	48	76.292	68	69.389	88	48.340
9	55.223	29	73.805	49	77.836	69	68.114	89	48.645
10	52.620	30	72.641	50	79.780	70	67.029	90	49.122
11	50.223	31	71.249	51	82.127	71	66.090	91	49.712
12	48.169	32	69.934	52	84.837	72	65.190	92	50.446
13	46.761	33	68.845	53	87.830	73	64.269	93	51.221
14	46.364	34	68.059	54	90.897	74	63.319	94	52.062
15	47.276	35	67.616	55	93.733	75	62.245	95	52.924
16	49.788	36	67.520	56	95.967	76	61.066	96	53.772
17	53.717	37	67.726	57	97.109	77	59.749	97	54.635

18 58.317	38 68.251	58 96.915	78 58.311	98 55.419
E1 62.474	39 69.002	E2 95.330	79 56.799	
20 65.549	40 69.884	E3 92.625	80 55.218	

Minimum: 46.364 Mean: 66.6841 Std. Dev.: 13.1859 Maximum: 97.109

Parameter # 8 : LEFT THIGH angles (degrees)

1	86.2754	21	82.9227	41	72.2746	61	77.8479	81	110.2565
2	87.9564	22	80.3928	42	73.3803	62	70.4117	82	113.1191
3	89.6901	23	78.4459	43	73.8971	63	63.3292	83	115.6840
4	91.4906	24	76.8624	44	73.9680	64	56.3528	84	118.0299
5	93.3732	25	75.4634	45	73.8562	65	49.5200	85	120.2206
6	95.2653	26	73.9026	46	73.9062	66	43.1199	86	122.3400
7	97.1685	27	72.0522	47	74.4040	67	38.2737	87	124.4572
8	99.1241	28	69.8954	48	75.5778	68	36.7177	88	126.6920
9	100.9554	29	67.5585	49	77.5447	69	39.4735	89	129.1398
10	102.5933	30	65.2884	50	80.4568	70	45.6610	90	131.8845
11	103.8586	31	63.3990	51	84.4227	71	53.4563	91	135.0354
12	104.5646	32	62.0205	52	89.6673	72	61.6037	92	138.5705
13	104.5701	33	61.3597	53	96.2550	73	69.3822	93	142.4601
14	103.7754	34	61.3549	54	103.8201	74	76.6313	94	146.4479
15	102.1171	35	62.0372	55	110.6119	75	83.2463	95	150.4160
16	99.6906	36	63.2237	56	113.3468	76	89.2257	96	154.0075
17	96.6345	37	64.8549	57	110.0480	77	94.5309	97	157.0288
18	93.1437	38	66.7329	58	102.7576	78	99.2475	98	159.4295
E1	89.4959	39	68.7472	E2	94.1949	79	103.3890		
20	86.0060	40	70.6739	E3	85.7493	80	107.0445		

Minimum: 36.7177 Mean: 89.88528 Std. Dev.: 27.30129 Maximum: 159.4295

Parameter # 9 : RIGHT SHANK angles (degrees)

1	93.5187	21	73.6203	41	64.3160	61	98.1581	81	90.9639
2	94.2905	22	70.4490	42	64.2187	62	99.6929	82	91.5383
3	95.0439	23	66.6268	43	64.9365	63	100.6452	83	92.1326
4	95.7250	24	62.1630	44	66.4642	64	100.9924	84	92.7343
5	96.2812	25	57.6808	45	68.6524	65	100.7171	85	93.3474
6	96.7427	26	54.2263	46	71.1686	66	99.9475	86	93.9524
7	97.0767	27	52.8025	47	73.8739	67	98.7609	87	94.5388
8	97.3603	28	53.6611	48	76.5564	68	97.3494	88	95.1199
9	97.4948	29	56.1672	49	79.2090	69	95.7682	89	95.7175
10	97.5485	30	59.2343	50	81.7205	70	94.2086	90	96.3017
11	97.3847	31	62.0963	51	83.9901	71	92.7657	91	96.9339
12	96.9199	32	64.3241	52	85.8493	72	91.5382	92	97.5552
13	96.0044	33	65.8174	53	87.2412	73	90.5753	93	98.2058
14	94.4736	34	66.6478	54	88.1824	74	89.8859	94	98.8459
15	92.2447	35	67.0137	55	88.8461	75	89.4890	95	99.4853
16	89.3543	36	67.0681	56	89.5599	76	89.3251	96	100.0913
17	86.0290	37	66.9005	57	90.5890	77	89.3945	97	100.6198
18	82.5724	38	66.4643	58	92.1281	78	89.6332	98	101.0786
E1	79.3342	39	65.7861	E2	94.0799	79	89.9919		
20	76.4397	40	64.9597	E3	96.2034	80	90.4514		

Minimum: 52.8025 Mean: 85.12029 Std. Dev.: 14.11096 Maximum: 101.0786

Parameter # 10 : LEFT SHANK angles (degrees)

1	91.1196	21	91.3739	41	65.3614	61	127.1908	81	122.1199
2	94.3080	22	84.6842	42	68.6524	62	127.3376	82	125.6976
3	97.8223	23	78.6654	43	72.0070	63	123.7483	83	129.4061
4	101.5839	24	73.6691	44	74.9704	64	118.5993	84	133.1957
5	105.4325	25	69.8521	45	77.1709	65	113.4340	85	137.0782

6	109.3341	26	67.3264	46	78.4318	66	108.7586	86	141.0494
7	113.2686	27	65.8652	47	78.7333	67	104.7361	87	145.0750
8	117.2090	28	65.2083	48	78.2371	68	101.4734	88	149.1219
9	121.0342	29	64.9613	49	77.2175	69	99.1817	89	153.1034
10	124.6584	30	64.8376	50	75.9536	70	98.1111	90	156.8644
11	127.7244	31	64.5839	51	74.8736	71	98.1875	91	160.3357
12	129.8708	32	64.1783	52	74.5877	72	99.1247	92	163.2478
13	130.6456	33	63.5931	53	75.7124	73	100.6522	93	165.6453
14	129.7126	34	62.8478	54	78.6700	74	102.5335	94	167.3978
15	127.0477	35	61.9356	55	83.5421	75	104.7054	95	168.6565
16	122.9104	36	61.0269	56	90.0454	76	107.0638	96	169.4643
17	117.7285	37	60.2933	57	97.7891	77	109.6620	97	170.0431
18	111.7619	38	60.1262	58	106.2929	78	112.4458	98	170.4303
E1	105.2221	39	60.8507	E2	114.9458	79	115.4625		
20	98.3335	40	62.6287	E3	122.5510	80	118.6876		

Minimum: 60.1262 Mean: 104.18378 Std. Dev.: 31.14482 Maximum: 170.4303

Parameter # 11 : RIGHT FOOT angles (degrees)

1	78.7964	21	55.3199	41	94.2692	61	84.8818	81	78.6079
2	78.0244	22	67.4489	42	99.5097	62	80.8962	82	78.1163
3	77.2559	23	75.9081	43	100.4828	63	78.1358	83	77.4927
4	76.5013	24	83.5026	44	93.6564	64	76.4527	84	76.7042
5	75.8162	25	91.2677	45	79.9929	65	75.7217	85	75.7798
6	75.1729	26	99.3496	46	63.4717	66	75.7601	86	74.6982
7	74.5399	27	107.0584	47	45.9806	67	76.3953	87	73.5458
8	73.7709	28	111.9605	48	38.2513	68	77.3968	88	72.2914
9	72.8445	29	110.1604	49	47.7615	69	78.5548	89	70.9540
10	71.6199	30	101.2404	50	61.3333	70	79.6151	90	69.5851
11	70.2039	31	89.4543	51	73.3964	71	80.4278	91	68.1783
12	68.6227	32	78.0228	52	85.7972	72	80.9186	92	66.7733
13	67.0232	33	68.1625	53	101.5165	73	81.0690	93	65.3647
14	65.4263	34	62.0603	54	126.0802	74	81.0121	94	63.9563
15	63.7402	35	61.4322	55	156.2920	75	80.7395	95	62.6170
16	61.5351	36	64.9390	56	141.1528	76	80.4186	96	61.3213
17	57.6805	37	70.1718	57	120.8605	77	80.0607	97	60.1393
18	49.4638	38	75.8102	58	107.2705	78	79.7118	98	59.0630
E1	34.0526	39	81.7801	E2	97.6094	79	79.3888		
20	36.0584	40	87.9551	E3	90.3465	80	79.0417		

Minimum: 34.0526 Mean: 77.93849 Std. Dev.: 19.20656 Maximum: 156.2920

Parameter # 12 : LEFT FOOT angles (degrees)

1	46.4580	21	57.3754	41	84.5670	61	83.0846	81	65.7036
2	37.8398	22	61.2419	42	84.1933	62	74.5445	82	69.0888
3	27.7197	23	66.8936	43	80.8647	63	66.5334	83	72.1749
4	23.7973	24	74.8399	44	75.6970	64	58.8530	84	74.9868
5	33.8719	25	85.2848	45	69.8448	65	51.5689	85	77.5725
6	46.8273	26	95.8273	46	64.6136	66	44.8512	86	79.9614
7	56.7253	27	101.5179	47	61.2256	67	39.0794	87	82.1794
8	63.1998	28	100.8346	48	61.3994	68	34.5811	88	84.3082
9	66.9151	29	97.0424	49	65.0789	69	31.5475	89	86.2897
10	68.5615	30	92.0712	50	70.8933	70	30.0973	90	88.1503
11	68.3078	31	86.7163	51	77.8623	71	30.2797	91	89.8907
12	66.6048	32	80.5725	52	86.0280	72	32.0119	92	91.4488
13	63.7832	33	73.3129	53	96.0970	73	34.8597	93	92.9023
14	60.5753	34	65.5050	54	108.9820	74	38.3777	94	94.1822
15	57.4790	35	61.8400	55	124.4378	75	42.2402	95	95.4186
16	55.1477	36	64.5089	56	134.9713	76	46.1068	96	96.4909
17	53.8577	37	69.2316	57	129.2359	77	50.1051	97	97.5472

18	53.3632	38	73.9443	58	115.9480	78	54.0849	98	98.5471
E1	53.7302	39	78.3141	E2	103.2817	79	58.0984		
20	54.9932	40	82.1722	E3	92.4870	80	62.0107		

Minimum: 23.7973 Mean: 70.57420 Std. Dev.: 23.14594 Maximum: 134.9713

APPENDIX D

Sample GRF, JRF, Moments,  
and  
Statistics

## Sample GRF, JRF, and Moments

s2b Horiz. GRF	s2b Vert. GRF	s2b Hip JRF	s2b Knee JRF
4.234	4.184	4.017	4.046
5.154	6.75	6.334	6.697
3.868	4.222	4.022	4.187
1.609	-0.04	0.174	-0.171
0.239	0.389	0.443	0.234
-0.226	1.754	1.636	1.613
-0.396	1.254	1.199	1.126
0.747	2.052	1.579	2.002
0.878	3.374	2.674	3.364
-1.325	3.218	2.794	3.167
-2.548	2.599	2.132	2.543
-2.494	1.488	0.943	1.475
-2.302	0.717	0.249	0.723
-1.397	1.367	0.783	1.348
-0.67	1.941	1.383	1.871
-0.358	2.018	1.563	1.878

s2b Ankle JRF	s2b Hip Moment	s2b Knee Moment	s2b Ankle Moment
4.156	-10.868	367.465	39.275
6.806	392.814	265.941	45.879
4.286	541.761	347.391	21.933
-0.059	263.157	201.557	22.606
0.33	88.540	-53.391	-0.671
1.700	80.749	115.428	13.846
1.184	138.408	107.167	7.713
2.013	23.345	-97.601	-37.188
3.398	-18.506	4.368	30.157
3.239	-376.760	-307.833	27.865
2.594	-452.081	-36.804	-1.619
1.48	-27.676	-128.869	-32.684
0.694	134.534	80.472	1.299
1.329	-245.627	-227.778	-17.723
1.915	-295.685	121.706	-11.477
1.997	28.073	-82.685	-9.801

### Statistics for Ground Reaction Forces

#### General Linear Models Procedure Class Level Information

Class	Levels	Values
S	6	2 3 4 5 6 8
JUMP	6	1 2 3 4 5 6
DIR	2	0 1
METHOD	2	0 1

#### General Linear Models Procedure Repeated Measures Analysis of Variance

##### Manova Test Criteria and Exact F Statistics for the Hypothesis of no TIME Effect

H = Type III SS&CP Matrix for TIME    E = Error SS&CP Matrix

Statistic	S=1	M=7	N=17		Pr > F
	Value	F	Num DF	Den DF	
Wilks' Lambda	0.06080110	34.7559	16	36	0.0001
Pillai's Trace	0.93919890	34.7559	16	36	0.0001
Hotelling-Lawley Trace	15.44707165	34.7559	16	36	0.0001
Roy's Greatest Root	15.44707165	34.7559	16	36	0.0001

##### Manova Test Criteria and Exact F Statistics for the Hypothesis of no TIME\*S Effect

H = Type III SS&CP Matrix for TIME\*S    E = Error SS&CP Matrix

Statistic	S=5	M=5	N=17		Pr > F
	Value	F	Num DF	Den DF	
Wilks' Lambda	0.00716958	3.9726	80	177.6268	0.0001
Pillai's Trace	0.93919890	3.3662	80	200	0.0001
Hotelling-Lawley Trace	15.44707165	4.4118	80	172	0.0001
Roy's Greatest Root	15.44707165	10.1824	16	40	0.0001

Manova Test Criteria and Exact F Statistics for  
the Hypothesis of no TIME\*JUMP(S) Effect

H = Type III SS&CP Matrix for TIME\*JUMP(S)      E = Error SS&CP Matrix

S=12                  M=1.5                  N=17

Statistic	Value	F	Num DF	Den DF	Pr > F
Wilks' Lambda	0.00024751	2.6502	192	373.5121	0.0001
Pillai's Trace	5.00168588	2.0994	192	564	0.0001
Hotelling-Lawley Trace	17.35887734	3.0890	192	410	0.0001
Roy's Greatest Root	6.15680489	18.0856	16	47	0.0001

Manova Test Criteria and Exact F Statistics for  
the Hypothesis of no TIME\*METHOD Effect

H = Type III SS&CP Matrix for TIME\*METHOD      E = Error SS&CP Matrix

S=1                  M=7                  N=17

Statistic	Value	F	Num DF	Den DF	Pr > F
Wilks' Lambda	0.63255188	1.3070	16	36	0.2456
Pillai's Trace	0.36744812	1.3070	16	36	0.2456
Hotelling-Lawley Trace	0.58089799	1.3070	16	36	0.2456
Roy's Greatest Root	0.58089799	1.3070	16	36	0.2456

Manova Test Criteria and Exact F Statistics for  
the Hypothesis of no TIME\*DIR Effect

H = Type III SS&CP Matrix for TIME\*DIR      E = Error SS&CP Matrix

S=1                  M=7                  N=17

Statistic	Value	F	Num DF	Den DF	Pr > F
Wilks' Lambda	0.17823281	10.3739	16	36	0.0001
Pillai's Trace	0.82176719	10.3739	16	36	0.0001
Hotelling-Lawley Trace	4.61063924	10.3739	16	36	0.0001
Roy's Greatest Root	4.61063924	10.3739	16	36	0.0001

Manova Test Criteria and Exact F Statistics for  
 the Hypothesis of no TIME\*DIR\*METHOD Effect  
 H = Type III SS&CP Matrix for TIME\*DIR\*METHOD      E = Error SS&CP  
 Matrix

Statistic	S=1	M=7	N=17		Pr > F
	Value	F	Num DF	Den DF	
Wilks' Lambda	0.61724395	1.3952	16	36	0.1988
Pillai's Trace	0.38275605	1.3952	16	36	0.1988
Hotelling-Lawley Trace	0.62010500	1.3952	16	36	0.1988
Roy's Greatest Root	0.62010500	1.3952	16	36	0.1988

Manova Test Criteria and Exact F Statistics for  
 the Hypothesis of no TIME\*DIR\*METHOD Effect  
 Test of Hypothesis for Between Subject Effects

Source	S=1		M=7		N=17	
	DF	Type III SS	Mean Square	F Value	Pr > F	
S	5	35.39575818	7.07915164	2.70	0.0309	
JUMP(S)	12	20.98439625	1.74869969	0.67	0.7752	
METHOD	1	6.13261137	6.13261137	2.34	0.1327	
DIR	1	643.40705069	643.40705069	244.98	0.0001	
DIR*METHOD	1	3.47978690	3.47978690	1.32	0.2551	
Error	51	133.94410746	2.62635505			

### Statistics for Joint Reaction Forces

#### General Linear Models Procedure Class Level Information

Class	Levels	Values
S	6	2 3 4 5 6 8
JUMP	6	1 2 3 4 5 6
DIR	3	0 1 2
JOINT	3	1 2 3

Number of observations in data set = 162

#### Manova Test Criteria and Exact F Statistics for the Hypothesis of no TIME Effect

H = Type III SS&CP Matrix for TIME    E = Error SS&CP Matrix

S=1                      M=6.5                      N=60

Statistic	Value	F	Num DF	Den DF	Pr > F
Wilks' Lambda	0.39832233	12.2856	15	122	0.0001
Pillai's Trace	0.60167767	12.2856	15	122	0.0001
Hotelling-Lawley Trace	1.51052961	12.2856	15	122	0.0001
Roy's Greatest Root	1.51052961	12.2856	15	122	0.0001

#### Manova Test Criteria and Exact F Statistics for the Hypothesis of no TIME\*S Effect

H = Type III SS&CP Matrix for TIME\*S    E = Error SS&CP Matrix

S=5                      M=4.5                      N=60

Statistic	Value	F	Num DF	Den DF	Pr > F
Wilks' Lambda	0.17178108	3.4883	75	588.5781	0.0001
Pillai's Trace	1.40753487	3.2911	75	630	0.0001
Hotelling-Lawley Trace	2.28039408	3.6608	75	602	0.0001
Roy's Greatest Root	1.03599769	8.7024	15	126	0.0001

Manova Test Criteria and Exact F Statistics for  
the Hypothesis of no TIME\*JUMP(S) Effect

H = Type III SS&CP Matrix for TIME\*JUMP(S)      E = Error SS&CP Matrix

	S=12	M=1	N=60		
Statistic	Value	F	Num DF	Den DF	Pr > F
Wilks' Lambda	0.03156513	2.8882	180	1175.153	0.0001
Pillai's Trace	2.81803008	2.7213	180	1596	0.0001
Hotelling-Lawley Trace	4.35437441	2.9069	180	1442	0.0001
Roy's Greatest Root	1.00656158	8.9248	15	133	0.0001

Manova Test Criteria and Exact F Statistics for  
the Hypothesis of no TIME\*JOINT Effect

H = Type III SS&CP Matrix for TIME\*JOINT      E = Error SS&CP Matrix

	S=2	M=6	N=60		
Statistic	Value	F	Num DF	Den DF	Pr > F
Wilks' Lambda	0.96711979	0.1371	30	244	1.0000
Pillai's Trace	0.03313181	0.1381	30	246	1.0000
Hotelling-Lawley Trace	0.03373792	0.1361	30	242	1.0000
Roy's Greatest Root	0.02180926	0.1788	15	123	1.0000

Manova Test Criteria and Exact F Statistics for  
the Hypothesis of no TIME\*DIR Effect

H = Type III SS&CP Matrix for TIME\*DIR      E = Error SS&CP Matrix

	S=2	M=6	N=60		
Statistic	Value	F	Num DF	Den DF	Pr > F
Wilks' Lambda	0.04803176	28.9778	30	244	0.0001
Pillai's Trace	1.23059819	13.1153	30	246	0.0001
Hotelling-Lawley Trace	14.01860437	56.5417	30	242	0.0001
Roy's Greatest Root	13.59180665	111.4528	30	123	0.0001

Manova Test Criteria and Exact F Statistics for  
 the Hypothesis of no TIME\*DIR\*JOINT Effect  
 H = Type III SS&CP Matrix for TIME\*DIR\*JOINT E = Error SS&CP Matrix

Statistic	S=4	M=5	N=60		
	Value	F	Num DF	Den DF	Pr > F
Wilks' Lambda	0.86777968	0.2950	60	478.4546	1.0000
Pillai's Trace	0.13602183	0.2934	60	500	1.0000
Hotelling-Lawley Trace	0.14801210	0.2973	60	482	1.0000
Roy's Greatest Root	0.11126634	0.9272	15	125	0.5362

General Linear Models Procedure  
 Repeated Measures Analysis of Variance  
 Test of Hypothesis for Between Subject Effects

Source	DF	Type III SS	Mean Square	F Value	Pr > F
S	5	108.49082823	21.69816565	3.11	0.0108
JUMP(S)	12	160.02982454	13.33581871	1.91	0.0379
JOINT	2	23.51059906	11.77529953	1.69	0.1892
DIR	2	1770.13557001	885.06778501	126.91	0.0001
DIR*JOINT	4	6.68269907	1.67067477	0.24	0.9155
Error	136	948.44022358	6.97382517		

### Statistics for Moments

#### General Linear Models Procedure Class Level Information

Class	Levels	Values
S	6	2 3 4 5 6 8
JUMP	6	A B C D E F
JOINT	3	ANKLE HIP KNEE

Number of observations in data set = 51

#### Manova Test Criteria and Exact F Statistics for the Hypothesis of no TIME Effect

H = Type III SS&CP Matrix for TIME    E = Error SS&CP Matrix

	S=1	M=6.5	N=8		
Statistic	Value	F	Num DF	Den DF	Pr > F
Wilks' Lambda	0.41378191	1.7001	15	18	0.1413
Pillai's Trace	0.58621809	1.7001	15	18	0.1413
Hotelling-Lawley Trace	1.41673206	1.7001	15	18	0.1413
Roy's Greatest Root	1.41673206	1.7001	15	18	0.1413

#### Manova Test Criteria and Exact F Statistics for the Hypothesis of no TIME\*S Effect

H = Type III SS&CP Matrix for TIME\*S    E = Error SS&CP Matrix

	S=5	M=4.5	N=8		
Statistic	Value	F	Num DF	Den DF	Pr > F
Wilks' Lambda	0.03906375	1.1670	75	90.43156	0.2403
Pillai's Trace	2.27412484	1.2236	75	110	0.1663
Hotelling-Lawley Trace	4.96768746	1.0863	75	82	0.3562
Roy's Greatest Root	1.83390074	2.6897	15	22	0.0172

Manova Test Criteria and Exact F Statistics for  
the Hypothesis of no TIME\*JUMP(S) Effect  
H = Type III SS&CP Matrix for TIME\*JUMP(S) E = Error SS&CP Matrix

	S=11	M=1.5	N=8		
Statistic	Value	F	Num DF	Den DF	Pr > F
Wilks' Lambda	0.00198873	1.1102	165	182.0705	0.2452
Pillai's Trace	4.38485185	1.2373	165	308	0.0561
Hotelling-Lawley Trace	9.58291968	0.9398	165	178	0.6567
Roy's Greatest Root	2.34596704	4.3791	15	28	0.0004

Manova Test Criteria and Exact F Statistics for  
the Hypothesis of no TIME\*JOINT Effect  
H = Type III SS&CP Matrix for TIME\*JOINT E = Error SS&CP Matrix

	S=2	M=6	N=60		
Statistic	Value	F	Num DF	Den DF	Pr > F
Wilks' Lambda	0.39668413	0.7053	30	36	0.8347
Pillai's Trace	0.67953320	0.6518	30	38	0.8853
Hotelling-Lawley Trace	1.32876135	0.7530	30	34	0.7834
Roy's Greatest Root	1.16364575	1.4740	15	19	0.2103

General Linear Models Procedure  
Repeated Measures Analysis of Variance  
Test of Hypothesis for Between Subject Effects

Source	DF	Type III SS	Mean Square	F Value	Pr > F
S	5	57845.70013047	11569.14002609	0.67	0.6505
JUMP(S)	11	404106.96372895	36736.99670263	2.12	0.0481
JOINT	2	18203.70411127	9101.85205564	0.53	0.5963
Error	32	554300.05473406	6.97382517		

General Linear Models Procedure  
Repeated Measures Analysis of Variance  
Univariate Tests of Hypothesis for Within Subject Effects

Source	DF	Type III SS	Mean Square	F Value	Pr > F
TIME	15	498733.62039	33248.90803	1.39	0.1473
TIME*S	75	3691635.65366	49221.80872	2.06	0.0001
TIME*JUMP(S)	165	6597057.23472	39982.16506	1.67	0.0001
TIME*JOINT	30	675775.19460	22525.83982	0.94	0.5576
Error (TIME)	32	11482216.00950	23921.28335		

## APPENDIX E

### Computer Program Used to Calculate Forces and Moments

{This computer program was written for the purpose of obtaining the ground reaction forces, and joint reaction forces using the complicated segmental method of calculation. The program reads in a set of values, written in ASCII code, and then produces force values. It should be noted that the **bold** type letters are the actual code, whereas the normal type letters are comments to inform the user of what sections do, or what certain variable represent}

**Program force\_calculation (input,output, file\_name, outfile);**

**const**

**r\_elbow = 1;**  
**r\_shoulder = 3;**  
**head\_neck = 5;**  
**l\_shoulder = 4;**  
**l\_elbow = 2;**  
**l\_hip = 8;**  
**l\_knee = 10;**  
**r\_knee = 7;**  
**l\_ankle = 12;**  
**r\_ankle = 9;**  
**r\_hip = 6;**  
**groundreaction = 11;**

**type**

{ The original data that is read into the computer from the files that are stored by the Peak5 software program}

**info = record**

**seg\_cg\_accelx: array [1..12, 1..55] of real;**  
**seg\_cg\_accely: array [1..12, 1..55] of real;**  
**seg\_cg\_accelz: array [1..12, 1..55] of real;**  
**seg\_cg\_accelr: array [1..12, 1..55] of real;**  
**ang\_accel: array [1..12, 1..55] of real;**  
**angle: array [1..12, 1..55] of real;**  
**CG\_accelerationx: array [1..20, 1..55] of real;**  
**CG\_accelerationy: array [1..20, 1..55] of real;**  
**CG\_accelerationz: array [1..20, 1..55] of real;**  
**CG\_accelerationr: array [1..20, 1..55] of real**

**end;**

{Calculated values of the forces and moments found values from 1-11 will represent the joint reaction forces, and joint

**cal\_value = record**

**moments, while 12 will contain the ground reaction forces}**

**forcex: array [1..13, 1..55] of real;**  
**forcey: array [1..13, 1..55] of real;**  
**moment: array [1..12, 1..55] of real**

**end;**

```

var
  data: info;           {original data values from Peak5}
  cal_force: cal_value; {calculated force and moment values}
  name: string [8];    {file name that is to be used without the extension}
  file_name, outfile: text; {Files used including the extension}
  temp_name: string [12]; {the file name plus the extension}
  last, a, joints, num_frames, num_points, touchdown, x, y: integer;
                        {x,y are counters}
  sex: char;           {sex of the athlete}
  height, weight: real; {height and weight of the subject}

```

---

This procedure will take the files produced by the peak5 system and read them into a set of arrays. There will be one array for each of the x,y,z,r values.)

```

Procedure Initialize_lin (var file_name:text; var data:info; last, q, touchdown,
                        num_points:integer);

```

{c - the first character read in by the computer, this will be converted from an ascii character into its numeric representation

pos\_exponent, neg\_exponent, left\_dec, right\_dec, done, neg - these are all boolean expressions that have either the value of "true" or "false".

When certain conditions are met, the value will be changed from one value to the other.

x, y, z, a, counter - are all counters used to run a series of lines over and over again until the required values have been met.

fac - a value used to increase the number by ten, if and only if the decimal point has not been read in yet.

exponent - the value that represents the exponent of the exponential notation

number - the converted value of the character representing the exponent

num - the converted value of the character representing the number being read into the array.

decfac - a value that starts at 1/10 and is continually decreased by a factor of 1/10, until there are no numbers left to be read into the array

totnum - the total value of the number being read into the array location}

```

var
  c: char;
  pos_exponent, neg_exponent, left_dec, right_dec, done, neg: boolean;
  x, y, z, a, fac, exponent, number: integer;
  num, decfac, totnum: real;

```

```

begin
  x:=0;
  repeat
    {this reads in the first set of numbers and discards
    them.}

```

```

read (file_name, c); {the number of values that are read in depends on
                    the number of frames digitized and the frame of
                    toe contact}

if c=' ' then
  x:=x+1;           {when the number of spaces is equal to 4 time the
                    number at touchdown, this loop is broken}
until x= (touchdown*4*num_points);

read (file_name, c); {read in the fist value to be kept}

```

{the next three for loops the computer reads in a frame number, then using that frame number, reads in the points one at a time. Then for each point it reads in the x, y, z, resultant values.

```

ie. frame 1 is read in
  point 1 is read in
  x, y, z, resultant values are read in
  point 2 is read in
  x, y, z, resultant values are read in
  .
  .
  .
  point n is read in
  x, y, z, resultant values are read in
  frame 2 is read in
  .
  .
  .
  etc. )

```

```

for x:=1 to last do
  for y:= 1 to num_points do
    for a:= 1 to 4 do
      begin {assignment of all the values to their initial value}
        done:= false;
        totnum:= 0;
        fac:= 1;
        decfac:= 10;
        neg:= false;
        left_dec:= true;
        right_dec:= false;
        z:=0;
        exponent:= 0;
        pos_exponent:= false;
        neg_exponent:= false;
        repeat {compares the value read in to the values of '-', '+', '.',
              'E' and then changes the appropriate boolean
              expression to the opposite value it had}

```

```

if c='- ' then
  neg:= true;
if c='.' then
  begin
    right_dec:= true;
    left_dec:= false;
  end;
if (c=' ') then
  done:= true;
if c='E' then
  begin
    fac:=0;
    read (file_name, c);
    if c='+' then
      pos_exponent:= true;
    if c='-' then
      neg_exponent:= true;
    repeat {calculates the value of the exponent}
      z:= z+1;
      read (file_name, c);
      exponent:= exponent * fac;
      number:= ord(c) - 48;
      exponent:= exponent + number;
    until z=2;
  end;
if (c in ['0'..'9']) then
  begin {calculates the value of the number}
    num:= ord(c) - 48;
    if left_dec then {if value is to the left of the decimal}
      begin {multiply by ten, read next value, add}
        z:=z+1; {the neww value to the existing value}
        if z=1 then
          fac:=1
        else
          fac:=10;
        totnum:= totnum * fac;
        totnum:= totnum + num;
      end;
    if right_dec then {if value is to the right of the decimal}
      begin {divide by ten, read next value, add}
        num:= num / decfac; {the neww value to the
          existing value}
        totnum:= totnum + num;
        decfac:= decfac * 10;
      end;
  end;
end;

```

```

    read (file_name, c);
until (done= true);

if neg then      {if value was negative multiply by (-1)}
    totnum:= totnum * (-1);
if pos_exponent then {if exponent was positive then multiply by
                    the value of the exponent}
    totnum:= totnum * exp(exponent * ln(10));
if neg_exponent then {if exponent was positive then multiply by
                    the value of the exponent}
    totnum:= totnum / exp(exponent * ln(10));
with data do
begin
    if q=1 then
        case a of          {assign calculated values to their respective
                            place holders}
            1: seg_cg_accelx [y,x]:= totnum;
            2: seg_cg_accely [y,x]:= totnum;
            3: seg_cg_accelz [y,x]:= totnum;
            4: seg_cg_accelr [y,x]:= totnum;
        end;
    if q=2 then
        case a of          {assign calculated values to their respective
                            place holders}
            1: CG_accelerationx [y,x]:= totnum;
            2: CG_accelerationy [y,x]:= totnum;
            3: CG_accelerationz [y,x]:= totnum;
            4: CG_accelerationr [y,x]:= totnum;
        end;
    end;
end;
end;
end;

```

{-----}  
{this procedure has the same variables, and performs the exact same  
function as the previous one. However, the one difference is that the values  
read in are from a file containing either angles or angular acceleration}  
**procedure initialize\_angle (var file\_name:text; var data:info; last, counter,  
touchdown, joints:integer);**

```

var
    c: char;
    pos_exponent, neg_exponent, left_dec, right_dec, done, neg: boolean;
    x, y, z, fac, exponent, number: integer;
    num, decfac, totnum: real;

```

```
begin
  x:=0;
  repeat
    read (file_name, c);
    if c=' ' then
      x:=x+1;
  until x= (touchdown*joints);
  read (file_name, c);
  for x:=1 to last do
    for y:= 1 to joints do
      begin
        done:= false;
        totnum:= 0;
        fac:= 1;
        decfac:= 10;
        neg:= false;
        left_dec:= true;
        right_dec:= false;
        z:=0;
        exponent:= 0;
        pos_exponent:= false;
        neg_exponent:= false;
        repeat
          if c='- ' then
            neg:= true;
          if c='.' then
            begin
              right_dec:= true;
              left_dec:= false;
            end;
          if (c=' ') then
            done:= true;
          if c='E' then
            begin
              z:=0;
              fac:=0;
              read (file_name, c);
              if c='+' then
                pos_exponent:= true;
              if c='- ' then
                neg_exponent:= true;
              repeat
                z:= z+1;
                read (file_name, c);
                exponent:= exponent * fac;
                number:= ord(c) - 48;
```

```

        exponent:= exponent + number;
    until z=2;
end;
if (c in ['0'..'9']) then
begin
    num:= ord(c) - 48;
    if left_dec then
        begin
            z:=z+1;
            if z=1 then
                fac:=1
            else
                fac:=10;
            totnum:= totnum * fac;
            totnum:= totnum + num;
        end;
    if right_dec then
        begin
            num:= num / decfac;
            totnum:= totnum + num;
            decfac:=decfac * 10;
        end;
    end;
    read (file_name, c);
until (done= true);
if neg then
    totnum:= totnum * (-1);
if pos_exponent then
    totnum:= totnum * exp(exponent * ln(10));
if neg_exponent then
    totnum:= totnum / exp(exponent * ln(10));
if counter = 1 then
    data.ang_accel [y,x]:= totnum;
if counter = 2 then
    data.angle [y,x]:= totnum;
end;
end;
end;

```

---

This procedure takes the values passed by the main program and calculates the forces and moment at the proximal joint. This procedure was used three times, once each for the right forearm, left forearm, and left foot}

```

procedure distal (var data:info; var values:cal_value; dist, prox, seg,
    last:integer; height, weight:real; sex:char);

```

{count- counter  
 last - the difference between the total number of frames digitized and the  
 point of first toe contact  
 angx, angy - the value obtained by taking the sine or cosine of the angle for  
 each frame  
 length - the length of the segment in question  
 L1, L2 - the respective distance from the proximal or distal segment to the  
 CG of the limb segment  
 mass - mass of the segment in question  
 inertia - the moment of inertia of the segment about the z-axis}

**var**

**count: integer;**  
**angx, angy, length, mass, inertia, L1, L2: real;**

**begin**

{forearm values for the force calculation}

**if (seg = 1) or (seg = 2) then**

**begin**

**length:= height \* (0.157);** {forearm length as a % of total body height}

**L1:= length \* (0.4176);** {distance from proximal point to CG}

**L2:= length \* (1 - 0.4176);** {distance from distal point to CG}

**if sex='m' then**

**mass:= weight \* (0.019)** {mass of male as % of total body weight}

**else**

**mass:= weight \* (0.0155);** {mass of female as % of total body weight}

**inertia:= 0.0076;** {inertia of forearms}

**end;**

{left foot values for force calculation}

**if (seg = 12) then**

**begin**

**length:= height \* (0.0425);** {length of foot as % of total body height}

**L1:= length \* (0.4176);** {distance from proximal point to CG}

**L2:= length \* (1 - 0.4176);** {distance from distal point to CG}

**if sex='m' then**

**mass:= weight \* (0.0195)** {mass of male as % of total body weight}

**else**

**mass:= weight \* (0.012);** {mass of female as % of total body weight}

**inertia:= 0.0038;** {inertia of foot}

**end;**

{for each of the frames from touchdown to the end of the landing, the forces and moments are calculated using the formuli presented in the methods section of the thesis. In Pascal, the formuli for the forces and moments are as follows.}

```

for count:= 1 to last do
  with values do
    begin
      forcex[seg, count]:= data.seg_cg_accelx[seg, count] * mass;
      forcey[seg, count]:= (data.seg_cg_accely[seg, count] * mass)+(mass * (-
9.81));
    end;
  end;
end;

```

---

This procedure takes the values passed by the main program and calculates the forces and moment at the proximal joint using the forces and moments from the distal joint. This procedure is used once for the head)

```

procedure head (var data:info; var values:cal_value; dist,prox, seg,
last:integer; height, weight:real; sex:char);

```

```

{count- counter

```

```

last - the difference between the total number of frames digitized and the
point of first toe contact

```

```

angx, angy - the value obtained by taking the sine or cosine of the angle for
each frame

```

```

length - the length of the segment in question

```

```

L1, L2 - the respective distance from the proximal or distal segment to the
CG of the limb segment

```

```

mass - mass of the segment in question

```

```

inertia - the moment of inertia of the segment about the z-axis

```

```

prev_seg - this is the distal segment that is attached to the segment that
we are trying to calculate.)

```

```

var

```

```

count, prev_seg: integer;

```

```

angx, angy, length, mass, inertia, L1, L2: real;

```

```

begin

```

```

  length:= height * (0.1075);      {head & neck length as a % of total body
height}

```

```

  L1:= length * (0.5);             {distance from proximal point to CG}

```

```

  L2:= length * (1 - 0.5);        {distance from distal point to CG}

```

```

  if sex='m' then

```

```

    mass:= weight * (0.096)       {mass of male as % of total body weight}

```

```

  else

```

```

    mass:= weight * (0.077);      {mass of female as % of total body weight}

```

```

  inertia:= 0.0248;               {inertia of head}

```

```

for count:= 1 to last do
  with values do
    begin
      forcex[seg, count]:= data.seg_cg_accelx[seg, count] * mass;
      forcey[seg, count]:= (data.seg_cg_accely[seg, count] * mass)+(mass * 9.81);
    end;
end;

```

-----  
This procedure takes the values passed by the main program and calculates the forces and moment at the proximal joint using the forces and moments from the distal joint. This procedure is used four times, once for the left upper arm, the right upper arm, the left shank, and the left thigh.)

```

procedure proximal (var data:info; var values:cal_value; dist, prox, seg,
last:integer; height, weight:real; sex:char);

```

```

{count- counter
angx, angy - the value obtained by taking the sine or cosine of the angle for
              each frame
length - the length of the segment in question
L1, L2 - the respective distance from the proximal or distal segment to the CG
          of the limb segment
mass - mass of the segment in question
inertia - the moment of inertia of the segment about the z-axis
prev_seg - this is the distal segment that is attached to the segment that we
            are trying to calculate.}

```

```

var
  count, prev_seg: integer;
  angx, angy, length, mass, inertia, L1, L2: real;

```

```

begin
{Upper arm values for force calculation}
  if (seg = 3) or (seg = 4) then
    begin
      length:= height * (0.172);      {length of upper arm as % of total height}
      L1:= length * (0.491);          {distance from proximal joint to CG}
      L2:= length * (1 - 0.491);      {distance from distal joint to CG}
      if sex='m' then
        mass:= weight * (0.033)      {male mass of upper arms as % of total}
      else
        mass:= weight * (0.03);      {female mass of upper arms as % of total}
      inertia:= 0.0213;               {body weight}
    end;

```

{shank values for force calculation}

```

if (seg = 10) then
  begin
    length:= height * (0.247);    {length of the shank as % of total height}
    L1:= length * (0.4179);      {distance from proximal joint to CG}
    L2:= length * (1 - 0.4179);  {distance from distal joint to CG}
    if sex='m' then
      mass:= weight * (0.045)    {male mass of upper arms as % of total}
    else
      mass:= weight * (0.0525);  {female mass of upper arms as % of total}
    inertia:= 0.0504;            {body weight}
  end;

```

{thigh values for force calculation}

```

if (seg = 8) then
  begin
    length:= height * (0.232);    {length of the thighs as % of total height}
    L1:= length * (0.4001);      {distance from proximal joint to CG}
    L2:= length * (1 - 0.4001);  {distance from distal joint to CG}
    if sex='m' then
      mass:= weight * (0.105)    {male mass of upper arms as % of total}
    else
      mass:= weight * (0.115);  {female mass of upper arms as % of total}
    inertia:= 0.1052;            {body weight}
  end;

```

{the following case statement finds out which segment is being used and then makes the variable "prev\_seg" equal to the number of the segment distal to the one in the calculation. This way segment 5, which is the r. upper arm can have the force and moment values of the right forearm summed to it (ie. the right forearm is segment 1)}

```

case seg of
  3: prev_seg:= r_elbow;
  4: prev_seg:= l_elbow;
  8: prev_seg:= l_knee;
  10: prev_seg:= l_ankle;
end;

```

{calculation of the forces and moments at the proximal joint of the segment in question}

```

for count:= 1 to last do
  with values do
    begin
      forcex[seg,count]:= forcex[prev_seg,count] +
        data.seg_cg_accelx[seg,count] * mass;
    end;

```

```

    forcey[seg,count]:= forcey[prev_seg,count]+
                        (data.seg_cg_accely[seg,count]*mass)+(mass*9.81);
  end;
end;

```

-----  
 The calculation of the forces and moments that occur at the right hip of the athlete. This procedure uses the values found at the left hip, right and left shoulders and the head to calculate the values.)

```

procedure trunk (var data:info; var values:cal_value; dist, prox, seg,
last:integer;          height, weight:real; sex:char);

```

```

{count- counter
last - the difference between the total number of frames digitized and the
point of first toe contact
angx, angy - the value obtained by taking the sine or cosine of the angle for
each frame
length - the length of the segment in question
L1, L2 - the respective distance from the proximal or distal segment to the CG
of the limb segment
mass - mass of the segment in question
inertia - the moment of inertia of the segment about the z-axis}

```

```

var
  count: integer;
  angx, angy, length, mass, inertia, L1, L2: real;

```

```

begin
  length:= height * (0.30);      {length of the trunk}
  L1:= length * (0.4383);        {distance from proximal point to CG of trunk}
  L2:= length * (1 - 0.4383);    {distance from distal point to CG of trunk}
  if sex='m' then
    mass:= weight * (0.458)      {male mass of the trunk}
  else
    mass:= weight * (0.463);     {female mass of the trunk}
  inertia:= 1.2606;              {moment of inertia of the trunk}

```

```

{calculation of the forces and moments at the right hip}
for count:= 1 to last do
  with values do
    begin
      forcex[seg,count]:= forcex[5,count]+forcex[3,count]+forcex[4,count]+
                          forcex[8,count]+data.seg_cg_accelx[seg,count]*mass;
    
```

```

forcey[seg,count]:= forcey[5,count]+forcey[3,count]+forcey[4,count]+
forcey[8,count]+data.seg_cg_accely[seg,count]*mass
+(mass*9.81);

```

```

end;
end;

```

---

The calculation of the forces and moments that occur at the right knee and ankle of the athlete. This procedure uses the values found at the right hip to calculate the values. The difference between this procedure and the previous proximal subroutine is that the forces are calculated at the distal end of the segment on question.)

```

procedure support (var data:info; var values:cal_value; dist, prox, seg, l
ast:integer; height, weight:real; sex:char);

```

```

var
count, prev_seg: integer;
angx, angy, length, mass, inertia, L1, L2: real;

```

```

begin

```

```

if (seg = 9) then

```

```

begin

```

```

length:= height * (0.247); {length of the shank as % of total height}

```

```

L1:= length * (0.4179); {distance from proximal joint to CG}

```

```

L2:= length * (1 - 0.4179); {distance from distal joint to CG}

```

```

if sex='m' then

```

```

mass:= weight * (0.045) {male mass of upper arms as % of total}

```

```

else {body weight}

```

```

mass:= weight * (0.0525); {female mass of upper arms as % of total}

```

```

inertia:= 0.0504; {body weight}

```

```

end;

```

```

if (seg = 7) then

```

```

begin

```

```

length:= height * (0.232); {length of the thighs as % of total height}

```

```

L1:= length * (0.4001); {distance from proximal joint to CG}

```

```

L2:= length * (1 - 0.4001); {distance from distal joint to CG}

```

```

if sex='m' then

```

```

mass:= weight * (0.105) {male mass of upper arms as % of total}

```

```

else {body weight}

```

```

mass:= weight * (0.115); {female mass of upper arms as % of total}

```

```

inertia:= 0.1052; {body weight}

```

```

end;

```

```

case seg of
  7: prev_seg:= r_hip;
  9: prev_seg:= r_knee;
end;

for count:= 1 to last do
  with values do
    begin
      forcex[seg,count]:= forcex[prev_seg,count]+
                          data.seg_cg_accelx[seg,count]* mass;
      forcey[seg,count]:= forcey[prev_seg,count]+
                          (data.seg_cg_accely[seg,count]*mass)+(mass*9.81);
    end;
  end;
end;

```

-----  
 the calculation of the GRF for the right foot upon landing a triple toe loop.)

```

procedure GRF (var data:info; var values:cal_value; dist, prox, seg,
               last:integer; height, weight:real; sex:char);

```

```

{count- counter
last - the difference between the total number of frames digitized and the
      point of first toe contact
length - the length of the segment in question
L1, L2 - the respective distance from the proximal or distal segment to the CG
          of the limb segment
mass - mass of the segment in question}

```

```

var
  count: integer;
  L1, L2, length, mass: real;

```

```

begin
  length:= height * (0.0425);      {length of the right foot}
  L1:= length * (0.4176);         {distance from proximal point to CG}
  L2:= length * (1 - 0.4176);     {distance from distal point to CG}
  if sex='m' then
    mass:= weight * (0.0195)      {male mass of right foot}
  else
    mass:= weight * (0.012);      {female mass of right foot}

```

```

(calculation of the GRF that occurs while landing the triple toe loop)
  for count:= 1 to last do
    with values do
      begin
        forcex[seg,count]:=data.seg_cg_accelx[seg,count]*mass+forcex[9,count];
        forcey[seg,count]:=(data.seg_cg_accely[seg,count]*mass)+(mass*9.81)+
          forcey[9,count];
      end;
    end;
  end;

```

```

{-----}
procedure moments (var data:info; var values:cal_value; dist, prox, seg,
                  last:integer; height, weight:real; sex:char);

```

```

var
  count, prev_seg: integer;
  angx, ange, length, mass, inertia, L1, L2: real;

```

```

begin

```

```

{Calculation of the moments at the ankle using the GRF and moving
proximally}

```

```

  seg := 9;
  for count := 1 to last do
    with values do
      begin
        length := height * (0.0425);
        L1 := length * (0.4176);
        L2 := length * (1 - 0.4176);
        if sex = 'm' then
          mass := weight * (0.0195);
        else
          mass := weight * (0.012);
        inertia := 0.0038;

        angx:= sin(data.angle[seg,count]);
        ange:= cos(data.angle[seg,count]);
        moment[seg,count]:=(- forcex[11,count]*L2+forcex[seg,count]*L1)*angx
          + (- forcey[11,count]*L2+ forcey[seg,count]*L1)*ange +
          (inertia*data.ang_accel[seg,count]);
      end;
    end;
  end;

```

{Calculation of the moments at the knee using the ankle JRF and moving proximally}

```

seg := 7;
for count := 1 to last do
  with values do
    begin
      length := height * (0.247);
      L1 := length * (0.4179);
      L2 := length * (1 - 0.4179);
      if sex = 'm' then
        mass := weight * (0.045);
      else
        mass := weight * (0.0525);
      inertia := 0.0504;

      angx:= sin(data.angle[seg,count]);
      ange:= cos(data.angle[seg,count]);
      moment[seg,count]:= moment[9, count] + (- forcex[9,count]*L1 +
        forcex[seg,count]*L2)*angx + (- forcey[9,count]*L1+
        forcey[seg,count]*L2)*ange +
      (inertia*data.ang_accel[seg,count]);
    end;

```

{Calculation of the moments at the hip using the knee JRF and moving proximally}

```

seg := 6;
for count := 1 to last do
  with values do
    begin
      length := height * (0.232);
      L1 := length * (0.4001);
      L2 := length * (1 - 0.4001);
      if sex = 'm' then
        mass := weight * (0.105);
      else
        mass := weight * (0.115);
      inertia := 0.1052;

      angx:= sin(data.angle[seg,count]);
      ange:= cos(data.angle[seg,count]);
      moment[seg,count]:= moment[7, count] + (- forcex[7,count]*L1 +
        forcex[seg,count]*L2)*angx + (- forcey[7,count]*L1+
        forcey[seg,count]*L2)*ange +
      (inertia*data.ang_accel[seg,count]);
    end;
end;

```

```

{-----}
the calculation of the GRF for the CG upon landing a triple toe loop.)

procedure CG_GRF (var data:info; var values:cal_value; seg, last:integer;
                  weight:real);

var
  {count- counter}
  count: integer;

begin
  {calculation of the GRF that occurs while landing the triple toe loop}
  for count:= 1 to last do
    with values do
      begin
        forcex[seg,count]:=(data.CG_accelerationx[20,count]*weight);
        forcey[seg,count]:=(data.CG_accelerationy[20,count]*weight +
                             weight *9.81);
      end;
    end;

  {division of the forces found above by the total weight of the athlete provides
  a force value as a % of total body weight}
  for count:= 1 to last do
    with values do
      begin
        forcex[seg,count]:=forcex[seg,count]/(weight*9.81);
        forcey[seg,count]:=forcey[seg,count]/(weight*9.81);
      end;
    end;
  end;

{-----}
{main program}
Begin
  temp_name:= ""; {initialize the temporary stings to the null string}
  name:= "";

  write ('Please enter the name of the file to be used (maximum of 8
          characters): ');

  readln (name);
  writeln;

  write ('Please enter the number of frames that were digitized: ');
  readln (num_frames);
  writeln;
  num_points := 19 + 1;

```

```

joints:= 12;

repeat {a repeat loop is used so that only a 'f' or a 'm' can be input}
  write ('Please enter the sex of the athlete (male=m, female=f): ');
  readln (sex);
until (sex='m') or (sex='f');
writeln;
write ('Please enter the frame when the foot first touches down: ');
readln (touchdown);
touchdown:=touchdown - 1;
writeln;

write ('Please enter the height of the subject (in meters): ');
readln (height);
writeln;

write ('Please enter the weight of the subject (in kilograms): ');
readln (weight);
writeln;

last:= num_frames - touchdown;
writeln ('      Working, please be patient.....');

```

{After assigning the input name to the temporary string with the extension of '.ala' which stands for the linear acceleration of each segment. This then opens the file chosen and sends control to the procedure Initialize\_lin to read in all values for the linear acceleration.}

```

x:=1;
temp_name:= name + 'a.ala';
assign (file_name, temp_name);
reset (file_name);
Initialize_lin (file_name, data, last, x, touchdown, joints);
close (file_name);

```

```

x:=2;
temp_name:= name + 'b.ala';
assign (file_name, temp_name);
reset (file_name);
Initialize_lin (file_name, data, last, x, touchdown, num_points);
close (file_name);

```

{assigning the input name to the temporary string with the extension of '.aaa' which stands for the angular acceleration. This then opens the file chosen and sends control to the procedure Initialize\_angle to read in all values for the angular acceleration.}

```

x:=1;
temp_name:= name + '.aaa';
assign (file_name, temp_name);
reset (file_name);
Initialize_angle (file_name, data, last, x, touchdown, joints);
close (file_name);

```

{assigning the input name to the temporary string with the extension of '.aad' which stands for the angular displacement. This then opens the file chosen and sends control to the procedure Initialize\_angle to read in all values for the angular displacement.}

```

x:=2;
temp_name:= name + '.aad';
assign (file_name, temp_name);
reset (file_name);
Initialize_angle (file_name, data, last, x, touchdown, joints);
close (file_name);

```

{A repetitive loop was used to calculate the forces and moments for each of the twelve segments used in the model. When 'a' was equal to any of the values between 1 and 12, the appropriate proximal and distal numbers were assigned, the segment number was assigned, and the control was sent to the procedure corresponding to the segment in question (ie. distal, proximal, trunk, GRF).}

```

for a:= 1 to 12 do
  case a of
    1: begin
      x:=1;
      y:=2;
      joints:= r_elbow;
      distal (data, cal_force, x, y, joints, last, height, weight, sex);
      end;
    2: begin
      x:=5;
      y:=4;
      joints:= head_neck;
      head (data, cal_force, x, y, joints, last, height, weight, sex);
      end;
    3: begin
      x:=8;
      y:=7;
      joints:= l_elbow;
      distal (data, cal_force, x, y, joints, last, height, weight, sex);
      end;

```

```
4: begin
  x:=19;
  y:=18;
  joints:= l_ankle;
  distal (data, cal_force, x, y, joints, last, height, weight, sex);
end;
5: begin
  x:=2;
  y:=3;
  joints:= r_shoulder;
  proximal (data, cal_force, x, y, joints, last, height, weight, sex);
end;
6: begin
  x:=7;
  y:=6;
  joints:= l_shoulder;
  proximal (data, cal_force, x, y, joints, last, height, weight, sex);
end;
7: begin
  x:=17;
  y:=16;
  joints:= l_knee;
  proximal (data, cal_force, x, y, joints, last, height, weight, sex);
end;
8: begin
  x:=16;
  y:=15;
  joints:= l_hip;
  proximal (data, cal_force, x, y, joints, last, height, weight, sex);
end;
9: begin
  x:=9;
  y:=4;
  joints:= r_hip;
  trunk (data, cal_force, x, y, joints, last, height, weight, sex);
end;
10: begin
  x:=11;
  y:=10;
  joints:= r_knee;
  support (data, cal_force, x, y, joints, last, height, weight, sex);
end;
```

```

11: begin
  x:=12;
  y:=11;
  joints:= r_ankle;
  support (data, cal_force, x, y, joints, last, height, weight, sex);
  end;
12: begin
  x:=14;
  y:=13;
  joints:= groundreaction;
  GRF (data, cal_force, x, y, joints, last, height, weight, sex);
  end;
end; {end of the case statement}

```

moments (data, cal\_force, x, y, joints, last, height, weight, sex);

{ the following two lines calculate the GRF using the entire body's CG}

```

joints:=13;
CG_GRF (data, cal_force, joints, last, weight);

```

{Calculates all force values as a % of body weight}

```

weight:= weight*9.81;
for y:= 6 to 11 do
  for x:= 1 to 55 do
    with cal_force do
      case y of
        6,7,9,11:begin
          forcex[y,x]:= forcex[y,x]/weight;
          forcey[y,x]:= forcey[y,x]/weight;
          moment[y,x]:= moment[y,x]/weight;
        end;
      end;
    end; {end of case statement}
  end;
end;

```

{the following section outputs the force values calculated at by both methods of force calculation. The complicated, segmental method is written by the variable cal\_force.forcey[11,x], while the calculation using the CG for the whole body is written by cal\_force.forcey[13,x]. These values are written to a file with the same name as the original data files but has the extension of '.GRF'.}

```

temp_name:="";
temp_name:= name + '.GRF';
assign (outfile, temp_name);
rewrite (outfile);
writeln (outfile,'x,y,CG - x,CG - y');
with cal_force do
for x:= 1 to 55 do
  writeln (outfile,forcex[11,x]:5:3,',',forcey[11,x]:5:3,',',forcex[13,x]:5:3,',',
          forcey[13,x]:5:3);
close (outfile);
{the following section outputs the force values calculated at the hip, knee and
ankle using the segmental method. These values are written to a file with
the same name as the original data files but has the extension of '.JRF'.}

temp_name:= name + '.JRF';
assign (outfile, temp_name);
rewrite (outfile);

writeln (outfile,'hip - x,hip - y,hip - moment');
with cal_force do
  for x:= 1 to 55 do
    writeln (outfile,forcex[6,x]:5:3,',',forcey[6,x]:5:3,',',moment[6,x]:5:3);
  writeln (outfile,'knee - x,knee - y,knee - moment');
  with cal_force do
    for x:= 1 to 55 do
      writeln (outfile,forcex[7,x]:5:3,',',forcey[7,x]:5:3,',',moment[7,x]:5:3);
    writeln (outfile,'ankle - x,ankle - y,ankle - moment');
  with cal_force do
    for x:= 1 to 55 do
      writeln (outfile,forcex[9,x]:5:3,',',forcey[9,x]:5:3,',',moment[9,x]:5:3);
    close (outfile);
end.

```